

**ICPEPA-10**

10<sup>th</sup> International Conference  
on Photoexcited Processes  
and Applications

[www.icpepa10.com](http://www.icpepa10.com)

# Book of Abstracts

[www.icpepa10.com](http://www.icpepa10.com)

**August 29–September 2, 2016, Brasov, Romania**



10<sup>th</sup> International Conference on Photoexcited Processes and Applications  
*August 29 – September 2, 2016, Brasov, Romania*

Organized by



with support of



Conference chairs:

- **Ion N. Mihailescu**, National Institute for Lasers, Plasma and Radiation Physics, Magurele, Romania
- **Ioan Vasile Abrudan**, Universitatea "Transilvania" Brasov, Romania

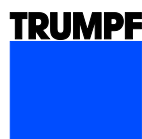
**ADMINISTRATIVE CONTACT:** [icpepa10@gmail.com](mailto:icpepa10@gmail.com)

Please visit: <http://icpepa10.com> for details regarding the conference

### LOCAL ORGANIZING COMMITTEE:

- Emanuel AXENTE, National Institute for Lasers, Plasma and Radiation Physics
- Mihaela BADEA, "Transilvania" University of Brasov
- Gabriela DORCIOMAN, National Institute for Lasers, Plasma and Radiation Physics
- Liviu DUTA, National Institute for Lasers, Plasma and Radiation Physics
- Dan FLOROIAN, "Transilvania" University of Brasov
- Claudiu HAPENCIUC, National Institute for Lasers, Plasma and Radiation Physics
- Dominic KRISTALY, "Transilvania" University of Brasov
- Adrian MANEA, "Transilvania" University of Brasov
- Alexandra MANEA, "Transilvania" University of Brasov
- Ioana MANEA, "Transilvania" University of Brasov
- Natalia MIHAILESCU, National Institute for Lasers, Plasma and Radiation Physics
- Irina NEGUT, National Institute for Lasers, Plasma and Radiation Physics
- Andrei POPESCU, National Institute for Lasers, Plasma and Radiation Physics
- Gianina POPESCU-PELIN, National Institute for Lasers, Plasma and Radiation Physics
- Paul SCHIOPU, "Politehnica" University Bucuresti
- Mihai SOPRONYI, National Institute for Lasers, Plasma and Radiation Physics
- Anita VISAN, National Institute for Lasers, Plasma and Radiation Physics

### Sponsors



VACUSERV SRL

## FOREWORD

The topics range from fundamental laser-material interactions, theory and modeling to applications with nanoparticles and nanophotonics as well as photoexcitations. The conference intends to create an atmosphere for scientific presentations at the forefront of the field and an informal exchange of ideas in a relaxing environment. Peer-reviewed papers submitted at the conference will be published in a Special Issue of Applied Surface Science.

### ICPEPA TOPICS

- Theoretical approach, simulation and modeling of photoexcited processes
- Fundamental phenomena of laser-matter interactions
- Dynamics and diagnostics of photoexcited processes
- Ultrafast Phenomena in chemical processes
- Photoexcited chemical processes
- Photo/laser-induced desorption from surfaces
- Resonant and non-resonant processes in photo/laser-induced materials processing
- Deposition and coating of thin films, multilayers, and nanostructured materials
- Synthesis of nanomaterials
- Photo/laser-induced nanoscale processing
- Plasmon-enhanced photon/laser processing
- Cutting, drilling, surface patterning and micromachining
- Surface modification including crystallization, amorphization, phase transformation, and doping
- Surface nanostructuring and nanoripple formation
- Volume and 3D internal processing
- 3D additive manufacturing
- Manipulated/shaped beam processing
- Ultrahigh-power laser applications
- Interactions with organic and biomaterials and applications including MALDI and laser microprobe mass analysis
- Lasers in nanobiomedicine
- Photon sources and laser systems for photoexcited processes
- Photocatalysis

### STEERING PANEL

- Chunlei Guo, University of Rochester, USA
- Peter Hess, University of Heidelberg, Germany
- Aaron Peled, Holon Institute of Technology, Israel
- Jørgen Schou, Technical University of Denmark, Denmark
- Koji Sugioka, RIKEN, Japan
- Yasuyuki Tsuboi, Osaka City University, Japan
- Leonid Zhigilei, University of Virginia, USA

**Venue:** “Sergiu T. Chiriacescu” Aula of the “Transilvania” University, 41A Iuliu Maniu Street, Brasov, Romania.



The city of BRASOV is located in the center of Romania, about 180 km north of Bucharest. It is an international resort, and well situated touristic city in Romania. Brasov, an old medieval city, gives you the opportunity to visit many old historical monuments and museums that reflect the cultural as well as other touristic important sites in the neighborhood. The biggest attraction in town is the Gothic Protestant Church built between 1385 and 1477. It is known as the name of the "Black Church" because of its smokeblackened walls after a fire in 1689.



# ICPEPA-10 PLENARY LECTURE

## Professor Stefan W. Hell

Max Planck Institute for Biophysical Chemistry, Göttingen  
German Cancer Research Center (DKFZ), Heidelberg  
GERMANY



## Optical microscopy: the optical revolution

V. Westphal, S.W. Hell

Max-Planck-Institute f. Biophysical Chemistry, Dept. f. NanoBiophotonics, Göttingen, Germany  
vwestph@gwdg.de

For more than a century, the resolution of a lens-based (far-field) optical microscope has been limited by diffraction, as shown by Abbe. However, in the 1990s it became evident that the limiting role of diffraction can be broken in lens-based fluorescence microscopy if certain fluorophore properties are judiciously integrated into the image formation<sup>1-3</sup>. The first viable concept of this kind is stimulated emission depletion (STED) microscopy, which, since its experimental validation, has been key to solving a number of problems in biophysics and cell biology.

Since its invention STED microscopy has done many steps forward, up to the point where imaging of living cells and fast dynamic processes with super-resolution has become possible. Also related techniques based on widefield microscopy have been developed. We will give an overview and the latest results.

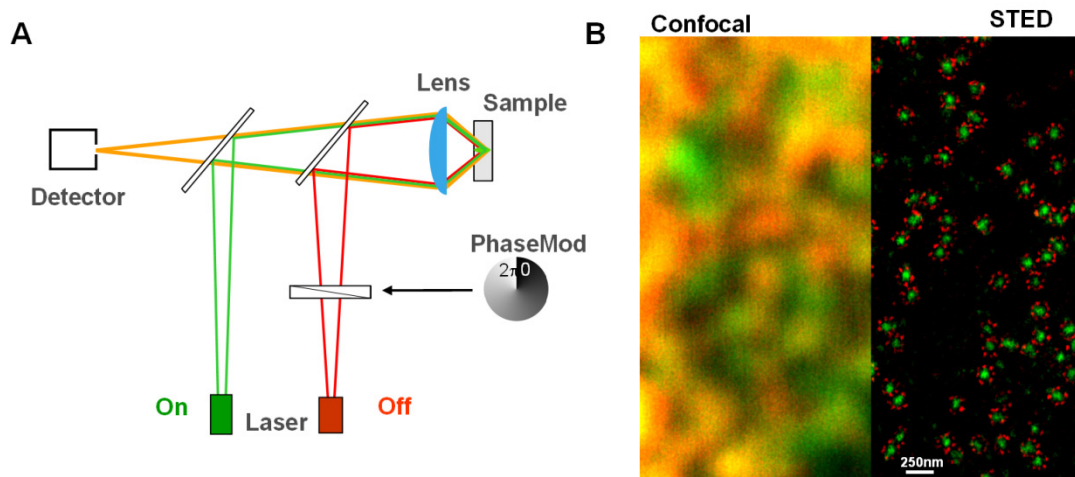


Figure 1: A) Schematic of a STED microscope B) Demonstration of the resolution enhancement, shown on nuclear pore complexes. Proteins stained: gp210 (red) and panFG (green).

1. S. W. Hell, J. Wichmann, *Opt. Lett.* **19**, 780 (1994);
2. S.W. Hell *Science* **316** 1153 (2007);
3. V. Westphal, S. O. Rizzoli, M. A. Lauterbach, D. Kamin, R. Jahn, S. W. Hell *Science*. **320**, 246 (2008).



# **INVITED PRESENTATIONS**





# Ultrafast laser light absorption in dielectrics: Focusing into the bulk versus surface irradiation

N.M. Bulgakova<sup>1,2</sup>, V.P. Zhukov<sup>3,4</sup>, I. Mirza<sup>1</sup>, A.V. Bulgakov<sup>2,5</sup>, T. Mocek<sup>1</sup>

<sup>1</sup> HiLASE Centre, Institute of Physics ASCR, Za Radnici 828, 25241 Dolní Břežany, Czech Republic

<sup>2</sup> S.S. Kutateladze Institute of Thermophysics SB RAS, 1 Lavrentyev Ave., 630090 Novosibirsk, Russia

<sup>3</sup> Institute of Computational Technologies SB RAS, 6 Lavrentyev Ave., 630090 Novosibirsk, Russia

<sup>4</sup> Novosibirsk State Technical University, 20 Karl Marx Ave., 630073, Novosibirsk, Russia

<sup>5</sup> EaStCHEM and School of Chemistry, University of Edinburgh, David Brewster Road, Edinburgh EH9 3FJ, UK  
bulgakova@fzu.cz

Femtosecond laser irradiation of dielectric materials enables deposition of laser energy in a highly localized region whose dimensions can be comparable with laser wavelength. This property of fs laser pulses is widely used for direct writing of micro- and nano-sized modifications and ultraprecise drilling and cutting for large variety of applications. Laser energy deposition into dielectric materials is largely governed by nonlinear processes (multi-photon ionization, electron avalanche, self-focusing, etc.). The spatiotemporal dynamics of these processes, accompanied with swift formation of a highly-localized free-electron population absorbing and scattering laser light, is extremely complicated.<sup>1,2</sup> The presence of ambient air at surface processing further complicates the phenomenon due to air ionization, corresponding attenuation of laser beam, and air plasma radiation that can increase material damage.<sup>3,4</sup> To produce gentle modifications of material properties or accurate ablation craters without creation of cracks around the laser-affected zone, irradiation parameters must be carefully selected, depending on material optical, thermal, and mechanical properties. The selection cannot be done without deep understanding of the overall phenomenon and contributing processes that requires close cooperation between experiment and theory.

In this work, we will report on several models developed to describe laser energy deposition in glass materials under the conditions of volumetric modification and surface ablation. For the case of laser beam focusing inside glass, the results of modeling based on Maxwell's equations will be reported while, for surface laser processing, a simplified 1D model of laser energy propagation is used. Ionization mechanisms are analyzed, depending on laser energy and pulse duration, with addressing the laser energy balance. Considerable difference in the dynamics of laser energy absorption is found for the regimes of surface ablation and volumetric modification, whose origin will be discussed. Simulations of laser damage and ablation of glass materials is supported by experimental data on crater shapes (Fig. 1) and white light spectra measurements. Possible role of air ionization in crater shape formation is considered.

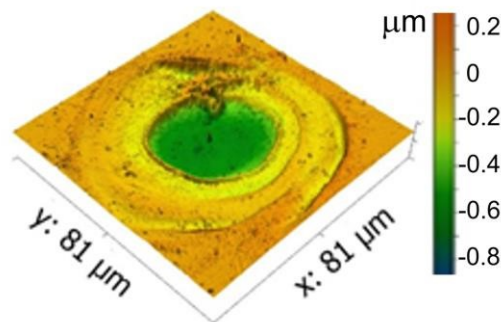


Figure 1: AFM profile of a single-shot ablation crater obtained by an fs laser pulse with an average fluence of  $112 \text{ J/cm}^2$ . Several annular rims correspond to the manifestation of different ablation mechanisms. The external rim diameter is threefold larger than the beam diameter ( $1/e^2$ ) that can be attributed to the effects of air ionization.

1. N.M. Bulgakova, V.P. Zhukov, S.V. Sonina, Yu.P. Meshcheryakov, Modification of transparent materials with ultrashort laser pulses: What is energetically and mechanically meaningful? *J. Appl. Phys.* **118**, 233108 (2015);
2. N.M. Bulgakova, V.P. Zhukov, I. Mirzaa, Yu.P. Meshcheryakove, J. Tomáščík, V. Michálek, O. Haderka, L. Fekete, A.M. Rubenchik, M.P. Fedoruk, T. Mocek, Ultrashort-pulse laser processing of transparent materials: Insight from numerical and semi-analytical models, *Proc. SPIE* 9735, 97350N (2016);
3. N.M. Bulgakova, A.V. Bulgakov, Comment on 'Time-Resolved Shadowgraphs of Material Ejection in Intense Femtosecond Laser Ablation of Aluminum', *Phys. Rev. Lett.* **101**, 099701 (2008);
4. N.M. Bulgakova, A.N. Panchenko, V.P. Zhukov, S.I. Kudryashov, A. Pereira, W. Marine, T. Mocek, A.V. Bulgakov, Impacts of ambient and ablation plasmas on short- and ultrashort-pulse laser processing of surfaces, *Micromachines* **5**, 1344-1372 (2014).

# MAPLE-deposited polymeric film and heterostructures towards innovative organic light-emitting devices

A.P. Caricato<sup>1,2</sup>, G. Accorsi<sup>2</sup>, M. Cesaria<sup>1</sup>, F. Mariano<sup>1</sup>, M. Martino<sup>1,2</sup>, M. Mazzeo<sup>1,2</sup>, C. Leo<sup>1</sup>

<sup>1</sup>Dipartimento di Matematica e Fisica "Ennio De Giorgi", Università del Salento, Via Arnesano, 73100 Lecce, Italy

<sup>2</sup>CNR-Nanotec, Istituto di Nanotecnologia, Polo di Nanotecnologia, c/o Campus Ecotekne, via Monteroni, 73100-Lecce, Italy  
anna.paola.caricato@unisalento.it

The matrix-assisted pulsed laser evaporation (MAPLE) technique is a laser based technique originally developed for the deposition of materials, such as organic and biological materials, in which the preservation of the original structure and functionality as well as minimal thermal degradation are critical factors. Over the years, MAPLE has demonstrated to be a very versatile and successful technique in enabling to deposit almost any kind of material (polymers, inorganics and hybrid organic–inorganic materials) and morphology (thin films, nanoparticles and nanostructured films) on even complex patterned substrates. All of this has recently prompted interest in MAPLE as a valuable alternative route to conventional methods, such as solution-phase and thermal evaporation approaches, for several emerging biological, biomedical and optoelectronic applications.

Operatively, the material of interest is dissolved/suspended in a volatile and laser absorbing solvent with concentration of few weight percentages and such solution (MAPLE-matrix) frozen at the liquid N<sub>2</sub> temperature forms the target to be irradiated by ultra-violet (UV) or infra-red (IR) laser sources. MAPLE exploits the energetic laser ablation mechanism to transfer the solute precursor material to a substrate where the deposit forms.

In this work, the peculiarities of the technique, which make it attractive in different fields, will be outlined and discussed together with its critical aspects. Particular emphasis will be given to its use in depositing low-roughness polymer single layer and multilayers for organic light emitting devices. In this respect, discussion of the interplay between the deposition parameters (fluence, laser repetition rate, number of deposition laser pulses and target-substrate distance) will point out the successful results enabled by the technique as well as the promising aspects about further optimization studies. In particular, MAPLE deposition of polymer multilayer architectures by sequential deposition lets overcome all the drawbacks still limiting the application of spin-coating and thermal evaporation approaches. This opens the way to the fabrication of low-cost innovative organic light-emitting devices for lighting applications.

## Angular distribution of ablated species from a multicomponent target in vacuum and background gas

S. Canulescu<sup>1</sup>, M. Döbeli<sup>2</sup>, J. Schou<sup>1</sup>

<sup>1</sup>Department of Photonics Engineering, Technical University of Denmark, Denmark

<sup>2</sup>Ion Beam Physics, ETH Zürich, Switzerland

There has been a growing interest in the fabrication of metal, alloys, oxides or chalcogenides by pulsed laser deposition (PLD). The properties of the PLD films are closely related to the composition of the laser ablated plume, but also on the angular distribution of the ablated species. Losses of volatile elements<sup>1</sup>, as well as variation in the composition of the films deposited at off-axis configuration were often observed<sup>2</sup>. This has been associated with variation in the angular distribution of the heavy atoms compared to the light atoms in the plume<sup>3,4</sup>. In order to have a comprehensive picture of the ablation process, we have investigated the ablation of a binary alloy consisting of heavy and light atoms in a similar atomic ratio (Au:Cu 1:1). The composition of the AuCu films was analysed by Rutherford Backscattering Spectrometry (RBS). The ablated material was collected on Si substrates placed over a wide range of angles in a symmetrical geometry with respect with normal incidence.

Ablation of the AuCu target at low fluence (1 J/cm<sup>2</sup>) results in a nearly congruent transfer over a large range of angles ranging from 0 to 90 degrees. At a laser fluence of 5 J/cm<sup>2</sup>, the ratio between the Cu to Au atoms deviates significantly from the target stoichiometry, resulting in a large depletion of the lighter elements (Cu) in the PLD-grown films. The deviation in composition of the films deposited at high fluence is significantly large at angles close to normal, while at the tail of the plume composition of the films approaches the composition of the target (Fig. 1). The data suggests that plume scattering plays a major role on the metal ratio of the deposited films. The effect of the background gas (Ne and Xe) on the angular distribution of the plume will also be discussed based on the RBS findings.

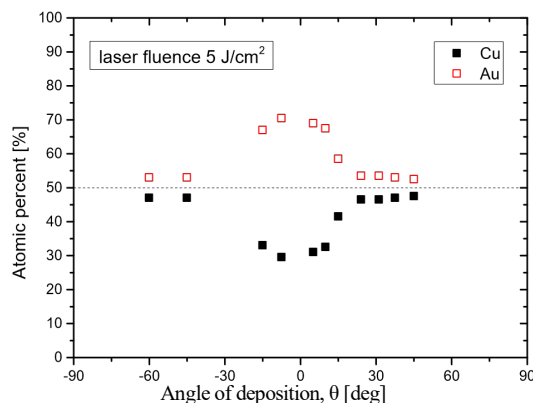


Figure 1: Chemical composition of the Au-Cu films deposited in vacuum in a hemispherical geometry

1. Alejandro Ojeda-G-P, Christof W. Schneider, Max Doebeli, Thomas Lippert and Alexander Wokaun, *Appl. Surf. Sci.* **336**, 150 (2015);
2. L Qiao and T C Droubay and V Shutthanandan and Z Zhu and P V Sushko and S.A.Chambers, *Journal of Physics: Condensed Matter* **22**, 312201 (2010);
3. S. Canulescu, E. L. Papadopoulou, D. Anglos, Th Lippert, C. W. Schneider and A. Wokaun, *J. Appl. Phys.* **105**, 063107 (2009);
4. W. Svendsen, J. Schou, T. N. Hansen and O. Ellegaard, *Appl. Phys. A-Mater. Sci. Process.* **66**, 493 (1998).

## Pulse Forge Curing of Electronic and Energy Materials

D.B. Chrisey<sup>1</sup>, B.C. Riggs<sup>1</sup>, R. Elupula<sup>1</sup>, S. Adireddy<sup>1</sup>, and S.M. Grayson<sup>1</sup>

<sup>1</sup>Tulane University, New Orleans, LA 70122

Polymer-ceramic nanocomposites have been thoroughly investigated previously for high-energy storage devices. However, the increase in performance of these nanocomposites has proven to be significantly lower than predicted values. Through surface functionalization of high dielectric constant nanoparticles (NP), the flaws that reduce composite performance can be eliminated to form high energy density composite materials. Functionalization methods utilize high throughput printing and curing techniques (i.e., inkjet printing and xenon flash lamp curing) that are crucial for rapid adoption into industrial production. (Ba,Ca) (Zr,Ti)O-3 NPs (50 nm) are synthesized through the solvothermal method and functionalized with alkene terminated methoxysilanes. A thiol-ene monomer ink system, PTD3 [pentaerythritol tetrakis (3-mercaptopropionate) (PEMP, P), 1,3Diisopropenylbenzene (DPB, D), 2,4,6-Triallyloxy-1,3,5-triazine (TOTZ, T)], is used as a high breakdown polymer matrix. Neat polymer, alkene terminated NP-polymer composites, and hydrophilic, TBAOH functionalized NP-polymer composites were spin coated onto both copper laminated glass slides and printed onto copper substrates in 1 cm<sup>2</sup> patterns for testing. Alkene functionalized NPs increased the breakdown strength by similar to 38% compared to the nonfunctionalized NPs. Functionalized NPs increased both the breakdown strength and dielectric constant compared to the neat polymer, increasing the energy density nearly 3-fold from 13.3 to 36.1 J/cm<sup>3</sup>.

# Laser fabrication of polymer ferroelectric nanostructures. Application for non-volatile organic memory devices

J. Cui<sup>1</sup>, M. Hernández<sup>2</sup>, D.E. Martínez-Tong<sup>1</sup>, A. Rodríguez-Rodríguez<sup>1</sup>, A. Nogales<sup>1</sup>,  
M.C. García-Gutiérrez<sup>1</sup>, T.A. Ezquerra<sup>1</sup>, E.Rebollar<sup>2</sup>

<sup>1</sup> Instituto de Estructura de la Materia, IEM-CSIC, Serrano 121, 28006 Madrid, Spain  
<sup>2</sup> Instituto de Química Física Rocasolano, IQFR-CSIC, Serrano 119, 28006 Madrid, Spain  
e.rebollar@csic.es

Information storage in organic materials is an essential aspect towards the development of organic electronic systems. Organic memory devices have focused attention on ferroelectric polymers as active storage components, where the poly(vinylidene fluoride) (PVDF) and its copolymer with trifluoro ethylene P(VDFTrFE) are the most used. Nanopatterning can play an important role to enhance information density by controlling molecular orientation<sup>1</sup>.

Polymer ferroelectric laser induced periodic surface structures (LIPSS) have been prepared on ferroelectric thin films of a P(VDF-TrFE) copolymer upon irradiation with the second harmonic of a Nd:YAG laser (532 nm, pulse duration 8 ns). Although not absorbing light at the laser wavelength, LIPSS on the copolymer can be obtained by forming a bilayer with other light absorbing polymer. In this case, poly(3-hexyl thiophene) (P3HT), which is a semiconducting polymer, was used as bottom layer<sup>2</sup>. The influence of the relative thickness of the bilayer components on LIPSS formation was evaluated by using different polymer concentrations. An optimal range of thicknesses was found in order to obtain periodic surface nanostructures.

The ferroelectric nature of the structured bilayer was proven by piezoresponse force microscopy measurements. Ferroelectric hysteresis was found on both bilayer and laser structured bilayer. We show that it is possible to write ferroelectric information at the nanoscale and in the case of the laser structured ferroelectric bilayer an increase in the information storage density of an order of magnitude in comparison to the original bilayer is observed. Since the performance of the bilayer, as defined by its capacity to storage information, can be strongly dependent on both the level of crystallinity and the orientation of the ferroelectric crystals along the thickness of the LIPSS bilayer the microstructure of the patterned bilayer was investigated by Grazing Incidence Wide and Small Angle X-ray Scattering (GIWAXS and GISAXS respectively) in order to elucidate the fine structures across the direction perpendicular to the free surface.

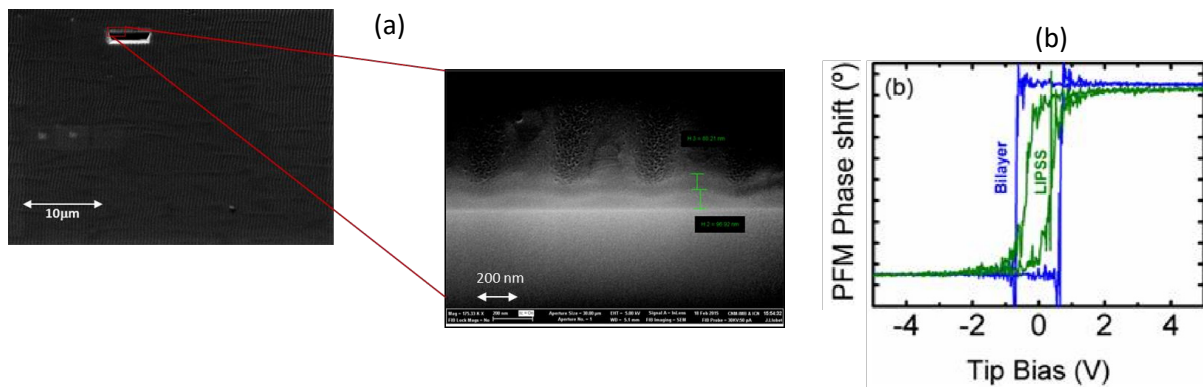


Figure 1: (a) Cross-section SEM images of a P(VDF-TrFE)/P3HT thin bilayer film after irradiation. (b) PFM phase shift as a function of applied bias for the LIPSS on the bilayer film (green) and continuous bilayer (blue) for comparison.

1. D.E. Martínez-Tong, M. Soccio, M.C. García-Gutiérrez, A. Nogales, A. D.R. Rueda, N. Alayo, F. Pérez-Murano, T.A. Ezquerra, Improving information density in ferroelectric polymer films by using nanoimprinted gratings, *Applied Physics Letters*, **102**,191601 (2013);
2. D.E. Martínez-Tong, A. Rodríguez-Rodríguez, A. Nogales, M.C. García-Gutiérrez, F. Pérez-Murano, J. Llobet, T.A. Ezquerra, E. Rebollar, Laser Fabrication of Polymer Ferroelectric Nanostructures for Non-volatile Organic Memory Devices., *ACS Applied Materials – Interfaces*, **7**, 19611 (2015).

# Pulsed Laser Ablation in Liquid for Nanoparticles production: fundamental aspects and perspectives

M. Dell'Aglio<sup>2</sup>, A. Santagata<sup>3</sup>, G. Valenza<sup>1</sup>, A. De Giacomo<sup>1,2</sup>

<sup>1</sup> Department of Chemistry, University of Bari, Italy

<sup>2</sup>National Council of Research-Institute of Nanotechnology, CNR-NANOTEC, Italy

<sup>3</sup>National Council of Research-Institute of Matter Structure, CNR-ISM, Italy  
alessandro.degiacomo@uniba.it, alessandro.degiacomo@nanotec.cnr.it

Laser induced plasma in liquid medium is getting a growing interest in technological fields spanning from medical applications to material production and chemical analysis. In particular laser ablation for the production of nanostructures is developing rapidly as a consequence of the numerous advantages it can provide, such as: clean methodology, easy set-up and long stability of the produced Nano-Particles (NPs). This technique, namely Pulsed Laser Ablation in Liquid (PLAL) is based on the ablation of a target submerged in a bulk liquid. The process consists in four different stages: laser matter interaction, plasma induction and evolution, cavitation bubble dynamics and material release in the liquid environment.

In this work plasma evolution, bubble cavitation and particles delivering are investigated both by an experimental and theoretical point of view in order to give a complete sketch of the processes occurring during laser ablation in bulk liquids. The basic mechanisms of PLAL, are discussed as well as the effect of different experimental configurations such as multipulse ablation, effect of external liquid pressure, target geometry and liquid thickness. In this frame a same example of practical applications in biochemistry and analytical chemistry will be discussed in order to show the potentiality of this methodology for the synthesis of nanostructures.

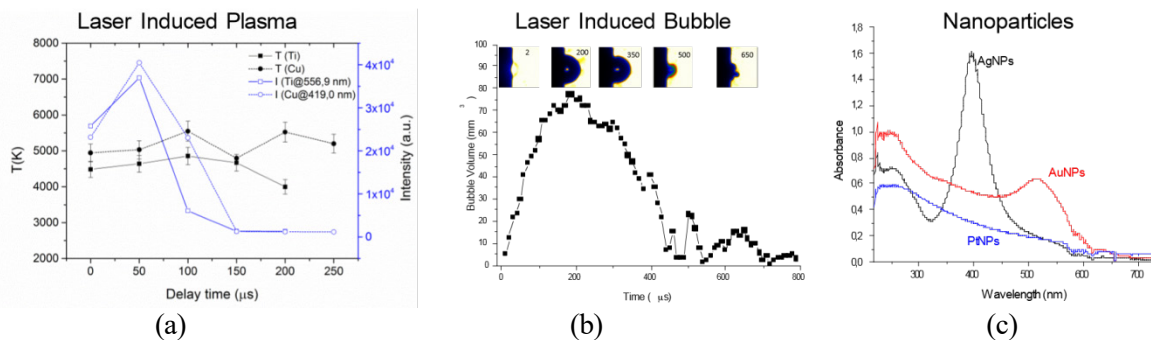


Figure 1: (a) Plasma temperature and intensity evolution, (b) bubble volume dynamic and (c) absorbance spectra of produced NPs during PLAL.

1. A. De Giacomo, M. Dell'Aglio, A. Santagata, R. Gaudiuso, O. De Pascale, P. Wagener, G. C. Messina, G. Compagnini and S. Barcikowski "Cavitation dynamics of laser ablation of bulk and wire-shaped metals in water during nanoparticles production" *Phys. Chem.* **15**, 3083 (2013);
2. A. De Giacomo, A. De Bonis, M. Dell'Aglio, O. De Pascale, R. Gaudiuso, S. Orlando, A. Santagata, G.S. Senesi, F. Taccogna, R. Teghil "Laser ablation of graphite in water in a range of pressure from 1 to 146 atm using single and double pulse techniques for the production of carbon nanostructures" *J. of Phys. Chem. C* **12**, 115 (2012);
3. M. Dell'Aglio, R. Gaudiuso, R. ElRashedy, O. De Pascale, G. Palazzo, A. De Giacomo, Collinear double pulse laser ablation in water for the production of silver nanoparticles, *Phys.Chem. Chem. Phys.*, **15**, 20868, (2013);
4. M. Dell'Aglio, R. Gaudiuso, O. De Pascale, A. De Giacomo "Mechanisms and processes of pulsed laser ablation in liquids during nanoparticle production" *Appl. Sur. Sci.* **348**, 4-9 (2015).

# Lasing out of thin air: Remote sensing using nonlinear optics

A. Dogariu

Mechanical and Aerospace Engineering Department, Princeton University, Princeton, NJ 08544, USA  
adogariu@princeton.edu

Remote detection and identification is of great interest for many applications including environmental, medical, and national security. Optical techniques can achieve standoff trace detection by identifying the atomic or molecular spectroscopic fingerprints. While linear optical methods such as LIDAR, Raman spectroscopy, absorption spectroscopy are considered for such tasks, they are less suitable for single-sided standoff detection in real-time, with both high specificity and sensitivity. Optical remote sensing methods, in particular standoff trace gas detection, can be greatly improved provided that a remote coherent source at the target emits backwards, towards the detection system. To achieve this goal, we have recently demonstrated remote air lasing in the backwards direction by dissociating the major species in air (molecular oxygen and nitrogen) and obtaining stimulated emission via two-photon excitation of the resulting atomic oxygen<sup>1</sup> and atomic nitrogen.<sup>2,3</sup> A highly elongated high gain region created by the focused UV pump can lead to coherent emission in both the forward and backward direction, where the stimulated emission gain is the strongest.

After reviewing the backwards air lasing from major species (oxygen and nitrogen), we are presenting lasing from atomic species in air, which has the benefit of not requiring molecular dissociation. We demonstrate backwards lasing in atomic argon directly excited via a three-photon pumping in air mixtures with argon mole fractions down to 10%. We achieve well collimated, narrowband coherent emission at 1327nm by using both broadband femtosecond excitation and narrow line-width picosecond excitation in the vicinity of 261nm.<sup>4</sup>

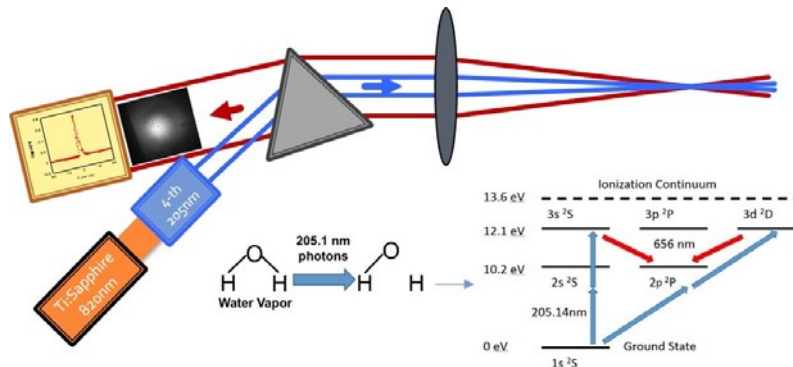


Fig. 1. Experimental setup and energy levels for hydrogen atomic lasing in atmospheric air with dissociation of water molecules.

We will then present a new type of air laser which makes use of the same air lasing recipe described for the major species (schematically presented in Fig. 1), but in this case, the gain medium is a minor species in atmospheric air, namely water vapor. By dissociating the water molecule we obtain atomic hydrogen, which is subsequently excited via a two-photon transition using 205nm photons. As shown in the inset of Fig. 1, this excitation leads to emission at 656nm, the well-known hydrogen alpha line.

In all cases of air lasing, we demonstrate that multi-photon dissociation and excitation can lead to strong stimulated emission from the atomic components in air (O, N, H, and Ar). The backwards emission is coherent, the pulses are bandwidth limited, and the pulses are on the order of tens of picoseconds, three orders of magnitude shorter than the spontaneous emission lifetime. The strong coherent emission is an example of a mirror-less atomic laser which can aid remote atmospheric trace species detection.

1. A. Dogariu, J. B. Michael, M. O. Scully, and R. B. Miles, "High Gain Backward Lasing in Air," *Science* **331**, 442 (2011);
2. A. Dogariu and R. B. Miles, "Nitrogen lasing in air," in *CLEO: 2013*, OSA Technical Digest (online) QW1E.1 (Optical Society of America, 2013);
3. A. Dogariu and R. Miles, "Lasing in Atmospheric Air: Similarities and Differences of Oxygen and Nitrogen," in *Frontiers in Optics 2013*, P. Delfyett, Jr. and D. Gauthier, eds., OSA Technical Digest (online) LTh2H.2 (Optical Society of America, 2013);
4. A. Dogariu and R. B. Miles, "Three-photon femtosecond pumped backwards lasing in argon", *Opt. Express* **24**, A544-A552 (2016).

# Laser Synthesis and Characterization of Photoresponsive Low-Dimensional Nanomaterials

D. B. Geohegan<sup>1</sup>, A. A. Puretzky<sup>1</sup>, K. Xiao<sup>1</sup>, X. Li<sup>1</sup>, K. Wang<sup>1</sup>, M. Mahjouri-Samani<sup>1</sup>, L. Liang<sup>1</sup>, B.C. Sumpter<sup>1</sup>, M. Tian<sup>3</sup>, G. Duscher<sup>3</sup>, M. Yoon<sup>1</sup>, G. Eres<sup>2</sup>, C. M. Rouleau<sup>1</sup>, R. Unocic<sup>1</sup>, M. Chi<sup>1</sup>, J. C. Idrobo<sup>1</sup>

<sup>1</sup>Center for Nanophase Materials Sciences, Oak Ridge National Laboratory, Oak Ridge, TN, USA

<sup>2</sup>Materials Science and Technology Division, Oak Ridge National Laboratory, Oak Ridge, TN, USA

<sup>3</sup>Dept. of Materials Science and Engineering, University of Tennessee, Knoxville, TN, USA

geohegandb@ornl.gov

Low-dimensional nanomaterials – from ultrasmall 0D nanoparticles such as TiO<sub>2</sub>, to atomically-thin 2D layered materials (e.g., GaSe and MoSe<sub>2</sub>) – can be especially photoresponsive and have unusual optical properties due to the pronounced influence of surface states and interactions, quantum confinement, and heterogeneity in the form of vacancies, structural disorder, and substitutional defects (dopants). Here we will report recent progress in the laserbased synthesis and diagnostics of low-dimensional nanomaterials, as well as the spectroscopic characterization of their structure, and optical interactions. First, we will describe strategies involving tuning the “building blocks” and growth kinetics in CVD and PLD from atoms/molecules to ultrasmall nanoparticles for the synthesis, deposition, and modification of photoresponsive metal oxide nanoparticle architectures and atomically-thin 2D metal chalcogenide crystals. Second, we will examine how heterogeneity in monolayer 2D crystals, and interlayer interactions in 2D bilayer homojunctions and heterojunctions, influence the electronic and vibrational properties of the heterostructures, as revealed by second harmonic generation, photoluminescence lifetime spectroscopy, white-light ultrafast pump-probe spectroscopy, and low-frequency Raman spectroscopy. These spectroscopy measurements are coupled with atomic-resolution, Z-contrast scanning TEM characterization and associated theory and modeling, to provide a comprehensive picture enabling laser spectroscopy to remotely identify atomistic characterization of structure and stacking in low-dimensional materials.

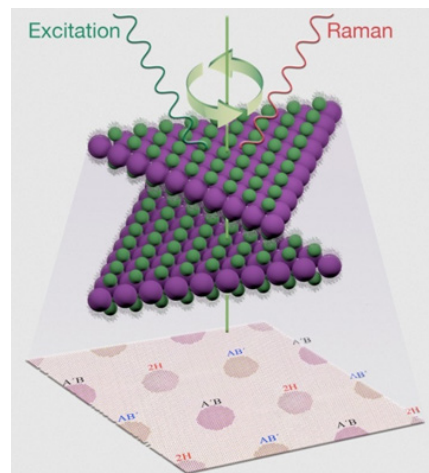


Figure 1: Schematic representation of two MoSe<sub>2</sub> monolayer crystals stacked at an arbitrary relative twist angle, forming a new bilayer material with periodic Moiré patterns that correspond to bulk stacking patterns. Low-frequency Raman spectroscopy of the breathing and shear modes between the layers can be used as “fingerprints” of such materials<sup>1,2</sup>.

**Acknowledgements:** Research sponsored by the U.S. Dept. of Energy, Office of Science, Basic Energy Sciences, Materials Science and Engineering Div. (synthesis science) and Scientific User Facilities Div. (characterization science).

1. A. A. Puretzky, L. Liang, X. Li, K. Xiao, K. Wang, M. Mahjouri-Samani, L. Basile, J. C. Idrobo, B. G. Sumpter, V. Meunier, and D. B. Geohegan, Low-Frequency Raman Fingerprints of Two-Dimensional Metal Dichalcogenide Layer Stacking Configurations *ACS Nano* 9(6) 6333 (2015);

2. A. A. Puretzky, L. Liang, X. Li, K. Xiao, B. G. Sumpter, V. Meunier, and D. B. Geohegan, Twisted MoSe<sub>2</sub> Bilayers with Variable Local Stacking and Interlayer Coupling Revealed by Low-Frequency Raman Spectroscopy, *ACS Nano* 10(2) 2736 (2016).

## Period of Laser-Induced Periodic Surface Structures (LIPSS) Described in the Frames of Hydrodynamic Models

E. Gurevich

Ruhr-University of Bochum

Laser-induced periodic surface structures (LIPSS or ripples) can be found on the surface of metals, dielectrics and semiconductor materials processed with single and multiple femtosecond laser pulses. Although the physical background of this phenomenon is studied for more than 50 years, the underlying physical mechanisms are still a topic of discussion. There are two main approaches to the problem of LIPSS formation based on: (1) interference of the incident laser light and the surface plasmons, which manifests itself in a periodically-modulated surface temperature of electrons and ions and (2) development of hydrodynamic instabilities on the surface. Here we compare the hydrodynamic and the plasmonic theories and look for possible mechanisms of the ripple formation. The question how the temperature profile can result in a periodically-modulated surface morphology in such a short time (less than 1 nanosecond) is addressed. Estimations made on the basis of different hydrodynamic instabilities allow us to sort out several mechanisms, which can bridge the gap between the temperature and the surface profile formation.



# Understanding the optical properties of ultrashort-pulselaser excited dielectric materials

L. Haahr-Lillevang<sup>1</sup>, Søren H. Møller<sup>1</sup>, and P. Balling<sup>1</sup>

<sup>1</sup>Department of Physics and Astronomy, Aarhus University, Ny Munkegade 120, DK-8000 Aarhus C, Denmark  
balling@phys.au.dk

Ultrashort-pulse laser excitation of dielectric materials is a topic of ongoing investigations<sup>1</sup>. An inherent property of such excitations is the rapid change in the optical properties of the material, a change which can be viewed as both an advantage and a complication for the understanding the excitation mechanisms. Clearly, the changes in the optical properties are useful for experimentally characterizing the dynamics of the excitation process through different time-resolved optical techniques such as time-resolved shadowgraphs, reflectance and spectral interference measurements. On the other hand, the rapid changes in the optical attributes complicate the theoretical description of the excitation process since the changes occur on time scales shorter than typical pulse durations of the exciting laser. This means that a good description of the time-dependent optical material parameters is necessary for a proper description of the material-excitation dynamics.

In this presentation, we will review the current understanding of the transient optical properties of dielectric materials. Experimentally, much information is provided by combining time-resolved reflectivity with time-resolved spectral interferometry experiments in either a crossed-beam geometry<sup>2-4</sup> or in a collinear setup<sup>5,6</sup>. Spectral interferometry measures the phase shift and the absorption of a probe pulse through an excited volume, thus permitting measurements of the changes in the real and imaginary parts of the refractive index. Generally, experiments demonstrate a fast negative phase shift, which is attributed to the promotion of electrons from the valence band to the conduction band. Such electrons are considered “free”, which means that they have Drude-like characteristics giving a negative real part and a finite imaginary part of the refractive index. At the same time – at sufficiently high laser fluences – a rapid increase in the reflectivity is also observed, again consistent with the rapid creation of a material with more “metal-like” properties.

In order to obtain a more quantitative understanding of the transient optical properties, detailed modeling of the material-excitation mechanisms in combination with the optical properties must be undertaken. In this talk, we will discuss the understanding, which can be obtained by comparison with a theoretical model based on the so-called multiple-rate equation approach originally proposed by Rethfeld<sup>7</sup> and later modified by us<sup>8,9</sup>.

In the current presentation, we will review the most recent time-resolved experimental results from short-pulse excitation and discuss the newest elaborations on the theoretical model towards a better understanding of the optical properties<sup>4,6</sup>.

1. P. Balling and J. Schou, *Femtosecond laser ablation dynamics of dielectrics: Basics and applications for thin films*, Reports on Progress in Physics, **76**, 036502 (2013);
2. K. Wædegaard, D. B. Sandkamm, A. Mouskeftaras, S. Guizard, and P. Balling, *Probing ultrashort-pulse laser excitation of sapphire: From the initial carrier creation to material ablation*, Europhysics Letters **105**, 47001 (2014);
3. L. Haahr-Lillevang, K. Wædegaard, D. B. Sandkamm, A. Mouskeftaras, S. Guizard, and P. Balling, *Short-pulse laser excitation of quartz: experiments and modelling of transient optical properties and ablation*, Appl. Phys. A **120**, 1221 (2015);
4. M. Garcia-Lechuga, L. Haahr-Lillevang, J. Siegel, P. Balling, S. Guizard, and J. Solis, *Simultaneous time-and-space resolved reflectivity and interferometric measurements of dielectrics excited with femtosecond laser pulses*, in preparation (2016);
5. T. Winkler, C. Sarpe, N. Jelzow, L. Haahr-Lillevang, N. Götte, B. Zielinski, P. Balling, A. Senfleben, and T. Baumert, *Probing spatial properties of electronic excitation in water after interaction with temporally shaped femtosecond laser pulses: Experiments and simulations*, Appl. Surf. Sci. in press (2016), doi:10.1016/j.apsusc.2015.11.182;
6. T. Winkler, L. Haahr-Lillevang, C. Sarpe, B. Zielinski, N. Götte, N. Jelzow, A. Senfleben, P. Balling, and T. Baumert, in preparation (2016);
7. B. Rethfeld, Phys. Rev. Lett., **92**, 187401 (2004); B. Rethfeld, Phys. Rev. B, **73**, 035101 (2006);
8. B. H. Christensen and P. Balling, *Modeling short-pulse laser ablation of dielectric materials*, Phys. Rev. B **79**, 155424 (2009);
9. K. Wædegaard, D. B. Sandkamm, L. Haahr-Lillevang, K. G. Bay, and P. Balling, *Modeling short-pulse laser excitation of dielectric materials*, Appl. Phys. A **117**, 7 (2014).

# Ultrafast Optical Switching in Hybrid Silicon-Vanadium Dioxide Nanophotonic Modulators

Richard F. Haglund, Jr.<sup>1</sup>, Sharon M. Weiss<sup>2</sup>

<sup>1</sup>Department of Physics and Astronomy, Vanderbilt University, Nashville, TN 37235-1807 USA

<sup>2</sup>Department of Electrical Engineering and Computer Science, Vanderbilt University, Nashville, TN 37235 USA  
richard.haglund@vanderbilt.edu

High-speed, low-power optical modulators are critical to the future of silicon photonics. We have recently demonstrated near-GHz modulation of a prototypical modulator — a hybrid silicon ring resonator incorporating vanadium dioxide (VO<sub>2</sub>) as the switching component<sup>1</sup>. Vanadium dioxide undergoes a semiconductor-to-metal transition near room temperature that can be triggered by ultrafast laser pulses<sup>2</sup> or electrically<sup>3</sup>. By free-space optically pumping a sub-micrometer-dimension patch of VO<sub>2</sub>, we have already achieved 10 dB switching of the hybrid ring resonators at an energy cost of less than 300 fJ/switch<sup>4</sup>.

The fabrication of these devices (Figure 1) requires double-layer electron-beam lithography and pulsed laser deposition (PLD), while optimal switching demands the smallest and thinnest patch of VO<sub>2</sub> consistent with the required mode structure in the resonator and the change in refractive index  $\Delta n$  needed to achieve the desired switching contrast. Laser-deposited thin films have higher switching contrast and larger defect-free grains compared to sputter-deposited films<sup>5</sup>; the present fabrication procedure is based on conventional nanosecond pulsed laser deposition at a wavelength of 248 nm and typical fluences of order 1-2 J/cm<sup>2</sup>.

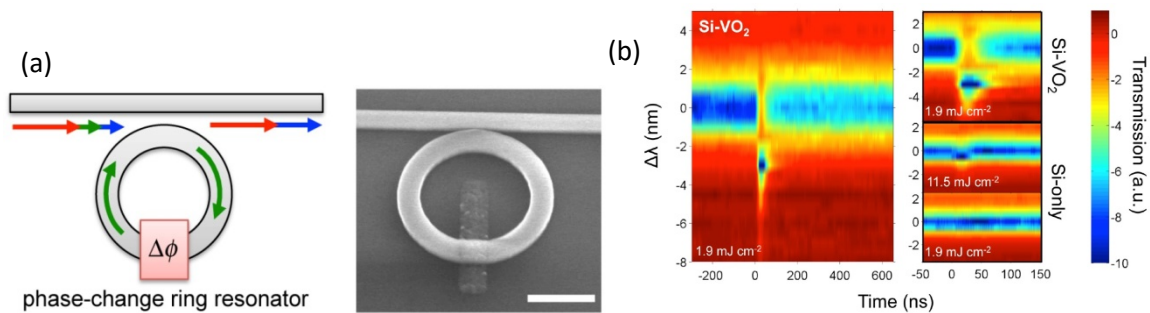


Figure 1: (a) Schematic showing wavelength-selective functionality and scanning-electron micrograph of e-beam fabricated silicon ring resonator with a sub-micron-dimension patch of excimer-laser-deposited VO<sub>2</sub> partially covering the resonator. The scale bar is 1  $\mu\text{m}$ . (b) False-color plots of wavelength shift vs time following nanosecond pulsed-laser excitation for hybrid Si-VO<sub>2</sub> and Si-only ring resonators. The Si-VO<sub>2</sub> resonator experiences a wavelength shift of 3 nm at 2 mJ/cm<sup>2</sup>, whereas the silicon-only ring resonator experiences a miniscule shift at six times that fluence.

We are currently aiming to achieve switching speeds exceeding 500 GHz at an energy cost of 100 fJ/switch in these hybrid Si photonics devices, with ring dimensions of 1-2  $\mu\text{m}$  diameter. This will require a number of changes in the present experimental geometry, primarily associated with on-chip, rather than free-space, optical pumping of the vanadium dioxide patch. We are also exploring the changes in the characteristics of the VO<sub>2</sub> phase transition when pumping the phase transition near the band edge (1500 nm) rather than at the 800 nm wavelength at which nearly all studies of the ultrafast photo-induced phase transition have been carried out. These studies already show significant differences in coherent phonon generation with near band-edge pumping.

**Acknowledgements:** Supported in part by the National Science Foundation (EECS-1509740, DMR-1207507) and the Air Force Office of Scientific Research

1. D. Wegkamp, M. Herzog, L. Xian, M. Gatti, P. Cudazzo, C. L. McGahan, R. E. Marvel, R. F. Haglund, Jr., A. Rubio, M. Wolf and J. Stähler, “Instantaneous band-gap collapse in photoexcited monoclinic VO<sub>2</sub> due to photocarrier doping,” *Physical Review Letters* **113**, 216401 (2014);
2. “Optically Monitored Electrical Switching in VO<sub>2</sub>”, Petr Markov, Robert E. Marvel, Hiram J. Conley, Kevin J. Miller, Kirill Bolotin, Richard F. Haglund, Jr. and Sharon M. Weiss, *ACS Photonics* **2**, 1175-1182 (2015);
3. J. D. Ryckman, K. A. Hallman, R. E. Marvel, R. F. Haglund, Jr. and S. M. Weiss, “An all-optical, reconfigurable, ultra-compact silicon ring resonator controlled by a semiconductor-to-metal transition,” J. D. Ryckman, K. A. Hallman, R. E. Marvel, R. F. Haglund, Jr. and S. M. Weiss. *Optics Express* **21** (9), 10753-10763 (2013);
4. “Influence of deposition process and substrate on the phase transition of vanadium dioxide thin films,” R. E. Marvel, R. Harl, V. Craciun, B. Rogers and R. F. Haglund, Jr., *Acta Materialia* **91**, 217-226 (2015).

# Laser induced nanoablation of diamond

V.I. Konov, V.V. Kononenko

*A.M. Prokhorov General Physics Institute of RAS, Vavilov str. 38, 119991 Moscow, Russia  
National Research Nuclear University MEPhI, Kashirskoye sh. 31, Moscow 115409, Russia*

It is found that at femtosecond pulsed laser fluence well below diamond surface graphitization threshold (requires surface temperature about 800°C) in the case of multiple-pulsed irradiation in oxidation atmosphere (air) the regime of the so called “nanoablation” can be realized. Diamond nanoablation rates as low as  $10^{-2}$ - $10^{-7}$  nm/pulse for pulse number up to  $10^8$  were measured. It allows to fabricate ultra fine diamond structures.

The mechanism of diamond nanoablation was proposed. It includes two steps. Initially electron-hole pairs (concentration up to  $10^{22}$  cm<sup>-3</sup>) are produced by multi-photon ionization. Part of the charge carriers energy can induce defect formation. Their life-time can be sufficient for carbon bonds transformation in the crystal. As a result at the irradiated surface sp<sub>2</sub> bonded carbon atoms appear. In the cause of the second step, namely photo-induced oxidation process, such atoms form volatile products (CO or CO<sub>2</sub>) and leave the sample.

The observed ultra-low ablation rates are determined by the two major factors. On one hand, concentration of the weekly bonded surface carbon atoms (clusters) is small. On the other, chemical ablation rate during the short-pulsed laser photo-thermal action is limited by the number of oxygen atoms adsorbed in air onto the diamond surface between laser pulses. It should be noted that diamond nanoablation technique can be not only ultra-precise but fast as well if laser pulse repetition frequency and mean power are high enough ( $\geq 1$  MHz and 1-10 W, correspondingly). The considered nanoablation model is supported by the experiments, establishing correlation between the material removal rates and laser pulse fluence, duration, wavelength, repetition frequency, number and charge carrier concentration in diamond crystal.

## Laser processing of low power integrated gas sensors with carbon materials sensing layers

T. Lippert

*Energy and Environment Division, Paul Scherrer Institut, 5232 PSI Villigen, Switzerland  
Thomas.lippert@psi.ch*

Sensors are widely used in many different fields, from safety related applications, to healthcare and biomedical related applications. Therefore, new and improved sensor systems are made possible both with new materials and processing technologies.

This talk summarizes the developments in laser based direct writing techniques of carbon based materials for applications as recognizing elements in miniaturized chemiresistor sensors.

Carbon materials such as carbon nanotubes (CNT) and hybrid CNT i.e. decorated with nanoparticles, are very promising sensor materials, with high sensitivity and fast response time. In this talk, laser direct writing of CNT and hybrid CNT onto nonconventional substrates, i.e. paper, plastics, tapes, etc. for the fabrication of sensors is presented. The direct writing technique is based on laser-induced forward transfer (LIFT), a simple process where a laser beam is focused through a transparent substrate onto a material film to be transferred. Every single pulse promotes the transfer of the thin film material onto a substrate that is usually placed parallel and facing the thin film at very short distances.

With LIFT, CNT and hybrid CNT materials are transferred, with a transfer yield of nearly 100%, to fabricate chemiresistive devices. The as printed carbon material maintains its original geometry, and the chemical and structural properties with high fidelity.

In addition, the performance of the LIFT-ed sensors, i.e. the sensitivity, and response time was evaluated at room temperature, by exposure of the sensors to different toxic vapors. Different sensitivities to the selected analytes i.e. acetone, ethanol, ammonia, etc. have been measured thus proving the feasibility of LIFT for applications in new and improved sensing devices.

*Acknowledgements: This work was supported by a grant from the Commission for Technology and Innovation CTI (project no. 16713.1 PFNM-NM).*

# Nano-fabrication by interference pattern of coherent beam

Y. Nakata<sup>1</sup>, M. Yoshida<sup>1</sup>, K. Osawa<sup>1</sup>, N. Miyanaga<sup>1</sup>

<sup>1</sup> Institute of Laser Engineering, Osaka University, Japan  
nakata-y@ile.osaka-u.ac.jp

Plasmonic devices consist of nano- or micron-sized unit structures in lattice have been fabricated by lithography, ion or electron beam figuring technique. On the other hand, our group has been investigating interference laser processing using ultrashort pulse laser. By processing metallic thin film, interference pattern can be transferred to the resultant structure in a single process. In the past experiment, a variety of unit structures such as nanowhisker, 1,2 nanobump, 3 MHA (Metallic-Hole Array), 3,4 nanodrop, 1,2,5 and designed pattern 5–7 have been fabricated. In this presentation, recent results of the fabrication of them and applications to plasmonic devices will be shown. In addition, interference pattern of 6 beams was applied to this technique, as shown in Figure 1. Figure 1 (a) shows the scheme of six beam correlation. The center wavelength was 785 nm, and the pulse width was 190 fs. The incidence angle  $\theta_n = 18^\circ$ , and  $\Delta\Phi_n = \pi/3$ . The target was 20 nm thick gold thin film on silica glass. It seems that nanostructures are in hexagonal lattice could be fabricated, as shown in Figure 1 (b). The averaged fluence was  $13.3 \text{ mJ/cm}^2$ , and the lattice constant was  $a_0 = 2.25 \mu\text{m}$ . In the presentation, a variety of nanostructures such as nanodrop, MHA fabricated by this technique will be shown.

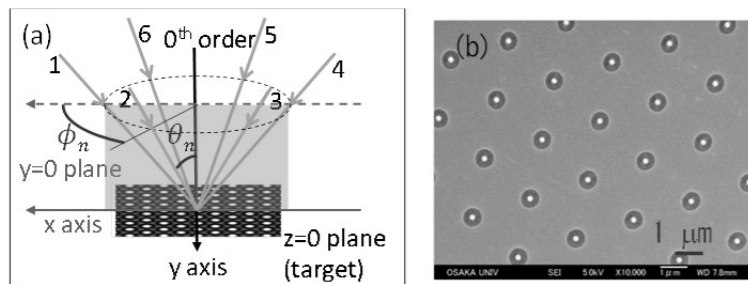


Figure 1: (a) scheme of six-beams interference processing. (b) top-view of the nanostructure in hexagonal lattice fabricated on 20 nm thick gold film.

1. Y. Nakata, N. Miyanaga, K. Momoo, and T. Hiromoto, *Appl. Surf. Sci.* **274**, 27 (2013);
2. Y. Nakata, N. Miyanaga, K. Momoo, and T. Hiromoto, *Jpn. J. Appl. Phys.* **53**, 096701 (2014);
3. Y. Nakata, T. Okada, and M. Maeda, *Japanese J. Appl. Physics, Part 2 Lett.* **42**, L1452 (2003);
4. Y. Nakata, Y. Matsuba, N. Miyanaga, and K. Murakawa, *Photonics Nanostructures - Fundam. Appl.* **17**, 10 (2015);
5. Y. Nakata, T. Hiromoto, and N. Miyanaga, *Appl. Phys. A Mater. Sci. Process.* **101**, 471 (2010);
6. Y. Nakata, K. Murakawa, K. Sonoda, K. Momoo, N. Miyanaga, and T. Hiromoto, *Appl. Phys. A* **112**, 191 (2012);
7. Y. Nakata, K. Murakawa, K. Sonoda, K. Momoo, and N. Miyanaga, *Appl. Opt.* **51**, 5004 (2012);

## Multi-scale architected materials: from vortex-induced to dual-color direct laser writing in silver-containing glasses

Y. Petit<sup>1,2</sup>, E. Lee<sup>1</sup>, K. Mishick<sup>1</sup>, E. Brasselet<sup>3</sup>, S. Danto<sup>2</sup>, I. M. Hö nninger<sup>1</sup>, T. Cardinal<sup>2</sup>, L. Canioni<sup>1</sup>

<sup>1</sup>University of Bordeaux, CNRS, CEA, CELIA, UMR 5107, 351 Cours de la Liberation, 33405 Talence Cedex, France

<sup>2</sup>University of Bordeaux, CNRS, ICMCB, UPR 9048, 87 avenue du Dr. A. Schweitzer, 33608 Pessac cedex, France

<sup>3</sup>University of Bordeaux, CNRS, LOMA, UMR 5798, 351 Cours de la Liberation, 33405 Talence Cedex, France

Lionel.Canioni@u-bordeaux.fr

Ultrashort laser pulses have shown a tremendous potential for precise microstructuring. Especially, the possibility to realize three-dimensionally localized modifications within the bulk of transparent materials has recently attracted increasing interest. When intense ultrashort pulses are tightly focused into the transparent material, the intensity in the focal volume can become high enough to initiate nonlinear absorption processes. This localized energy deposition results in permanent structural changes inside the sample without affecting the surface. Depending on the processing parameters, either isotropic refractive index changes, self-organized sub-wavelength structures leading to form birefringence or microvoids can be generated in the focus. Among several lithographic techniques, Direct Laser Writing (DLW) considered as a maskless patterning process, presents numerous advantages over usual techniques. DLW offers rapid patterning at sub-micrometer resolutions, with flexibility and scalability. At last, true three-dimensional structuration is allowed thanks to non-linear interaction in optical transparent materials. In this context, DLW of materials containing photosensitive agents can initiate photochemical processes, opening routes toward the design of nanocomposites. DLW techniques can modify the

size, the shape, and the arrangement of the metal clusters. It is a powerful and flexible tool to control and optimize the linear and nonlinear properties of metallo- dielectric composites. Many groups have shown interest in patterning metals in three dimensions in transparent media such as glasses or polymers. This becomes particularly challenging when structures much smaller than the diffraction limit need to be patterned for infrared or optical applications.

## 3D additive manufacturing of highly bioactive alkali-free glass scaffolds for healthcare applications

B.C.G. Silva<sup>1</sup>, A.C. Marques<sup>1</sup>, S.H. Olhero<sup>1</sup>, H.R. Fernandes<sup>1</sup>, A. Brito<sup>2</sup>, J.M.F. Ferreira<sup>1</sup>

<sup>1</sup>Department of Ceramics and Glass Engineering, University of Aveiro, CICECO, 3810-193 Aveiro, Portugal

<sup>2</sup>Reg4life-Regeneration Technology, S.A., Biocant, Parque Tecnológico de Cantanhede, 3060-197 Cantanhede, Portugal

jmf@ua.pt

An alkali-free bioactive glass composition, FastOs<sup>®</sup>BG (38.49% SiO<sub>2</sub> – 36.07% CaO – 19.24% MgO – 5.61% P<sub>2</sub>O<sub>5</sub> – 0.59% CaF<sub>2</sub>)<sup>1</sup> belonging to the diopside (CaMgSi<sub>2</sub>O<sub>6</sub>)–fluorapatite (Ca<sub>5</sub>(PO<sub>4</sub>)<sub>3</sub>F)–tricalcium phosphate (Ca<sub>3</sub>(PO<sub>4</sub>)<sub>2</sub>) system possesses a number of distinctive features, being promising for demanding applications in healthcare and tissue engineering. It exhibits fast *in vitro* biomineralization and bonding ability to living tissues *in vivo*, and osteogenic properties that foster early cellular differentiation and proliferation. The purpose of the present study is to investigate the processing ability of this bioactive glass in aqueous media and obtaining high concentrated (up to 50 vol.% solids loading) inks for additive manufacturing. The effects of the type and amounts of the processing additives on the rheological properties of the fluid suspensions and on their transformation into extrudable pastes with enough stiffness for the cylindrical filaments to maintain the shape after extrusion, green and sintered properties were investigated. The excellent processing and sintering ability of FastOs<sup>®</sup>BG resulted in amorphous well densified and structures as shown in Figure 1, which exhibited strong mechanical properties after sintering. This bioactive glass compositions revealed a fast biomineralization activity *in vitro*, resulting in the formation of a hydroxycarbonate apatite (HCA) layer on their surface after immersion for 1 h in simulated body fluid (SBF)<sup>1</sup>.

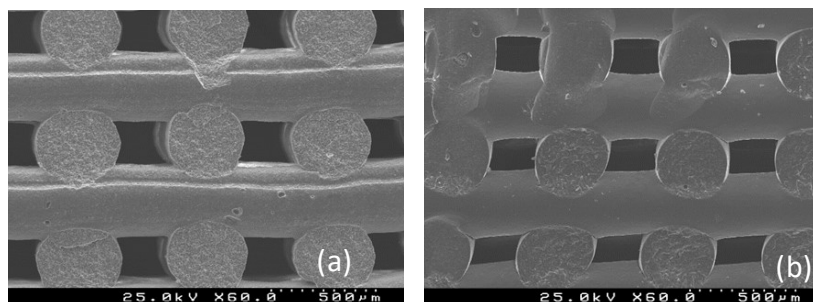


Figure 1: Scaffolds of the FastOs<sup>®</sup>BG bioactive glass sintered at 800°C derived from suspensions containing different solids loading: (a) 47 vol.%; (b) 48 vol.%.

These features, essential for 3D porous scaffolds intended for bone regeneration and tissue engineering applications<sup>2</sup>, contrasting with those obtained for 45S5 Bioglass<sup>®</sup> 3-4. This last material is difficult to process in aqueous media, exhibits poor sintering ability and is highly prone to crystallisation, leading to scaffolds with poor mechanical properties.

1. A. Goel, S. Kapoor, R.R. Rajagopal, M.J. Pascual, H.-W. Kim, J.M.F. Ferreira, Alkali-free bioactive glasses for bone tissue engineering: a preliminary investigation, *Acta Biomater.* 8, 361–372 (2012);
2. P.P. Cortez, A.F. Brito, S. Kapoor, A.F. Correia, L.M. Atayde, P.D. Pereira, A. Afonso, A. Goel, J.M.F. Ferreira, The *in vivo* performance of an alkali-free bioactive glass for bone grafting, FastOs<sup>®</sup>BG, assessed with an ovine model, *J. Biomed. Mater. Res. Part B Appl. Biomater.* n/a–n/a, (2015);
3. S. Eqtesadi, A. Motealleh, P. Miranda, A. Lemos, A. Rebelo, J.M.F. Ferreira, A simple recipe for direct writing complex 45S5 Bioglass<sup>®</sup> 3D scaffolds, *Mater. Lett.*, 93 68-71 (2013);
4. S. Eqtesadi, A. Motealleh, P. Miranda, A. Pajares, A. Lemos, A. Rebelo, J.M.F. Ferreira, Robocasting of 45S5 bioactive glass scaffolds for bone tissue engineering, *J. Eur. Ceram. Soc.* 34 (1), (2014) 107-118.

# Laser printing: an alternative approach

P. Sopeña<sup>1</sup>, S. González-Torres<sup>1</sup>, J.M. Fernández-Pradas<sup>1</sup>, X. Arrese<sup>2</sup>, A. Cirera<sup>2</sup>, P. Serra<sup>1</sup>

<sup>1</sup>Universitat de Barcelona, IN2UB, Applied Physics Department

<sup>2</sup>Universitat de Barcelona, MIND-IN2UB, Engineering Department: Electronics  
Martí i Franquès 1, 08028-Barcelona, Spain  
pserra@ub.edu

Laser-induced forward transfer (LIFT) constitutes an interesting alternative to conventional printing techniques in microfabrication applications. Originally developed to print inorganic materials from solid films, it was later proved that LIFT was feasible for printing liquids as well, which substantially broadened the range of printable materials. Any material which can be suspended or dissolved in an ink can be in principle printed through LIFT.

The principle of operation of LIFT relies on the localized absorption of a focused laser pulse in a thin film of the ink containing the material to print (donor film). This results in the generation of a cavitation bubble which expansion displaces a fraction of the liquid around it, leading to the formation of a jet which propagates away the donor film and towards the acceptor substrate, placed at a short distance. The contact of the jet with this acceptor substrate results in the deposition of a sessile droplet. Thus, each droplet results from a single laser pulse, and the generation of micropatterns is achieved through the overlap of successive droplets.

In this work we review our main achievements on the LIFT of inks, and propose a new mode of operation that contrasts with the ones developed so far. This new mode of operation allows reducing dramatically the costs of industrial implementation of the technique.

## Hybrid Subtractive and Additive 3D Microprocessing Using Femtosecond Laser for Functional Biochip Fabrication

K. Sugioka, F. Sima, J. Xu, D. Wu, K. Midorikawa

RIKEN Center for Advanced Photonics, Wako, Saitama 351-0198, Japan  
ksugioka@riken.jp

The rapid development of femtosecond laser has revolutionized materials processing due to its unique characteristics of ultrashort pulse width and extremely high peak intensity<sup>1</sup>. In particular, the high peak intensity allows nonlinear interactions such as multiphoton absorption and tunneling ionization to be induced in transparent materials, which provides versatility in terms of the materials that can be processed. More interestingly, irradiation with tightly focused femtosecond laser pulses inside transparent materials makes three-dimensional (3D) micro- and nanofabrication available due to efficient confinement of the nonlinear interactions within the focal volume.

Using this feature, both types of subtractive and additive 3D manufacturing are available<sup>2</sup>. Specifically, the former process involves femtosecond laser internal modification followed by wet chemical etching (Femtosecond Laser Assisted Wet Etching: FLAE) which directly fabricate 3D microfluidic structures inside glass, while the latter one is two-photon polymerization (TPP) of photocurable resin to create 3D polymer micro and nanostructures even with complicated geometries. Recently, we have proposed to integrate these two processes to further enhance performance of femtosecond laser 3D processing for fabrication of highly functional biochips<sup>3-5</sup>.

The hybrid femtosecond laser microprocessing consists of two main steps as shown in Fig. 1. The first step is to fabricate 3D microfluidic structure by FLAE of photosensitive Foturan glass (a-c). The second step is to integrate functional microcomponents into the resulting glass 3D microfluidic structure for device functionalization by the successive TPP procedure (f-d).

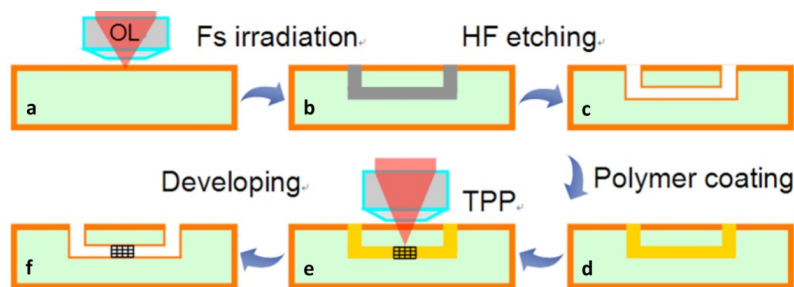


Figure 1: Schematic illustration of the fabrication procedure for ship-in-a-bottle biochips by hybrid femtosecond laser 3D microprocessing. It mainly consists of (a) fs laser 3D direct writing of photosensitive Foturan glass followed by (b) a thermal treatment, (c) HF etching, (d) polymer filling, (e) TPP, and (f) developing.

This technique successfully demonstrated to fabricate true 3D biochips with high functionalities<sup>3-5</sup>. The fabricated device has been termed a “ship-in-a-bottle” biochip, since the polymer 3D micro and nano structures are created in the closed 3D glass microfluidic structure after the microfluidics fabrication. The ship-in-a-bottle biochips were then applied for biological and chemical experiments including efficient mixing of fluids, separation of microparticles, parallel cell counting with a 100% success rate, and investigation of cancer cell metastasis.

1. K. Sugioka and Y. Cheng, “Ultrafast lasers - reliable tools for advanced materials processing”, *Light Sci. Appl.* **3**, e149 (2014);
2. K. Sugioka and Y. Cheng, “Femtosecond laser three-dimensional micro- and nanofabrication”, *Appl. Phys. Rev.* **1**, 041303 (2014);
3. D. Wu, S. Wu, J. Xu, L. Niu, K. Midorikawa, and K. Sugioka, “Hybrid femtosecond laser microfabrication to achieve true 3D glass/polymer composite biochips with multiscale features and high performance: the concept of ship-in-a-bottle biochip”, *Laser Photon. Rev.* **8**, 458-467 (2014);
4. D. Wu, J. Xu, L. Niu, S. Wu, K. Midorikawa, and K. Sugioka, “In-channel integration of designable microoptical devices using flat scaffold-supported femtosecond-laser microfabrication for coupling-free optofluidic cell counting”, *Light Sci. Appl.* **4**, e228 (2015);
5. D. Wu, L. G. Niu, S. Z. Wu, J. Xu, K. Midorikawa, and K. Sugioka, “Ship-in-a-bottle femtosecond laser integration of optofluidic microlens arrays with center-pass units enabling coupling-free parallel cell counting with 100% success rate,” *Lab Chip* **15**, 1515-1523 (2015).

## Photo-excited electrons from plasmonic nanostructures inducing surface photochemistry

G. Toker, L. Zilberberg, H. Shankar and M. Asscher

*Institute of Chemistry, The Hebrew University of Jerusalem Jerusalem 91904, Israel  
micha.asscher@mail.huji.ac.il*

The search for direct evidence of plasmon enhanced photochemistry and catalysis at the vicinity of metal nanostructures is accelerating in recent years due to its potential importance in solar energy related applications<sup>1,2</sup>. Such enhancement has been predicted theoretically more than 3 decades ago, during the early reports on Surface Enhanced Raman Spectroscopy (SERS) but has not yet been demonstrated under well controlled UHV environment. Extreme enhancement of photo-desorption cross section at nanometer size sharp edges and tips of silicon has been earlier demonstrated in our group<sup>3</sup>. In this report<sup>4,5</sup> we present the first attempt to address this issue under well-defined ultra-high vacuum conditions, on top of clean (non-colloidal) silver nanoparticles at the size range of 10-120nm. Ethyl chloride molecules adsorbed at 45K on silver clusters decorated SiO<sub>2</sub>/Si(100) substrate were used as our probe molecule for photo-reactivity and selectivity studies. Photo-excited/photo-emitted electrons are the source for photochemical activity via dissociative electron attachment (DEA) mechanism.

Experimental parameters included gradual increase of the silver particles size and total coverage, excitation laser wavelength and in particular varying the distance of the probe molecule from the silver particle's surface via Xe spacer layers (see figure 1 below). Pump-probe experiments employing two laser wavelengths were used to dissociate the molecule (355nm) and to excite the TiO<sub>2</sub> film modified surface plasmon resonance of the silver particles (532nm). This experiment has revealed that no observable enhancement of photo-reactivity could be detected when the two nsec laser pulses overlap in time. The overall list of observations has led us to conclude that the photo-induced mechanism is governed by hot-electrons excitation. Following the excited electrons energy, affected by work function modifications, with respect to the ethyl chloride affinity level confirm our proposed mechanism.

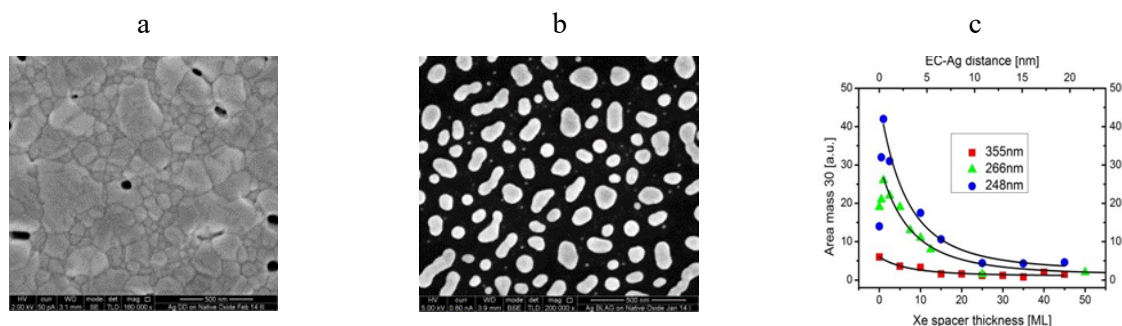


Figure 1: (a) Continuous Ag layer (b) Separated 120nm Ag particles (c) Excitation wavelength effect on EC photochemistry yield as a function of Xe spacer layer thickness.

1. N. J. Halas et. al., *JACS*, 136, 64 (2014) ;
2. P. Christopher et. al., *ACS Catalysis*, 4, 116 (2014) ;
3. G. Toker and M. Asscher, *Phys. Rev. Lett.*, 107, 167402 (2011);
4. Toker, G., et. al., *Nano Letters*, 15(2), 936-42 (2015); 5. L. Zilberberg et. al., 119(52), 28979-28991 (2015).

# Ultrafast laser-induced processes on surfaces at the micro/nano-scale by temporally-shaped fs laser pulses

G. D. Tsibidis, E. Stratakis, P. A. Loukakos

*Institute of Electronic Structure and Laser, Foundation for research and Technology – Hellas, N. Plastira 100, 71110 Heraklion, Greece  
loukakos@iesl.forth.gr*

The application of temporally shaped femtosecond laser pulses in the micro/nano-structuring of semiconductor surfaces is investigated. As an initial step towards full pulse shaping, sequences of equal-intensity double pulses with variable temporal spacing in the ps time domain have been used. Following the laser-surface interaction with appropriate irradiation conditions craters decorated with nm-sized ripples are formed. The area, depth and strikingly the ripple periodicity (Fig. 1a) show a dependence on the temporal delay between the individual components of the double pulses (Fig 1b). Our analysis and explanation for the dependence of the micro and nano-morphological features on the pulse delay is based on our recently developed theoretical model that combines the laser-triggered ultrafast excitation and relaxation mechanisms on a semiconductor surface such as carrier excitation, ultrafast carrier-lattice energy exchanges and energy transport along with the slower phenomena of melting, the corresponding hydrodynamics and re-solidification that follow until the final surface morphology is established. The details of our model and our experimental investigations on laser-irradiated Si and ZnO surfaces will be reviewed and discussed<sup>1-4</sup>. Also, our latest results on the inclusion of the polarization parameter along with the temporal shaping will be also discussed in the nanostructuring processes. Thereby, we find that the nanostructure morphology can be shaped according to the combined effect of temporal delay and polarization relevance between the two components of the double laser pulse sequences.

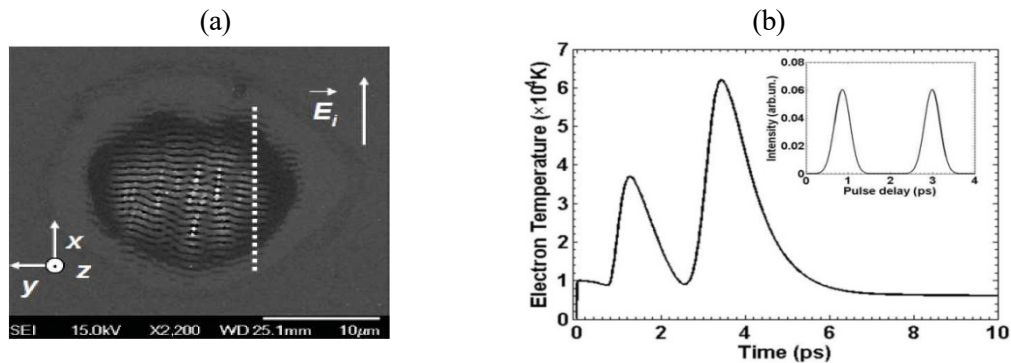


Figure 1: (a) Crater decorated with ripples following irradiation by ultrashort double laser pulses. (b) Main: Electron temperature evolution following double pulse irradiation of a Si surface. Inset: Temporal profile of double ultrashort laser pulses of equal intensity used to irradiate the semiconductor surfaces.

1. G. D. Tsibidis, M. Barberoglou, P. A. Loukakos, E. Stratakis, and C. Fotakis, *Phys. Rev. B* **86**, 115316 (2012);
2. M. Barberoglou, D. Gray, E. Magoulakis, C. Fotakis, P. A. Loukakos, and E. Stratakis, *Opt. Express* **21**, 18501 (2013);
3. M. Barberoglou, G. D. Tsibidis, D. Gray, E. Magoulakis, C. Fotakis, E. Stratakis, and P. A. Loukakos, *Appl. Phys. A* **113**, 273 (2013);
- 4) G. D. Tsibidis, E. Stratakis, P. A. Loukakos, and C. Fotakis, *Appl. Phys. A* **114**, 57 (2014).

## 4D-Printed Hydrogel Based Composite Structures by Additive Processing

A. Vaseashta<sup>1,2</sup> and N. Bolgen<sup>2</sup>

<sup>1</sup>International Clean Water Institute, Herndon, VA, USA

<sup>2</sup>Mersin University, Mersin, TURKEY  
prof.vaseashta@ieee.org

Hydrogels are materials consisting of a permanent, three-dimensional network of hydrophilic polymers and water filling the space between the polymer chains with applications in diverse fields ranging from bio-medical applications and stimuli sensitive systems for agricultural, personal care, environmental, and industrial applications. We have used multidisciplinary approach and advances in programmable materials assembly to create transformable architectures. Using microscale 3D printing technology and fourth time dimensional parameter by environmental response, we have developed 4D printed hydrogel composite structures. Although, the investigation is in its preliminary stages, we anticipate using meta-materials to detect and capture organic materials, volatile organic compounds and an extension of our work on capturing pharmaceuticals. Since, hydrogel composites contain cellulose fibrils derived from wood, response to environment is likely to produce biomimicking to external stimuli.



# Femtosecond laser treatment of biomaterials and biological tissues surfaces

R. Vilar<sup>1</sup>, V. Oliveira<sup>2</sup>, L. Canguero<sup>1</sup>, Tri Le Quang<sup>1</sup>

<sup>1</sup>CeFEMA – Centre of Physics and Engineering of Advanced Materials and Instituto Superior Técnico, University of Lisbon, Av. Rovisco Pais, 1049-001, Lisboa, Portugal

<sup>2</sup>CeFEMA – Center of Physics and Engineering of Advanced Materials, Instituto Superior Técnico Instituto Superior de Engenharia de Lisboa, Instituto Politécnico de Lisboa, Estrada de Benfica, 529, 1549-020, Lisboa, Portugal  
rui.vilar@ist.utl.pt

The presentation will review recent results on the ultrafast laser surface treatment of metallic materials and biological hard tissues for biomedical applications.

Ultrafast lasers were applied to the texturing of titanium alloys aiming at favouring matrix mineralisation and bone formation and reduce bacteria adhesion and biofilm formation in dental and orthopaedic implants. Different femtosecond laser surface treatment direct writing methods were applied to create a range of surface structures including: (a) Low-frequency Laser-Induced Periodic Surface Structures (LIPSS), (b) nanopillars arrays (NP), and (c) arrays of microcolumns covered with LIPSS, forming a bimodal roughness distribution (MC-LIPSS). The surface texture was combined with biofunctionalisation by covalent grafting of a RGD peptide sequence. The biological behaviour was assessed by wetting measurements and by studying the behaviour of human mesenchymal stem cells (hMSCs) and *Staphylococcus aureus* bacteria brought into contact with the treated surfaces in appropriate controlled conditions. All these textures enhance surface wettability by water and Hank's balanced salt solution (HBSS). Moreover, LIPSS and MC-LIPSS textures induce an anisotropic wetting behaviour, which superwetting appearing in the LIPSS direction. Matrix mineralisation is observed for all surfaces of both Ti alloys when human mesenchymal stem cells (hMSCs) are cultured in osteogenic medium. Matrix mineralisation and formation of bone-like nodules are significantly enhanced on LIPSS and NP textured surfaces. On the contrary, *Staphylococcus aureus* adhesion and biofilm formation are significantly reduced for LIPSS and NP textured surfaces. The biofunctionalisation of the laser textured surfaces of cp Ti is successfully achieved. In general, these results suggest that surface texturing of Ti alloys using femtosecond laser direct writing is a promising method for enhancing surface wettability of dental and orthopaedic implants by biological fluids and their osseointegration (osteoblastic differentiation and matrix mineralisation), while reducing *Staphylococcus aureus* adhesion and biofilm formation. Finally, the combination of laser texturing and covalent grafting of a RGD peptide sequence may be potentially useful for increasing cell adhesion and facilitating bone formation.

Lasers have also been applied to the ablation of mineralised biological tissues, in particular bone, dentin and enamel. Due to their extremely high intensity and short pulse duration, ultrafast lasers favour nonthermal ablation mechanisms and the thermal impact on the neighbouring tissues is negligible. Furthermore, the laser-tissue interaction is highly nonlinear, so the laser effects are confined to the focal volume (a few tens to a few hundred cubic micrometres), enabling highly precise excisions. The laser treatments were performed with a femtosecond infrared laser (pulse duration 500 fs, wavelength 1030 nm). For cortical bone the laser treated surfaces are usually free of melting, cracks and redeposited debris. A slight decrease on the bone organic material content as well as a partial recrystallization of hydroxyapatite was observed. The average ablation threshold of bone was 0.79 J/cm<sup>2</sup>. A similar result is obtained for human dentin treated with fluences ranging from 1 to 3 J/cm<sup>2</sup>. They present an irregular and rugged appearance, with no significant traces of melting, deformation, cracking or carbonization. The average ablation threshold in these conditions is 0.6±0.2 J/cm<sup>2</sup>. Independently on the laser processing parameters used no subsuperficial cracking was observed and the dentin constitution and chemical composition is not significantly modified. In particular, the organic matter is not preferentially removed from the surface and no traces of high temperature phosphates, such as the β-tricalcium phosphate, is observed. For higher fluences (7 to 14 J/cm<sup>2</sup>) the surface is covered with a poorly adherent layer of ablation debris consisting of amorphous Ca phosphate. Once this layer is removed a flat surface with opened dentinal tubules with negligible traces of melting but having partially lost some of its collagen is revealed. This layer is less than 1 μm thick. The achieved results are compatible with an athermal ablation mechanism. On the contrary, in the case of enamel, a layer of resolidified material between 100 – 900 nm thick is observed on the ablation surface, indicating melting of the tissue, but no changes in the structure and chemical constitution of the tissue are observed below this layer. This behaviour shows that there is a thermal contribution for the ablation mechanism of enamel in these experimental conditions. The differences between the ablation mechanisms of these biological tissues are related to their constitution and optical properties.

# Extreme Light Infrastructure-Nuclear Physics (ELI-NP): present status and perspectives

N. V. Zamfir

*ELI-NP, Horia Hulubei National Institute for Physics and Nuclear Engineering, Bucharest-Măgurele, Ilfov 077125 Romania*

Extreme Light Infrastructure (ELI) Pan-European project represents a major step forward in scientific research with extreme high electromagnetic fields. Extreme Light Infrastructure – Nuclear Physics (ELI-NP), one of the three pillars of ELI, will be located in Bucharest-Magurele, Romania. The ELI-NP Project, worth 300 million euro, is co-financed by the European Regional Development Fund. The project implementation started in 2013 and the facility will be operational in 2018. At ELI-NP, a high power laser system (2x10PW) together with a very brilliant gamma beam system are the two main research equipment. ELI-NP will be a research center for ultra-high intensity lasers and nuclear physics. This multidisciplinary facility will provide completely new opportunities to study fundamental processes that occur in ultra-intense laser fields during light-matter interaction. Basic and applied physics research as well will be presented in the scientific program of the new Center. The status of the project implementation, the planned high power laser system and the gamma beam system will be presented, together with the main directions of the scientific program ([www.eli-np.ro](http://www.eli-np.ro)).

## Quantitative phase imaging of nanofabricated structures

R. Zhou, C. Edwards, L. Goddard, G. Popescu

*Department of Electrical and Computer Engineering  
Beckman Institute for Advanced Science and Technology  
University of Illinois at Urbana-Champaign  
gpopescu@illinois.edu | <http://light.ece.illinois.edu/>*

We present a novel, nondestructive approach for imaging nanostructures. We developed diffraction phase microscopy (wDPM) as a laser-based quantitative phase imaging method that combines the single shot measurement benefit associated with off-axis methods, high temporal phase stability associated with common path geometries, and high spatial phase sensitivity due to the white light illumination. A spatiotemporal filtering method pushes the limit of the pathlength sensitivity to the sub-angstrom level at practical spatial and temporal bandwidths. This capability allows us to measure with nanometer level precision nanofabricated structures nondestructively and dynamically. Specifically, we present recent results on defect detection in semiconductor wafers, imaging the dynamic etching process of semiconductor structures, as well as Si dissolution kinetics.

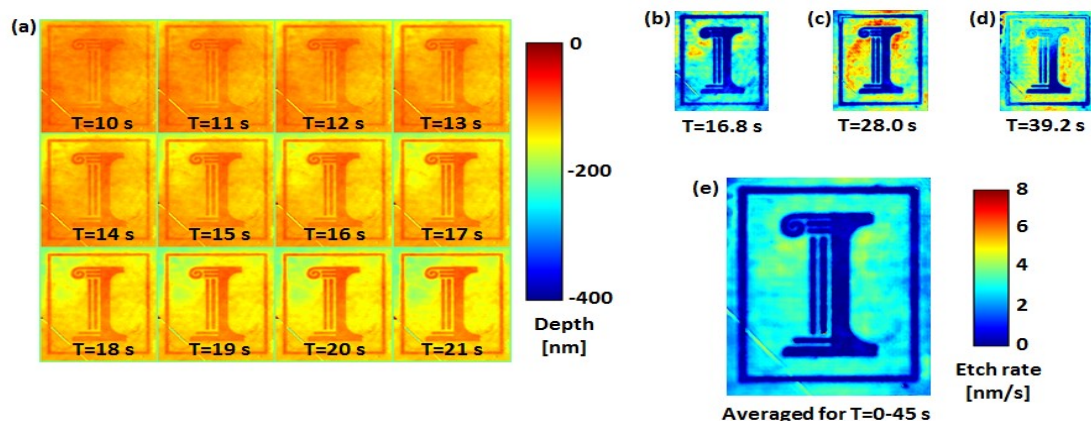


Figure 1: Dynamic monitoring of semiconductor etching using diffraction phase microscopy. a) Time-lapse series that shows the Illinois logo becoming visible as the background etches away. b-e) Etching rate in nanometers per seconds at discrete time points and time-averaged.



# ORAL PRESENTATIONS



# Three-dimensional Cu micropatterns fabricated using femtosecond laser-induced CuO nanoparticle reduction

S. Arakane, M. Mizoshiri, J. Sakurai, S. Hata

Dept. of Micro-Nano Systems Eng., Graduate School of Eng., Nagoya Univ., Furo-cho, Chikusa-ku, Nagoya, Aichi, 464-8603 Japan  
arakane.shun@b.mbox.nagoya-u.ac.jp

Direct-writing technology has attracted much attention in recent years for 3D additive manufacturing. Especially, 3D bulk metal structures are fabricated by selective laser sintering and electron-beam melting. In these processes, it is difficult to apply them to metal micropatterning because raw metal powders are easily oxidized by downsizing the metal powders. On the other hand, 2D Cu micropatterning by laser-induced CuO nanoparticle (NP) reduction has been reported.<sup>1</sup> We have also reported this process by using femtosecond laser pulses.<sup>2</sup> To date, 2D Cu- and Cu<sub>2</sub>O-rich micropatterns, which exhibited respectively metal- and semiconductor-like temperature coefficient of resistance, were selectively formed by controlling laser irradiation conditions.<sup>3</sup> In this presentation, the 3D Cu micropatterns were fabricated using femtosecond laser reduction of CuO NPs and its lamination process.

3D Cu micropatterns were fabricated by the following procedure. First, CuO NP solution, which included CuO NPs and the 2-propanol/polyvinylpyrrolidone (PVP) solution, was coated onto the glass substrate by a dispenser (ML-808GX, Musashi Engineering, Inc.). Then, femtosecond laser pulses were irradiated onto the CuO NP solution film on a glass substrate to form the Cu micropatterns by reducing CuO NPs to Cu. Coating of CuO NP solution and laser patterning were repeatedly conducted to fabricate 3D Cu micropatterns by laminating 2D Cu micropatterns. Finally, 3D Cu micropatterns were obtained by rinsing the sample substrate into ethanol to remove the non-irradiated CuO NP solution.

Dependences of Cu micropattern thickness and its resistance on the layer number were examined as shown in Fig. 1. The thickness increased and the resistance decreased by increasing the layer numbers, which indicate that each layer of 2D Cu micropattern is electrically-connected. However, the resistivity of the micropatterns slightly increased by increasing the layer number. When the 2<sup>nd</sup> or more upper layers were fabricated on the previously formed 2D Cu micropatterns, thermal diffusion to the underlying layer was increased due to the larger thermal conductivity than that of the glass substrate. As a result, the heating temperature of CuO NPs is expected to decrease with increasing the layer numbers, which is consistent with the increasing the resistivity with the layer numbers.

We demonstrated the fabrication of the microbridge heater using this method as shown in an optical scope and a SEM images (Figs. 4). The microbridge heater was composed of the 1<sup>st</sup>-3<sup>rd</sup> layers electrode pads and the 4<sup>th</sup> layer microbridge. A hollow under the microbridge heater was to heat it efficiently without thermal diffusion. It was confirmed that only the microbridge was heated by applying a voltage of 18 V. This 3D micropatterning technique is expected to directly fabricate microsensors such as high response thermal type flow or pressure sensors.

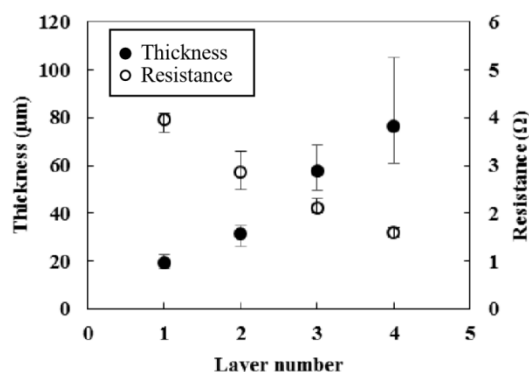


Figure 1. The thickness and resistance vs layer number of the 3D Cu micropatterns.

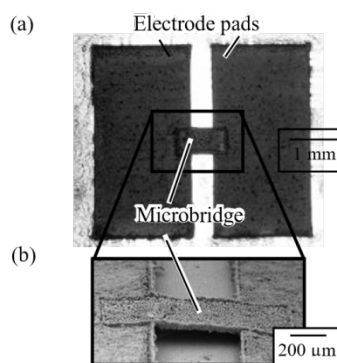


Figure 2. (a) Optical scope and (b) SEM image of the microbridge heater.

1. B. Kang, S. Han, J. Kim, S. Ko and M. Yang, One-step fabrication of copper electrode by laser-induced direct local reduction and agglomeration of copper oxide nanoparticle, *J. Phys. Chem. C* **115** 23664 (2011);
2. S. Arakane, M. Mizoshiri, J. Sakurai, S. Hata, Direct patterning of Cu microstructures using femtosecond laser-induced CuO nanoparticle reduction, *Jpn. J. Appl. Phys.* **54** art. no. 06FP07. (2015);
3. M. Mizoshiri, S. Arakane, J. Sakurai, S. Hata, Direct writing of Cu-based micro-temperature detectors using femtosecond laser reduction of CuO nanoparticles, *Appl. Phys. Express*, **9** 036701 (2016).

# Gamma-beam system at ELI-NP and highlights of the experimental program

D. L. Balabanski

ELI-NP, IFIN-HH, 077125 Magurele, Romania

The Extreme Light Infrastructure (ELI) Pan-European facility initiative represents a major step forward in quest for extreme electromagnetic fields. Extreme Light Infrastructure – Nuclear Physics (ELI-NP), which is under construction in Magurele, Romania, is one of the three laboratories of ELI, and aims at utilization of extreme electromagnetic fields for nuclear physics and quantum electrodynamics research and applications. It is one of the three Pan-European nuclear physics laboratories, which are at present under construction in the EU under the ESFRI scheme. At ELI-NP, high-power laser systems together with brilliant gamma beams are the main research tools. The expected performance of the ELI-NP gamma-beam system (GBS) will be reported. The emerging experimental program with brilliant gamma beams at the GBS will be presented with emphasis on the prepared day-one experiments and the related instruments designed for their realization.

*Acknowledgements:* This work is supported by Extreme Light Infrastructure – Nuclear Physics (ELI-NP) – Phase II, a project cofinanced by the European Union through the European Regional Development Fund.

## Improvement in Ultraviolet Based Decontamination rate Using Meta-materials

S. Bazgan<sup>1</sup>, M. Turcan<sup>1</sup>, T. Paslari<sup>1,2</sup>, N. Ciobanu<sup>1,3</sup>, C. Ristoscu<sup>4</sup>, I. N. Mihailescu<sup>4</sup>, A. Vascashta<sup>5</sup>, N. Enaki<sup>1,2</sup>

<sup>1</sup>Quantum Optics and Kinetic Processes Lab, Institute of Applied Physics of Academy of Sciences of Moldova, Chişinău, Moldova

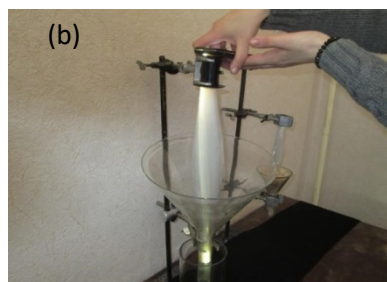
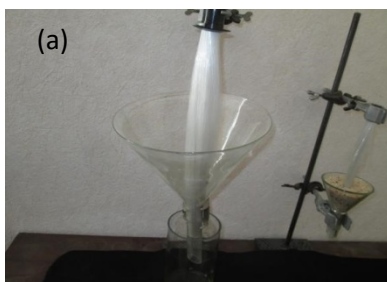
<sup>2</sup>Department of Physics and Engineering, Moldova State University, Chisinau, Moldova

<sup>3</sup>Department of Human Physiology and Biophysics, State University of Medicine and Pharmacy “Nicolae Testemitanu”, Chisinau, R. Moldova

<sup>4</sup>National Institute for Lasers, Plasma and Radiation Physics, Bucharest, Romania

<sup>5</sup>International Clean Water Institute, NUARI, SUA  
enache@asm.md

Using meta-materials, such as optical fibers or periodic photon structures open the new possibilities to manipulate and kill viruses and bacteria in contaminated zones of liquids or organic tissue<sup>1</sup>. For example, the good contact area between the implant and cells can not only be accomplished, but also guided by UV radiation along the implant surface, maintaining the good medical assistance against possible viruses or bacterias. The UV action against bacteria and viruses depends on the dimension and volume of the evanescent zone of the photonic periodical waveguide structures. In Fig. 1, we represented such a periodical structure (fibers and spherical structures) introduced into a funnel through which the contaminated fluid flows. To improve the deficient decontamination of this waveguide material, we propose a simple periodical structure of the set of planar waveguides. Periodical Fiber structures and periodical spherical materials were proposed for carrying out the required measurements in the decontamination procedures as a function of the intensity and pulse duration of UV pulses. The efficient action of UV pulse on the chemical reactions, which take place in the microorganisms is in the initial stage of our studies. Here we take into consideration the quantified structure of the energy of quasiparticle, transmitted from one DNA segment to another, or in connection of coupled protein microtubule. According to our investigations the cooperative effects between the atoms in the process of absorption and emission of photons lies on the photo-transformation process cellular DNA of bacterias. Development of nonlinear models<sup>2</sup> of interaction of UV radiation with microorganisms opens new possibilities concerning decontamination and diagnosis of the new collective processes which take place in viruses, bacteria or other cellular structures under the influence of external UV pulses in the process of its propagation through the multi-cellular tissue. The possibilities of the



selective actions of the UV radiation on the microorganisms with minimal effects on the human tissue are studied.

*Figure 1: The transmission of UV radiation through the periodic optical SiO<sub>2</sub> structures in interaction with the contaminated fluids.*

*Acknowledgement:* This paper was supported by the projects: No. 15.817.02.07F, 15.820.18.02.04/It and EAP SFP 984890.

1. S. Bazgan, C. Ristoscu, I. Negut, C. Hapenciu, M. Turcan, N. Ciobanu, I.N. Mihailescu and N. Enaki, Propagation of UV radiation through meta-materials and its application in bio decontamination, Rom. Rep. in Phys., **67**, 1602–1607 (2015).

2. N.A. Enaki, Non-Linear Cooperative Effects in Open Quantum Systems (Nova Science Publisher, Hauppauge, United States) (2015).

# Evaluation of mechanical and physicochemical properties of Si-DLC and Ti-DLC coatings

D. Bociaga<sup>1</sup>, A. Sobczyk-Guzenda<sup>2</sup>, W. Szymanski<sup>3</sup>, A. Jadrzejczak<sup>1</sup>, A. Olejnik<sup>1</sup>, A. Jastrzebska<sup>3</sup>, K. Jastrzebski<sup>1</sup>

<sup>1</sup> Division of Biomedical Engineering and Functional Materials, Institute of Material Science and Engineering, Lodz University of Technology, 1/15 Stefanowskiego St., 90-924 Lodz, Poland

<sup>2</sup> Division of coatings engineering and non-metallic materials, Institute of Material Science and Engineering, Lodz University of Technology, 1/15 Stefanowskiego St., 90-924 Lodz, Poland

<sup>3</sup> Division of Biophysics, Institute of Material Science and Engineering Lodz University of Technology, 1/15 Stefanowskiego St., 90-924 Lodz, Poland, krzysztof.jastrzebski@p.lodz.pl

Constantly increasing market of implants and medical devices is characterised by the enhancing the diversification of portfolio of products that support more successful surgical outcome<sup>1</sup>. Among the solutions that satisfy the demand for new implants of rapidly aging population, as well as victims of traumatic accidents is doping of diamond like carbon coatings (DLC). By introduction of various elements, it is possible to influence or even tailor the features of synthesized thin films. From the point of view of biological properties among the fields of researches are coatings inducing: bacteriostatic or bactericidal effect (for example: Ag-DLC, Cu-DLC, Si-DLC), haemocompatibility (for example: Si-DLC, Ca-DLC, P-DLC) and proliferation of cells in proximity of graft (for example: Si-DLC, Ti-DLC).

To compare the mechanical and biological properties, as well as chemical composition of carbon coating and its doped derivatives, the DLC Ti-DLC and Si-DLC films were synthesized by means of physical vapour deposition method (PVD). Magnetron sputtering was conducted at process pressure of 0.6 Pa and argon flow rate of 10 sccm. The source of carbon were two graphite targets sputtered with DC power, while dopant was introduced by RF sputtering. Films for potential biomedical applications were deposited on metallic materials used for the implants manufacturing: Ti6Al7Nb and stainless steel AISI 316 LVM.

Introduction of Si or Ti resulted in the improvement of surface hardness in comparison to the both substrate materials. By varying the sputtering power of Si source between 10 and 80W it was possible to increase Si-DLC hardness (up to about 15GPa) above the level of undoped films (about 9-10 GPa). In literature, lack of reduction of hardness resulting in addition of silicon is uncommon<sup>2,3</sup>. In case of Ti-DLC manufactured with sputtering powers between 20 and 80W, the hardness of synthesized coatings did not drop below the value achieved for undoped DLC, however no further improvement of hardness was observed.

Incorporation of silicon to the carbon matrix resulted in values of adhesion on at least the same level as for DLC coatings. About 1.8 at.% of silicon or over 13.9 at.% led to the significant improvement of the critical force of delamination. For the over 20 at.% of Si, its value was even 40% higher than for carbon film. In contrary, addition of Ti showed the improvement of adhesion only in case of its maximum examined amount.

The chemical analysis of synthesized coatings was performed by means of Fourier Transform Infrared Spectroscopy (FTIR) and Raman spectroscopy. Conducted researches enabled to define the change of the bonds systems type with the increase of the sputtering power of dopant source and, as a result, rising amount of elements of interest.

To evaluate the potential of biomedical application of Ti-DLC and Si-DLC, their biological activity and wettability examination was performed. The microbiological test involved the use of liquid culture of *E. coli* bacteria. Conducted test revealed for example that coatings manufactured on Ti6Al7Nb substrate reduced by about one third the number of colony forming units in comparison to the unmodified substrate. Nevertheless, there was no statistically significant difference in bacteriostatic effect between films with various amounts of silicon, which is in opposition to results obtained in researches involving other bacterial strains<sup>4</sup>.

**Acknowledgements** This research has been supported by the National Centre for Research and Development under the grant no. LIDER/040/707/L-4/12/NCBR/2013 entitled „MOBIOMED: Modified BIOMaterials – MEDicine future”.

1. Analysis of the Global Orthopedic Implant Market. Fost & Sullivan (2014);
2. K-R. Lee, M-G. Kim, S-J. Cho, K. Y. Eun, T-Y. Seong, Structural dependence of mechanical properties of Si incorporated diamond-like carbon films deposited by RF plasma-assisted chemical vapor deposition, *Thin Solid Films* 308-309, 1997, 263-267;
3. M. Lubwama, B. Corcoran, K. Sayers, J.B. Kirabira, A. Sebbit, K.A. McDonnell, D. Dowling Adhesion and composite micro-hardness of DLC and Si-DLC films deposited on nitrile rubber. *Surface & Coatings Technology*, 206, (2012) 4881-4886;
4. D.W. Ren, Q. Zhao, A. Bendavid, Anti-bacterial property of Si and F doped diamond-like carbon coatings. *Surface & Coatings Technology* 226 (2013) 1-6.



# Initiation of air ionization by ultrashort laser pulses: Evidence for a role of metastable-state air molecules

A.V. Bulgakov<sup>1,2</sup>, I. Mirza<sup>3</sup>, N.M. Bulgakova<sup>1,3</sup>, V.P. Zhukov<sup>4,5</sup>, E.E.B. Campbell<sup>2</sup>, T. Mocek<sup>3</sup>

<sup>1</sup> S.S. Kutateladze Institute of Thermophysics SB RAS, 1 Lavrentyev Ave., 630090 Novosibirsk, Russia

<sup>2</sup> EaSiCHEM and School of Chemistry, University of Edinburgh, David Brewster Road, Edinburgh EH9 3FJ, UK

<sup>3</sup> HiLASE Centre, Institute of Physics ASCR, Za Radnici 828, 25241 Dolni Břežany, Czech Republic

<sup>4</sup> Institute of Computational Technologies SB RAS, 6 Lavrentyev Ave., 630090 Novosibirsk, Russia

<sup>5</sup> Novosibirsk State Technical University, 20 Karl Marx Ave., 630073, Novosibirsk, Russia  
bulgakov@itp.nsc.ru

Vast majority of scientific and technological applications of short and ultrashort laser processing of materials are performed in a gas environment, mainly in air under atmospheric conditions. However, the role of ambient gases is still poorly understood due to complexity of the phenomenon of laser beam propagation in ionizable medium and a large variety of involved processes. It has been shown that the presence of a gas environment can lead to higher target absorptivity,<sup>1</sup> ultradeep crater formation,<sup>2,3</sup> and can cause misinterpretation of laser ablation mechanisms.<sup>4</sup> Here we report on a discovery of accumulation effects upon multipulse laser processing of materials in air. While various accumulation effects of laser-induced formation of defects states and morphological changes on materials surfaces and in volume have widely been studied, little attention is paid to the fact that excited molecular and atomic states in ambient gases can also be accumulated, thus facilitating gas ionization by subsequent laser pulses.

In this work, transmission measurements for femtosecond laser pulses (800 nm, 120 fs) through the focal region have been carried out in air of various pressures and compared with the vacuum conditions. A spectroscopic study of air plasma emission was also performed. Nitrogen molecule lines were detected at laser fluences well below the breakdown threshold determined from the transmission measurements. The plasma absorption effects are found to depend on the pulse repetition rate and are considerably stronger at 1 kHz as compared to 1-10 Hz (Fig. 1). This suggests that metastable states of air molecules play an important role in initiation of air breakdown, enhancing the ionization efficiency at high repetition rates. Analysis of the spectroscopic data indicates that the ionization process involves the  $N_2(A^3\Sigma_u^+)$  state with a decay time in a 10ms timescale. Modeling of laser-induced gas ionization<sup>3</sup> has been performed which shows good agreement with the experimental data (Fig. 1). The role of ambient gas effects in laser material processing is discussed.

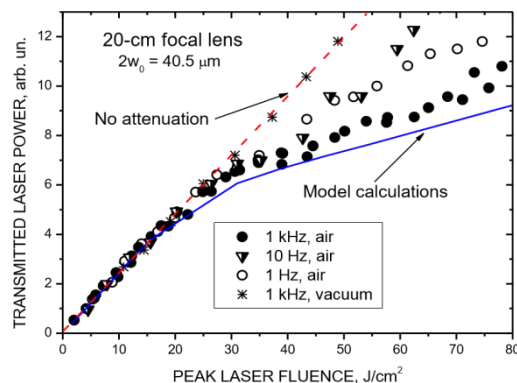


Figure 1: Transmitted power of a central part of a Gaussian laser pulse (800 nm, 120 fs) through a focal region in air and vacuum as a function of peak laser fluence for different repetition rates. The straight dashed line corresponds to the pulse transmission without attenuation. The solid line shows the calculated transmitted power assuming multiphoton air ionization by individual laser pulses.

1. N.M. Bulgakova, V.P. Zhukov, A.Y. Vorobyev, C. Guo, Modeling of residual thermal effect in femtosecond laser ablation of metals: role of a gas environment, *Appl. Phys. A* **92**, 883-889 (2008);
2. N.M. Bulgakova, A.B. Evtushenko, Yu.G. Shukhov, S.I. Kudryashov, A.V. Bulgakov, Role of laser-induced plasma in ultradeep drilling of materials by nanosecond laser pulses, *Appl. Surf. Sci.* **257**, 10876-10882 (2011);
3. N.M. Bulgakova, A.N. Panchenko, V.P. Zhukov, S.I. Kudryashov, A. Pereira, W. Marine, T. Mocek, A.V. Bulgakov, Impacts of ambient and ablation plasmas on short- and ultrashort-pulse laser processing of surfaces, *Micromachines* **5**, 1344-1372 (2014);
4. N.M. Bulgakova, A.V. Bulgakov, Comment on "Time-Resolved Shadowgraphs of Material Ejection in Intense Femtosecond Laser Ablation of Aluminum", *Phys. Rev. Lett.* **101**, 099701 (2008).

# Compression of dry lysozyme targets: A new parameter in protein thin film production

C. Constantinescu<sup>1,2,3</sup>, A. Matei<sup>1,3</sup>, M. Dinescu<sup>3</sup> and J. Schou<sup>1,\*</sup>

<sup>1</sup> DTU Fotonik, Technical University of Denmark, DK-4000 Roskilde, Denmark

<sup>2</sup> Université de Limoges, CNRS, Laboratoire SPCTS (UMR 7315), F-87068 Limoges, France

<sup>3</sup> INFILPR – National Institute for Laser, Plasma and Radiation Physics, 409 Atomistilor St, RO-077125, Magurele, Romania  
josco@fotonik.dtu.dk

The protein lysozyme is used as a model system for film deposition of complex organic molecules<sup>1</sup>. Its properties are well-known, it has a significant signal for the mass analysis by MALDI (Matrix-Assisted Laser Desorption/Ionization) and an activity test which is not too complicated. We have recently demonstrated that such films can be produced by laser irradiation without an external matrix, but by utilizing the residual water in lysozyme powder as a matrix<sup>2</sup>. Thin film production of an organic material without an external matrix, e.g. toluene or water ice, reduces the background pressure considerably and facilitates the deposition of organic molecules without compounds between the film molecules and the matrix molecules. Uniform thin films of proteins in a dry environment are difficult to produce in the thickness range of 10-100 nm, and typically these films can be used for sensors and for patterning of organic systems, as well as for other biotechnical and pharmaceutical applications.

In contrast to most inorganic powders, lysozyme powder can be prepared to a target with a pressure that varies by more than one order of magnitude, i.e. from 10 to 130 bar. A standard deposition at 2 J/cm<sup>2</sup> with laser light at 355 nm and a target preparation pressure of 60 bar leads to a deposition of about 6 ng/cm<sup>2</sup> per pulse. The pressed target density at 60 bar is about 0.6 of the crystalline lysozyme density. The target preparation was carried out by pressing the lysozyme powder with a calibrated piston.

The increase of target preparation pressure leads to a higher internal pressure of the target powder which is held back by the grain friction. It means that the laser must supply more energy and thereby a higher temperature and pressure to release material. The higher temperature and pressure lead to a significantly higher deposition rate measured by weight increase on the substrate. However, the number of intact molecules transferred to the film on a substrate falls off by almost two orders of magnitude in the same pressure interval, as determined by quantitative MALDI and described in ref. [2]. The lysozyme molecules are presumably destroyed early in the ablation process by the high laser-induced pressure and temperature increase and not by the preparation pressure. Films deposited at high target pressure are thus of limited quality, even though they are faster to produce.

1. A. Purice, J. Schou, P. Kingshott and M. Dinescu, "Production of active lysozyme films by matrix assisted pulsed laser evaporation at 355 nm", Chem. Phys. Lett. **435**, 350 (2007);

2. M. Tabetah, A. Matei, C. Constantinescu, N. P. Mortensen, M. Dinescu, J. Schou and L. V. Zhigilei, "The minimum amount of "matrix" needed for matrix-assisted pulsed laser deposition of biomolecules", J. Phys. Chem. B **118**, 13290 (2014).

# Investigations of Radiation Effects in Pulsed Laser Deposited Thin Films

D. Craciun<sup>1</sup>, G. Socol<sup>1</sup>, S. Behdad<sup>2</sup>, B. Boesl<sup>2</sup>, E. Lambers<sup>3</sup>, D. Pantelica<sup>4</sup>, P. Ionescu<sup>4</sup>,  
B. S. Vasile<sup>5</sup>, H. Makino<sup>6</sup>, L. M. Trinca<sup>7,8</sup>, A. C. Galca<sup>7</sup>, D. Simeone<sup>9</sup>, and V. Craciun<sup>1</sup>

<sup>1</sup>National Institute for Lasers, Plasma and Radiation Physics, Măgurele, Romania

<sup>2</sup>Florida International University, Miami, USA

<sup>3</sup>MAIC, University of Florida, Gainesville, USA

<sup>4</sup>Horia Hulubei National Institute for Physics and Nuclear Engineering, Măgurele, RO

<sup>5</sup>Polytechnic University Bucharest, Bucharest, Romania

<sup>6</sup>Research Institute, Kochi University of Technology, Kochi, Japan

<sup>7</sup>National Institute for Materials Physics, Magurele, Ilfov, Romania

<sup>8</sup>Faculty of Physics, University of Bucharest, Magurele, Ilfov, Romania

<sup>9</sup>CEA/DEN/DANS/DM2S/SERMA/LEPP-LRC CARMEN CEN Saclay, France

valentin.craciun@infplpr.ro

For many years studies investigating the effects of radiation on the structure and properties of various materials have been focused on single crystals or sintered pellets having large grain sizes. However, more and more applications are using materials that are nanostructured or even amorphous. Investigations of the effects of radiation on such materials, which have been recently performed, found interesting differences with respect to the results obtained for large grain or single crystal materials. The absence of a long distance order allows for very short diffusion distances of the irradiation generated defects before encountering sites in the network or grain boundaries that could act as sinks. Therefore, the structure and properties are not so strongly affected by exposure to radiation. To investigate in detail the radiation effects on such materials we used the Pulsed Laser Deposition (PLD) technique, which is very suitable to grow nanocrystalline or amorphous thin films of almost any materials starting from inexpensive targets. By simple changes of the deposition parameters, films possessing different chemical compositions and/or structures could be readily obtained. In addition, the surface morphology of the deposited films is flat and very smooth, allowing for the use of characterization techniques such as X-ray reflectivity, grazing incidence X-ray diffraction, or nanoindentation that all possess depth resolutions of the order of few nm. The effect of ions, gamma and X-ray irradiation on the structure, chemical composition, mechanical, optical and electrical properties of transparent and conductive indium zinc oxide films with various In and Zn compositions and several ceramic materials such as ZrC, ZrN and SiC that are widely used in nuclear reactors were investigated<sup>1-3</sup> and compared with those obtained on polycrystalline or single crystal materials.

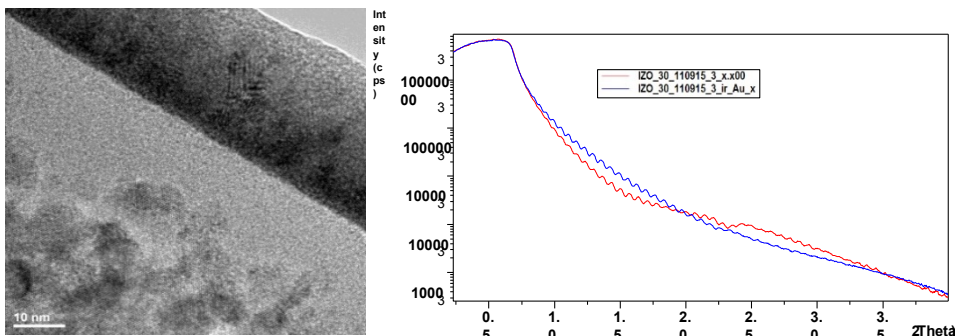


Figure 1: TEM cross-section image of a ZrC thin film deposited on Si after irradiation by 800 keV Ar ions at a fluence of  $1 \times 10^{15}$  ions/cm<sup>2</sup>; XRR curves recorded from IZO films before and after irradiation with 1 MeV Au ions at a fluence of  $10^{14}$  ions/cm<sup>2</sup>.

1. D. Craciun, G. Socol, D. Simeone, S. Behdad, B. Boesl, B.S. Vasile, V. Craciun, Structural and mechanical properties changes induced in nanocrystalline ZrC thin films by Ar ion irradiation, *Journal of Nuclear Materials* **468**, 78-83 (2016);
2. V. Craciun, D. Craciun, G. Socol, S. Behdad, B. Boesl, C. Himcinschi, H. Makino, M. Socol, D. Simeone, Investigations of Ar ion irradiation effects on nanocrystalline SiC thin films, *Appl. Surf. Sci.*, In Press, Corrected Proof, Available online 7 January 2016;
3. D. Craciun, G. Socol, S. Le Caër, L. M. Trinca, A.C. Galca, D. Pantelica, P. Ionescu, V. Craciun, Gamma irradiation effects on the properties of indium zinc oxide thin films, *Thin Solid Films*, In Press, Accepted Manuscript, Available online 29 April 2016.

# Femtosecond-Laser-Induced Periodic Surface Structures on Magnetic Layer Targets: the Role of Magnetization

K. Czajkowski, M. Ratzke, O. Varlamova, J. Reif

Brandenburg. Tech. Univ. – BTU Cottbus-Senftenberg Platz der Deutschen Einheit 1; 03046 Cottbus; Germany  
reif@b-tu.de

We investigate femtosecond LIPSS on a complex multilayer target, namely a computer hard disk (HD), consisting of a metallic substrate, a magnetic layer, and a thin polymeric protective layer. As shown previously<sup>1</sup>, according to the local dose (fluence  $\times$  number of pulses) first the polymeric cover layer is completely removed. Then, the magnetic layer morphology is strongly modified by laser-induced periodic structures and, finally, kind of an etch stop is reached at the bottom of the magnetic layer. The LIPS modulation shows very high modulation depth below and above the original surface level.

In the present work, we investigate the role of magnetization and magneto-mechanic forces in the structure formation process, monitoring the bit-wise magnetization of the HD with a magnetic force microscope. WE study, in particular, the problem of transient overcoming the Curie temperature and associated loss of magnetic order, as well as the influence of residual magnetization on the structure formation.

The results are compared with our model of LIPS/LIPSS formation by self-organized relaxation from a laserinduced thermodynamic instability.

1. J. Reif, O. Varlamova, M. Ratzke, S. Uhlig; Appl. Phys. A **122**, 338 (2016)

## High power, high intensity contrast hybrid femtosecond laser systems

R. Dabu

National Institute for Nuclear Physics and Engineering, Extreme Light Infrastructure-Nuclear Physics,  
Str. Reactorului 30, 077125 Bucharest-Magurele, Romania  
razvan.dabu@eli-np.ro

For many research applications a very high laser intensity of more than  $10^{22}$  W/cm<sup>2</sup> in the focused beam is required. If a laser intensity of about  $10^{11}$  W/cm<sup>2</sup> is reached on the target before the main laser pulse, the generated pre-plasma disturbs the experiment. High power femtosecond lasers must be tightly focused to get a high intensity and in the same time must have a high enough intensity contrast of the temporally compressed amplified pulses. Reaching an intensity contrast in the range of  $10^{12}$  represents a challenging task for a Ti:sapphire CPA laser. Hybrid femtosecond lasers combine the chirped pulse amplification (CPA) in laser active media with optical parametric chirped pulsed amplification (OPCPA) in nonlinear crystals<sup>1</sup>. OPCPA provides large amplification spectral bandwidth and improves the intensity contrast of the amplified pulses. A key feature of these systems consists in the adaptation of the parametric amplification phase matching bandwidth of nonlinear crystals to the gain spectral bandwidth of laser amplifying media, like Ti:sapphire crystals<sup>2-4</sup> and Nd doped glasses<sup>5</sup>.

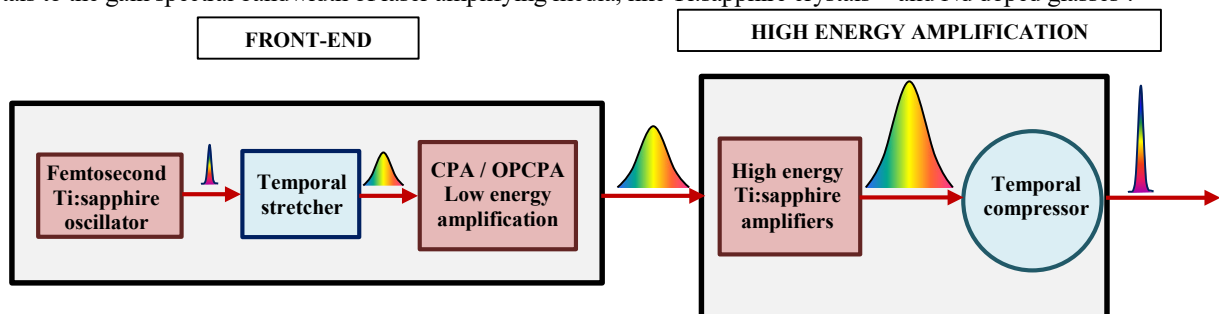


Figure 1: Schematic drawing of a hybrid femtosecond laser system.

OPCPA in BBO, LBO crystals up to mJ energy level in the laser amplifier Front-End, followed by CPA in Ti:sapphire crystals up to ten/hundred Joules, represents a suitable solution for PW-class femtosecond lasers with high intensity contrast (Figure 1). The configuration, technical solutions, and expected output beam characteristics of the hybrid amplification 2 x 10 PW ELI-NP laser are presented<sup>1,6</sup>.

1. R. Dabu, "Lumina Extrema. Lasere de Mare Putere" (Editura Academiei Romane, Bucuresti, Romania), Chapter 3.4 (2015);
2. H. Kyriama et al, "High-spatiotemporal-quality petawatt-class laser system", Appl. Opt. **49** (11), 2105 (2010);
3. J. P. Chambaret, "The Extreme Light Infrastructure Project ELI and its prototype APOLLON/ ILE", LEI Conference, Braşov, Romania, October 21, 2009;
4. Z. Wang et al, "High-contrast 1.16 PW Ti:sapphire laser system combined with a doubled chirped-pulse amplification scheme and a femtosecond optical-parametric amplifier", Opt. Lett. **36**(16), 3194 (2011);
5. E.W. Gaul et al, "Demonstration of 1.1 petawatt laser based on a hybrid optical parametric chirped pulse amplification/mixed Nd:glass amplifier", Appl. Opt. **49**(9), 1676-1681 (2010);

## Formation of silicon nanocrystals by continuous wave laser annealing of SiO<sub>x</sub> films

T. Fricke-Begemann<sup>1</sup>, K. Rewerts<sup>1</sup>, N. Wang<sup>2</sup>, P. Peretzki<sup>2</sup>, M. Seibt<sup>2</sup>, J. Ihlemann<sup>1</sup>

<sup>1</sup>Laser-Laboratorium Göttingen e.V., Hans-Adolf-Krebs-Weg 1, 37077 Göttingen, Germany

<sup>2</sup>IV. Physikalisches Institut, Universität Göttingen, Friedrich-Hund-Platz 1, 37077 Göttingen, Germany  
juergen.ihlemann@llg-ev.de

Silicon nanocrystals (Si-NC) are of interest as integrated light emitters in silicon based photonics. They are mainly generated by high temperature annealing of substoichiometric SiO<sub>x</sub> leading to a phase separation into Si and SiO<sub>2</sub>. Laser annealing instead of furnace annealing offers the possibility to generate nanocrystals spatially controlled. Previous attempts have been made with freestanding films in order to reach sufficiently high temperatures by avoiding heat diffusion to any underlying substrate<sup>1</sup>. In the present work, we show that the generation of silicon nanocrystals by laser induced phase separation can be accomplished in substrate bound SiO<sub>x</sub> while preserving the optical quality of the film<sup>2</sup>. A continuous wave laser emitting at 405 nm is focused to a 6 μm diameter spot on 530 nm thick SiO<sub>x</sub> films deposited on fused silica substrates. Irradiation of lines is performed by focus scanning in nitrogen environment. The irradiated material exhibits photoluminescence in the visible to infrared spectral range (Fig. 1 (a)) indicating the presence of amorphous and/or crystalline Si-nanoparticles. The formation of the crystalline phase is verified by transmission electron microscopy (Fig. 1 (b)) and Raman spectroscopy. At a laser power of 35 mW corresponding to an irradiance of about  $1.2 \times 10^5$  W/cm<sup>2</sup> the formation of Si-nanocrystals in the film without any deterioration of the surface is observed. At higher laser power the central irradiated region is oxidized to SiO<sub>2</sub> and exhibits some porous character, while the surface remains optically smooth, and nanocrystals are observed beside and beneath this oxidized region. Amorphous Si-nanoclusters are formed at lower laser power and around the lines written at high power.

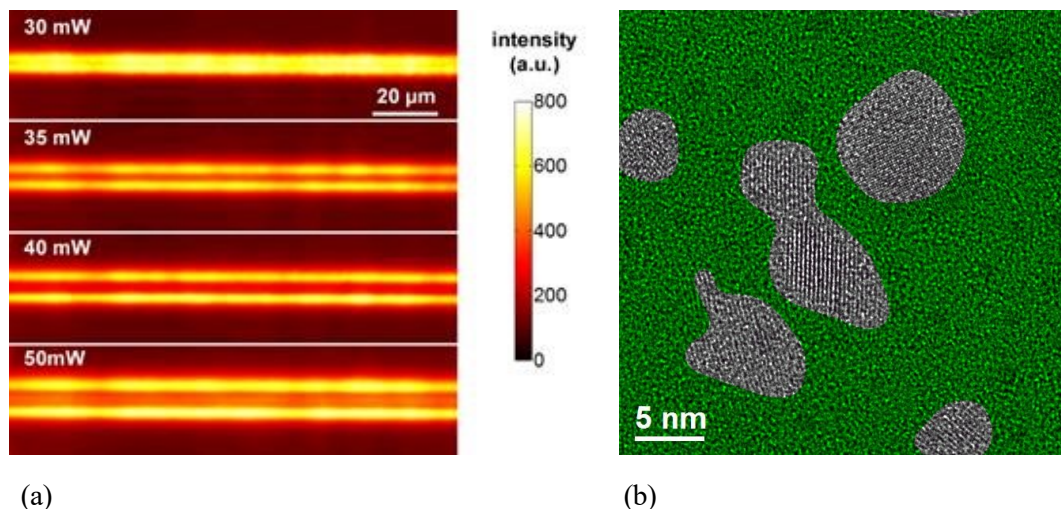


Figure 1: (a) Photoluminescence images recorded from laser annealed lines in SiO<sub>x</sub> written with varying laser power as indicated. (b) High-resolution TEM image showing crystalline particles (grey) embedded in an amorphous matrix (green) obtained for laser irradiation at  $1.4 \times 10^5$  W/cm<sup>2</sup> (40 mW).

Further investigations including the surrounding medium show that the surface of the laser-annealed films irradiated in **air** is smoother than that of films irradiated in **nitrogen**. In a region close to the surface rather large nanocrystals are formed (~20 nm diameter), and the extent of the porous region is diminished. The oxygen supply during irradiation potentially limits the formation of oxygen vacancies, which may increase the structural stability of Si-NC.

1. L. Khriachtchev, T. Nikitin, M. Räsänen, A. Domanskaya, S. Boninelli, F. Iacona, A. Engdahl, J. Juhanoja, S. Novikov, Continuous-wave laser annealing of Si-rich oxide: A microscopic picture of macroscopic Si-SiO<sub>2</sub> phase separation, *J. Appl. Phys.* **108**, 124301 (2010);

2. T. Fricke-Begemann, N. Wang, P. Peretzki, M. Seibt, J. Ihlemann, Generation of silicon nanocrystals by damage free continuous wave laser annealing of substrate-bound SiO<sub>x</sub> films, *J. Appl. Phys.* **118**, 124308 (2015).

# Oscillatory behaviour and double-layer effects in high-fluence laser ablation plasmas

S. Gurlui<sup>1</sup>, P. Nica<sup>2</sup>, M. Agop<sup>2</sup>, M. Ziskind<sup>3</sup>, C. Focsa<sup>3</sup>

<sup>1</sup>Facultatea de Fizica, Universitatea "Alexandru Ioan Cuza", 700506 Iasi, Romania

<sup>2</sup>Universitatea Tehnica "Gheorghe Asachi", 700513 Iasi, Romania

<sup>3</sup>Laboratoire de Physique des Lasers, Atomes et Molécules (UMR CNRS 8523),  
Université de Lille 1 Sciences & Technologies, 59655 Villeneuve d'Ascq cedex, France

Understanding the complex processes triggered by the pulsed laser interaction with the condensed matter is key for the development and optimization of a huge number of applications in various fields, from nuclear fusion to precision micromachining and nanoscale synthesis of high technological potential materials. At high-fluence, this interaction leads to the formation of a transient plasma plume which may exhibit peculiar effects as fragmentation (plume splitting and sharpening), oscillations (in the MHz-GHz frequency range), (multiple) double-layer occurrence, electron and ion acceleration etc.

In this frame, we have performed systematic experimental studies on the characterization of plasma plumes generated by laser ablation in various temporal regimes (ns, ps, fs) at fluences up to 1 kJ/cm<sup>2</sup> and irradiances up to 1 PW/cm<sup>2</sup>. Optical (fast gate intensified CCD camera imaging and space- and timeresolved emission spectroscopy) and electrical (mainly Langmuir probe and mass spectrometry) methods have been applied to experimentally investigate the dynamics of the plasma plume and its constituents. A new theoretical method based on a fractal hydrodynamic approach has been proposed to describe the expansion of the plasma plume. Our results provide strong arguments for the occurrence of these peculiar effects in a multiple double-layer scenario intimately linked to the existence of hot and cold electrons in two-electron-temperature (TET) laser ablation plasmas.

## Combinatorial Photocatalyst Screening using Photo-Electrochemical Scanning Droplet Cell Microscopy

A. W. Hassel<sup>1,2</sup>, J. P. Kollender<sup>1,2</sup>, A. I. Mardare<sup>1,2</sup>

<sup>1</sup>Institute for Chemical Technology of Inorganic Materials, Johannes Kepler University Linz, Altenberger Str. 69, 4040 Linz, Austria

<sup>2</sup>Christian Doppler Laboratory for Combinatorial Oxide Chemistry, Institute for Chemical Technology of Inorganic Materials, Johannes Kepler University Linz, Altenberger Str. 69, 4040 Linz, Austria  
achimwalter.hassel@jku.at

A vast amount of work is presently devoted to the search and development of new photocatalysts. Hopefully, they will hopefully help us solving or at least reducing our energy problems. Heterogeneous and homogeneous catalysts are considered in various approaches. The preparation of modified or entirely new photoactive materials requires effective screening methods. The photo-electrochemical scanning droplet cell PE-SDC that was introduced in its initial form some 10 years ago<sup>1</sup> has been further developed to a fully automatized method. The basic idea is using a glass capillary with a tip diameter of e.g. 100 µm that is wetting a small part of a substrate. An in build reference electrode guarantees a full 3 electrode arrangement. In the set up presented here various light sources can be randomly used to illuminate the investigated small spot. The light sources are either diode lasers with fixed wavelength or a continuous emitter for which the wavelength of interest is chosen using a monochromator<sup>2</sup>.

As a proof of concept this system is applied to traditional semiconductors namely n-Si, p-Si and III-IV semiconductors proving that: **o** photo potential (continuous or chopped) **o** photo current (continuous or chopped); **o** photo impedance (full spectra and/or fixed frequency bias scanning) can be automatically performed.

Transition metal oxide material libraries have been prepared by multi source co-deposition and have been screened using PE-SDCM. These materials produce promising candidates for water splitting photo electrodes. In the comparison of MeOx-WOx libraries in which the metal Me is a ferrous metal like Fe, Ni or Co differences in the mechanisms are explained. There are striking differences resulting from the differences in the watersplitting capacity of compositions within these libraries. Their common application however is the successful application of a combinatorial photo-electrochemical approach in which samples are prepared and investigated in the CALMAR.

An alternative application is the screening of homogeneous or immobilized catalysts. Complex bifunctional materials with an intramolecular donor acceptor pair are rather difficult to synthesize and therefore may exist only in very small amounts of some 10 µg in the beginning. The PE-SDCM provides a method for a comprehensive characterizing of such materials under these limited conditions<sup>3</sup>.

1. A. W. Hassel, M. Seo, Localised Photoelectrochemical Measurements with the Scanning Droplet Cell in Passivity and Localised Corrosion, Proc. Electrochem. Soc. (1999) 337;

## Laser-based realization of 1D guided topographical wedge waves with unrivaled nonlinearity

P. Hess<sup>1</sup>, A. M. Lomonosov<sup>1-3</sup>, A. P. Mayer<sup>2</sup>

<sup>1</sup>*Institute of Physical Chemistry, University of Heidelberg, D-69120 Heidelberg, Germany*

<sup>2</sup>*HS Offenburg, University of Applied Sciences, D-77723 Gengenbach, Germany*

<sup>3</sup>*General Physics Institute, Russian Academy of Sciences, 119991 Moscow, Russia*

*peter.hess@urz.uni-heidelberg.de*

Nonlinear wave phenomena such as shock formation, solitons or turbulence occur in various fields of science and technology. The build-up of steep wave fronts to shocks and the formation of sharp spikes may be regarded as cumulative nonlinear effects resulting from a resonant interaction of harmonics of the wave field, which is possible in the absence of dispersion. Apart from rare exceptions, the acoustic modes of conventional onedimensional (1D) waveguides such as fibers and channel waveguides are normally dispersive, which inhibits the growth of higher harmonics. However, the fundamental modes of 1D wedge waves (WWs) are localized within a depth of approximately one wavelength at the wedge tip and the elastic strain energy remains concentrated there due to the nondispersive and non-diffractive nature. WWs are subsonic, i.e. their phase velocity is below the phase velocities of surface and bulk waves and therefore they do not couple with these 2D and 3D elastic waves. To launch a transient WW pulse with sufficient magnitude, the absorption layer technique was employed, where a 1ns pulse of a Nd:YAG laser operating at 1.064  $\mu\text{m}$  was focused into a small spot of a highly absorbing liquid layer deposited on one wedge face near the edge. The resulting local surface inclination, associated with the transient WW pulse, was detected by the probe-beam-deflection method at two different spots near the tip, using a 532 nm continuous-wave Nd:YAG laser. While in isotropic materials, well defined antisymmetric flexural (ASF) modes are excited, such a simple description cannot be applied to low symmetry anisotropic wedges.

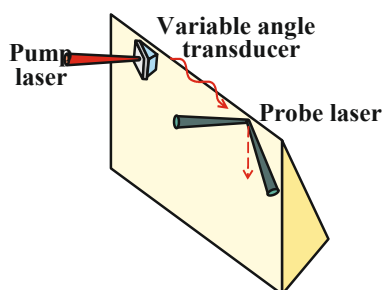


Figure 1: All-optical setup to launch and detects WWs

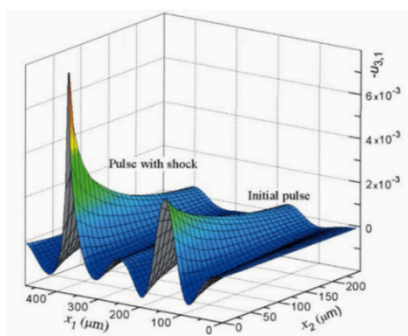


Figure 2: Development of nonlinear pulse profiles

The rectangular silicon wedge studied had the wedge faces  $(-1-1-1)$   $90^\circ(-110)$ . The low symmetry removes the restrictions responsible for the nonexistence of second-order nonlinearity. This allowed for the first time the observation of a new type of efficient second-order nonlinearity with dominating frequency-up conversion. The acoustic pulses, showing steepening, narrowing, and spiking to shock-like profiles, were generated and detected by the laser-based pump-probe setup. The shock formation process is described theoretically by a nonlinear evolution equation, which also allows for prediction of the characteristic features of 1D shock waves differing from their bulk and surface wave analogs. This includes besides simulations of the nonlinear pulse profile, the explanation of the more efficient frequency-up than frequency-down conversion, and the resulting shorter shock formation distance as compared to surface and bulk waves. The conditions required to realize this type of strong nonlinearity can be easily fulfilled in anisotropic materials such as single-crystal silicon. Therefore, these observations open the door to the new field of dispersion-free 1D waveguides with unrivaled nonlinear behavior.

1. A. M. Lomonosov, P. D. Pupyrev, P. Hess, and A. P. Mayer, *Phys. Rev. B* 92, 014112 (2015).

# Anisotropy evaluation in polarization second harmonic generation imaging of collagen in histopathological samples

R. Hristu, S. G. Stanciu, D. E. Tranca, G. A. Stanciu

Center for Microscopy-Microanalysis and Information Processing, University Politehnica of Bucharest, 313 Splaiul Independentei, Bucharest, Romania  
hristu\_radu@yahoo.com

Laser scanning microscopy techniques exploiting nonlinear optical effects have been proven to be useful tools in biomedical tissue imaging.<sup>1</sup> One of these techniques, second harmonic generation (SHG) has the advantage of imaging endogenous structures without the need of staining.<sup>2</sup> Due to its coherent nature, the SHG intensity dependence on the laser polarization is sensitive to the structure and arrangement of the molecules that produces the signal<sup>3</sup> and offers additional information and means of contrast beyond intensity-based SHG microscopy. By applying polarization-sensitive measurements different metrics such as the anisotropy factor ( $\beta$ )<sup>3</sup> can be computed and used in quantitative image analysis. The anisotropy factor  $\beta$  is a pixel-wise measure of the alignment of molecular dipoles relative to the incident laser polarization and provides additional information on the collagen ultra-structural characteristics which are complementary to the spatial distribution provided by intensity-based SHG. In this paper we evaluate SHG-based collagen imaging depending on the incident laser polarization for the case of histopathological samples.

Series of images at different polarization angles were acquired to investigate the dependence of the SHG and of the anisotropy parameter on the polarization angle of the excitation light. As expected, the image contrast among the different SHG images is polarization dependent. In this set of experiments, we found that the minimum SHG intensity was obtained when the incoming polarization was perpendicular to the collagen orientation. The SHG parallel and perpendicular components for each input polarization were then acquired for the calculation of the anisotropy factor (Fig. 1). The anisotropy factor was calculated from each set of images on a pixel-by-pixel basis by:  $\beta = \frac{I_{\parallel} - I_{\perp}}{I_{\parallel} + 2I_{\perp}}$ , where  $I_{\parallel}$  and  $I_{\perp}$  are the SHG intensity detected with the analyzer parallel and perpendicular to the laser polarization, respectively. This polarization information allows reconstructing the anisotropy maps with a resolution corresponding to the image pixel.

We have shown that the anisotropy factor used previously for cancer assessment in different types of samples follows a polarization dependence similar to that of the SHG intensity. For random distributions of collagen across the investigated areas the dependence is less evident, while for aligned collagen fibers,  $\beta$  strongly depends on the incident laser polarization.

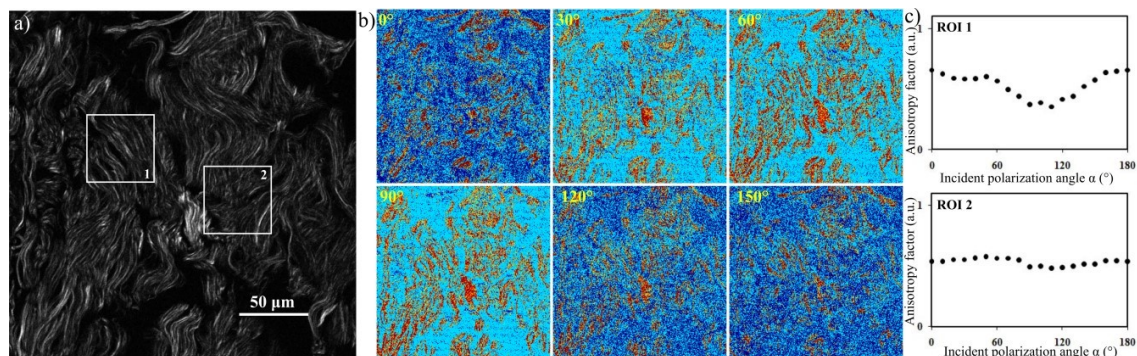


Figure 1: SHG and anisotropy factor images for human skin samples prepared for the histopathological examination. (a) SHG image obtained as the sum of all the images acquired with tunable linear incident polarization; (b) Anisotropy maps for six different incident polarizations, displayed as a color-coded map, where the  $\beta$  values are represented from blue to red; (c) Average value of the anisotropy factor  $\beta$  for aligned (ROI 1) and for random distribution (ROI 2) of collagen fibers.

1. W.R. Zipfel, R.M. Williams, R. Christie, A.Y. Nikitin, B.T. Hyman, W.W. Webb, Live tissue intrinsic emission microscopy using multiphoton-excited native fluorescence and second harmonic generation, *Proceedings of the National Academy of Sciences*, 100(12), 7075-7080 (2003);
2. P.J. Campagnola and L.M. Loew, Second-harmonic imaging microscopy for visualizing biomolecular arrays in cells, tissues and organisms, *Nature biotechnology*, 21(11), 1356-1360 (2003);
3. X. Chen, O. Nadiarynkh, S. Plotnikov, P.J. Campagnola, Second harmonic generation microscopy for quantitative analysis of collagen fibrillar structure, *Nature protocols*, 7(4), 654-669(2012).



# Hybrid laser technology and doped biomaterials

M. Jelínek<sup>1,2</sup>

<sup>1</sup>*Institute of Physics of the Czech Academy of Sciences, Na Slovance 2, 182 21 Prague 8, Czech Republic*

<sup>2</sup>*Czech Technical University in Prague, Faculty of Biomedical Engineering, nam. Sitna, 3105, 27201 Kladno, Czech Republic  
jelinek@fzu.cz*

To improve physical, mechanical and biocompatible properties of implant coatings the layer can be doped (enriched) with another element - nanocomposites are created. For laser fabrication of nanocomposite films the cheapest way is to cover rotated target material (matrix) with a piece of dopant material. The laser beam ablates one material and subsequently the second, etc. The method is not flexible, do not make possible the fast dopant changes and materials (dopant and matrix) are accumulated in layer separately, independently. In our contribution we are concentrated on fabrication of doped thin films by hybrid laser deposition technology. Especially on technology using a) two beams of two lasers focused on two different targets (matrix target material and dopant material), or b) on laser deposition running simultaneously with magnetron sputtering. In the case of double beam pulsed laser deposition (PLD) technology two independent fluxes of high energetic particles (up to 1 keV) intersect on the substrate. In combination of PLD with magnetron sputtering the layer is continuously growing by continuous condensation of low energetic material flux produced by magnetron (~ 5 eV) and high energetic pulsed material flux ablated by PLD. Both fluxes are directed on the substrate. The two different hybrid technologies result in different properties of doped films even for the same concentration of dopants in matrix (film). Hybrid based laser technologies make possible the easy fabrication of nanocrystalline, doped, nanocomposite and gradient layers by changing of material fluxes.

In our contribution we compare properties of doped layers created by the two hybrid deposition technologies, for various dopant concentrations and various deposition conditions. The focus was on titanium and chromium doped diamond like carbon (DLC) layers. Properties as morphology and roughness (profilometer, scanning electron microscope, atomic force microscope), and contact angle and surface free energy were studied. Layers of Cr doped DLC, prepared by PLD + magnetron, were smoother, contact angle was higher and the surface free energy was lower compared to double PLD deposition, for the same dopant concentrations. The fabrication of layers of low dopant concentrations is easier to arrange with double PLD because of PLD + magnetron arrangement exhibits instabilities in glow magnetron discharge for a low magnetron power (needed for deposition of low dopant concentrations). Advantages and disadvantages of both hybrid laser technologies will be discussed and detailed results, including titanium doped DLC layers, will be given.

## Laser-lithography as a micro-machining tool for 3D laser target engineering

F. Jipa<sup>1</sup>, I. Tiseanu<sup>1</sup>, C. Luculescu<sup>1</sup>, M. Cernaianu<sup>2</sup>, D. Ursescu<sup>2</sup>, M. Zamfirescu<sup>1</sup>

<sup>1</sup>*National Institute for Laser, Plasma and Radiation Physics, Atomistilor 409, Magurele, Romania*

<sup>2</sup>*National Institute for Nuclear Physics and Engineering, ELI-NP department, Reactorului 30, Magurele, Romania  
florin.jipa@infpr.ro*

The fabrication of 3D targets for ultra-intense laser interactions is demonstrated in this work, using as processing technic the 3D laser-lithography. According to Particle-In-Cell (PIC) numerical simulations<sup>1,2</sup>, an engineered cone-shaped micro-target, increase the absorption of the electromagnetic field, prevent the plasma expanding and improve the divergence and the efficiency of the emitted particle, compared with the standard planar thin foils.

Due to the small dimensions of the targets proposed by us, usually few tens of micrometers, the fabrication technology are limited to photo-lithographic methods. One of these is Laser-lithography which use a femtosecond laser to induces Two-Photon-Polymerization (TPP)<sup>3</sup> mechanism in the volume of photo-resist materials. Translating the focused beam through the photo-resist volume, complex 3D microstructures with resolution of the order of 100 nm can be fabricated, according to a computer controlled design<sup>4</sup>.

We propose to use the technology of 3D laser lithography for fabrication of targets for efficient laser-mater interactions in high field regime. We proof the concept of 3D fabrication of a cone shaped structure (Fig.1) using the Photonic Professional system from Nanoscribe GmbH, installed at the Center for Advanced Laser Technologies - CETAL facility. The designed shape was fabricated in the IP-L photo-resist on the top of a thin aluminium foil with thickness of 3  $\mu\text{m}$ . The sample was investigated by Scanning Electron Microscopy (SEM) (Fig. 1a,b) and X-ray Tomography (Fig. 1c).

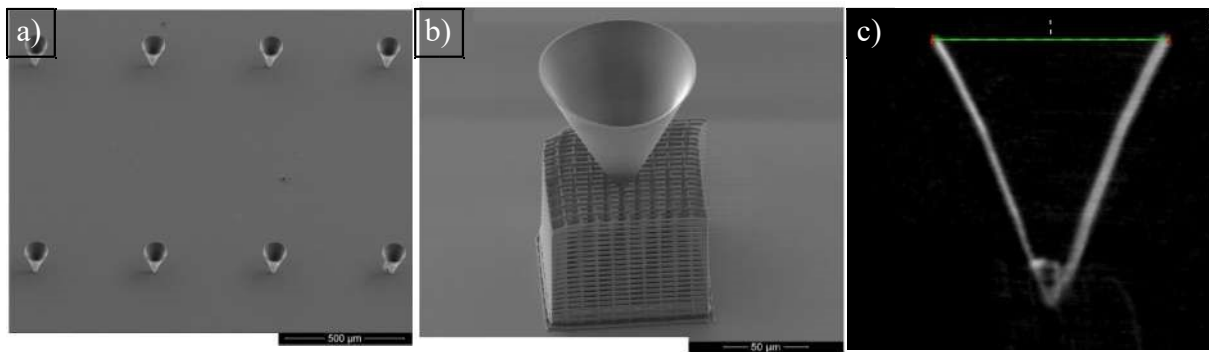


Figure 1: Micro-structures fabricated in IP-L foto-resist using the Professional 3D Nanoscribe laser lithography work-station. a) An array of cone structures; b) The cone structure is located on a woodpile base; c) A tomography image of a single cone shaped structure.

1. N. Renard-le Galloudec and E. D'humieres, New micro-cones targets can efficiently produce higher energy and lower divergence particle beams, *Laser and Particle Beams*, **28**, 513–519 (2010);
2. G Y Hu, A. Lei, W. Wang, J. Wang, L. Huang, X. Wang, Y. Xu, J. Liu, B. Shen, W. Yu, R. Li, Z. Xu, Enhanced surface acceleration of fast electrons by using subwavelength grating targets, *Phys. Plasmas* **17**, 083102 (2010);
3. S. Maruo, O. Nakamura, S. Kawata, Three-dimensional microfabrication with two-photon-absorbed photopolymerization, *Optics Letters*, **22**, 132–134 (1997);
4. T. Tanaka, H. Sun, S. Kawata, Rapid sub-diffraction-limit laser micro/nanoprocessing in a threshold material system, *Appl. Phys. Lett.*, **80**, 312-314 (2002).

## Numerical investigation of the temperature modulation relaxation on the surfaces of Au, Ti and SiO<sub>2</sub> upon femtosecond laser irradiation above the damage threshold

Y. Levy<sup>1</sup>, E. L. Gurevich<sup>2</sup>, N. M. Bulgakova<sup>1,3</sup>

<sup>1</sup>HiLASE Centre, Institute of Physics CAS, Za Radnici 828, 25241 Dolní Břežany, Czech Republic

<sup>2</sup>Chair of Applied Laser Technologies, Ruhr-Universität Bochum, Universitätsstraße 150, 44801 Bochum, Germany

<sup>3</sup>S.S. Kutateladze Institute of Thermophysics, SB RAS, 1 Lavrentyev ave., 630090 Novosibirsk, Russia  
levy@fzu.cz

We study numerically the evolution of a temperature modulation on surfaces of two different kinds of materials, metals (Au, Ti) and dielectric (fused silica), exposed to femtosecond laser pulses of linearly polarized light at 800 nm wavelength, in the regime of LIPSS formation. It is assumed that the incident laser light experiences an intensity modulation upon coupling to the target due to interference with the scattered surface electromagnetic wave that is considered as the main mechanism of formation of laser-induced periodic surface structures (LIPSS)<sup>1</sup>. Absorption of light results in modulation of the deposited laser energy along polarization direction and our study is aimed at examining the post-irradiation temperature evolution.

Our simplified 2D simulations<sup>2</sup> are based on the two-temperature model (TTM) and accounts for the local changes in material optical properties through the Drude model. The growth and decay of the modulation of the lattice temperature, that can govern the LIPSS formation, is followed during the period of electron-lattice thermalization and beyond. We first present the case of metals by addressing the irradiation of gold and titanium, thus comparing temperature dynamics of materials of the same kind. It has been demonstrated that even materials of the same family can behave differently in respect of modulated temperature profile evolution due to difference in thermodynamic and optical properties. A more pronounced difference is observed, at similar irradiation conditions, between metals and dielectrics (fused silica as an example) where for the latter the model considers the dynamics of free carrier excitation and relaxation.

To gain insight into the role of swiftly changing optical response of metals to ultrashort laser radiation in dynamics of temperature modulation, modeling was also performed with constant optical properties as often used in the TTM simulations. A strong enhancement of temperature modulation has been found due to the change in reflectivity and absorptivity during the laser pulse action. The effects of different modeling parameters in the description of ionization rates for SiO<sub>2</sub> are discussed.

1. J.E. Sipe, J.F. Young, J.S. Preston, H.M. van Driel, Laser-induced periodic surface structure. I. Theory, *Phys. Rev. B*, **27**, 1141–1154 (1983);

2. Y. Levy, T.J.-Y. Derrien, N.M. Bulgakova, E.L. Gurevich, T. Mocek, Relaxation dynamics of femtosecond-laser-induced temperature modulation on the surfaces of metals and semiconductors, *Appl. Surf. Sci.*, **374**, 157-164 (2016).

# Far-field nanostructuring in dielectric materials enabled by near-field enhancement of laser-induced nanoplasma

Yang Liao, and Ya Cheng

State Key Laboratory of High Field Laser Physics, Shanghai Institute of Optics and Fine Mechanics, Chinese Academy of Sciences, Shanghai 201800, China, [superliao@vip.sina.com](mailto:superliao@vip.sina.com); [ya.cheng@siom.ac.cn](mailto:ya.cheng@siom.ac.cn)

Due to the unique characteristics of ultrashort pulse width and extremely high peak intensity, femtosecond lasers have established themselves as excellent tools for high-precision and flexible fabrication of 3D microstructures. By taking advantage of the well-defined ablation threshold as well as the suppressed thermal diffusion, one can beat the diffraction limit by choosing the peak laser fluence slightly above the threshold value<sup>1</sup>. However, due to the high nonlinearity of photoionization, the structuring process will become extremely sensitive to the fluctuation of laser intensity, especially when the laser intensity is near the threshold intensity. Thus, a compromise has to be made between improving the resolution and maintaining the stability of the fabrication process.

To address this issue, we present far-field nanostructuring in dielectric materials enabled by near-field enhancement of laser-induced nanoplasma<sup>2</sup>. In multi-pulse irradiation regime, nanoplasmas can be generated in dielectric materials by defect-induced photo-ionization, and the local field enhancement at the boundary of nanoplasma could lead to the formation of a stable nanoplane as narrow as tens of nanometers under the action of many laser shots<sup>3</sup>. This unique mechanism enables reliable nanostructuring not only on the surface but also inside dielectric materials with a reproducible fabrication resolution. Moreover, the single isolated nanoplanes can be connected into a continuous structure for construction of 3D nanochannels in glass, as shown in Figure 1<sup>4</sup>.

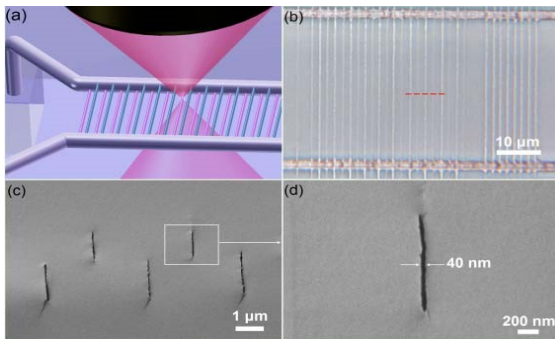


Figure 1: (a) Schematic diagram of an array of double-layer nanochannels to bridge two microchannels. (b) Top view optical micrograph of double-layer nanochannels after postannealing. (c) Cross-sectional SEM micrograph of the nanochannels cleaved along the red dashed line in Figure 4b. (d) Close-up SEM micrograph of cross section of a nanochannel.

1. P. P. Pronko, S. K. Dutta, J. Squier, J. V. Rudd, D. Du, and G. Mourou, *Opt. Commun.*, **114**, 106 (1995);
2. Y. Liao, Y. Shen, L. Qiao, D. Chen, Y. Cheng, K. Sugioka, and K. Midorikawa, *Opt. Lett.*, **38**, 187 (2013);
3. Y. Liao, J. Ni, L. Qiao, M. Huang, Y. Bellouard, K. Sugioka, and Y. Cheng, *Optica*, **2**, 329 (2015);
4. Y. Liao, Y. Cheng, C. N. Liu, J. X. Song, F. He, Y. L. Shen, D. P. Chen, Z. Z. Xu, Z. C. Fan, X. B. Wei, K. Sugioka, and K. Midorikawa, *Lab Chip*, **13**, 1626 (2013).

## Nanostructuring of dielectric surfaces using nanosecond laser radiation

P. Lorenz, I. Zagoranskiy, J. Zajadacz, F. Frost, C. Grüner, L. Bayer, K. Zimmer

Leibniz-Institut für Oberflächenmodifizierung e. V., Permoserstr. 15, 04318 Leipzig, Germany  
[pierre.lorenz@iom-leipzig.de](mailto:pierre.lorenz@iom-leipzig.de)

Nanostructures have a widespread field of applications. The laser-induced nanostructuring of fused silica and sapphire surfaces was studied assisted by a laser-induced molten phase transformation of a thin metal film where a homogenous as well as a structured metal film was irradiated. The structuring process is split into two steps: STEP 1: The low laser fluence irradiation of thin metal layers and structured films on dielectric surfaces, respectively, results in a melting and nanostructuring process due to the surface tension of the liquid metal layer. STEP 2: The high laser fluence irradiation of the pre-structured metal nanostructures/dielectric system results in a nanostructuring of the dielectric surfaces where different processes like pattern transfer (see Figure 1 (b) and (c)), self-organized surface nanostructuring and nanodrilling can be found. As laser sources an ultraviolet and an infrared nanosecond laser were used. As UV laser source a KrF excimer laser with a wavelength of  $\lambda = 248$  nm, a pulse duration of  $\Delta t_p = 25$  ns and a variable beam profile (top hat beam and periodically modulated profiles) were applied. Further, as IR laser source a fiber laser with a Gaussian beam profile, a wavelengths of  $\lambda = 1064$  nm as well as an adjustable pulse duration of 1–600 ns with a resolution of 1 ns was used. The method allows the fabrication of randomly distributed structures using a top hat beam profile for STEP 1 (see Figure 1 (a)). Further the fabrication of periodic structures is possible, using a periodic beam profile (at STEP 1) and structured metal films, respectively (see Figure 1 (a)). The resulting structures were investigated by atomic force (AFM) and scanning

electron microscopy (SEM). Several samples were structured by focused ion beam (FIB) and subsequently measured by SEM.

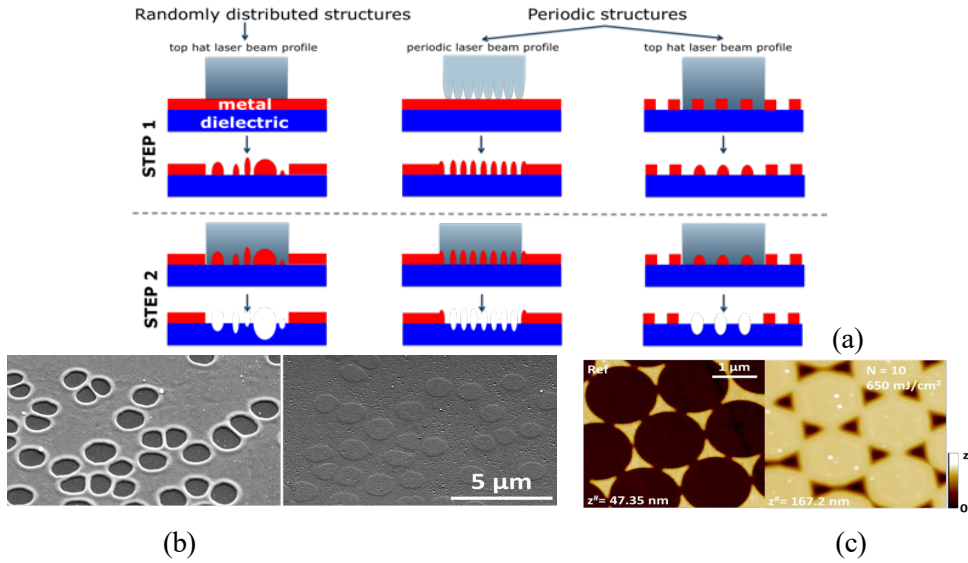


Figure 1: (a) Schematic illustration of the different laser structuring methods. (b) SEM images of (left) a low-fluence irradiated 20 nm molybdenum layer on sapphire (STEP 1:  $\Phi = 330 \text{ mJ/cm}^2$ ,  $N = 9$ ) and (right) highfluence irradiation of the pre-structured system (STEP 2:  $\Phi = 1.1 \text{ J/cm}^2$  and  $N = 1024$ ). AFM images of untreated and treated 30 nm chromium triangles on fused silica, irradiated by a KrF excimer laser with  $\Phi = 650 \text{ mJ/cm}^2$  and  $N = 10$  (STEP 2).

## Power Splitting of 1x16 in Multicore Photonic Crystal Fibers

D. Malka and A. Peled

Holon Institute of Technology, Electrical Engineering Department, Holon 5810201, Israel  
 dmalka@hit.ac.il

Photonic Crystal Fiber (PCF) structures add a new dimension to photonic distribution power design<sup>1</sup>. One specific application of such structures is to achieve an optical power splitter/coupler. The coupling characteristics of multicore PCF based 1x4 power splitters in 5.8-mm-long multicores have been studied e.g., [2], and in ref. [3] the authors have obtained an effective splitting of energy in a 5.35-mm-long multicore with with a splitting ratio of (1x8). The splitting into eight ports was achieved by changing the diameter of the air holes affecting thus the coupling coefficients between the cores. In this paper, we investigate yet another approach to obtain a multicore PCF which divides the single optical beam power equally into sixteen ports. The new method combines two different diameters sizes of small air tubes with variable distances between the neighboring cores to optimize the propagation distance-thus obtaining the required optical power outputs. Also the coupled-mode analysis is increased from 9 cores to 17 cores to resolve better the supermode patterns and the coupling characteristics between the neighboring cores. We use the beam propagation method (BPM) to investigate this new design of multicore PCF based (1x16) splitters. Thus an optical signal at a wavelength of  $1.55 \mu\text{m}$  inserted into the central core of a PCF (Fig. 1(a)) is equally divided into sixteen cores, each with a 6.25% of the single core input power (Fig. 1(b)). The numerical simulations show the optical signal splitting modes equally divided in PCF structures with dimensions of  $60 \mu\text{m} \times 60 \mu\text{m} \times 3.582 \text{ mm}$  (x,y,z). The power coupling characteristics obtained from the coupled-mode analysis are in very good agreement with those calculated using the BPM solver.

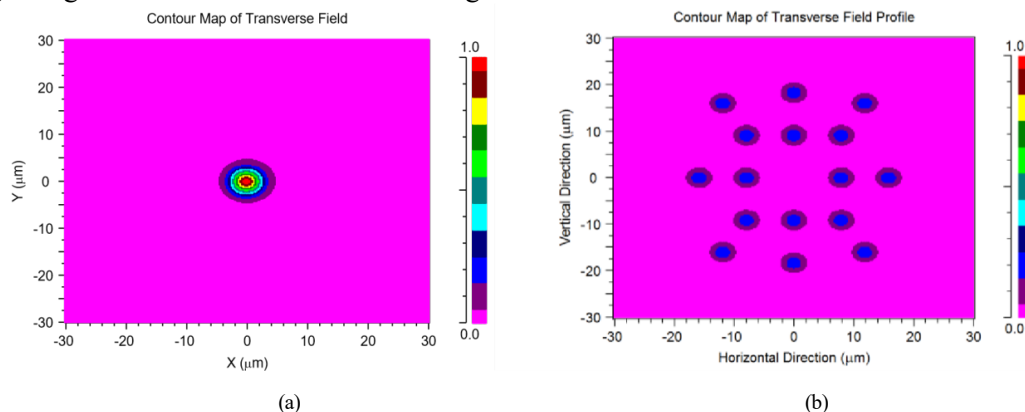


Figure 1. Modal Field Distribution plots of the intensity splitting in a 1x16 PCF splitter of optical signals at  $\lambda=1.55 \mu\text{m}$  for two xy cross sections: (a)  $z=0$ . (b)  $z=3.582 \text{ mm}$ .

1. J. D. Joannopoulos, S. G. Johnson, J. N. Winn and R. D. Meade, "Molding the Flow of Light," 2nd Edition, Princeton University Press, (2008);
2. M. Koshiba, "Coupling Characteristics of Multicore Photonic Crystal Fiber-Based 1 x 4 Power Splitters", J. Lightwave Technol. 27, 2062-2068 (2009);
3. D. Malka and Z. Zalevsky, "Multicore Photonic Crystal Fiber Based 1x8 Two-Dimensional Intensity Splitters/Couplers," Electromagnetics 33, 413–420 (2013).

## Copper-based thin film combinatorial libraries screening for sensor applications

A. I. Mardare<sup>1,2</sup>, I. Pötzelberger<sup>1</sup>, C. C. Mardare<sup>1,3</sup>, A. W. Hassel<sup>1,2,3</sup>

<sup>1</sup>Institute for Chemical Technology of Inorganic Materials, Johannes Kepler University Linz, Altenberger Str. 69, 4040 Linz, Austria

<sup>2</sup>CEST Competence Center for Electrochemical Surface Technology, Viktor Kaplan Str. 2, 2700 Wiener Neustadt, Austria

<sup>3</sup>Christian Doppler Laboratory for Combinatorial Oxide Chemistry, Institute for Chemical Technology of Inorganic Materials, Johannes Kepler University Linz, Altenberger Str. 69, 4040 Linz, Austria  
andrei.mardare@jku.at

Combinatorial approaches for development of new materials are the most efficient ways toward identifying compositions with enhanced properties. Thin film combinatorial libraries are obtained from vapour phase using multiple source geometries where each alloying source is purposefully positioned off axis with respect to the substrate center. The obtained compositional spread along the substrate is screened and compositional mappings of the property of interest are performed<sup>1</sup>. Copper and Cu alloys are presenting a widely varied field of application. Besides the predominant use of pure Cu for electrical conductors a number of alloys possess high industrial importance due to their high mechanical strength, good thermal conductivity and excellent corrosion resistance. In the present work Cu-Ni, Cu-Zn and Cu-Pd thin film combinatorial libraries are evaluated for use in electrooxidative sensing<sup>2,3</sup>. Enhanced electrocatalytic activity was identified in each library for certain compositions during the oxidation of formaldehyde and glucose. After a compositional mapping, for all analyzed Cu-based libraries compositionally induced microstructural and crystallographic changes were identified and their influence on the sensing behaviour was evaluated. In part (a) of Figure 1 the principle of glucose detection via electrooxidation is schematically presented. The same principle is used for formaldehyde.

The electrochemical response to both formaldehyde and glucose was investigated using scanning droplet cell microscopy with flowing electrolyte (FT-SDCM). The technique allows for localised addressing of a well defined area on the surface of the library due to its contact operation mode. Using 3D printing the body of the flow cell was realized accommodating a counter electrode (CE) and a reference electrode (RE) together with the electrolyte inlet and outlet as shown in part (b) of Figure 1. At the tip of the cell a predefined opening allows the electrolyte to come in contact with the investigated surface and the sealing is ensured by using a patterned silicone O-ring. The diameter of the area addressed for a single measurement can vary in a wide range from 50  $\mu\text{m}$  to several mm providing a very good spatial resolution. All Cu-based thin film libraries were scanned in this way with a compositional resolution of maximum 0.5 at.% allowing a precise identification of interesting alloys to be further used for actual sensors development.

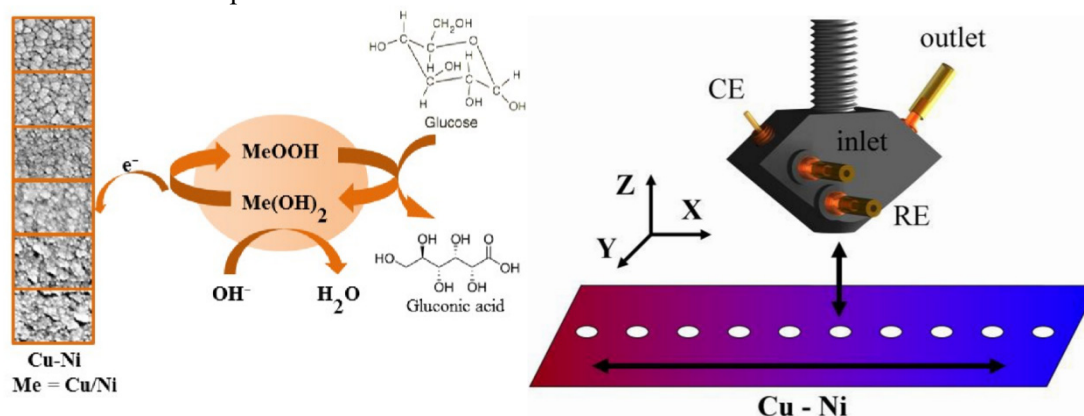


Figure 1: (a) Principle of glucose detection via electrooxidation.

(b) Flow-type scanning droplet cell microscope.

1. A.I. Mardare, A. Ludwig, A. Savan, A.W. Hassel, Sci. Technol. Adv. Mater., **15** 015006 (2014);
2. I. Pötzelberger, A.I. Mardare, A.W. Hassel, Phys. Status Solidi A, **212**, 1184–1190 (2015);
3. I. Pötzelberger, A.I. Mardare, A.W. Hassel, Phys. Status Solidi A, **In press** DOI: 10.1002/pssa.201532590.

# Laser assisted design of mesoporous carbon with embedded magnetic metal nanoparticles

C. Matei Ghimbeu<sup>1</sup>, M Sopronyi<sup>2,3</sup>, F Sima<sup>2</sup>, L Delmotte<sup>1</sup>, C Vaultot<sup>1</sup>, C Zlotea<sup>4</sup>, V Paul-Boncour<sup>4</sup>, J-M Le Meins<sup>1</sup>

<sup>1</sup>Institut de Science des Matériaux de Mulhouse, CNRS UMR 7361, 15 rue Jean Starcky, 68057 Mulhouse, France.

<sup>2</sup>Lasers Department, National Institute for Lasers, Plasma and Radiation Physics, Atomistilor 409 bis, RO-77125, Magurele, Romania

<sup>3</sup>University of Bucharest, Faculty of Physics, 405 Atomistilor Str., Magurele, Ilfov, Romania

<sup>4</sup>Institut de Chimie et des Matériaux Paris-Est CNRS-UMR 7182, UPEC, 2-8, rue Henri Dunant – 94320, Thiais, France  
camelia.ghimbeu@uha.fr

A green, simple and rapid laser synthetic approach to prepare mesoporous carbon with embedded Co particles is presented herein. This consists in the exposure of a solution containing a phenolic resin, a structure directing agent and a cobalt salt to the UV laser source followed by thermal annealing<sup>1,2</sup>. Very short irradiation times (5 to 60 min) are only required to polymerize and cross-link the phenolic resin compared to one day for classical approaches. The influence of several metallic salts on the phenolic resin and carbon characteristics (structure, texture and particle size/distribution) was systematically studied and a formation mechanism proposed based on <sup>13</sup>C and <sup>1</sup>H NMR techniques. Mesoporous carbon with uniform pore size distribution and homogeneously dispersed particles were obtained (Fig. 1a and b). The precursor salt proved to have an impact on the cobalt particle size distribution rather than on the carbon texture. Particularly, using cobalt acetate, very small particles (average particle size ~ 3.5 nm) were obtained (Fig 1b).

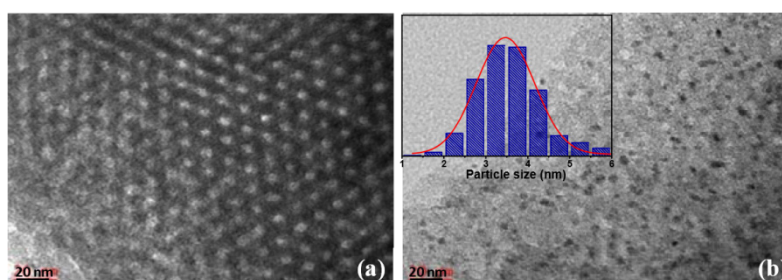


Figure 1: TEM pictures of (a) mesoporous carbon and (b) mesoporous carbon containing Co nanoparticles.

The magnetic properties of cobalt nanoparticles proved to be size-dependent: large Co nanoparticles (50 nm) behave as bulk Co whereas small Co nanoparticles are superparamagnetic (Fig. 2a, b). The particle surface chemistry, i.e., oxidation level was found to be responsible for the decrease in the magnetic moment (Fig. 2b).

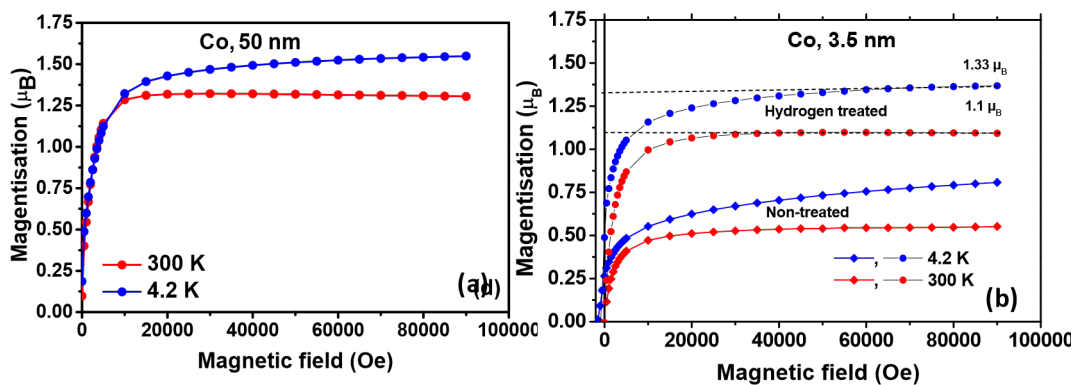


Figure 2: Magnetization curves of carbon containing cobalt nanoparticle of (a) 50 nm and (b) 3.5 nm.

1. C M Ghimbeu, M Sopronyi, F Sima, Luc Delmotte, Cyril Vaultot, C Zlotea, V Paul-Boncour, JM Le Meins, One-pot laser-assisted synthesis of porous carbon with embedded magnetic cobalt nanoparticles, *Nanoscale*, **7**, 10111 (2015);
2. C M Ghimbeu, M Sopronyi, F Sima, C Vaultot, L Vidal, J-M Le Meins and L Delmotte, "Light-assisted evaporation induced selfassembly": an efficient approach toward ordered carbon materials, *RSC Advances*, **5**, 2861(2015).

# Molecular resonances: from electron/ion to photon/neutral collisions and backwards

J. Zs. Mezei<sup>1,2,3,4</sup>, F. Colboc<sup>1</sup>, D. A. Little<sup>5</sup>, N. Pop<sup>6</sup>, K. Chakrabarti<sup>7</sup>, O. Motapon<sup>8</sup>, A. Bultel<sup>9</sup>, K. Hassouni<sup>2</sup>, J. Tennyson<sup>5</sup>, Ch. Jungen<sup>3</sup> and I. F. Schneider<sup>1,3</sup>

<sup>1</sup>Laboratoire Ondes et Milieux Complexes, CNRS, Université du Havre, Normandie Université, France

<sup>2</sup>Laboratoire des Sciences des Procédés et des Matériaux, CNRS, Université Paris 13, France

<sup>3</sup>Laboratoire Aimé Cotton, CNRS, ENS Cachan and Université Paris-Sud, Orsay, France

<sup>4</sup>Institute of Nuclear Research of the Hungarian Academy of Sciences, Debrecen, Hungary

<sup>5</sup>Department of Physics and Astronomy, University College London, United Kingdom

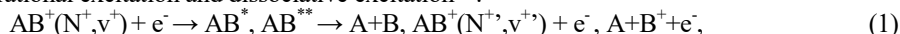
<sup>6</sup>Department of Physical Foundation of Engineering, Politehnica University Timișoara, Romania

<sup>7</sup>Department of Mathematics, Scottish Church College, Kolkata, India

<sup>8</sup>Department of Physics, Faculty of Sciences, University of Douala, Cameroon

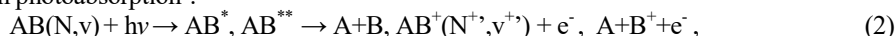
<sup>9</sup>Complexe de Recherche Interprofessionnel en Aérothermochimie, CNRS, Université de Rouen, France, ioan.schneider@univ-lehavre.fr

Dissociative recombination, ro-vibrational excitation and dissociative excitation<sup>1-4</sup>:



are major elementary processes in numerous cold ionized gases, including those produced within the Laser Induced Breakdown Spectroscopy (LIBS), or within the Ion Implantation Plasma (IIP) technique. The quantum interference between the *direct* mechanism – capture into the doubly-excited states  $AB^{**}$  – and the *indirect* one – temporary capture into a Rydberg state  $AB^*$  – induces resonances in the cross section, as illustrated in the left and side of Fig. 1 for the dissociative recombination of  $HD^+$ .

Similar resonant processes appear in photoabsorption<sup>5</sup>:



where, as in the case of  $H_2$ , they may amplify by an order of magnitude the cross section.

We provide cross sections and rate-coefficients, as illustrated in the right-hand side of Fig. 1 for  $HD^+$ , in order to understand or predict the kinetics of the above-invoked plasmas.

The account of the resonant captures is the main condition to reach high accuracy of these ratecoefficients and, consequently, of the collisional-radiative models<sup>6</sup>. Further examples will be provided for  $CO^+$ <sup>3</sup>,  $N_2^+$ <sup>4</sup> and  $BF^+$  during the conference.

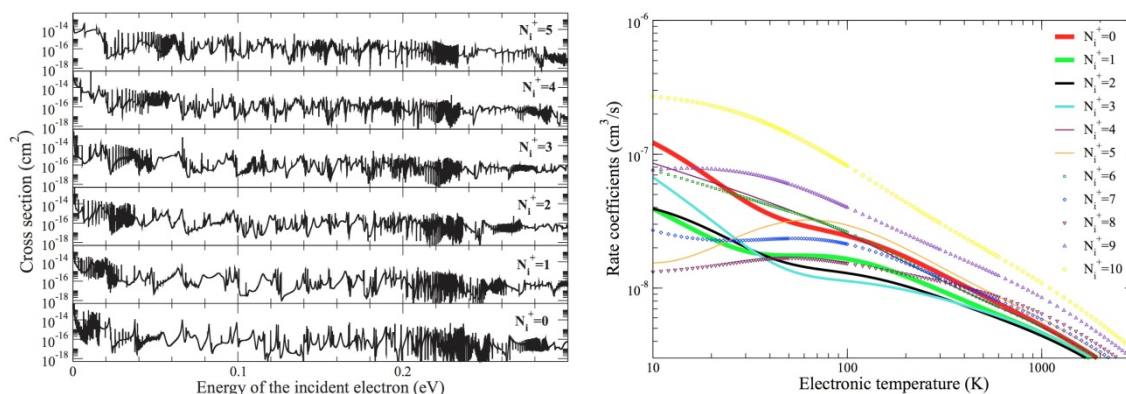


Figure 1. Dissociative Recombination of vibrationally relaxed ( $v_i^+=0$ )  $HD^+$  on its lowest rotational  $N_i^+$  states: cross sections (left) and Maxwell rate coefficients (right)<sup>2</sup>.

1. I. F. Schneider, O. Dulieu, J. Robert, editors, Proceedings of DR2013: The 9th International Conference on Dissociative Recombination: Theory, Experiment and Applications, Paris, July 7-12, 2013, *EPJ Web of Conferences* **84** (2015);
2. O. Motapon *et al*, *Phys. Rev. A* **90**, 012706 (2014);
3. J. Zs. Mezei *et al*, *Plasma Sources Science and Technology* **24**, 035005 (2015);
4. D. A. Little *et al*, *Phys. Rev. A* **90** 052705 (2014);
5. J. Zs. Mezei *et al*, *Phys. Rev. A* **85**, 043411 (2012);
6. Yu. Ralchenko (ed.), «Modern Methods in Collisional-Radiative Modeling of Plasmas», Springer Series on Atomic, Optical, and Plasma Physics **90** (2016).

# Ultrashort pulse laser processing of glass material surfaces

I. Mirza<sup>1</sup>, N. M. Bulgakova<sup>1,2</sup>, V. Michálek<sup>3</sup>, O. Haderka<sup>3,4</sup>, L. Fekete<sup>5</sup> and T. Mocek<sup>1</sup>

<sup>1</sup>HiLASE Centre, Institute of Physics ASCR, Za Radnici 828, 25241 Dolní Břežany, Czech Republic

<sup>2</sup>Institute of Thermophysics SB RAS, 1 Lavrentyev Ave., 630090 Novosibirsk, Russia

<sup>3</sup>Institute of Physics ASCR, Joint Laboratory of Optics of Palacký University and Institute of Physics ASCR, 772 07 Olomouc, Czech Republic

<sup>4</sup>Regional Centre of Advanced Technologies and Materials, Joint Laboratory of Optics of Palacký University and Institute of Physics ASCR, Palacký University, 17. listopadu 12, 771 46 Olomouc, Czech Republic

<sup>5</sup>Institute of Physics ASCR, Na Slovance 1999/2, 18221 Praha, Czech Republic

mirza@fzu.cz

With increasing use of glasses and transparent crystals in different fields of science and applications, ranging from electronics, radiation protection, automotive to life sciences and biomedical technologies, there is a growing interest in better and cleaner processing (cutting, drilling and micromachining) of such materials using available laser technologies. Femtosecond (fs) lasers have proven to be an excellent tool for this procedure, as they are able to produce high quality ablation craters and structures<sup>1,2</sup> due to reduced heat affected zone as compared to pico- and nanosecond pulsed lasers. Due to the complexity of ultrafast laser ablation processes of transparent dielectrics, numerous studies have been performed understand better the photo-excitation, electron energy relaxation and material blow off mechanisms. Stuart *et al.*<sup>3</sup>, when studying the damage threshold of fused silica (SiO<sub>2</sub>) by 800 nm fs and ps laser pulses, found that, for fs pulses, the damage threshold depends only slightly on the pulse duration with a slight decrease toward very short fs pulses. At the same irradiation conditions, Du *et al.*<sup>4</sup> investigated plasma lightning from fused silica. Comparing these two studies, it becomes evident that the damage and plasma lightning thresholds coincide for pulses longer than 10 ps while, at fs pulse durations, the luminous plasma emission appears at fluences much higher than the ablation threshold. By inspecting the crater morphologies, Lenzner *et al.*<sup>1</sup> discovered dramatic improvement in the ablation crater quality towards few cycle laser pulses.

In this work, we link the studies<sup>1,3,4</sup> to verify an existing concept that, by using very short fs pulses and moderate fluence, the energy of free electrons produced by laser light absorption can be considerably reduced due to insufficient time for inverse bremsstrahlung and, hence, avalanche ionization. As a result, within a certain range of irradiation parameters, ablation of glass matrix is believed to be produced without substantial heating and at reduced thermal stresses that is sometimes called “cold ablation”. The experimental studies have been carried out on the example of Corning<sup>®</sup> Willow glass irradiated by single pulses of 800 nm, 130 fs Ti:Sapphire laser. The damage threshold, crater formation at different laser fluences as well as the plasma lightning threshold and spectra with increasing laser fluence were investigated. Surprisingly, the plasma lightning threshold coincides for Willow and fused silica glasses. To gain better insight into the processes connected with free electron plasma emission, numerical modelling of free electron plasma formation and lattice heating through electron-lattice relaxation and electron recombination into excitonic states in fused silica has been performed.<sup>5</sup> Contrary to the concept of “cold ablation”, simulations reveal very high free electron energies even near the ablation threshold. Furthermore, heating of the glass matrix takes place at fs time scale that must culminate in material ejection from the target at ultrashort timescales. Inspecting morphology of craters created at different laser fluences, we have revealed manifestation of coexistence of several mechanisms of ablation. Finally we extend our discussion to the regimes of burst-mode laser ablation with hundreds of MHz intraburst repetition rate<sup>6</sup> with an analysis of the possible impacts of high repetition rates on laser processing of materials.

1. M. Lenzner, F. Krausz, J. Krüger, and W. Kautek, Photoablation with sub-10 fs laser pulses, *Appl. Surf. Sci.* **154-155**, 11-16 (2000);

2. A. Ostendorf, G. Kamlage, U. Klug, F. Korte, B.N. Chichkov, Femtosecond versus picosecond laser ablation, *Proc. SPIE* **5713** (2005); doi:10.1117/12.597975;

3. B.C. Stuart, M.D. Feit, S. Herman, A.M. Rubenchik, B.W. Shore, M.D. Perry, Optical ablation by high-power short-pulse lasers, *J. Opt. Soc. Am. B* **13**, 459-468 (1996);

4. D. Du, X. Liu, G. Korn, J. Squier, and G. Mourou, Laser-induced breakdown by impact ionization in SiO<sub>2</sub> with pulse widths from 7 ns to 150 fs, *Appl. Phys. Lett.* **64**, 3071-3073 (1994);

5. N.M. Bulgakova, V.P. Zhukov, I. Mirza, Yu.P. Meshcheryakove, J. Tomáščík, V. Michálek, O. Haderka, L. Fekete, A.M. Rubenchik, M.P. Fedoruk, T. Mocek, Ultrashort-pulse laser processing of transparent materials: Insight from numerical and semi-analytical models, *Proc. SPIE* **9735**, 97350N (2016);

6. C. Kerse, H. Kalaycıoğlu, P. Elahi, K. Yavuz, I. Mirza, N.M. Bulgakova, F. Ömer İlday, Ultrafast micromachining of Cu and Si at ultrahigh repetition rates with pulse bursts', *Conference on Lasers and Electro-Optics Pacific Rim (Busan)* (2015), 27E2\_4.



# Direct-writing of Cu-Ni micropatterns using femtosecond laser reduction of CuO/NiO nanoparticles

M. Mizoshiri, J. Sakurai, S. Hata

Department of Micro-Nano Systems Engineering, Graduate School of Engineering, Nagoya University,  
Furo-cho, Chikusa-ku, Nagoya, Aichi, 464-8603 Japan  
mizoshiri@mech.nagoya-u.ac.jp

Direct-writing of metal micropatterns have received attention as additive manufacturing and printed electronic technology. To date, Cu and Ni micropatterns have been fabricated in air by reductive sintering and melting of CuO and NiO nanoparticles, respectively, using continuous-wave and nanosecond pulse lasers.<sup>1,2</sup> We have also studied femtosecond laser direct-writing of Cu-based micropatterns. Cu-rich and Cu<sub>2</sub>O-rich micropatterns were selectively formed in air by controlling femtosecond laser irradiation conditions.<sup>3</sup> However, alloy micropatterning has not been reported. In this presentation, Cu-Ni micropatterns were fabricated using femtosecond laser reduction of CuO/NiO mixed nanoparticles (NPs).

CuO/NiO NP solution were prepared by mixing of commercially available CuO NPs (<50 nm), NiO NPs (<50 nm), ethylene glycol (EG), and polyvinylpyrrolidone (PVP). The concentration of CuO NPs, NiO NPs, EG, and PVP, were 30 wt.%, 30 wt.%, 27 wt.%, and 13 wt.%, respectively. The solution was spin-coated on a glass substrate (thickness: ~1 mm). Femtosecond fiber laser with operating wavelength of 780 nm, pulse duration of 120 fs, and repetition rate of 80 MHz was used for direct-writing of micropatterns. The laser pulses were focused onto the surface of the solution film using an objective lens of 0.80 numerical aperture. After writing the micropatterns, non-irradiated CuO and NiO NPs were removed by rinsing the sample substrate into EG and ethanol. The crystal structures of the micropatterns were examined by an X-ray micro-diffractometer (Rigaku RINT RAPID-S). Electrical conductivity of the micropatterns was evaluated using 4 probe method. The micropattern (1 mm × 20 mm) was used for XRD analysis and measurement of electrical conductivity. Laser writing was conducted by raster scanning of the focal spot with the pitch of 5 μm.

Figure 1 show XRD spectra of the micropatterns fabricated at the pulse energy of 0.22-0.62 nJ and the writing speed of 20 mm/s. When the pulse energy was 0.62 nJ, the intense CuNi diffraction peaks were observed. The CuO and NiO peak intensities were increased by decreasing pulse energy. These results indicate that CuNi alloy is composed under the large laser irradiation energy. The electrical conductivity of the micropatterns is shown in Fig. 2. An optical microscope image of the micropattern for measurement was also shown in an insert of Fig. 2. The electrical conductivity of the micropatterns was increased with increasing the pulse energy at pulse energy of 0.22-0.62 nJ, which is consistent with the increases of CuO and NiO peak intensities in Fig. 1. Dependence of the electrical conductivity on the laser writing speed and its application for the fabrication of microdevices are also reported in the presentation.

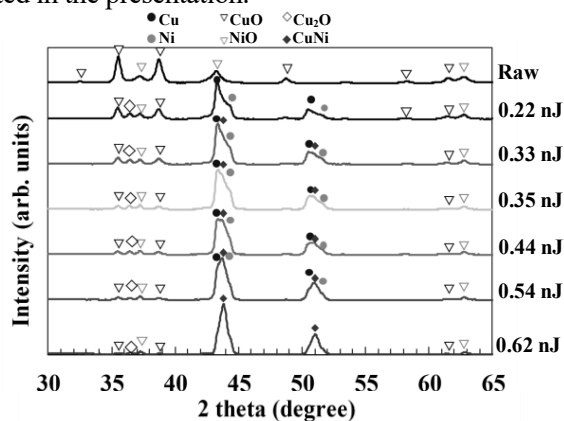


Fig. 1: XRD spectra of the micropatterns fabricated at pulse energy of 0.22-0.62 nJ and the writing speed of 20 mm/s

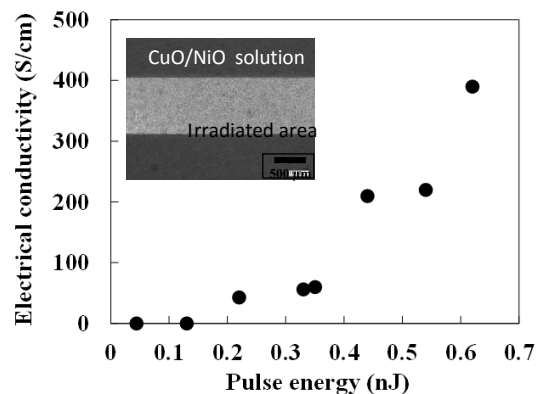


Fig. 2: Dependence of electrical conductivity of the micropatterns on pulse energy at writing speed of 20 mm/s

1. B. Kang, S. Han, J. Kim, S. Ko, and M. Yang, One-step fabrication of copper electrode by laser-induced direct local reduction and agglomeration of copper oxide nanoparticle, *J. Phys. Chem. C*, **115**, 23664-23670 (2011);
2. D. Paeng, D. Lee, J. Yeo, J.-H. Yoo, F. I. Allen, E. Kim, H. So, H. K. Park, A. M. Minor, and C. P. Grigoropoulos, *J. Phys. Chem. C*, **119**, 6363-6372 (2015);
3. M. Mizoshiri, S. Arakane, J. Sakurai, S. Hata, Direct writing of Cu-based micro-temperature detectors using femtosecond laser reduction of CuO nanoparticles, *Appl. Phys. Express*, **9**, 036701 (2016).

# Laser-induced pressure waves in glass: time-resolved studies

A. Mouskeftaras<sup>1</sup>, B. McMillen<sup>1</sup>, Y. Bellouard<sup>1</sup>

<sup>1</sup> Galatea Lab, STI/IMT, Ecole Polytechnique Fédérale de Lausanne (EPFL), CH-2002 Neuchâtel, Switzerland  
alexandros.mouskeftaras@epfl.ch

We present an experimental study of laser-induced acoustic waves generated in bulk glass (fused silica, borosilicate). These waves present a fundamental and applied scientific interest since they drive both void formation and modification to the surrounding material<sup>1</sup>, making them an elementary process in laser material processing. Although numerous studies have been performed on this subject<sup>2,3,4</sup>, very little is known about the actual pressure generated by these sound waves. In this study, we use tightly-focused femtosecond laser pulses (150 fs) at 1035 nm to locally modify the dielectric constant of the medium and reach energy densities that are above the damage threshold of the bulk substrate. Energy relaxation takes place through the release of a pressure wave, which propagates in the surrounding medium. To measure the properties of these waves and their effects on the surrounding material, an in-situ optical microscopy setup has been implemented to obtain time-resolved images in transmission (see Fig. 1). Furthermore, we use polarization sensitive analysis<sup>5</sup> to measure the laser-induced birefringence, which we relate to stress using photoelasticity. In parallel, we use a spatially-separated, time-delayed double-pulse processing scheme to study the effects of “simultaneous” and “sequential” processing. Our results obtained with different focusing conditions, pulse energies, and polarization states will be discussed in detail.

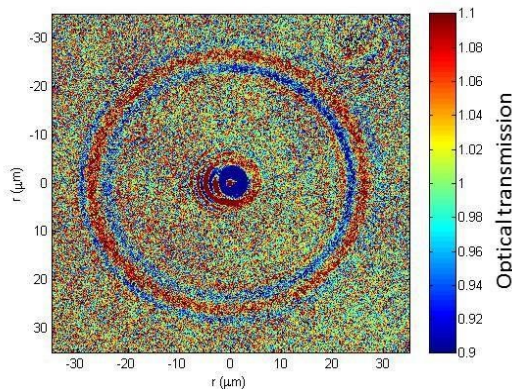


Figure 1: Light transmission 6 ns after the laser pulse excitation inside the bulk of a microscope slide. Single-pulse excitation is used with the following laser characteristics: pulse energy is 800 nJ, pulse duration is 150 fs and a NA=0.4 microscope objective is used to focus the laser pulse.

Figure 1: Light transmission 6 ns after the laser pulse excitation inside the bulk of a microscope slide. Single-pulse excitation is used with the following laser characteristics: pulse energy is 800 nJ, pulse duration is 150 fs and a NA=0.4 microscope objective is used to focus the laser pulse.

1. E. Gamaly, et al., Laser-matter interaction in the bulk of a transparent solid: Confined microexplosion and void formation, *Phys. Rev. B* 73, 214101 (2006);
2. A. Mermillod-Blondin, et al., Dynamics of femtosecond laser induced void like structures in fused silica, *Applied Physics Letters*, 94(4), 041911 (2009);
3. M. Sakakura, et al., Observation of pressure wave generated by focusing a femtosecond laser pulse inside a glass, *Optics Express*, 15, 5674-5686 (2007);
4. Y. Hayasaki, et al., Time-resolved interferometry of femtosecond laser-induced processes under tight focusing and close-to-optical breakdown inside borosilicate glass, *Optics Express*, 19, 5725-5734 (2011);
5. T. Tochio, et al., Transient stress imaging after irradiation with a focused femtosecond laser pulse inside a single crystal, *Japanese Journal of Applied Physics*, 51(12R), 126602 (2012).

## Comparison of pulsed electron beam deposition and pulsed laser deposition methods

M. Nistor

National Institute for Lasers, Plasma and Radiation Physics (NILPRP), Plasma Physics and Nuclear Fusion Laboratory (L 22),  
Str. Atomistilor 409, P.O. Box. MG-36, 77125 Bucharest-Magurele, Romania  
mnistor@infim.ro

The pulsed electron beam deposition (PED) is a relatively recent thin film growth method which uses a pulsed electron beam (110 ns, polyenergetic electron distribution up to 16 keV) to ablate a target material. PED and pulsed laser deposition (PLD) present some similar characteristics: the pulsed nature of process, the very anisotropic character of the ablation plume and the high energy of species. The main difference between PED and PLD is the use of electrons instead of photons which leads, via the specificities of the electron-matter interactions, to an extension of the range of materials that could be ablated, e.g. to those that are transparent to laser wavelengths used in PLD. As a result, thin films of complex materials, whatever their composition or properties are easily obtained by PED, even thin films of polymers and organic compounds can be grown by this method. To study the potential of the PED method to grow high quality thin films, we have developed a compact pulsed electron beam source based on a channel-spark discharge<sup>1</sup>. We have established the relationship between the discharge parameters and the electron beam distribution and their influence on the thin films. *In situ* diagnostics of ablation plasma produced in PED showed that the kinetic energy of the species emitted by the target is roughly in the 10 to 60 eV range, leading to high surface mobility to these species in the growing film. As a result, the growth of high crystalline quality thin films at relatively low temperatures has been obtained<sup>2,3</sup> and epitaxial films are easily obtained. Moreover, it is possible to control the density of structural defects via the growth conditions, and thus to tune the physical properties of the films. In this frame, metal-semiconductor transition was evidenced in epitaxial un-doped

ZnO thin films grown by PED on c-cut single crystal substrates and their interpretation in the frame of the quantum corrections to conductivity in disordered oxides was addressed<sup>2</sup>. Physical properties of oxide thin films grown by PED will be compared with those observed for PLD method<sup>4</sup>, evidencing the differences and specificities of each method for thin film growth.

1. M. Nistor, N.B. Mandache, J. Perrière, Pulsed Electron Beam Deposition of Oxides Thin Films, *J. Phys. D: Appl. Phys.* **41**, 165205 (2008);
2. M. Nistor, F.Gherendi, N.B.Mandache, C. Hebert, J. Perrière, W.Seiler, Metal-semiconductor transition in epitaxial ZnO thin films, *J.Appl. Phys.* **106**, 103710 (2009);
3. W.Seiler, M.Nistor, C.Hebert, J.Perrière, Epitaxial undoped indium oxide thin films: Structural and physical properties, *Solar Energy Materials and Solar Cells* **116**, 34 – 42 (2013);
4. M. Nistor, L. Mihut, E. Millon, C. Cachoncille, C. Hebert, J. J.Perrière, Tailored electric and optical properties of Nd doped ZnO: from transparent conducting oxide to photon down-shifting thin films, *RSC Adv.* **6**, 41465-41472 (2016).

## Surface structuring of silicon with femtosecond optical vortex laser beams generated by a q-plate

J. JJ Nivas<sup>1,2</sup>, Zhenming Song<sup>1,3</sup>, F. Cardano<sup>1</sup>, A. Rubano<sup>1,2</sup>, A. Vecchione<sup>4</sup>,  
R. Fittipaldi<sup>4</sup>, D. Paparo<sup>5</sup>, L. Marrucci<sup>1</sup>, R. Bruzzese<sup>1,2</sup>, S. Amoruso<sup>1,2</sup>

<sup>1</sup>Dipartimento di Fisica, Università di Napoli Federico II, Complesso Universitario di Monte S. Angelo, Via Cintia, I-80126 Napoli, Italy.

<sup>2</sup>CNR-SPIN UOS Napoli, Complesso Universitario di Monte S. Angelo, Via Cintia, I-80126 Napoli, Italy.

<sup>3</sup>School of Science, Tianjin Polytechnic University, Binshuixi Road 399#, Xiqing District, Tianjin, 300387 P. R. China.

<sup>4</sup>CNR-SPIN, UOS Salerno, Via Giovanni Paolo II 132, I-84084 Fisciano (SA), Italy.

<sup>5</sup>National Research Council, Institute of Applied Science & Intelligent Systems (ISASI) 'E. Caianiello', Via Campi Flegrei 34, 80078 Pozzuoli (NA), Italy.  
amoruso@na.infn.it; salvatore.amoruso@umina.it

There is increasing interest for surface structures at the micro- and nano-scale. Femtosecond laser surface structuring with a Gaussian beam has already distinguished itself as a versatile method to fabricate surface structures on metals and semiconductors.<sup>1</sup> In this communication, we report on femtosecond laser surface structuring with an optical vortex (OV) beam generated by a *q-plate*. The laser source is a Ti:Sa laser system delivering linearly polarized  $\approx 35$  fs pulses at 800 nm with a Gaussian beam spatial profile, at a repetition rate of 100 Hz, in air. The *q-plate* allows producing cylindrical vector beams with a state of polarization (SoP) that varies spatially retaining an axial symmetry.<sup>2</sup> In particular, we use a *q-plate* with a topological charge  $q=1/2$  which allows generating optical vortex (OV) beams carrying an orbital angular momentum (OAM)  $\ell=\pm 1$ . These OV beams present an annular spatial distribution of the laser intensity and can be tuned to several different spatial distributions of the SoP, like for example azimuthal, radial, spiral or linear. The OV beam produced by the *q-plate* is focused onto a silicon target, mounted on a computer-controlled XY-translation stage, at normal incidence. An electromechanical shutter controls the number of laser pulses,  $N$ , irradiated on the target surface. The morphological modifications of the irradiated surface are studied by field emission scanning electron microscopy (SEM). The different SoP of the OV beam result in the generation of several regular surface patterns on the silicon target (see Fig. 1, e.g.). Here, we report first a thorough analysis of the regular structures (ripples and grooves) as a function of the number of pulses  $N$  and laser pulse energy  $E_p$ .<sup>3</sup> Then, we discuss the novel possibility of generating non-symmetric surface structure patterns by appropriate tuning of the *q-plate* voltage and illustrate an interpretative framework explaining the experimental observations. Our findings suggest that direct femtosecond laser surface structuring is a versatile approach both to generate a variety of surface patterns and to characterize complex femtosecond laser beams.

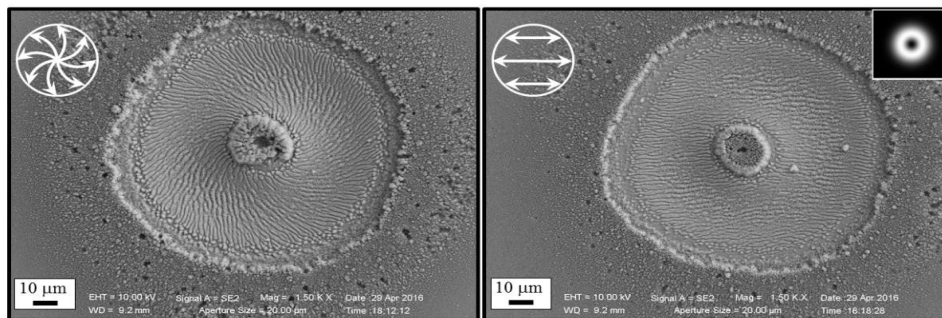


Figure 1: SEM images illustrating two examples of surface structure patterns generated by irradiating a silicon target with an OV beam with  $\ell=1$  and two different SoP: spiral (left panel) and linear (right panel). The SoP is indicated by the cartoon reported in the upper-left corner of each image. The inset in the upper-right corner of the left panel reports the typical annular spatial intensity distribution of the OV beam. The SEM images show the presence of various regions characterized by a different morphology. The central and external regions of the beam spot are decorated with assemblies of nanoparticles produced during the target ablation. The peripheral regions of lower energy at the two outer edges of the annular OV beam are namely characterised by subwavelength ripples oriented along the normal to the local laser polarization, while the internal region of the OV beam, at higher energy, presents microgrooves preferentially directed along the local laser polarization.

1. A.Y. Vorobyev and C. Guo, Direct femtosecond laser surface nano/microstructuring and its applications, *Laser Photonics Rev.*, **7**, 385–407 (2013);
2. Q. Zhan A. Cylindrical vector beams: from mathematical concepts to applications, *Advances in Optics and Photonics* **1**, 1–57 (2009);
3. J. JJ Nivas, S. He, A. Rubano, A. Vecchione, D. Paparo, L. Marrucci, R. Bruzzese, S. Amoroso, Direct Femtosecond Laser Surfaces Structuring with Optical Vortex Beams Generated by a q-plate, *Scientific Reports* **5**, 17929 (2015).

## DFT Study of Photocatalytic Degradation of Common Antibiotics on TiO<sub>2</sub> Nanoclusters

C. I. Oprea and M. A. Gîrțu

*Faculty of Applied Sciences and Engineering, Ovidius University of Constanța, Constanța - 900527, Romania  
mihai.girtu@univ-ovidius.ro*

We report results of density functional theory calculations of penicillin G, penicillin V, ampicillin and amoxicillin in solution as well as adsorbed on a TiO<sub>2</sub> nanoclusters, in order to study the photocatalytic degradation under visible light irradiation. We analyze the absorption spectrum of the free and adsorbed penicillin, the binding configurations, the energy spectrum and the density of states and discuss the likelihood of the charge-transfer from the pollutant to the titania substrate. We compare and contrast the photodegradation processes for the four types of antibiotics, discussing the possible mechanisms relevant for the residual water cleaning.

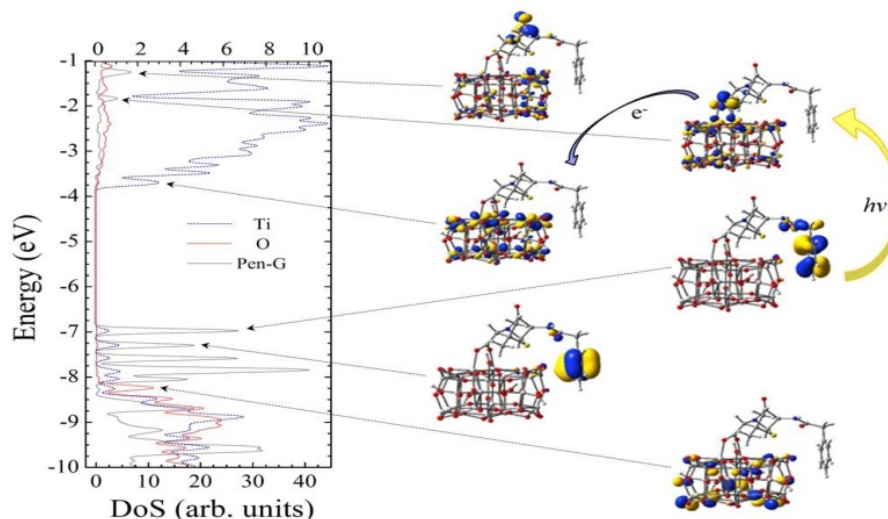


*Figure 1: Density of states and electron density of key molecular orbitals of Penicillin G on TiO<sub>2</sub> nanoclusters*

The orbitals with mixed character, having contributions from both the antibiotic and the catalyst lead to the occurrence of weak but allowed transitions in the visible range. We suggest that such optical transitions induce the electron transfer from the pollutant to the catalyst. The extra electron may be further transferred from the semiconductor to the water molecules in solution, causing the appearance of superoxide, O<sub>2</sub><sup>-</sup>, which attacks the antibiotic degrading it.

*Acknowledgements:* The financial support of UEFISCDI/CNCS through the grant PN2-ID-PCE-14/2013 is gratefully acknowledged.

1. C.I. Oprea, L.C. Petcu, and M.A. Gîrțu, IEEE Conference Proceedings: E-Health and Bioengineering Conference (EHB), 2015.

# Nanostructure and optical properties of noble metal particles prepared by nanosecond and picosecond ablation in liquid

P. M. Ossi<sup>1</sup>, M. Santoro<sup>2</sup>, E. Fazio<sup>2</sup>, S. Trusso<sup>3</sup>, P. Calandra<sup>4</sup>, M. Tommasini<sup>5</sup>, C. Zanchi<sup>6</sup>, R. Saija<sup>2</sup>, F. Neri<sup>2</sup>

<sup>1</sup>Dipartimento di Energia & NEMAS, Politecnico di Milano, Via Ponzio 34-3, 20133 Milano, Italy

<sup>2</sup>Dipartimento di Scienze Matematiche e Informatiche, Scienze Fisiche e Scienze della Terra, Università di Messina, Viale Ferdinando Stagno d'Alcontres 31, 98166 Messina, Italy

<sup>3</sup>CNR-IPCF Istituto per i Processi Chimico-Fisici, Viale F. Stagno d'Alcontres 37, 98158 Messina, Italy

<sup>4</sup>CNR-ISMN Istituto per lo studio dei materiali nanostrutturati, Sede Montelibretti, Monterotondo Stn, Roma, Italy

<sup>5</sup>Dipartimento di Chimica, Materiali, Ingegneria Chimica, Politecnico di Milano, Piazza L. da Vinci 32, 20133 Milano, Italy

<sup>6</sup>Dipartimento di Energia, Politecnico di Milano, Via Ponzio 34-3, 20133 Milano, Italy

paolo.ossi@polimi.it

In the last decade, nanometer-sized noble metal (Au; Ag) structures have been widely used for optics applications in the visible range because of their remarkable plasmonic ability to enhance local electromagnetic fields. Noble metal nanoparticles (NPs) are among the most extensively studied colloidal systems, due to their characteristic surface plasmon resonances (SPR) of interest for biological sensing and imaging. Ag and Au NPs are exploited for their optical, anti-microbial, anti-inflammatory properties and excellent biocompatibility. Chemical reduction of silver/gold salt by borohydride, citrate and ascorbate is the most frequently applied route to prepare Ag and Au NPs as stable, colloidal dispersions in water or organic solvents. The synthesis of NPs by chemical reduction methods often requires the presence of stabilizers to avoid colloid agglomeration. The alternative and convenient method, that does not need any surfactant to stabilize the metallic colloid, is the topdown approach of Pulsed Laser Ablation in Liquid (PLAL). Here, we report the use of nanosecond ( $\lambda=532\text{ nm}$ ;  $\tau=5\text{ ns}$ ) and picosecond ( $\lambda=532\text{ nm}$ ;  $\tau=6\text{-}8\text{ ps}$ ) PLAL at varying fluences (from 0.1 to 1.5 J/cm<sup>2</sup>) and irradiation times (from 2 to 20 min) to synthesize Ag and Au NPs in water-based solutions. Highly stable and chemically pure NPs, with average size ranging from 5 to 100 nm, different degrees of agglomeration and considerably different optical properties were synthesized by ns- and respectively ps-PLAL. The morphology and the size distribution of the particles were investigated carrying out STEM and Dynamic Light Scattering (DLS) measurements. A theoretical method based on the multipole expansion of the electromagnetic field in the framework of the transition matrix formalism was used to reproduce the optical absorption response as well as to discriminate whether the samples are characterized by nanostructures with large or small aspect ratio. Both for ns and for ps irradiations is remarkable the intrinsic feature of PLAL to produce clean, stable species making it attractive as an eco-compatible technique. In particular, by ps-PLAL chemically and morphologically stable nanocolloids with a narrow size distribution are synthesized in short times (few minutes).

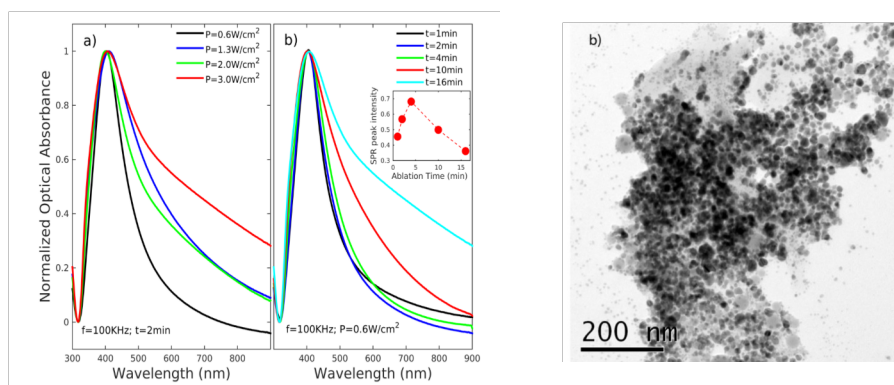


Figure 1: (a) Optical absorbance and STEM images of Ag nanocolloids prepared by ps-PLAL

Au<sub>1-x</sub>Ag<sub>x</sub> (x=25; 50; 75) alloyed NPs were synthesized mainly by ns-PLAL. Their optical properties were investigated as a function of NP stoichiometry and synthesis history. The SERS activity of the AuAg alloys was tested in liquid and in solid state. UV-Vis Spectroscopy helped to determine the appropriate laser wavelength for the resonant excitation of the localized surface plasmon. SERS spectra obtained at increasingly lower concentrations of the standard reference dye Rhodamine 6G (R6G) were acquired as a preliminary step towards application to biomedical sensors. The optical limiting properties were investigated by the Z-scan method, using a nanosecond pulsed laser. Both the different solvents and the NP morphological properties play a driving role in the nonlinear optical response.

# Light-induced spatial phase modulation in films of DNA-CTMA-DR1 investigated using a pump – probe interferometric method

A. Petris<sup>1</sup>, P. Gheorghe<sup>1</sup>, V. I. Vlad<sup>1</sup>, I. Rau<sup>2</sup>, A. M. Manea<sup>2</sup>, F. Kajzar<sup>2</sup>

<sup>1</sup>National Institute for Laser, Plasma and Radiation Physics, 409 Atomistilor Street, 077125 Bucharest – Magurele, Romania

<sup>2</sup>University Politehnica of Bucharest, Faculty of Applied Chemistry and Materials Science, 1-7 Polizu Street, 011061, Bucharest, Romania  
adrian.petris@infpr.ro

The deoxyribonucleic acid (DNA) is intensively studied in the last years as a new “green” photonic material with promising applications in organic photonics<sup>1-5</sup>. The DNA bio-polymer has a wide range of transparency in visible and near-infrared and it can be functionalized with chromophores, ensuring a tuning of the optical properties of the resulted complexes.

We report the results obtained in an experimental study of the spatial phase modulation induced by light in the DNA – Cetyltrimethyl-Ammonium Chloride (CTMA) – Disperse Red (DR1) films.

The experiments have been performed using an interferometric pump-probe method, recently introduced<sup>4,6</sup>. This method is briefly described here. A focused pump beam is exciting locally the nonlinear response of the investigated sample, which is placed in the test arm of a Mach-Zehnder interferometer. A weak laser beam, incident in the interferometer, is split in two beams which pass along the test and reference arms of the interferometer, respectively, and are super-imposed on the sensitive array of a laser beam analyzer, producing an interference pattern. The spot size of the weak test beam is larger than the spot size of the focused pump beam, in the sample plane. The interference fringe pattern recorded when the pump beam is switched ON contains the information about the refractive index change induced in the sample by the pump light. Using an appropriate Fourier transform method for the Direct Spatial Reconstruction of the Optical Phase (DSROP)<sup>7-9</sup> implemented by us<sup>4,6</sup>, the spatial distribution of the phase modulation induced by the pump light in the sample can be extracted from a single fringe pattern.

In the experimental investigation performed in DNA-CTMA-DR1 films, the second harmonic ( $\lambda=532$  nm) of a c.w. Nd:YAG laser is used as pump light and a He-Ne laser beam ( $\lambda=633$  nm) as probe beam. Using the interferometric method, the spatial distribution of the optical phase change, its magnitude and its dependence on the incident pump intensity were determined in the investigated DNA-CTMA-DR1 films. As example, in Fig. 1 are shown the locally distorted fringe pattern, for the pump intensity  $I=56$  W/cm<sup>2</sup>, and the corresponding light-induced phase modulation,  $\Delta\Phi$ , extracted from it using the implemented DSROP method. The results are important for nonlinear photonics in applications based on all-optical spatial light modulation.

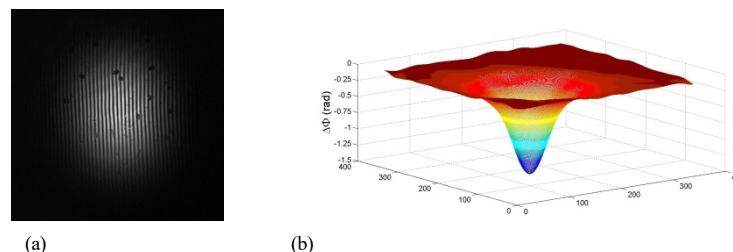


Figure 1: The locally distorted fringe pattern (a) and the corresponding light-induced phase modulation (b) for pump intensity  $I = 56$  W/cm<sup>2</sup>,

**Acknowledgments:** This work has been financed by the project UEFISCDI Partnerships 3/2012 “Bio-Nano-Photo” and by the National Authority for Scientific Research and Innovation in the frame of Nucleus programme- contract 4N/2016.

1. A. J. Steckl, DNA – a new material for photonics?, *Nature Photonics* **1**, 3-5 (2007);
2. I. Rau, J. G. Grote, F. Kajzar, A. Pawlicka, DNA-novel nanomaterial for applications in photonics and in electronics, *Comptes Rendus Physique* **13**, 853-864 (2012);
3. T. Bazaru Rujoiu, A. Petris, V.I. Vlad, I. Rau, A.M. Manea, F. Kajzar, Lasing in DNA-CTMA doped with Rhodamine 610 in butanol, *Phys. Chem. Chem. Phys.* **17**, 13104-13111 (2015);
4. A. Petris, P. Gheorghe, V. I. Vlad, I. Rau, F. Kajzar, Interferometric method for the study of spatial phase modulation induced by light in dye-doped DNA complexes, *Rom. Rep. Phys.* **67**, 1373-1382 (2015);
5. P. Gheorghe, A. Petris, V. I. Vlad, I. Rau, F. Kajzar, A. M. Manea, Temporal evolution of the laser recording of gratings in DNA-CTMARh610 films, *Rom. Rep. Phys.* **67**, 1412-1420 (2015);
6. I. Dancus, S. T. Popescu, A. Petris, Single shot interferometric method for measuring the nonlinear refractive index, *Optics Express* **21**, 31303-31308 (2013);
7. M. Takeda, H. Ina, S. Kobayashi, Fourier-transform method of fringe-pattern analysis for computer-based topography and interferometry, *J. Opt. Soc. Am.* **72**, 156-160 (1982);
8. V. I. Vlad and D. Malacara, Direct spatial reconstruction of optical-phase from phase-modulated images, *Prog. Opt.* **33**, 261-317 (1994);
9. V. I. Vlad, D. Malacara, A. Petris, Real-time holographic interferometry using optical phase conjugation in photorefractive materials and direct spatial phase reconstruction, *Opt. Eng.* **35**, 1383-1388 (1996).

# Femtosecond laser modification of NiPd single and 5xNi/Pd multilayer thin films

S. Petrović<sup>1</sup>, B. Gaković<sup>1</sup>, D. Peruško<sup>1</sup>, B. Radak<sup>1</sup>, M. Zamfirescu<sup>2</sup>, C. R. Luculescu<sup>2</sup> and I. N. Mihailescu<sup>2</sup>

<sup>1</sup>Institute of Nuclear Sciences Vinča, University of Belgrade, POB 522, 11001 Belgrade, Serbia

<sup>2</sup>National Institute for Laser, Plasma and Radiation Physics, Magurele, Bucharest, Romania  
spetro@vinca.rs

Modification of complex nickel-palladium samples by laser processing in the femtosecond time domain is unexplored field. This work included a study of the effects caused by changes in the morphology of the compact NiPd thin layer and multi-layer 5x(Ni/Pd) structure. Alloys and thin layers of nickel and palladium have specific physical, chemical and mechanical properties, such as high corrosion resistance, good stability, high strength and porosity<sup>1</sup>. Alloy of Ni and Pd possesses high catalytic activity and can easily hydrogenated, however, recently implemented an effective catalysts and materials for hydrogen storage. Excellent synergistic effect occurs between Ni and Pd, because NiPd alloy and/or multilayer can be used as a new generation of catalysts completely different properties from individual Ni and Pd catalysts<sup>2</sup>.

The samples were processed by focused Ti:Sapphire laser beam (Clark CPA-2101) with 775 nm laser wavelength, 2 kHz repetition rate, 200 fs pulse duration. The laser-induced morphological and composition modifications have shown dependence on applied intensities and number of laser pulses. The formed surface nanostructures on the NiPd complex systems are compared with individual Ni and Pd thin films. The results show an increase in surface roughness, formation of parallel periodic surface structures, appearance of hydrodynamic features and ablation of surface material. At low number of pulses (less than 10 pulses) and low pulse energies range (not over 1.7  $\mu\text{J}$ ), the two types of LIPSS can be observed: low and high spatial frequency LIPSS (HSFL and LSFL). The low spatial frequency LIPSS (LSFL), oriented perpendicular to the laser polarization with periods slightly lower than the irradiation wavelength, was typically formed at elevated laser fluences<sup>3</sup>. On the contrary, high spatial frequency LIPSS (HSFL) was created with uniform period of two times shorter than the period of LSFL, parallel to the laser light polarization. The high spatial frequency LIPSS (HSFL) appeared at low laser energies, as well as in the wings of the Gaussian laser beam distribution for higher used pulse energy. At higher number of pulses and/or higher energy, the structures observed in center of the spot seem to be more on the Si substrate than on the metallic film.

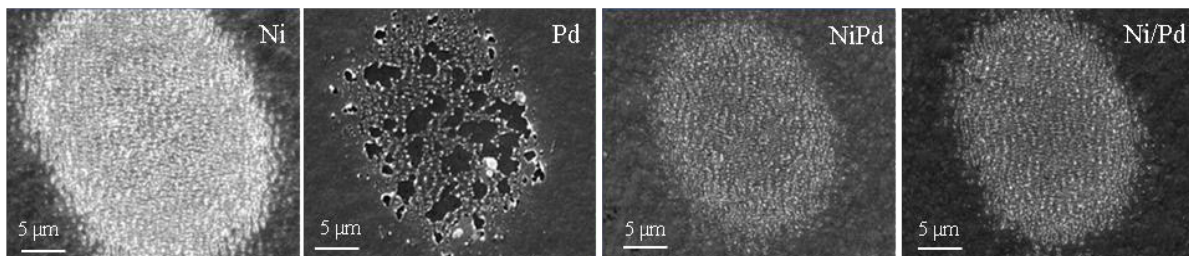


Figure 1: Comparison between the fs-induced morphology of the irradiated surfaces for single pulse regime at  $E = 1.7 \mu\text{J}$

From the comparison between irradiated samples, the morphology of LIPSS on Ni, Ni/Pd and 5xNi/Pd seems similar. In contrast, the single Pd film is much easier removed under the laser irradiation from the first pulse, the sequent pulses modifying the Si substrate.

1. M. Kasprzak, D. Baither, G. Schmitz, Diffusion-induced recrystallization in nickel/palladium multilayers, *Acta Materialia* **59**, 1734, (2011);
2. S. Yun, S.T. Oyama, Correlations in palladium membranes for hydrogen separation: A review, *Journal of Membrane Science* **375**, 28, (2011);
3. S.M. Petrovic, B. Gakovic, D. Perusko, E. Stratakis, I. Bogdanovic'-Radovic, M. Cekada, C. Fotakis, B. Jelenkovic, Femtosecond laserinduced periodic surface structure on the Ti-based nanolayered thin films, *Journal of Applied Physics* **114**, 233108 (2013).

# Effects of the quencher diffusion and the photoinitiator depletion on the spatial resolution and performance of direct laser writing by multiphoton polymerization

A. Pikulin,<sup>1</sup> N. Bituryn,<sup>1</sup> V. I. Sokolov<sup>2</sup>

<sup>1</sup>Institute of Applied Physics of Russian Academy of Sciences, 46, Ul'yanov Str., Nizhny Novgorod, 603950, Russia

<sup>2</sup>Institute on Laser and Information Technologies, Russian Academy of Sciences, Svyatoozerskaya St. 140700 Shatura Moscow Region, Russia  
pikulin@uifp.appl.sci-nnov.ru

Diffusion-assisted direct laser writing (DA-DLW) by multiphoton polymerization has been recently shown to be one of the most promising methods for the high-resolution 3D nanofabrication.<sup>1,2</sup> The improvement of the writing spatial resolution (see Fig. 1) has been observed under certain conditions when the mobile radical quencher (polymerization inhibitor) is added to the photosensitive composition. Due to the quencher diffusion, the simple idea of the polymerization threshold related to the local quencher depletion should be revised.

Here, we present a theoretical study of the laser writing in the presence of the radical quencher, focusing on the resolution capabilities and optimal writing parameters. The laser beam absorption in the polymerizable composition causes the localized depletion of the quencher molecules. If the quencher depletion is balanced by its diffusion from the outside of the focal volume, the quasi-stationary non-equilibrium concentration spatial profile with nearly-zero minimum can be obtained. The polymer is then effectively formed only in the vicinity of this minimum. The spatially-distributed quencher, in this case, has the effect similar to that of the vortex beam in two-beam writing techniques<sup>3</sup> inspired by STimulated Emission Depletion (STED) microscopy.

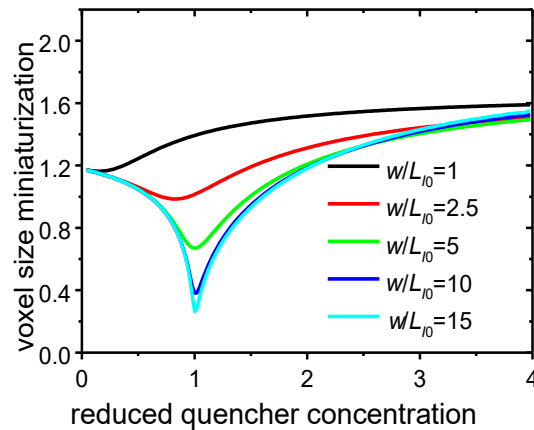


Figure 1: Voxel radius normalized by the beam waist size ( $w$ ) is plotted against the dimensionless quencher concentration in the resin.  $w/L_{10}$  is the ratio of the beam waist size and the characteristic problem scale that depends on the composition of the resin and the beam average power

We present a theoretical model of the photoinitiator depletion accompanied by its diffusion into the irradiated volume during the writing process. An analytical formula for the maximal achievable photoinitiation rate was derived. The deteriorative effect of the photoinitiator depletion both on the writing spatial resolution and performance emphasises the benefits of the writing schemes without photoinitiators.

**Acknowledgements:** This work was financially supported by the Russian Science Foundation (RSF) under project No. 14-1901659.

1. I. Sakellari, E. Kabouraki, D. Gray, V. Purlys, C. Fotakis, A. Pikulin, N. Bituryn, M. Vamvakaki, M. Farsari, Diffusion-Assisted HighResolution Direct Femtosecond Laser Writing, *ACS Nano*, **6**, 2302–2311 (2012);
2. A. Pikulin, N. Bituryn, and V. I. Sokolov, Model of diffusion-assisted direct laser writing by means of nanopolymerization in the presence of radical quencher, *AIP Adv.*, **5**, 127215 (2015);
3. J. Fischer and M. Wegener, Three-dimensional optical laser lithography beyond the diffraction limit, *Laser Photon. Rev.*, **7**, 22–44 (2013).



# Ablation behavior of dentin by femtosecond laser

Q. T. Le<sup>1,2</sup>, C. Bertrand<sup>2</sup>, R. Vilar<sup>1</sup>

<sup>1</sup>*Instituto Superior Técnico and CeFEMA – Center of Physics and Engineering of Advanced Materials, Lisbon University  
Avenida Rovisco Pais, 1049-001 Lisboa, Portugal*

<sup>2</sup>*Laboratoire ICMCB – CNRS- UPR9048, 87, Avenue du Dr Albert Schweitzer, 33608, PESSAC Cedex, France  
quang.le@tecnico.ulisboa.pt*

Thanks to their capability to ablate materials with negligible thermal effects, femtosecond lasers are extremely promising tools for minimally invasive dental surgery. Early experiments on the femtosecond ablation of dentin and enamel, the two main constituents of human teeth<sup>1,2</sup>, showed that these tissues could be effectively ablated by near infrared femtosecond lasers with no signs of carbonization and/or melting on the laser treated surface in particular when the ablation experiments are performed with low radiation intensity and low pulse repetition rates. This result was explained by a predominantly electrostatic ablation mechanism. Recently, the present authors observed a layer less than 1  $\mu\text{m}$  thick of resolidified material on enamel surfaces resulting from ablation with a wide range of radiation fluences, from near-threshold values (4  $\text{J}/\text{cm}^2$ ) to 14  $\text{J}/\text{cm}^2$ , and for a number of laser pulse as low as 5<sup>3</sup>. The existence of traces of collapsed bubbles in the resolidified material layer and the presence of amorphous calcium phosphate in this layer, detected by Raman spectroscopy, indicates that the ablation of enamel in those experimental conditions involves melting of enamel hydroxyapatite, followed by the partial decomposition of this phase accompanied by gas release, and resolidification. In the present work, the ablation behavior of dentin by using the same laser system and fluences within the range 1.5 – 14  $\text{J}/\text{cm}^2$  was studied. The morphology of the ablation surface was observed by SEM. In addition, the ablation debris were collected during the laser processing of dentin and analysed by scanning and transmission electron microscopies.

As hydroxyapatite is the dominant phase in both dentin and enamel, one would expect the ablation behavior of dentin to be similar to that of enamel. Nevertheless, no traces of resolidified material were found in the laser treated dentin surface and the pristine structure of dentin could be clearly observed by SEM, even at the radiation fluence of 14  $\text{J}/\text{cm}^2$ . Despite the absence of resolidified material in the ablation surface, TEM and SEM analysis of the ablation debris collected during the ablation of dentin showed that the amorphous calcium phosphate was the predominant phase in the debris, even at the radiation fluence of 1.5  $\text{J}/\text{cm}^2$ . The observation implies that the inorganic phase in dentin also underwent laser-induced heating processes, similar to the behavior of enamel, and the resolidified material might have been removed by the explosive ablation of collagen and water, which exist in dentin with significantly higher contents than in enamel and have rather low ablation threshold (0.06  $\text{J}/\text{cm}^2$  for collagen<sup>4</sup>, 1.12  $\text{J}/\text{cm}^2$  for pure water<sup>5</sup>). In order to confirm the suggested influence of water and collagen on the ablation behavior of dentin, the ablation experiments were performed on dentin specimens, which were treated by immersion in NaOCl solution or dehydration in vacuum to reduce the contents of collagen and water, respectively, before the experiments. The SEM analysis of craters ablated in those samples showed traces of resolidified material and collapsed bubbles, even at the radiation fluence of 1.5  $\text{J}/\text{cm}^2$ .

1. Alves, S., Oliveira, V. & Vilar, R. Femtosecond laser ablation of dentin. *J. Phys. D: Appl. Phys.* **45**, 245401 (2012);

2. Rode, A. V *et al.* Subpicosecond laser ablation of dental enamel. *J. Appl. Phys.* **92**, 2153–2158 (2002);

3. Q. T. Le, C. Bertrand, R. Vilar. *Femtosecond laser ablation enamel.* (2016);

4. Oraevsky, A. A. *et al.* Plasma mediated ablation of biological tissues with nanosecond-to-femtosecond laser pulses: relative role of linear and nonlinear absorption. *Selected Topics in Quantum Electronics, IEEE Journal of* **2**, 801–809 (1996);

5. Vogel, A., Linz, N., Freidank, S. & Paltauf, G. Femtosecond-Laser-Induced Nanocavitation in Water: Implications for Optical Breakdown Threshold and Cell Surgery. *Phys. Rev. Lett.* **100**, 38102 (2008).

# ***In vitro* behaviour of human mesenchymal stem cells on smart biointerfaces obtained by laser methods for tissue engineering applications**

L. Rusen<sup>1</sup>, L. E. Sima<sup>2</sup>, M. Icriverzi<sup>2,3</sup>, N. Mihailescu<sup>1</sup>, I. Anghel<sup>1,4</sup>, A. Bonciu<sup>1,4</sup>, S. Brajnicov<sup>1,5</sup>,  
A. Cimpean<sup>3</sup>, M. Dinescu<sup>1</sup>, A. Roseanu<sup>2</sup> and V. Dinca<sup>1</sup>

<sup>1</sup>National Institute for Lasers, Plasma and Radiation Physics, Atomistilor 409, 077125, Magurele, Bucharest, Romania

<sup>2</sup>Institute of Biochemistry, Romanian Academy, 296 Splaiul Independentei, Bucharest, Romania

<sup>3</sup>University of Bucharest, Faculty of Biology, Department of Biochemistry and Molecular Biology, Splaiul Independentei 90-94, Bucharest, Romania

<sup>4</sup>University of Bucharest, Faculty of Physics, RO-077125, Magurele, Romania

<sup>5</sup>University of Craiova, Faculty of Mathematics and Natural Sciences, RO-200585, Craiova, Romania  
laurentiu.rusen@inflpr.ro

Providing controlled and tunable interfacial properties of materials represents a key strategy for modulating the behaviors of cells, aiming the development of new generation of high-performance biomaterials for regenerative medicine applications.

In this work, we focus on laser-based approaches (such as Matrix-Assisted Pulsed Laser Evaporation (MAPLE) and laser texturing) for the design of polymeric and ceramic bio-interfaces aiming the control of stem cell behaviour *in vitro*. MAPLE was used to prepare smart thermo responsive coatings based on pNIPAM and its derivatives (e.g. amine terminated pNIPAM, azide terminated pNIPAM, and amide terminated pNIPAM). Fourier transform infrared spectroscopy (FTIR), Scanning Electron Microscopy (SEM) and atomic force microscopy (AFM) were used to determine the pNIPAM based thin films chemical and morphological characteristics. For biointerfaces obtained by direct laser texturing, a fs laser system was used to structure Zirconia ceramic sheets.

The *in vitro* biological assays showed that the early mesenchymal stem cell (MSC) growth was conditioned by specific chemistry and microtopography for both thermo responsive coatings and microstructured Zirconia ceramic. The cell culture-based studies (fluorescence microscopy, MTT assays) have proved a good biocompatibility and a cell behavior correlated with the chemical composition of biomaterial substrates. Contact guidance efficiency of MSCs on lines and grids geometries depended on specific periodicities of Zirconia patterns. Our results give indications on the use of laser methods for obtaining controlled surface chemical functionalization and surface topographies for tissue engineering applications.

**Acknowledgments:** This work was supported by Romanian National Authority for Scientific Research (CNCS – UEFISCDI), under the projects PNII-PT-PCCA-2013-4-199, PN-II-RU-TE-2014-4-2434, PN0939, Nucleus programme- contract 4N/2016 and Romanian Academy project 1/2015-2016.

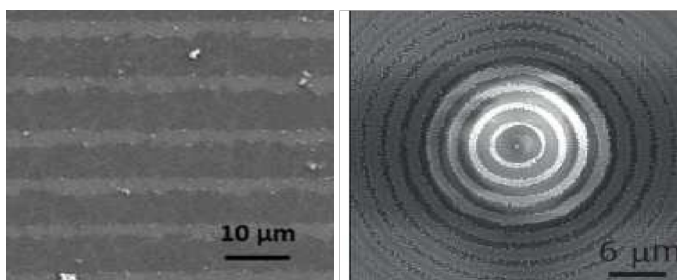
## **Diffraction-Free Femtosecond Laser Beams for Nanoscale Patterning of 2D Materials and Thin Films**

R. Sahin<sup>1</sup>, T. Ersoy<sup>1</sup>, E. Simsek<sup>2</sup>, S. Akturk<sup>1</sup>

<sup>1</sup>Istanbul Technical University, Department of Physics, Istanbul 34469

<sup>2</sup>George Washington University, Washington DC, 20052  
selcuk.akturk@itu.edu.tr

It is well-known that femtosecond-pulsed lasers can yield material modification with dimensions below the diffraction limit, by restraining the pulse fluence at focus near ablation threshold<sup>1</sup>. On the other hand, tightly focused Gaussian beams needed for such processes diffract very rapidly, making them very sensitive to alignment and sample surface variations. We show that diffraction-free beams with radial electric field amplitudes of zeroth and first order Bessel function profiles significantly enhance the facility of the process. Within the Bessel-zone, these beams have constant transverse width, and the intensity varies much slower in the longitudinal direction as compared to Gaussian beams. We apply the approach on different types of surfaces. In the first case, we generate



sub-micron size strips on single-layer graphene surfaces on Si/SiO<sub>2</sub> substrates. We show that, by properly choosing the laser scan rate and pulse energy, it is possible to ablate graphene without doing any damage on the substrate<sup>2</sup>. Secondly, we pattern metallic thin-film surfaces and investigate plasmonic behaviors of the generated structures<sup>3</sup>.

Figure 1: SEM micrographs of graphene surface patterned with zeroth order Bessel beams (left) and gold thin film patterned with first order Bessel beams (right).

1. A. P. Joglekar, H. Liu, E. Meyhöfer, G. Mourou, and A. J. Hunt, "Optics at critical intensity: Applications to nanomorphing," *Proceedings of the National Academy of Sciences of the United States of America* **101**, 5856–5861 (2004);
2. R. Sahin, E. Simsek, and S. Akturk, "Nanoscale patterning of graphene through femtosecond laser ablation," *Applied Physics Letters* **104**, 053118 (2014);
3. R. Sahin, Y. Morova, E. Simsek, and S. Akturk, "Bessel-beam-written nanoslit arrays and characterization of their optical response," *Applied Physics Letters* **102**, 193106 (2013).

## Simulation of Laser Induced Absorption Phenomena in Transparent Materials

**D. Savastru<sup>1</sup>, R. Savastru<sup>1</sup>, S. Miclos<sup>1</sup>, I. Lancranjan<sup>1</sup>**

<sup>1</sup> *The National Institute of Research and Development for Optoelectronics - INOE 2000*  
 409 Atomistilor Street, Magurele, Ilfov, RO-077125, Romania  
 dsavas@inoe.ro

In the last over sixty years of laser physics, the laser-induced damage and breakdown in transparent optical materials has been an important active field of research part of laser-material interactions studies. As laser systems continually advance, new opportunities to study laser-material interactions arise. An important part of research activities in this field are aiming to transparent optical materials, glasses and ceramics, laser microprocessing<sup>1-4</sup>. As a classical example, drilling micro channels through a glass plate is worth to be reminded. Of particular interest are optic fibers laser micro-processing techniques, i.e. drilling holes through clad and core, transverse welding and designing and fabrication of all photonic devices. Among others, one important purpose of these research activities consists in the development of Optic Micro-Nano Fiber sensors with improved capabilities. It is worth to observe that future developments of these research activities impose accurate theoretical models as base for improved correlated simulations and designs. The paper begins by analyzing the damage mechanisms and absorption phenomena that lead to laser-induced breakdown at the surface and in the bulk of optical materials. Electron density variation, growth in a material exposed to a high intensity laser field is analyzed as considered the main breakdown, damage mechanism. An in depth understanding of these processes are the foundation of the development of rate equations that describe occurrence and evolution of damage in a transparent material exposed to a strong electromagnetic wave. These rate equations are the base for a theoretical model. By using variable laser and material parameter inputs, the model calculates the laser induced electron density in a material in order to predict damage occurrence. Simulations are compared with literature reported experimental results in order to determine the accuracy of the model. Simulations are performed for different optical ceramics, chalcogenide, germanate, tellurite and silicate glasses. Simulations are performed considering ultrafast ultra-intense lasers (UULs) as the tool for inducing damages in transparent materials. Simulations are done for different laser wavelengths in the range 500-2500 nm and considering different half-measure time duration (FWHM) impulses. An important first stage of simulation procedure consists in modelling the laser intensity distribution over the irradiation zone of the material. Simulation results show great promise, but additional work must be done to increase confidence. Future developments of the model will lead to better accuracy and additional capabilities. The world's desire to push the limits of technology with these lasers have led to advancements in a variety of fields including homeland security, renewable energy, and advanced medical analysis. The focus of this paper stems from UULs applications in the area of transparent optical materials processing. Many wide use laboratory research, industrial, and military devices rely on optical systems for a variety of different purposes such as imaging systems, guidance systems, defense mechanisms, and much more. Explaining the mechanisms of energy deposition from an UUL pulse to a transparent optical solid and diagnosing the ensuing material modifications is important for improving the design and manufacturing of such optical devices<sup>2</sup>. By studying and understanding the interactions in materials that arise in nonlinear optics, steps can be taken to utilize material behavior in this ultrashort ultra-intense regime. If material responses and the ability of a material to maintain its initial properties when subject to ULLs are well understood, the possibilities to both improve optical systems as well as acquire valuable information on an existing optical system can be realized.

1. A. Du, X. Liu, G. Kom, and J. Squier, *Applied Physics Letters*, **64**, 3071 (1994);
2. L. S. C. Jones, P. Braunlich, R. T. Casper, and X.-A. Shen, *Optical Engineering*, **28**, 1039 (1989);
3. A. S.H. Lin, A. A. Villaeys, and Y. Fujimura, *Advances in Multi-Photon Processes and Spectroscopy* (World Scientific, Singapore), 2011.
4. D. Savastru, S. Miclos, R. Savastru, I. Lancranjan, *Romanian Reports in Physics*, **67**, 1586–1596 (2015).

# New achievements in laser scanning microscopy based on far field and near field

G. A. Stanciu, C. Stoichita, S. G. Stanciu, D. E. Tranca, R. Hristu

Center for Microscopy-Microanalysis and Information Processing, University Politehnica of Bucharest,  
313 Splaiul Independentei, 060042, Bucharest, Romania

In our work we present a new multimodal system which includes several microscopy techniques working in far field or in near field. Our new multimodal system integrates several microscopy techniques which offer the possibility for investigations at micro and nanoscale on the same area. By using an apertureless near field optical module upgrading an atomic force microscope we are able to image simultaneously the topography as well as optical characteristics at nanoscale resolution. The best resolution was less than 10 nm and it is connected with the tip size. The two techniques upgraded a confocal microscope. By using the same microscope and an external setup, our system may be used as a nanoscope based on the far field radiation (stimulated emission depletion and transient absorption microscopy). The system may be also used for second or third harmonic imaging and also for two photon excitation imaging. The schematic diagram of the multimodal system is shown in the fig. 1.

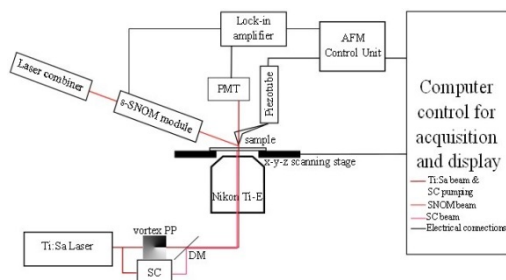


Figure 1: Schematic diagram of the multimodal system

The images on the collagen structures are shown in the Fig. 2. Four microscopy techniques integrated in the multimodal system have been used used.

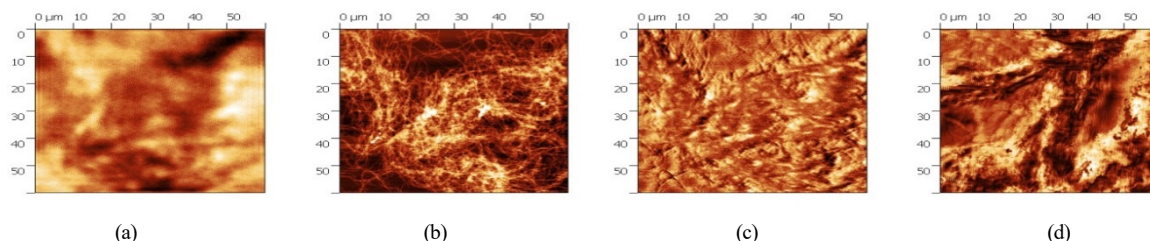


Figure 2: Images of the collagen: a) Confocal; b) AFM; c) s-SNOM, d) fluorescence –SNOM

**Acknowledgements:** This work has received support from the European Community's Seventh Framework Programme (FP7/2012-2015) under grant agreement no. 280804 (LANIR, [www.lanir.eu](http://www.lanir.eu)) and no. 212533 (BioElectricSurface, [www.bioelectricsurface.eu](http://www.bioelectricsurface.eu)). This communication reflects the views only of the authors, and the Commission cannot be held responsible for any use which may be made of the information contained therein. The presented work has been supported as well by the Romanian Executive Agency for Higher Education, Research, Development and Innovation Funding through the research grants PN-II-PT-PCCA-2011-3.2-1162 (NANOLASCAN) and PN-II-RU-TE-2014-4-1803 (MICRONANO).

## Influence of focusing depth for the Nanogratings Formation and Etching Selectivity in Fused Silica

V. Stankevič<sup>1,2</sup>, G. Račiukaitis<sup>2</sup>

<sup>1</sup>Center for Physical Sciences and Technology, Savanoriu Ave. 231, LT-02300, Vilnius, Lithuania

<sup>2</sup>ELAS UAB, Savanoriu Ave. 235, LT-02300, Vilnius, Lithuania

[valdemar.s@e-lasers.com](mailto:valdemar.s@e-lasers.com)

The nanogratings in Fused Silica are widely known phenomena and for the first time they were mentioned by Shimotsuma *et al.*<sup>1</sup>, however, their origin is not entirely understood yet. Focusing conditions of writing laser beam strongly influence formation of nanogratings<sup>2</sup>. Depending on the focusing depth and the used wavelength, different morphology of nanogratings can be achieved. For conventionally used focusing objectives of 0.2-0.6 NA, aberrations play a significant role in getting the required intensity field distribution needed for nanograting formation. In this work, the influence of different focusing depth for nanogratings formation is reviewed. The longitudinal internal modifications formed along the horizontal plane were fabricated with objectives of two different numerical apertures (NA 0.25 and NA 0.55). For the first step to evaluate the etching selectivity of the microchannels, the sample with longitudinal modifications using 515 nm and 1030 nm laser wavelengths was etched in 15% HF acid for 30 min. Hereafter, the sample was side polished to have the direct access to the vertical modification plane and etched for 1 min in 5% HF acid to reveal the nanogratings. The measured results link the length of the etched microchannels with the quality and morphology of the nanogratings formed at various depths extracted from the scanning electron microscope images. This association helps us to understand how critical is the

quality of the nanogratings for the etching selectivity of the microchannels. For a better understanding of phenomena involved and to take into account polarization of the focused beam at tight focusing, the Debye vectorial focusing calculations was used to model the intensity field distribution at different focusing depths and compare them with the experimental data.

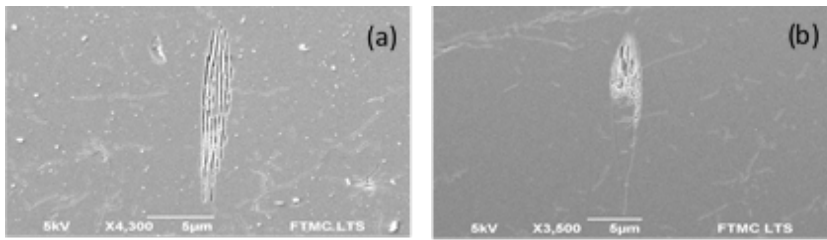


Figure 1: SEM images of self-organized nanogratings in the vertical observation plane formed at the 50  $\mu\text{m}$  depth with (a) 1030 nm wavelength; (b) 515 nm wavelength. The sample was polished and etched for 1 min in 5% HF acid.

1. Y. Shimotsuma, P. G. Kazansky, J. Qiu and K. Hirao, Self-Organized Nanogratings in Glass Irradiated by Ultrashort Light Pulses, *Phys. Rev. Lett.*, **91**, 247405-1 (2003);
2. C. Hnatovsky, R.S. Taylor, E. Simova, V. R. Bhardwaj, D.M. Rayner and P. B. Corkum, High-resolution study of photoinduced modification in fused silica produced by a tightly focused femtosecond laser beam in the presence of aberrations, *J. Appl. Phys.*, **98**, 013517 (2005).

## Laser interference lithography in case of nanosecond and picosecond laser pulses

E. Stankevičius, E. Daugnoraitė, M. Garliauskas, I. Matulaitienė, G. Niaura and G. Račiukaitis

Center for Physical Sciences and Technology, Savanoriu Ave. 231, LT-02300, Vilnius, Lithuania  
estankevicius@ftmc.lt

The fabrication technique based on the laser interference lithography (LIL)<sup>1-4</sup> is among the most practical and elegant approaches to the manufacture of extended periodic structure<sup>5</sup>. LIL has certain advantages over the direct laser writing (DLW) technique<sup>6</sup> due to the rapid fabrication of periodic structures. LIL allows fabricating periodic structures over a large area relatively fast and that makes this technique attractive and promising for mass-fabrication of the functional devices such as hydrophobic structures, microlens array<sup>7</sup>, scaffolds, microtubes, etc. Fabrication of useful and precise microstructures using the techniques based on photopolymerization processes requires an understanding of photo-chemical mechanisms occurring during the photopolymerization processes. Such studies would allow optimizing the experimental setups and the photo-polymers by tailoring their composition and chemical enhancement for the required resolution or sensitivity in structuring applications.

In this presentation, we compare and analyse the photo-polymerization process by using nanosecond and picosecond laser pulses with the same pulse peak intensity. The results of experiments by using two different laser pulse duration (10 ns and 300 ps) with the same peak pulse intensity ( $\sim 31 \text{ MW/cm}^2$ ) are shown in Fig. 1. As can see from the results: the structures fabricated by nanosecond pulses are strong and stable compared to the structures fabricated by the picosecond pulses. The structures fabricated by picosecond laser pulses (with the same peak pulse intensity as ns pulses) can not survive the development process (Fig. 1b). The reason of it is the density of generated radicals (which is much higher in the case of ns pulses) and various kinetic and transport processes in both cases.

Additionally, in this presentation, we demonstrate the ability to manipulate the light beam characteristics using a different shape of microstructures and show other functional structures fabricated using laser interference lithography.

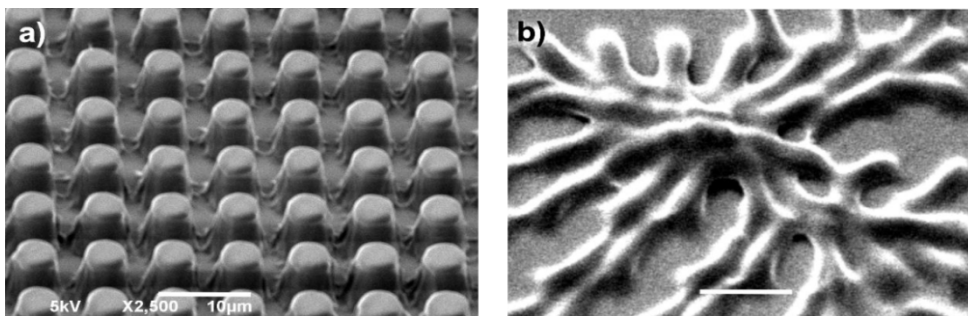


Figure 1: Structures fabricated using the laser interference lithography and different laser pulse duration: a) 10 ns and b) 300 ps. The peak pulse intensity of the generated pulses and the exposure time was the same, respectively:  $\sim 31 \text{ MW/cm}^2$  and 60 s. The scale bars represent 10  $\mu\text{m}$ .

1. V. Berger, O. Gauthier-Lafaye, and E. Costard, Photonic band gaps and holography, *J. Appl. Phys.* **82**, 60-64 (1997);
2. M. Campbell, D.N. Sharp, M.T. Harrison, R.G. Denning, and A.J. Turberfield, Fabrication of photonic crystals for the visible spectrum by holographic lithography, *Nature* **404**, 53-56 (2000);
3. T. Kondo, S. Matsuo, S. Juodkazis, and H. Misawa, Femtosecond laser interference technique with diffractive beam splitter for fabrication of three-dimensional photonic crystals, *Appl. Phys. Lett.* **79**(6), 725-727 (2001).

4. E. Stankevičius, M. Garliauskas, M. Gedvilas, and G. Račiukaitis, Bessel-like beam array formation by periodical arrangement of the polymeric round-tip microstructures, *Opt. Express* **23**(22), 28557-28566 (2015);
5. T. Kondo, S. Juodkakis, V. Mizeikis, S. Matsuo, and H. Misawa, Fabrication of three-dimensional periodic microstructures in photoresist SU-8 by phase-controlled holographic lithography, *New J. Phys.* **8**(10), 250 (2006);
6. M. Malinauskas, A. Zukauskas, G. Bickauskaitė, R. Gadonas, and S. Juodkakis, Mechanisms of three-dimensional structuring of photopolymers by tightly focussed femtosecond laser pulses, *Opt. Express* **18**(10), 10209-10221 (2010);
7. E. Stankevičius, M. Gedvilas, and G. Raciukaitis, Investigation of laser-induced polymerization using a smoothly varying intensity distribution, *Appl. Phys. B* **119**(3), 525-532 (2015).

## Mechanical and biological properties of multi-doped Diamond-Like Carbon coatings (DLC-Si/Ag) fabricated using modified chemical vapour deposition method

L. Swiatek<sup>1</sup>, A. Olejnik<sup>1</sup>, J. Grabarczyk<sup>1</sup>, A. Jedrzejczak<sup>1</sup>, A. Sobczyk-Guzenda<sup>2</sup>,  
M. Kaminska<sup>3</sup>, W. Jakubowski<sup>3</sup>, W. Szymanski<sup>3</sup>, D. Bociaga<sup>1</sup>

<sup>1</sup>*Division of Biomedical Engineering and Functional Materials, Lodz University of Technology, Institute of Materials Science and Engineering, 1/15 Stefanowskiego St., 90-924, Poland*

<sup>2</sup>*Division of coatings engineering and non-metallic materials, Institute of Material Science and Engineering, Lodz University of Technology, 1/15 Stefanowskiego St., 90-924 Lodz, Poland*

<sup>3</sup>*Division of Biophysics, Institute of Material Science and Engineering Lodz University of Technology, 1/15 Stefanowskiego St., 90-924 Lodz, Poland  
swiatek.lidia@gmail.com*

Nowadays, there is an increasing emphasis placed on a healthy lifestyle and physical activity what may lead to various injuries. In order to re-establish mechanical and biological functions of the impaired organs and tissues, the biomaterial implantation is often required. Recently a lot of attention is given to surface modification of biomaterials in order to improve the biological response of the organism towards an implanted material. One of most efficient and commonly applied solutions involves the use of diamond-like carbon (DLC) coatings, which combine both good biological and mechanical properties<sup>1</sup>. Despite numerous advantages, some DLC coatings exhibit also certain undesirable properties, such as poor adhesion resulting from high internal stress level or low thermal stability<sup>2</sup>. These kind of problems scientist solve doping with different metallic elements, such as Ti, Si, Ag, Mo, Cr, W or Al, which reduce disadvantages of carbon coatings<sup>3</sup>.

Silicon and silver dopands, exhibit highly desirable properties in the context of medical applications. Silicon improves not only the physiochemical, mechanical and tribological properties, but also enhances the biocompatibility of carbon coatings. Sliver, on the other hand, increases the antibacterial properties of DLC films. The combination of those properties would allow to obtain a biomaterial fulfilling all mechanical and biological requirements and hence, the DLC-Si/Ag coatings are potentially a very good material for biomedical applications.

Therefore, in this work the Si/Ag-incorporated DLC coatings have been manufactured and examined in terms of chemical composition and structure, surface morphology, mechanical and surface properties, wettability as well as biological response. Since one of the most commonly applied synthesis method for the deposition of Si-DLC coatings is radio frequency plasma assisted chemical vapour deposition (RF PACVD)<sup>4,5</sup> technique, it has been modified in order to allow simultaneous doping with both Si and Ag in one process. Films for potential biomedical applications were deposited on metallic materials used for the implants manufacturing: Ti6Al7Nb. The manufactured DLC-Si/Ag layers are characterized by a granular structure and the silver contained within the carbon matrix shows the tendency to form conglomerates. It was revealed that the Ag binds chemically with the DLC coatings. The DLC-Si/Ag coating, exhibited not only improved hardness, but also the best biocompatibility. The obtained results demonstrated that the incorporation of Ag and Si dopants (at proper ratio) allows to obtain coatings of good biocompatibility and high antibacterial properties, which are due to the bactericidal properties of Ag. High biocompatibility is in turn due to the positive influence of Si on the cell's proliferation, which compensates for the possible cytotoxicity of Ag.

**Acknowledgements** This research has been supported by the National Centre for Research and Development under the grant no. MERA.NET/2012/02/ 2014 entitled "CarLa – Ag/Si doped carbon layer for bio-medical application".

1. R. Hauert, A review of modified DLC coatings for biological applications, *Diam. Relat. Mater.* **12** 583-589 (2003);
2. M.M. Morshed, B.P. McNamara, D.C. Cameron, M.S.J. Hashmi, Stress and adhesion in DLC coatings on 316L stainless steel deposited by a neutral beam source, *J. Mater. Process. Technol.* **143-144**, 922-926 (2003);
3. J. Vetter, 60 years of DLC coatings: Historical highlights and technical review of cathodic arc processes to synthesize various DLC types, and their evolution for industrial applications, *Surf.Coat. Technol.* **257**, 213-240 (2014);
4. S. Mitura, E. Mitura, A. Mitura, Manufacture of amorphous carbon layers by r. f. dense plasma CVD, *Diam. Relat. Mater.* **4**, 302-303 (1995);
5. J. Grabarczyk, Long-term termination of carbon layers synthesized using RF PACVD method onto metal substrates, *Diam. Relat. Mater.* **20** 1133-1136 (2011).

# Fabrication of metal nanostructures on various dielectric substrates: the effect of thermal diffusivity

A. Takami<sup>1</sup>, Y. Nakajima<sup>1</sup>, N. Nedyalkov<sup>2</sup>, M. Terakawa<sup>1,3</sup>

<sup>1</sup>School of Integrated Design Engineering, Keio University, 3-14-1 Hiyoshi, Kohoku-ku, Yokohama, 223-8522, Japan

<sup>2</sup>Institute of Electronics, Bulgarian Academy of Sciences, Tsarigradsko Shose 72, 1784 Sofia, Bulgaria

<sup>3</sup>Department of Electronics and Electrical Engineering, Keio, University, 3-14-1, Hiyoshi, Kohoku-ku, Yokohama-shi 223-8522, Japan  
terakawa@elec.keio.ac.jp

Periodically aligned metal nanowire gratings (MNGs) are nanostructures which show unique optical properties. Novel optical and electronic devices such as band-selective micro polarizers and sensitive photodetectors have been realized by using MNGs. Different substrates have been used for such applications because device properties are dependent on the substrate. In our previous study, we have demonstrated the fabrication of MNGs of platinum by femtosecond laser irradiation to a platinum thin film on a fused silica substrate<sup>1</sup>. The mechanism of the MNGs formation is not fully revealed; however, it is probably related to that of LIPSS as well as to the melting of the metal thin film.

In this study, we report the fabrication of MNGs on various substrates by using femtosecond laser and discuss the effect of thermal diffusivity of substrates on the fabricated shapes. Femtosecond laser pulses (wavelength 800 nm, pulse duration 500 fs, repetition rate 1kHz, laser fluence 180 mJ/cm<sup>2</sup>, number of pulses 10000 shots) were irradiated to platinum thin films deposited on three different substrates; silicon carbide, aluminum nitride and fused silica (thermal diffusivity of respective substrate:  $2.1 \times 10^{-4} \text{ m}^2\text{s}^{-1}$ ,  $1.2 \times 10^{-4} \text{ m}^2\text{s}^{-1}$ ,  $8.0 \times 10^{-7} \text{ m}^2\text{s}^{-1}$ ). Figure 1 shows the scanning electron microscopy (SEM) images of the samples after the laser irradiation. While MNGs were fabricated on higher thermal diffusivity substrates, nanoparticles were mainly fabricated on lower thermal diffusivity substrates possibly via melting of metal thin films. As shown in figure 2, a calculational result by two temperature model indicates that the lattice temperature at the film-substrate boundary become higher for lower-thermal-diffusivity substrates. These results suggest that the metal thin film on the lower thermal diffusivity substrate would melt easily because of confinement of generated heat by femtosecond laser irradiation.

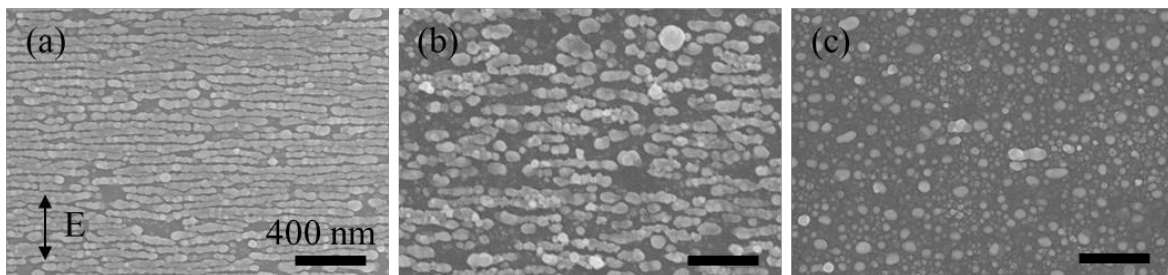


Figure 1: SEM images of laser-irradiated platinum thin films deposited on (a) silicon carbide, (b) aluminum nitride and (c) fused silica substrates. The double-headed arrow shows the direction of laser polarization.

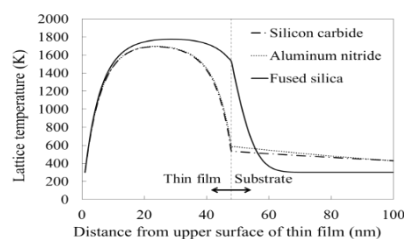


Figure 2: Calculated spatial distribution of lattice temperature in platinum thin film and the different substrates - silicon carbide, aluminum nitride and fused silica 30 ps after laser irradiation. The central dotted-line shows the thin film - substrate boundary.

I. Y. Nakajima, N. Nedyalkov, A. Takami, M. Terakawa, "Formation of periodic metal nanowire grating on silica substrate by femtosecond laser irradiation," *Appl. Phys. A* **119**, 1215 (2015).

# Combined laser-gamma beam experiments at ELI-NP

O. Tesileanu<sup>1</sup>, K. Homma<sup>2,3</sup>, S. Ataman<sup>1</sup>, M. Cuciuc<sup>1</sup>, L. D'Alessi<sup>1</sup>, Y. Nakamiya<sup>4</sup>, K. Seto<sup>1</sup>, Y. Xu<sup>1</sup>, M. Zeng<sup>1</sup>

<sup>1</sup>ELI-NP, "Horia Hulubei" National Institute for Physics and Nuclear Engineering, 30 Reactorului Street, RO-077125, Bucharest-Magurele, Romania

<sup>2</sup>Graduate School of Science, Hiroshima University, Higashihiroshima, Hiroshima, Japan

<sup>3</sup>International Center for Zetta-Exawatt Science and Technology, Ecole Polytechnique, France

<sup>4</sup>Institute of Chemical Research, Kyoto University, Gokasho, Uji-city, Kyoto, Japan

ovidiu.tesileanu@eli-np.ro

The unique capability of ELI-NP to deliver for experiments a high intensity, tunable gamma ray beam and at the same time two high power ultrashort laser pulses will be employed to tackle problems of fundamental physics, in experimental setups with increasing complexity. The beams themselves will have characteristics much beyond the present-day state of the art. A Technical Design Report (TDR) has been developed for these experiments with the contribution of the international scientific community<sup>1</sup>.

The isomer production and photoexcitation experiment will start at the beginning of the operation phase of ELINP with the production of isomers with the help of the 1PW/10PW laser pulses. After optimizing the isomer production setup the gamma ray beam will be employed as a second step of the experiment in order to study the photoneutron emission from the isomer levels. The study of radiation reaction, pair creation in vacuum and vacuum birefringence are also topics of interest, starting when the electron beam from the linac will be available for experiments in the E7 area at ELI-NP.

Using the two 100TW laser beams available in the E4 experimental area, we propose a setup for the study of the four-wave mixing in search of Dark Matter candidates in the sub-eV range<sup>2</sup>, followed by an experiment with a table-top gamma-gamma collider. These experiments will be also performed at 1PW in a second phase, when the upgrade to this power is completed.

In addition, there are two generic Research and Development tasks proposed in the TDR, related to the development of a detection system, the Gamma Polari-Calorimeter (GPC), commonly applicable to energy measurements for electrons, positrons and gamma rays above the 0.1 GeV energy scale and the preparatory tests for laser plasma acceleration of electrons up to necessary energies of 210 MeV, 2.5 GeV and 5 GeV for the later stage experiments, respectively.

An overview of the experimental programme proposed for the "Combined laser-gamma beam experiments" research activity will be given, as well as a discussion of phasing of the experiments and implementation challenges.

1. K. Homma et al, Romanian Reports in Physics, Vol. 68, Supplement, S233–S274 (2016).

2. K. Homma, D. Habs, T. Tajima, Appl. Phys. B 106:229-240 (2012).

## Polymer thin film surface patterning by direct laser writing

N. Tosa<sup>1</sup>, E. Pavel<sup>2</sup>, S. Jinga<sup>3</sup>, V. Marinescu<sup>4</sup>, R. Trusca<sup>5</sup>

<sup>1</sup>National Institute for R&D of Isotopic and Molecular Technologies, 400297 Cluj-Napoca, Romania

<sup>2</sup>Storex Technologies, 020892 Bucharest, Romania

<sup>3</sup>Faculty of Applied Chemistry and Materials Science, "Politehnica" University of Bucharest, 011061 Bucharest, Romania

<sup>4</sup>National Institute for R&D in Electrical Engineering, 030138 Bucharest, Romania

<sup>5</sup>METAV R&D, 020011 Bucharest, Romania

nicoleta.tosa@itim-cj.ro

The aim of our work was to create dedicated patterns in polymer thin film<sup>1</sup> surfaces by direct laser writing at micro- and submicrometric scale in a controlled and reproducible manner. The optical lithography process has been developed in a chromophore<sup>2</sup> doped polymer compatible as absorption spectral range with the wavelength of the laser used for uniform thin film patterning. The size of the patterned structures is very sensitive to the laser power, varying from a few microns down to hundred of nanometers for reduced powers. Optical microscopy and SEM morphological investigations of the patterned structures demonstrated that their size rose when the laser power increased, meanwhile the structures width maintained constant along the entire pattern (Figure 1).

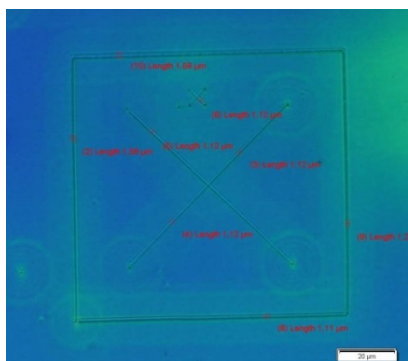


Figure 1: Optical image of an X pattern structure, placed inside of a square frame, recorded in bright field in transmitted light, using an 100x oil-immersed objective at 63x magnification.



At higher laser power the “written” structures display a pit at the central part of the structure due to an additional ablation process at the laser spot-structure contact. In this view, the spatial temperature gradient in the active layer, that is directly dependent on the laser photo-excitation process and on the laser power control, will definitely influence the shape and the position of the generated pits<sup>3</sup>. The complex geometries and the controllable shapes/sizes of the structures patterned by direct laser writing in thin films allow developing issues for increased data storage capacity<sup>4</sup>.

1. M. Farsari, G. Filippidis, C. Fotakis, Fabrication of three-dimensional structures by three-photon polymerization, *Optics Letters*, 30, 3180-3182 (2005);
2. S.T. Thompson and E. Stellwagen, Binding of Cibacron blue F3GA to proteins containing the dinucleotide fold, *Proc. Nat. Acad. Sci. USA, Biochemistry*, 73, 361-365 (1976);
3. B. Tieke, G.R. Langereis, E.R. Meinders, J.G.F. Kablau, R. Woundenber, R.A.J. van Kollenburg, Thermally Balanced Writing for HighSpeed Compact Disc Recordable (CD-R) Recording, *Japanese Journal of Applied Physics*, 41, 1735-1738 (2002);
4. E. Pavel, S.I. Jinga, B.S. Vasile, A. Dinescu, V. Marinescu, R. Trusca, N. Tosa, Quantum optical lithography from 1 nm resolution to pattern transfer on silicon wafer, *Optics & Laser Technology*, 60, 80–84 (2014).

## Development of flexible oxide thin films grown by photo-assisted MOD

T. Tsuchiya, T. Nakajima, T. Nakamura, I. Yamaguchi, H, Matsui

*National Institute of Advanced Industrial Science and Technology (AIST) Japan, 1-1-1 Higashi, Tsukuba, Ibaraki, Japan.  
tetsuo-tsuchiya@aist.go.jp*

To construct low carbon society more and more in the world, it is necessary to develop a high performances new green device such as a solar cell, a lithium battery, a power semiconductor, and light emitting diode (LED) lighting, superconducting device and so on. Metal oxides are expected to be key materials which are used for a new device by controlling metal composition, a crystal structure, orientation or multilayer of the film, a carrier, a spin, etc. In order to fabricate the new devices, their parameters controllable process would be effective. Another important problem is the development of the low cost and power saving process for constructing sustainable society in the world. For these purpose, chemical solution process (CSP) would be suitable because it does not require vacuum and high facility investments and any complicated etching process. In addition, precise metal composition control is possible when the materials are made from the more than 3 or 4 metal components. For the thin film processing, we have developed the photo-induced chemical solution process such as excimer laser-assisted metal organic deposition (ELAMOD) and photo reaction of nano-particle (PRNP), and photo reaction of hybrid solution (PRHS) for the preparation of the patterned metal oxide thin film on organic, glass and single crystalline substrates. In this presentation, we demonstrate a preparation of flexible ITO and phosphor thin films on PET and SiN substrates. Also, we show the preparation of resistor thin films on PI substrate at low temperature in air for SiC power electronics.

### ***Flexible ITO film by PRNP method***

By using the PRNP process, ITO and phosphor thin films were prepared on glass and PET substrates at room temperature. The Sheet resistance of the ITO film on PET by using the PRNP method was 150Ω/sq. Thus, PRNP method is useful for the preparation of polycrystalline oxide film on PET at low temperature, and the flexible display and lightning devices.

### ***Flexible luminescent or resistor films by PRHS method***

As shown in Fig.1, flexible RuO<sub>2</sub> film was successfully prepared by PRHS process at room temperature. The resistivity of the flexible RuO<sub>2</sub> film was 4.8×10<sup>-4</sup>Ωcm. The resistance change was 2.4% at the temperature range from 300 to 25°C. In addition, at the time of implementation, flexible resistor would be expected to relax the crack that comes from the difference in the thermal mechanical properties.

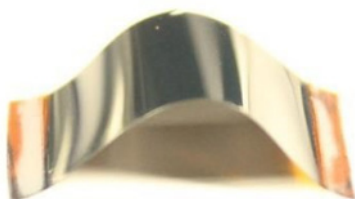


*Figure 1: Flexible resistor by PRHS*

1. T. Tsuchiya et al., *Appl. Surf. Sci.*, **186** (2002) 173;
2. T. Tsuchiya et al., *Appl. Phys. A* **99** (2010) 745;
3. T. Tsuchiya et al., *Mater. Res. Soc. Symp. Proc.* **1454** (2012) 189;
4. T. Nakajima et al., *Chem. Soc. Rev.* **43** (2014) 2027.

# Optical means to probe orbital ordering in epitaxial vanadate films fabricated by pulsed-laser ablation

I. Vrejoiu<sup>1</sup>, C. Himcinschi<sup>2</sup>, L. Bussmann<sup>1</sup>, P. H. M. van Loosdrecht<sup>1</sup>

<sup>1</sup>University of Cologne, II. Physics Institute, Zùlpicher Str. 77, 50937 Cologne,

<sup>2</sup>TU Bergakademie Freiberg, Institute of Theoretical Physics, Freiberg, Germany  
vrejoiu@ph2.uni-koeln.de

Orbital ordering is a fascinating ordering phenomenon in complex oxide materials, which has been largely investigated in bulk single crystals with perovskite structure, such as  $\text{LaVO}_3$ , as more physical techniques can be employed for probing the ordering in such samples. Investigations of orbital ordering in thin films are often rendered very difficult by the hindering and often dominant contributions of the single crystal substrates. By temperature-dependent Raman scattering spectroscopy we probed and evidenced the transition to orbital ordering in epitaxial  $\text{LaVO}_3$  film samples fabricated by pulsed-laser deposition.<sup>1</sup> To the best of our knowledge we are the first to report on Raman scattering spectroscopy of  $\text{LaVO}_3$  thin film samples and, moreover, we are the first to evidence that, similar to the bulk parent compound, orbital ordering occurs in epitaxial films as well. This opens up the possibility to explore further subtle aspects of the orbital ordering such as the influence of different epitaxial strain (compressive *vs.* tensile) and of epitaxy-induced distortions of oxygen octahedra on the orbital ordering, in epitaxial perovskite vanadate films. Raman scattering spectroscopy in conjunction with future temperature-dependent optical conductivity and X-ray spectroscopy measurements, corroborated with  $\text{VO}_6$  octahedra observations by electron microscopy can provide a comprehensive insight in the structure-electronic property relations of epitaxially modified  $\text{LaVO}_3$ .

$\text{LaVO}_3$  is a prototypical Mott-Hubbard insulator with a  $3d^2$  electronic configuration of  $\text{V}^{3+}$ . At 143 K  $\text{LaVO}_3$  single crystals undergo a magnetic transition from a paramagnetic to an antiferromagnetic state and a first order structural phase transition from orthorhombic  $Pbnm$  to monoclinic  $P2_1/b$  following right below the magnetic ordering temperature, at 141 K.<sup>1,2</sup> The AFM state is a C-type spin-ordered state with ferromagnetically arranged  $\text{V}^{3+}(S=1)$  spins along the  $c$ -axis and the antiferromagnetic alignment in the  $ab$  plane. Along with the structural transition, a G-type orbital order sets in below 141 K as well, with commonly occupied  $t_{2g}$   $d_{xy}$  orbitals and  $d_{yz}$  or  $d_{zx}$  orbitals that are alternately occupied in all directions.

The fabrication of phase pure  $\text{LaVO}_3$  films requires oxygen pressures lower than about  $10^{-6}$  mbar, so that the competing  $\text{LaVO}_4$  phase does not form. The fabrication of the  $\text{LaVO}_x$  films under high vacuum conditions affects the stoichiometry of the film and oxygen content of the substrates. Our  $\text{LaVO}_3$  and  $\text{La}_{0.75}\text{Sr}_{0.25}\text{VO}_3$  epitaxial films were fabricated by pulsed-laser deposition (PLD), assisted by reflective high energy electron diffraction (RHEED) for *in situ* control of the growth. The film deposition was performed in reducing atmosphere of Ar/4%  $\text{H}_2$  at a substrate temperature of 700°C.

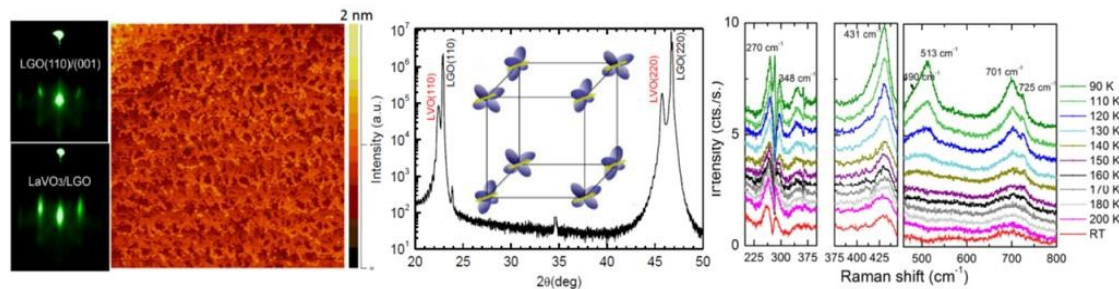


Figure 1: Epitaxial films of  $\text{LaVO}_3$  grown on  $\text{LaGaO}_3(110)$  crystals, fabricated by RHEED-assisted PLD (left most images show RHEED patterns taken at the growth temperature). The transition to orbital-ordered state was probed by temperature-dependent resonant Raman scattering spectroscopy (data shown on the right).

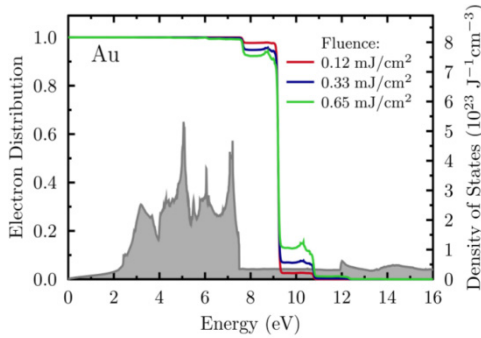
I. I. Vrejoiu, C. Himcinschi, L. Jin, C. -L. Jia, N. Raab, J. Engelmayer, R. Waser, R. Dittmann, P. H. M. van Loosdrecht, Probing orbital ordering in  $\text{LaVO}_3$  epitaxial films by Raman scattering, *APL Materials*, 4, 046103 (2016).

# Nonequilibrium electron dynamics in laser-excited copper and gold

S. Weber and B. Rethfeld

Department of Physics and Research Center OPTIMAS, Technical University of Kaiserslautern, Germany  
weber@physik.uni-kl.de

After excitation with an ultrashort laser pulse, the electrons in a metal are in a strong nonequilibrium state. During thermalization, they interact also with the lattice, transferring energy to the phonons. On the basis of complete Boltzmann-type collision integrals, a method allowing to treat materials with an arbitrary density of states has been developed<sup>1</sup>. This method provides insights into the response of different material classes to ultrafast laser excitation. Here we focus on the study of noble metals which possess characteristic densities of states with an elevated area at a certain distance below the Fermi edge.



The figure 1 shows the distribution of the excited electron system in gold after a laser irradiation of 10 fs duration. Different fluencies have been applied. Characteristic features of the density of states are visible. In the contribution we analyze the details of the excited distribution for copper and gold, discuss the timescales of thermalization and study the coupling of the electrons with the phononic system. We find that the electron-phonon coupling hinders the electrons' complete thermalization as long as the temperature of both subsystems differ from each other.

Figure 1: Electron distribution in gold after excitation with a 10 fs laser pulse of different fluencies

I. B. Y. Mueller and B. Rethfeld, Relaxation dynamics in laser-excited metals under nonequilibrium conditions, Phys. Rev. B **87**, 035139 (2013).

## Effect of pulse duration on ultrafast energy deposition in copper

J. Winter<sup>1</sup>, H. Huber<sup>1</sup>

<sup>1</sup>Department of Applied Sciences and Mechatronics, Munich University of Applied Sciences,  
Lothstrasse 34, 80335 Munich, Germany  
jan.winter@hm.edu

Experimental and theoretical studies on efficiency of laser material processing from metals have been demonstrating a high degree of dependence on spatial as well as temporal laser pulse parameters. A general trend indicates a steep increase of ablation efficiency with reduction of the laser pulse duration. The scope of this study was to investigate the ultrafast energy deposition in a copper metal target after irradiation with a 500 fs and 10 ps ultra-short laser pulse.

A numerical analysis of laser-matter interaction was performed by using the optical Drude critical point (DCP)<sup>1,2</sup> and the thermal two temperature model (TTM) model. The DCP model was incorporated into the TTM to simulate the time-resolved ultrafast laser energy deposition and thermal material response in copper irradiated by femto- and picosecond laser pulses. In addition the thermomechanical effect was considered in the TTM model fully coupled with the thermoelasticity theory for calculation of the temporal and spatial evolution of the compressive thermoelastic pressure in the stress-confinement regime.

It was found that a dynamic change in reflectivity and absorption coefficient induced by a rapid temperature increase affects the laser energy deposition during the irradiation and leads to a higher penetration depth for shorter laser pulses. The simulations indicate that the laser pulse energy is converted into an ultrafast heat source leading to

a factor of 2 deeper energy deposition into the target material, as shown in Fig. 1.

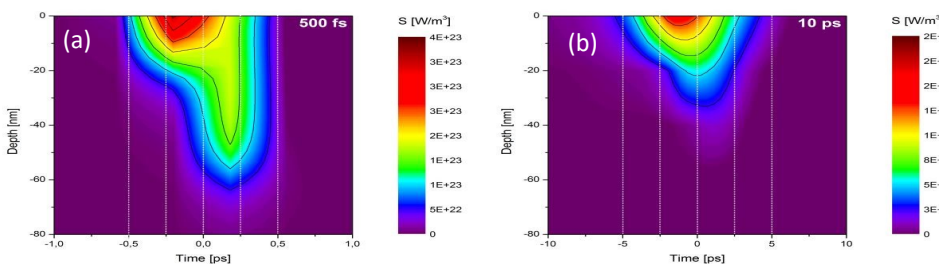


Figure 1: (a) Contour plots of volumetric laser heat source distribution in the depth of the material for simulating of laser irradiation with a 500 fs in (a) and 10 ps in (b) ultra-short laser pulses on the Cu material.

The simulations

indicate that the thermal energy is deposited deeper into the target material due to the improved optical energy deposition and higher electron temperatures as a driving force for heat diffusion into the depth. These results implicate the differences in the ultra-fast energy deposition and laser ablation efficiency for 500 fs and 10 ps laser pulses and accordingly give a trend towards a better understanding of ultra-short laser ablation

1. Y. Ren, J. K. Chen, Y. Zhang, and J. Huang, Ultrashort laser pulse energy deposition in metal films with phase changes, *Appl. Phys. Lett.* 98, 191105 (2011);  
 2. S. Y. Wang, Y. Ren, C. W. Cheng, J. K. Chen, and D. Y. Tzou, Micromachining of copper by femtosecond laser pulses, *Appl. Surf. Sci.* 265, 302–308, (2013).

## Simulations of short pulse laser ablation and nanoparticle formation under spatial confinement: From background gas to liquid environment and to solid overlayer

C. Wu,<sup>1</sup> C.Y. Shih,<sup>1</sup> H. Wu,<sup>1,2</sup> E. T. Karim,<sup>1</sup> M. V. Shugaev,<sup>1</sup> L. V. Zhigilei<sup>1</sup>

<sup>1</sup>Department of Materials Science and Engineering, University of Virginia, USA

<sup>2</sup>Institute of Modern Optics, Nankai University, China

lz2n@virginia.edu

While the general mechanisms of laser melting, spallation, and ablation in vacuum have been extensively studied experimentally, theoretically, and computationally, the effect of spatial confinement by a high (1 atm or higher) background gas pressure, liquid environment, and a solid transparent overlayer on the laser-induced processes still remains largely unexplored. In this work, the mechanisms of laser ablation of metal targets under conditions of spatial confinement are investigated in a systematic computational study covering various degrees of spatial confinement, from 1–10 atm background gas, to liquid environment, and to the solid overlayer placed on the irradiated surface. The ablation process is simulated for Al and Ag targets irradiated by femtosecond laser pulses. The simulations are performed with atomistic molecular dynamics model combined with a coarsegrained representation of the liquid environment (parameterized for water) and implementing special acoustic impedance matching boundary condition for representation of the solid overlayer (parameterized for silica glass). The results of the simulations suggest a surprisingly strong effect of the gas environment on the initial plume expansion and evolution of the cluster size distribution, with almost complete suppression of the generation of small atomic clusters in the front part of the ablation plume, Figure 1. The confinement by the liquid environment results in the formation of a mixing region where the liquid is brought to the supercritical state by the interaction with the ejected metal vapor and droplets. The conditions in the mixing region facilitate rapid cooling and condensation of metal vapor leading to the formation of metal nanoparticles, Figure 2. Even stronger confinement by a solid overlayer prevents the expansion and phase decomposition of the top part of the superheated metal target, leading to a gradual cooling of the hot compressed supercritical metal down to the liquid state and eventual solidification of the target.

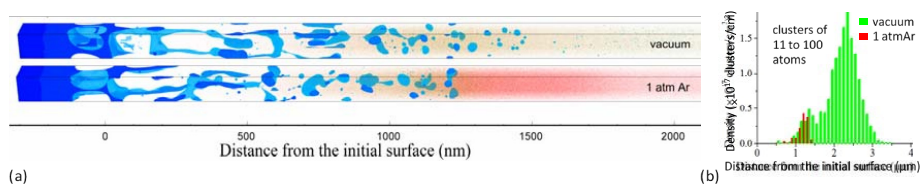


Figure 1: Snapshots of the ablation plume (a) and distribution of small clusters (b) generated by irradiation of an Al target by a 100 fs laser pulse in vacuum and 1 atm Ar and an absorbed fluence of 200 mJ/cm<sup>2</sup>. The snapshots are taken at 600 ps after the laser pulse. The atoms are colored by their potential energies, with the scale ranging from -3.4 eV (blue) to 0 eV (red).

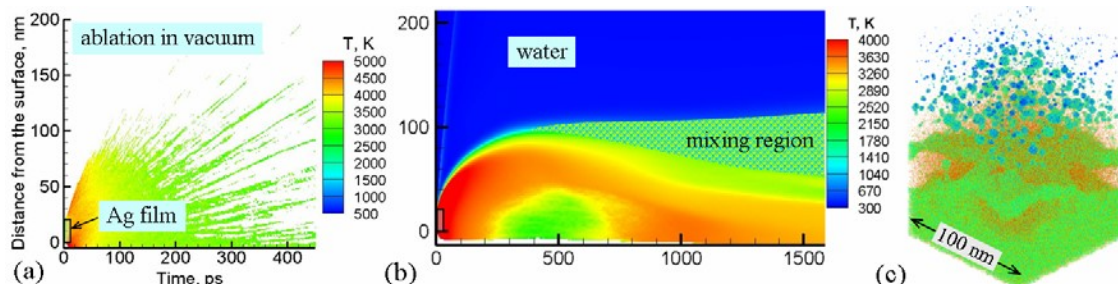


Figure 2: Temperature contour plots obtained in atomistic simulations of a 20 nm Ag film deposited on a silica substrate and irradiated by a femtosecond laser pulse at an absorbed fluence of 40 mJ/cm<sup>2</sup> in vacuum (a) and in water environment (b,c). In the snapshot shown in (c) for 2 ns after the laser pulse, water is blanked to expose Ag clusters in the Ag-water mixing region.

# Enhanced photocatalytic activities of PLD TiO<sub>2</sub> films supporting Au nanoparticles under UV irradiation

T. Yoshida<sup>1</sup>, T. Tabuchi<sup>1</sup>, F. Kikuchi<sup>2</sup>, I. Umezu<sup>3</sup>, and M. Haraguchi<sup>2</sup>

<sup>1</sup>Course of Chemical Engineering, National Institute of Technology, Anan College, Anan, Tokushima 774-0017, Japan

<sup>2</sup>Department of Optical Science and Technology, Tokushima University, Tokushima 770-8506, Japan

<sup>3</sup>Department of physics, Konan University, Kobe 658-8501, Japan  
takehito@anan-nct.ac.jp

In recent several years, plasmonic excitation phenomena of nanostructured metals have realized high performance photocatalysts, in particular the visible light operation. Pulsed laser ablation (PLA) in reactive background gases is a candidate process to synthesize high performance nanocrystalline TiO<sub>2</sub> photocatalysts. We have already prepared TiO<sub>2</sub> nanocrystalline films supporting Au nanoparticles using PLA, and confirmed plasmonic-excited photocatalytic activities under visible light irradiation.<sup>1</sup> In this work, we evaluate photocatalytic activities of the (Au nanoparticles)/(anatase nanocrystalline films) synthesized by full PLA process, under UV irradiation. Because Au shows absorption band of the interband transition in UV region and strong coupling with anatase surface (interfacial electron transfer: IET).<sup>2</sup>

The TiO<sub>2</sub> nanocrystalline films were formed by the PLA of a TiO<sub>2</sub> target in O<sub>2</sub> background gases. O<sub>2</sub> gas was introduced into the vacuum chamber and maintained at 13 Pa. The fourth harmonics of a Nd:YAG laser beam (wavelength: 266 nm, pulse width: 6 ns, energy density: 2.4 J/(cm<sup>2</sup>·pulse), repetition rate: 10 Hz) was focused onto the TiO<sub>2</sub> target for 15 min. Distance from the target to the unheated deposition substrates (T/S) was 25 mm. Post-annealing by a furnace was carried out at 400°C for 10 min. In this condition, crystal structure of the nanocrystalline TiO<sub>2</sub> film was anatase. Au was deposited on the anatase nanocrystalline films using the same PLA process chamber. The process conditions were as follows: background gas: 266 Pa (He), energy density: 0.7 J/(cm<sup>2</sup>·pulse), T/S: 40 mm, deposition time: 10-75 sec. The specimens were annealed at 300°C for 180 min in the furnace. During the annealing process, as-deposited island-like Au balled to nanoparticles. We used a methylene blue (MB) decomposition method. The anatase nanocrystalline films supporting Au nanoparticle on the substrates in MB aqueous solution (0.01 mmol/L), were irradiated by a Xe arc lamp (wavelength: 365 ± 10nm, energy density: 1.00 mW/cm<sup>2</sup>).

Figure 1 shows optical transmittance spectra in dependence on the Au deposition time. Transmittances were recovered more than 85%, in the longer wavelength region (>700 nm). In spite of the low coverage factors, strong and sharp absorption bands appeared in wavelength range of 510-600 nm (in particular, deposition time: 60 sec), this is the reason why we infer the absorption bands of the balled Au nanoparticles in wavelength range of 510-600 nm were attributed to localized surface plasmonic resonance. In the shorter wavelength region (<450 nm), absorption remained, especially in deposition time longer than 60 sec. This phenomenon was presumably due to the interband transition in Au. We selected deposition time 60 sec for the photocatalytic evaluation. In plane-view FESEM observations for the Au nanoparticles of deposition time 60sec, it was found that the Au nanoparticles which had mean diameter and distribution: 18 ± 4.7 nm were well-dispersed. The photocatalytic activities were described by normalized MB concentration  $C/C_0$  (Fig. 2). The absorbance was monitored at the main peak position (wavelength: 664 nm). The  $C/C_0$  decreased with increasing irradiation time. The anatase nanocrystalline film supporting Au nanoparticles had about two times higher activity, in comparison with the control sample (without Au nanoparticles). As well-known, dechlorization of MB is caused by reduction. This photocatalysis enhancement is supposed to be ascribed to the Au interband transition and the strong coupling with anatase surface (IFT).

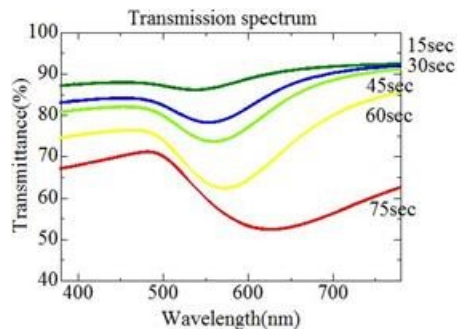


Figure 1: Optical transmittance of anatase nanocrystalline films supporting Au nanoparticles. Dependence on deposition time.

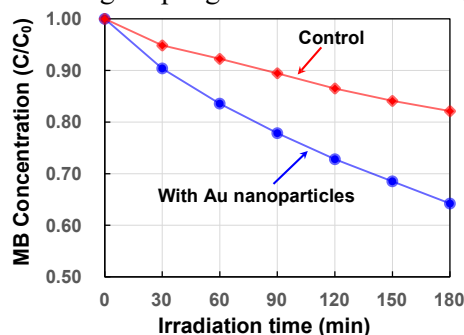


Figure 2: Photocatalytic activity of anatase nanocrystalline film supporting Au nanoparticles and control sample.

# Electronically induced rapid sub-ps structural transitions in tungsten upon ultrafast laser excitation

H. Zhang<sup>1</sup>, C. Li<sup>1,2</sup>, E. Bévilion<sup>1</sup>, J. P. Colombier, R. Stoian<sup>1</sup>

<sup>1</sup>Laboratoire Hubert Curien, UMR 5516 CNRS, Université de Lyon, Université Jean Monnet, 42000 St. Etienne, France

<sup>2</sup>State Key Laboratory of Transient Optics and Photonics, Xi'an Institute of Optics and Precision Mechanics, CAS, 710119 Xi'an, China  
razvan.stoian@univ-st-etienne.fr

The time needed for a metal to structurally respond to electronic excitation is key in defining behaviors under extreme conditions. In current views it is usually set by electron-phonon coupling and defines the limitations in the achievement of non-thermal rapid structural phases. We show that ultrashort laser excitation of metallic tungsten determines unexpectedly fast optical and structural transformations, almost on the timescale of the laser pulse. Driven by Fermi redistribution of carriers around a d-band pseudogap in the vicinity of the damage threshold, quasi-resonant optical excursions occur upon pumping with near-infrared photons, initiating a transient plasmonic state for the initial non-plasmonic metal.<sup>1</sup> Beyond this range, sub-ps ablation occurs, challenging current thermally-driven scenarios relying on vibrational coupling and phase transformations. We indicate a correlated action towards structure destabilization involving charge depletion and electronic pressure. If, at low excitation, primarily localized states are populated due to Fermi smearing, screening the electron-ion potential, the transfer reverses between low-lying bands to delocalized states with increasing electronic temperature, and a strong charge deficit appears on bonding orbitals.<sup>2</sup> In the presence of pressure gradients, this is prone to rapidly destabilize the structure even in a metallic environment. Using time-resolved ellipsometry, first principle molecular dynamics and hydrodynamic calculations we demonstrate that various mechanisms concur in a correlated way.<sup>3</sup> They include mutual effects of charge-induced bond-softening, swift mechanical pressure drives, or thermodynamic supercritical trajectories. An ultrafast competition between non-classical charge distortions, electron-driven mechanical stress, and classical electron-phonon dynamics appears, with coexistence of thermal and non-thermal effects on scales believed prohibitive for the former.

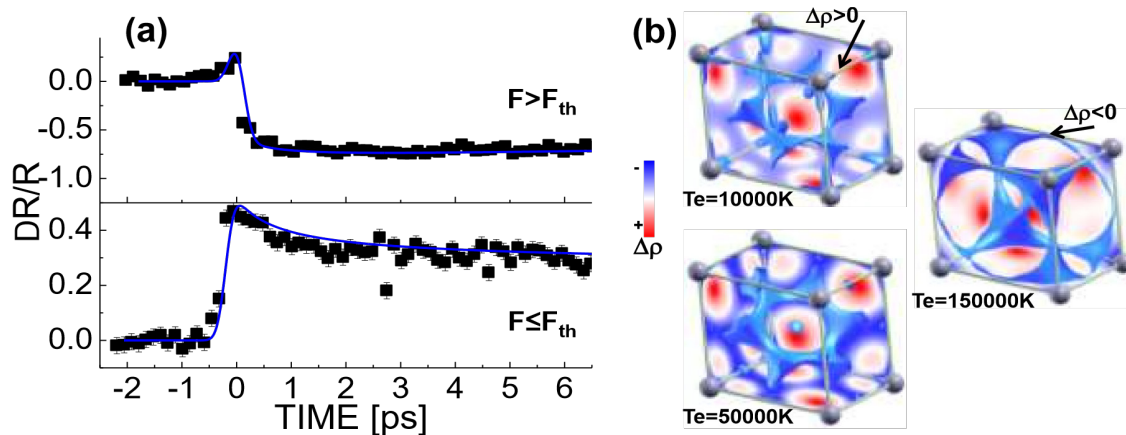


Figure 1: (a) Time-resolved reflectivity measurements on W surfaces close and above the ablation threshold. (b) Iso-surface normalized charts of charge redistribution (loss and gain  $\Delta\rho$  domains) in W relative to the unexcited material for a range of electronic temperatures.

1. E. Bévilion, J. P. Colombier, V. Recoules, H. Zhang, C. Li, and R. Stoian, Phys. Rev. B (2016);
2. S. T. Murphy, S. L. Daraszewicz, Y. Giret, M. Watkins, A. L. Shluger, K. Tanimura, and D. M. Duffy, Phys. Rev. B 92 134110 (2015);
3. H. Zhang, C. Li, E. Bévilion, G. Cheng, J. P. Colombier, and R. Stoian, submitted (2016).

# Ab-initio and classical molecular dynamics simulations of ultrafast structural phenomena in laser excited solids

T. Zier, B. Bauerhenne, V. Lipp, D. S. Ivanov, E. S. Zijlstra and M. E. Garcia

*Institute of Physics, Universität Kassel, Heinrich-Plett-Str. 40, 34132 Kassel, Germany  
garcia@physik.uni-kassel.de*

Intense femtosecond-laser pulses are able to induce ultrafast nonthermal melting of different materials along pathways that are inaccessible under thermodynamic conditions. In order to investigate the nonthermal motion of atoms upon femtosecond laser excitation we performed *ab-initio* molecular-dynamics simulations on laserexcited potential energy surfaces using our code CHIVES (Code for Highly excited Valence Electron Systems). We found surprising results, like excitation of squeezed thermal phonons, which constitute the precursor of nonthermal melting as a function of fluence<sup>1</sup>, or atomic fractional diffusion, as a transient state preceding the formation of a nonthermal liquid<sup>2</sup>. Different experimentally measurable signatures of nonthermal melting and the differences to thermal melting were also identified<sup>3</sup>. In particular, we will show that the energy flow from the excited electron system to the phonon modes is extremely anisotropic in the nonthermal regime<sup>4</sup>. In order to extend our method for the study of nucleation phenomena, we developed an analytical interatomic potential for laser-excited silicon, which depends on the electronic temperature. Effects like bond softening in the presence of hot electrons are taken into account. With the help of this potential we were able to perform large-scale simulations and study nucleation dynamics during nonthermal melting.

Moreover, we applied a hybrid atomistic-continuum model capable of capturing the essential mechanisms responsible for the laser-induced nanostructuring of gold surfaces upon excitation with spatially modulated ultrashort UV pulses. Our TTM-MD approach allowed us to perform calculations on experimental spatial and time scales and to a one-to-one comparison with experiments. Theoretical results are in excellent agreement with experiment. Our simulations show the presence of voids beneath the surface as a consequence of the laser excitation, explaining the formation of nanobumps and their sizes depending on the laser fluence<sup>5</sup>.

1. E. S. Zijlstra, A. Kalitsov, T. Zier and M. E. Garcia, Squeezed Thermal Phonons Precursor Nonthermal Melting of Silicon as a Function of Fluence, *Physical Review X* **3**, 011005 (2013);
2. E. S. Zijlstra, A. Kalitsov, T. Zier and M. E. Garcia, Fractional Diffusion in Silicon, *Advanced Materials* **25**, 5605-5608 (2013);
3. T. Zier, E. S. Zijlstra, A. Kalitsov, I. Theodonis and M. E. Garcia, Signatures of nonthermal melting, *Structural Dynamics* **2**, 054101 (2015);
4. T. Zier, E. S. Zijlstra and M. E. Garcia, Quasimomentum-Space Image for Ultrafast Melting of Silicon, *Phys. Rev. Lett.* **116**, 153901 (2016);
5. D. S. Ivanov, V. P. Lipp, A. Blumenstein, F. Kleinwort, V. P. Veiko, E. Yakovlev, V. Roddatis, M. E. Garcia, B. Rethfeld, J. Ihlemann, and P. Simon, Experimental and Theoretical Investigation of Periodic Nanostructuring of Au with Ultrashort UV Laser Pulses near the Damage Threshold, *Phys. Rev. Applied* **4**, 064006 (2015).

# Modeling of propagation of femtosecond laser pulses with spatiotemporal coupling through glass materials

V.P. Zhukov<sup>1,2</sup>, N.M. Bulgakova<sup>3,4</sup>, Y. Morova<sup>5</sup>, S. Aktürk<sup>5</sup>

<sup>1</sup>*Institute of Computational Technologies SB RAS, 6 Lavrentyev Ave., 630090 Novosibirsk, Russia*

<sup>2</sup>*Novosibirsk State Technical University, 20 Karl Marx ave., 630073, Novosibirsk, Russia*

<sup>3</sup>*HiLASE Centre, Institute of Physics ASCR, Za Radnici 828, 25241 Dolni Březany, Czech Republic*

<sup>4</sup>*Institute of Thermophysics SB RAS, 1 Lavrentyev Ave., 630090 Novosibirsk, Russia*

<sup>5</sup>*Department of Physics, Istanbul Technical University, Maslak 34469 Istanbul, Turkey*  
zukov@ict.nsc.ru

Ultrashort laser pulses are usually described in terms of temporal and spatial dependences of their electric field, assuming that the spatial dependence is separable from time dependence. However, in most situations this assumption is incorrect as generation of ultrashort pulses and their manipulation lead to couplings between spatial and temporal coordinates resulting in various effects such as pulse front tilt (PFT) and spatial chirp. One of the most interesting spatiotemporal coupling effects is the so-called “lighthouse effect”, the phase front rotation with the beam propagation distance.<sup>1,2</sup> The interaction of spatiotemporally coupled laser pulses with transparent materials have interesting peculiarities, such as a violation of axial symmetry of laser energy coupling and the effect of nonreciprocal writing, which can be used to facilitate microfabrication of photonic structures inside optical glasses.

In paraxial approach, the PFT and the phase front rotation can be described by the spatiotemporal terms in the boundary condition for the electric field as

$$E = E_0 \exp(-r^2/w^2 - ikr^2 / (2f) - (t - p_R x - i p_I x)^2 / t_L^2 + i\beta t^2)$$

Here  $w$  is the laser beam waist;  $t_L$  is the pulse duration;  $p_R$ ,  $p_I$ , and  $\beta$  are the parameters determining the PFT and its rotation.<sup>1</sup> In this work, we investigate the influence of these parameters on the distribution of absorbed laser energy inside fused silica glass. The model, which is based on nonlinear Maxwell’s equations supplemented by the hydrodynamic equations for free electron plasma, is applied.<sup>3</sup> As three-dimensional solution of such problems would require huge computational resources, a simplified two-dimensional model has been proposed which enables a qualitative insight to a number of PFT effects appearing at volumetric laser modification of transparent materials, including violation of axial symmetry of laser energy absorption and the effect of nonreciprocal writing.

**Acknowledgements:** The work was jointly supported by RFBR (Russian Foundation for Basic Research, Grant 15-51-46007) and TUBITAK (the Scientific and Technological Research Council of Turkey, Grant 114F502).

1. S. Akturk, X. Gu, P. Gabolde, R. Trebino, The general theory of first-order spatio-temporal distortions of Gaussian pulses and beams, *Opt. Express* **13**, 8642-8661 (2005);
2. J.A. Wheeler, A. Borot, S. Monchocé, H. Vincenti, A. Ricci, A. Malvache, R. Lopez-Martens, F. Quéré, Attosecond lighthouses from plasma mirrors, *Nature Photonics* **6**, 829–833 (2012);
3. N.M. Bulgakova, V.P. Zhukov, S.V. Sonina, Y.P. Meshcheryakov, Modification of transparent materials with ultrashort laser pulses: What is energetically and mechanically meaningful? *J. Appl. Phys.* **118**, 233108 (2015).





# POSTERS



# Fluorescence emission structure of a side-pumped Rh6G dye-doped micro-droplet

I.R. Andrei<sup>1</sup>, M. Boni<sup>1,2</sup>, A. Staicu<sup>1</sup>, M.L. Pascu<sup>1,2</sup>

<sup>1</sup>National Institute for Lasers, Plasma, and Radiation Physics, str. Atomistilor 409, 077125 Magurele, Romania

<sup>2</sup>Faculty of Physics, University of Bucharest, str. Atomistilor 405, 077125 Magurele, Romania  
ionut.andrei@inflpr.ro

This paper presents results about the interaction of a laser pulse with individual pendant Rhodamine 6G (Rh6G) dye-doped water droplets at different concentration. When the laser radiation is partially or fully absorbed by the droplet's components the interaction is called resonant.

Following absorption, laser induced fluorescence (and even lasing) effects are produced and are investigated through fluorescence spectra analysis. In the reported experiments resonant interaction was studied, a single droplet behaving as an optical closed spherical cavity in which optical signal/radiation is amplified<sup>1</sup>. By varying the dye concentration, pumping energy and droplet volume, typical broadband fluorescence was obtained and a narrow peak assigned to lasing effect was evidenced<sup>2</sup>.

The excitation is made with the second harmonic generated by a pulsed Nd:YAG laser system at 532 nm through a lens with a focus length of 150 mm, and the droplet was positioned at about 122 mm from the lens so that the pumping beam covered, at the limit, the droplet (Fig. 1a). The energy domain of the pumping beam was chosen in such way that resonant effects are obtained at the lowest energy values, and at the same time strong mechanical effects (liquid expulsion) are avoided (Fig. 1b). At the highest pumping energies the mechanical effects (e.g. droplet deformation) were present after the first pulse (Fig. 1c).

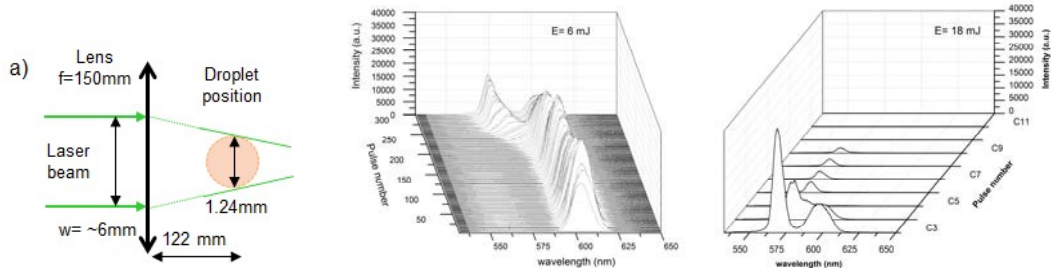


Figure 1: a) Scheme of interaction geometry of the laser beam with a dye-doped water droplet of  $V= 1\mu\text{l}$ ; b) and c) emission spectra for continuous irradiation with a pulsed laser beam at two energies, 6 and 18 mJ.  $D$ , droplet diameter;  $w$ , beam waist;  $d$ , lens – droplet distance.

The pendant microdroplets containing laser dye exhibit an enhanced fluorescence emission signal. This effect may be explained as being due to the spherical/quasi-spherical geometry of the pendant droplet. The droplet acts as an optical resonator amplifying the fluorescence signal with the possibility of producing a lasing effect. We also investigated how Rhodamine 6G concentration, pumping laser beam energies and number of pumping laser pulses influence the fluorescence radiation behavior.

The results can be useful in optical imaging, since they can lead to the use of smaller quantities of fluorescent dyes to obtain the same quality of results.

**Acknowledgements:** This work was supported by the Romanian ANCS/CNDI–UEFISCDI program, projects PN-II-ID-PCE-2011-30922, PN-II-PT-PCCA-2011-3.1-1350, and NUCLEU program, project PN 1647 / 2016.

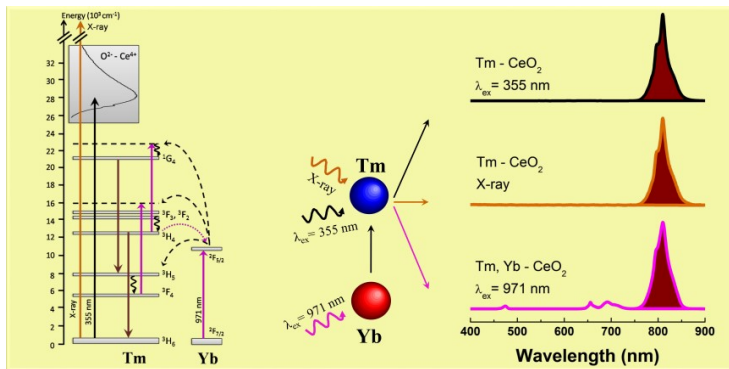
1. X.-Y. Pu, W.-K. Lee, Lasing characteristics of a pendant drop deformed by an applied electric field, *Optics Letters* vol. 25, No. 7 (2000);
2. M. Boni, V. Nastasa, I.R. Andrei, A. Staicu, M. L. Pascu, Enhanced fluorescence emitted by microdroplets containing organic dye emulsions, *Biomicrofluidics* 9, 014126 (2015).

# X-ray and pulsed UV to NIR optical excitation of luminescence in doped nanoparticles for bioimaging and spectral converters

D. Avram<sup>1</sup>, I. Tiseanu<sup>1</sup>, C. Tiseanu<sup>1</sup>

<sup>1</sup> National Institute for Lasers, Plasma and Radiation Physics, Atomistilor Str. 409, Bucharest-Magurele, 077125, ROMANIA  
radu.avram@infpr.ro

We present our latest results on the X-ray and ultraviolet (UV) to near - infrared (NIR) excited luminescence of lanthanide doped nanoparticles. Optical (down and up - conversion excitation) spanned large UV to NIR range (250 to 1500 nm) by use of a tunable ns pulsed laser. The investigated nanoparticles (size between 30 and 100 nm) are composed of CeO<sub>2</sub> and BiOCl as hosts and Tm (Yb) and Er as lanthanide (co)dopants, respectively. The up - conversion mechanisms were differentiated by the analysis of time - gated up - conversion emission measured at different delay times after the laser pulse.<sup>1-3</sup>



From the applications side, the pure NIR emission around 800 nm that has been observed under UV, X-ray and up - conversion excitation of Tm (Yb) - CeO<sub>2</sub> (Figure 1) may be attractive for both spectral converter and theranostic applications.<sup>3</sup> The remarkable emission at 980 nm which accounts for 98% of the total emission measured between 500 and 1000 nm under pulsed excitation at ~ 1500 nm suggests that Er - CeO<sub>2</sub> may be a promising system for second biological window applications.

Figure 1: NIR (~800 nm) emission of Tm and Tm, Yb - CeO<sub>2</sub> measured under different excitation modes: UV, X-ray and up - conversion excitation.

**Acknowledgements:** The authors acknowledge the Romanian National Authority for Scientific Research (CNCS-UEFISCDI) (project number PN-II-ID-PCE-2011-3-0534) and program NUCLEU, contract 4N/2016 for the financial support.

1. D. Avram, B. Cojocaru, M. Florea, V. Teodorescu, I. Tiseanu and C. Tiseanu, NIR to Vis-NIR up-conversion and X-ray excited emission of Er doped high Z BiOCl, *Optical Materials Express* **5**(5), 951-962 (2015);
2. D. Avram, M. Florea, I. Tiseanu and C. Tiseanu, Time delay and excitation mode induced tunable red/near-infrared to green emission ratio of Er doped BiOCl, *Journal of Physics D: Applied Physics* **48**(35), 355501 (2015);
3. D. Avram, B. Cojocaru, A. Urda, I. Tiseanu, M. Florea and C. Tiseanu, Pure and almost pure NIR emission of Tm and Tm, Yb-CeO<sub>2</sub> under UV, X-ray and NIR up-conversion excitation: key roles of level selective antenna sensitization and chargecompensation, *Physical Chemistry Chemical Physics* **17**, 30988-30992 (2015).

## Analysis of thin films for micro-electronics via laserinduced breakdown pectroscopy

E. Axente<sup>1</sup>, J. Hermann<sup>2</sup>, G. Socol<sup>1</sup>, C.R. Luculescu<sup>1</sup>, P. Ionescu<sup>3</sup>, D. Pantelica<sup>3</sup> and V. Craciun<sup>1</sup>

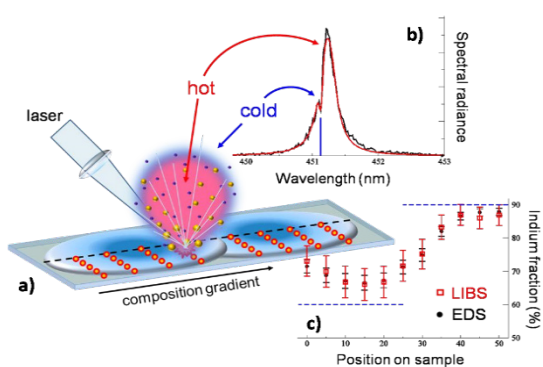
<sup>1</sup>Laser-Surface-Plasma Interactions Laboratory, National Institute for Lasers, Plasma and Radiation Physics, 077125 Măgurele, Romania

<sup>2</sup>LP3, CNRS/Aix-Marseille Université, 163 av. Luminy, 13288 Marseille, France

<sup>3</sup> National Institute of Physics and Nuclear Engineering Horia Hulubei, RO-077125, Măgurele, Ilfov, Romania  
emanuel.axente@infpr.ro, hermann@lp3.univ-mrs.fr

The main fields related to thin films nowadays, having both research and industrial impact are micro-optoelectronics, computer science and manufacturing, and physical devices miniaturization. Thin (<1 μm) and very thin films (<100 nm) materials have already proven to be key elements for continued advances in several emerging cutting edge technologies. Among these, indium zinc oxide (IZO) and silicon-germanium (SiGe) thin films are promising materials for applications like new thin film transistors and displays, thermoelectrics, photovoltaics, and nanoelectronics. However, a fast but precise quantitative investigation of thin films composition is mandatory, preferably *in-situ* and in real time. With decreasing the films thickness, some of the classical investigation tools suffer due to limited accuracy or depth resolution, some other could alter the composition during analyses. The advantages and limitations of LIBS, in comparison with other analytical techniques, are well known. Accurate analysis of thin films is a difficult task compared to that of bulk samples, since pulse energy employed in conventional LIBS analysis ranges typically from 10 to 100 mJ.

Here we report on the influence of the background gas on the analytical performances of LIBS based on plasma modeling during analyses of IZO (500 nm) and SiGe (<100 nm) compositional libraries thin films. The results were compared with complementary measurements using EDX and RBS. Accurate analysis of IZO films via LIBS in air based on the calculation of the spectral radiance of the nonuniform plasma is proven, the metal fractions being in good agreement with the values obtained by EDX (Figure 1). As the fractions measured by both methods differ by



only 5%, the effective LIBS measurement uncertainty is shown to be better than the value of 10% expected from the imprecision of spectroscopic data. Similar LIBS measurements on very thin SiGe films were conducted in air and Argon backgrounds. It is proven that analyses based on the assumption of uniform spatial distributions may be applied to material analyses in ambient air as long as the gate delay is short enough and no transitions of strong optical thickness are involved.<sup>2</sup> A good agreement when compared to EDX and RBS was achieved, despite the large variation of the film thickness and moderate accuracy of available spectroscopic data for germanium.

Figure 1: Schematic representation of thin film irradiation geometry and plasma expansion a). Measured spectrum (black line) and computed spectral radiance (red line) of In I 451.13 nm spectral line for a non-uniform plasma in local thermodynamic equilibrium b). Atomic fraction of indium compared to the total metal content within the thin film versus the longitudinal position on the sample c).

1. E. Axente, J. Hermann, G. Socol, L. Mercadier, S.A. Beldjilali, M. Cirisan, C.R. Luculescu, C. Ristoscu, I.N. Mihailescu, V. Craciun, J. Anal. At. Spectrom. 29 (2014) 553;
2. J. Hermann, C. Gerhard, E. Axente, C. Dutouquet, Spectrochimica Acta Part B 100 (2014) 189.

## Film continuity studies of refractory metal nano-layers obtained using an improved set-up of the high voltage anodic plasma

M. Badulescu<sup>1</sup>, A. Anghel<sup>1</sup>, A. M. Vlaicu<sup>2</sup>, C. Surdu-Bob<sup>1</sup>, R. Gavrilă<sup>3</sup>, B. Bită<sup>3</sup>

<sup>1</sup>Low Temperature Plasma Lab., National Institute for Lasers, Plasma and Radiation Physics, Magurele – Romania

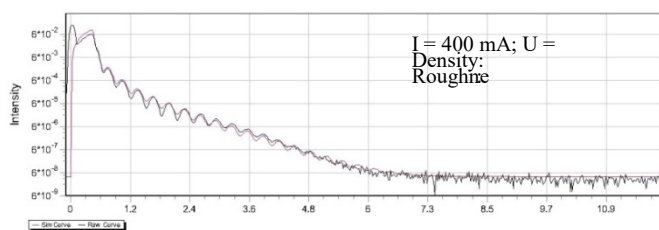
<sup>2</sup>National Institute for Materials Physics, Magurele – Romania

<sup>3</sup>Microtechnology Institute – Baneasa, Romania  
 marius.badulescu@infpr.ro

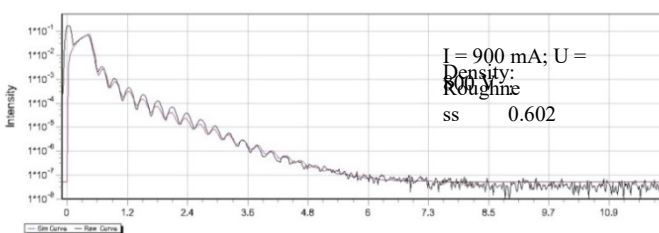
Refractory metals are elements with a high melting point (above 2000°C), high density and high hardness. Nano-films of such materials are attractive for a large range of applications, from wear protection to photovoltaics. They are also attractive for optics of high energy radiation applications where high reflection power and temperature resistance are needed. In order to be used for these applications, the most important qualities of refractory metal nano-films are high smoothness, high density and compactness.

In order to assess the potential of our high voltage anodic plasma coating technique for the synthesis of high quality layers for X-ray optics, nano-layers of W, Ta, B and Mo refractory metals were deposited onto very smooth glass substrates. The nano-layers were investigated by Scanning Electron Microscopy, Atomic Force Microscopy and X-Ray Reflectivity in terms of roughness, density and film continuity at a given thickness. The results obtained are presented and discussed with respect to the influence of deposition conditions on these film characteristics.

The optimal deposition conditions needed for obtaining full substrate coverage at a minimum film thickness for each refractory metal studied is reported.



(a)



(b)

Figure 1: Boron film deposited with higher (a) and lower (b) ion energy. The influence of plasma deposition parameters on film density and roughness

1. E.O. Filatova, I.V. Kozhevnikov et al, X-ray and photoelectron spectroscopic nondestructive methods for thin films and interfaces study. Application to SrTiO<sub>3</sub> based heterostructures, Microelectronic Engineering Name, **109**, 13-16 (2013).

2. N. Ghafoor, Growth and Nano-structural Studies of Metallic Multilayers for X-ray Mirrors (Linkoping University, Linkoping, Sweden), PhD Thesis (2005).

# Calculation of ionization probability of Nitrogen in gas jets for the Laser Plasma Wakefield Acceleration experiments at ELI-NP

S. Balascuta

*The National Institute for R&D in Physics and Nuclear Engineering, Department of ELI-NP, 077125, Magurele, Ilfov, Romania*

New QED phenomena are planned to be studied at Extreme Light Infrastructure Nuclear Physics (ELI-NP), where a 10 PW Laser beam (with 20 femtoseconds pulses at frequency 1/60 Hz), with central wavelength 0.8  $\mu\text{m}$ , will be focused in a long plasma guide<sup>1</sup> to accelerate electrons up to 10 GeV. In the first experiments the Laser pulse will be focused by a long focal length parabolic mirror (e.g.  $f/20$ ) in a less than 75  $\mu\text{m}$  spot radius, in a gas jet, to assure a Laser field intensity above  $10^{20}$  W/cm<sup>2</sup>. At this field intensity and for gas densities between  $10^{18}$  cm<sup>-3</sup> and  $10^{19}$  cm<sup>-3</sup>, the electrons from plasma are expected to be self-injected in a bubble-like plasma wake formed behind the Laser pulse<sup>2</sup>. To increase the electric charge per pulse, small amount of Nitrogen (up to 10%) can be added into a Helium gas jet<sup>2</sup>. The probability of Nitrogen ionization in a range of field intensities was computed analytically, according to previous used methods<sup>3</sup>. The number of the seven Nitrogen species and the charge density of the electron bunches, were calculated along the Laser propagation direction, with the particle-in-cell code EPOCH<sup>4</sup>. The optimum plasma densities for two concentrations of Nitrogen in Helium, were computed function of the Laser pulse length. The charge, energy and emittance of the electron bunch were computed for Nitrogen concentrations from 1% to 10%. The results show that for each Laser pulse length, there is an optimum plasma density for which the electron bunch charge and average energy are maximum.

1. I.C.E. Turcu, S. Balascuta, F. Negoita, D. Jaroszynski, P. McKenna "Strong field physics and QED experiments with ELI-NP 2x10 PW laser beams", AIP Conf. Proc. 1645, 416 (2015);
2. A. Pak, K. A. Marsh, S. F. Martins, W. Lu, W. B. Mori, and C. Joshi, Physical Review Letters 104, 025003 (2010);
3. L. V. Keldysh, Ionization in the field of a strong electromagnetic wave, Soviet Physics JETP, 20, 5, 1307-1314, 1965;
4. T.D.Arber, et al, Contemporary particle-in-cell approach to laser-plasma modeling. Plasma Physics and Controlled Fusion, 57 (11), 113001, 2015.

## Alignment laser procedure and beam wavefront optimization using adaptive optics loop

I. Barbut<sup>1</sup>, L. Neagu<sup>1,2</sup>, M. Serbanescu<sup>2</sup>, I. Dancus<sup>1</sup>, R. Ungureanu<sup>2</sup>, G. Cojocaru<sup>2</sup>, P. Ghenuche<sup>1</sup>, M. O. Cernaianu<sup>1</sup>, I. Nicolae<sup>2</sup>, E. Lalla<sup>1</sup>, D. Ursescu<sup>1</sup>

<sup>1</sup>Extreme Light Infrastructure – Nuclear Physics, Horia Hulubei National Institute for Physics and Nuclear Engineering, Magurele, Ilfov, Romania

<sup>2</sup>INFLPR, Magurele, Ilfov, Romania iulia.barbut@eli-np.ro

Since 2013 a petawatt class laser system has been installed in the Center for Advanced Laser Technologies (CETAL)<sup>1</sup>. This laser system is fully Ti: Sapphire based, using a double stage chirped-pulse amplification technique<sup>2</sup> and was produced by THALES company.

In this type of laser system thermal drift and other long term mechanical instabilities have the consequences of changing the optical path of the laser beam in time, and as a consequence, the position and quality of the laser focal spot used in experiments. Monitoring the optical path and the use of a procedure for laser alignment is thus necessary.

In this work we present the method we used at the CETAL 1PW laser for monitoring the laser beam path, based on near field and far field monitoring with common optics and CCD cameras. We have implemented this type of beam monitoring in specific locations important for the general alignment of the laser system. By developing specialized software we have integrated this system into the general control system of the laser.

Another important subject of this work is the quality of the focal spot and its optimization. One of the important parameters in reaching a good focal spot is the wavefront of the laser beam. All optics involved in the production, amplification and propagation of high power lasers have aberrations. This static aberration added to the transient aberration, in general produced by transient thermal effects in air and amplification medium, leads to an imperfect wavefront of the laser beam at the output of the system. Experiments using this type of lasers require thus controlling the focus of the laser beam. Here we will present the implementation of an adaptive optics system, including a focal spot optimization loop, in order to correct the wavefront distortions and obtain the best focus, based on an Imagine Optic Inc. technology.

1. Matras Guillaume, François Lureau, Sébastien Laux, Olivier Casagrande, Christophe Radier, Olivier Chalus, Frédéric Caradec, Laurent Boudjemaa, Christophe A. Simon-Boisson, Razvan Dabu, Florin Jipa, Liviu Neagu, Ioan Dancus, Dan Sporea, Constantin Fenic, Constantin Grigoriu, "First sub-25fs PetaWatt laser system", CLEO: Science and Innovations, United States (2013);

2. D. Strickland and G. Mourou, *Compression of amplified chirped optical pulse*, Optics Communications, Vol. 56 (3), 219-221 (1985).

# Laser scribing of perovskite thin-film solar cells

L. Bayer<sup>1</sup>, M. Ehrhardt<sup>1</sup>, P. Lorenz<sup>1</sup>, S. Pisoni<sup>2</sup>, S. Buecheler<sup>2</sup>, K. Zimmer<sup>1</sup>

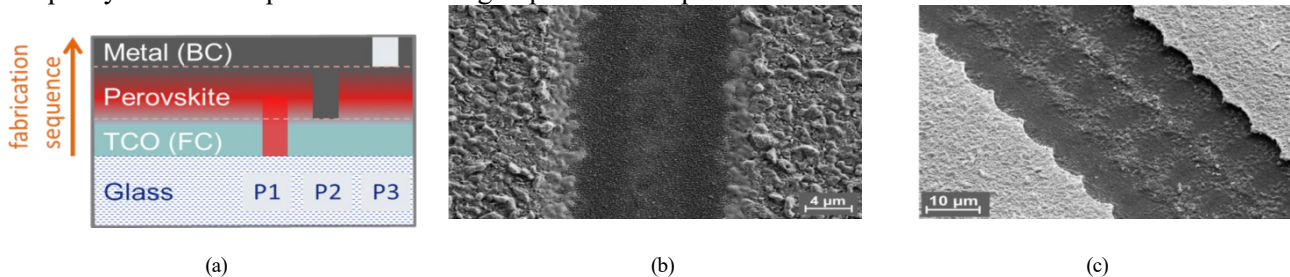
<sup>1</sup>Leibniz-Institut für Oberflächenmodifizierung e. V., Permoserstr, 15, 04318 Leipzig, Germany

<sup>2</sup>EMPA, Überlandstr, 129, 8600 Dübendorf, Switzerland  
klaus.zimmer@iom-leipzig.de

Perovskite thin-film solar cells exhibit a rapid growing attention in scientific and commercial applications due to the potential of combining high efficiency and low production costs. For a low-cost production of PV modules a fast and cost-effective structuring of the solar cell material with small dead areas is necessary where laserscribing methods seem to be the most promising.

The solar cell, based on a gold back contact, CH<sub>3</sub>NH<sub>3</sub>PbI<sub>2</sub> perovskite and a TCO front contact, must be laserscribed in three steps (see Figure 1 (a)): P1: scribing of the TCO front contact material, P2: scribing of the perovskite, and P3: scribing of the gold back contact. The laser scribing process of the particular films were investigated with a picosecond laser with a pulse duration of 10 ps at different wavelengths (1064 nm and 355 nm) as well as with a femtosecond laser with a pulse duration of 150 fs and a wavelength of 780 nm. The samples were irradiated from the film side as well as from the rear side (irradiated through the glass substrate). The morphology, structure and modifications of the film materials after the laser scribing were analyzed by optical microscopy (reflective, interference) and scanning electron microscopy (SEM). Additional characterizations were performed by energy-dispersive X-ray spectroscopy (EDX). In Figure 1 (b) and (c) typical scribing results are shown.

The modifications of the scribed material in dependence on the applied laser parameters were analyzed in detail for both used lasers. Especially the edge quality of the laser-generated structures was investigated in order to ensure the quality of the subsequent manufacturing steps of the complete solar cell module.



(a) Cross section of an interconnection area of a Perovskite thin-film system.  
(b) SEM image of a P2 scribe using picosecond laser radiation ( $\lambda = 1064$  nm,  $\Delta t_p = 10$  ps, front side irradiation).  
(c) SEM image P3 scribe using picosecond laser radiation ( $\lambda = 355$  nm,  $\Delta t_p = 10$  ps, front side irradiation).

## Comparison between HiPIMS and PLD Deposition of ZnO and TiO<sub>2</sub> thin films

N. Becherescu<sup>1,5</sup>, I.N. Mihailescu<sup>2</sup>, G. Socol<sup>2</sup>, C. Luculescu<sup>2</sup>, V. Tiron<sup>3</sup>, G. E. Stan<sup>4</sup> and M. Udrea<sup>5</sup>

<sup>1</sup>University of Bucharest, Faculty of Physics, 405 Atomistilor, P. O. Box MG-11, 077125, Magurele, (Ilfov), Romania

<sup>2</sup>National Institute for Lasers, Plasma and Radiation Physics, 409 Atomistilor St., 077125, Magurele (Ilfov), Romania

<sup>3</sup>Faculty of Physics, Alexandru Ioan Cuza University, 11, Carol I Blvd., 700506, Iasi, Romania

<sup>4</sup>National Institute of Materials Physics, 405A, Atomistilor St., 077125, Magurele, (Ilfov), Romania

<sup>5</sup>Apel Laser SRL, 25 Vantorilor St., 077135, Mogosoaia (Ilfov), Romania  
nicu.becherescu@apellaser.ro

Zinc oxide (ZnO) and titanium dioxide (TiO<sub>2</sub>) thin films were deposited on Si (100) and SiO<sub>2</sub> substrates using two different techniques: high-power impulse magnetron sputtering (HiPIMS) and pulsed laser deposition (PLD). The structure and morphological characteristics of the obtained thin films were compared. The X-ray diffraction patterns showed similar characteristics in both cases. The morphological characteristics of the films have been studied by using SEM. For the PLD experiment we have used a UV KrF\* ( $\lambda = 248$  nm,  $\tau_{FWHM}$  aprox. 7 ns) excimer laser source, operated at 2.8 J/cm<sup>2</sup> incident fluence value, target diameter 1". For the HiPIMS samples, we have used a circular magnetron, target diameter 2", magnetic field induction at the target surface of 1000 Gauss, a high voltage pulse generator for HiPIMS technology, power density: 0.5-10 kW cm<sup>-2</sup>, adjustable pulse duration 2-50 μs, adjustable pulse period between 0.2 and 6 ms, with a response time of less than 500 nanoseconds. In figure a1 and a2 we have the XRD patterns for TiO<sub>2</sub> samples deposited by HiPIMS and PLD, respectively, and in figure b1 and b2 we have the SEM images of the TiO<sub>2</sub> samples. We have similar, comparative results, for ZnO and for the optical characteristics of the deposited thin films as well. The specific advantages and disadvantages of these deposition methods are presented.



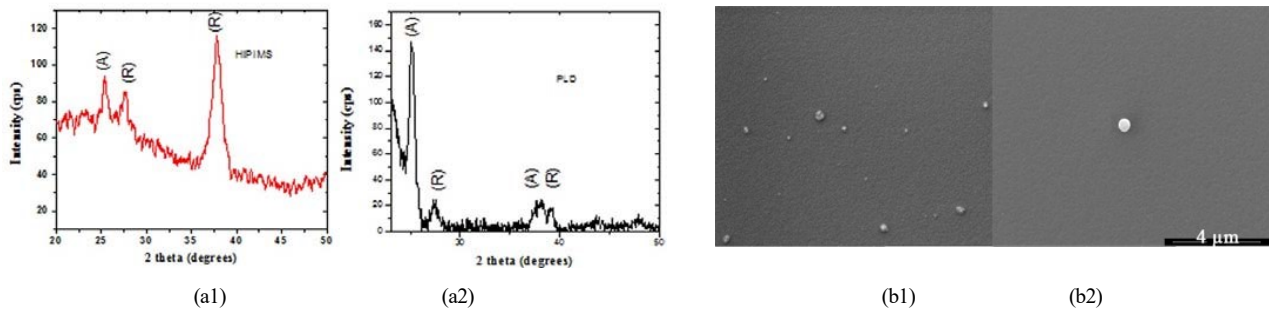


Figure 1: X-ray diffraction patterns of  $\text{TiO}_2$  films deposited with HiPIMS (a1) and PLD (a2); SEM images of  $\text{TiO}_2$  films deposited with HiPIMS (b1) and PLD (b2).

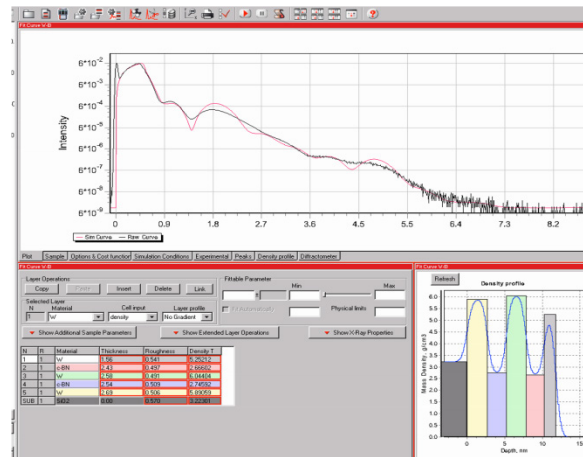


Figure 2: XRR spectrum of a W-B nano-multilayer

1. E.O. Filatova, I.V. Kozhevnikov et al, X-ray and photoelectron spectroscopic nondestructive methods for thin films and interfaces study. Application to  $\text{SrTiO}_3$  based heterostructures, *Microelectronic Engineering Name*, **109**, 13-16 (2013);
2. N. Ghafoor, Growth and Nano-structural Studies of Metallic Multilayers for X-ray Mirrors (Linkoping University, Linkoping, Sweden), PhD Thesis (2005).

## Dose calculations in cell monolayers from proton beams generated by femtosecond lasers

M. Bobeica<sup>1</sup>, S. Aogaki<sup>1</sup>, M. Tomut<sup>2</sup>, T. Asavei<sup>1</sup>, M. Cernaianu<sup>1</sup>, P. Ghenuche<sup>1</sup>, F. Negoita<sup>1</sup>, D. Stutman<sup>1,3</sup>

<sup>1</sup>ELI-NP, Horia Hulubei National Institute for Physics and Nuclear Engineering, Magurele, Romania

<sup>2</sup>GSI, Planckstraße 1, 64291 Darmstadt, Germany

<sup>3</sup>Johns Hopkins University, 3400 N Charles St., Baltimore, Maryland 21218, USA  
mariana.bobeica@eli-np.ro

The interaction of a high power laser (1PW, 25 fs) with a solid target at Extreme Light Infrastructure - Nuclear Power facility (ELI-NP) can generate pulsed proton beams (initial parameters: energy up to 60 MeV and a number of particles per pulse of  $10^9$ ) and other types of irradiation beams like electrons, gamma, X-rays. Of particular interest are irradiation experiments of biological samples (proteins, DNA, cells, tissue, plants and seeds) with multi-component, multi-energetic particle beams (example protons and electrons) in the context of deep space missions and establishment of permanent human habitats on Mars. Modelling of space radiation exposures in these type of experiments will lead to understanding of biological material responses and improved radiation shielding, or development of sustainable extra-terrestrial resources. Also, future therapeutic and adjuvant solutions as countermeasures for prolonged exposures to low or acute dose radiation could be investigated and tested. An experimental set-up was designed, according to results from Geant4 calculations, for a high throughput proton irradiation setup of bio-samples in a standard 96 well plate. This setup will be tested with protons and further with other types of irradiation beams (electrons, gamma, X-rays) in preparation for use with a multicomponent “cocktail” radiation that will become available at ELI-NP in the future. Geant4 simulations with proton beams (energy up to 60 MeV) provided insight in the spatial distribution of the deposited dose, total dose estimations, as well as input for the experimental set-up optimization.

# Biological evaluation and surface characteristics of Si-DLC and Ti-DLC coatings deposited by magnetron sputtering

D. Bociaga<sup>1a</sup>, M. Kaminska<sup>1b</sup>, A. Sobczyk-Guzenda<sup>1c</sup>, L. Swiatek<sup>1a</sup>, K. Jastrzebski<sup>1a</sup>, A. Olejnik<sup>1a</sup>

<sup>1</sup>Lodz University of Technology, Institute of Materials Science and Engineering, 1/15 Stefanowskiego St., 90-924 Lodz, Poland

<sup>a</sup>Division of Biomedical Engineering and Functional Materials

<sup>b</sup>Division of Biophysics

<sup>c</sup>Division of Coatings Engineering and Non-metallic Materials  
dorota.bociaga1@gmail.com

Recently, a rapid growth of the medical implants market may be observed as a consequence of both technological development as well as the increasing number of people suffering from disabilities. Due to the rising incidence of trauma injuries and cardiovascular diseases, the orthopedic and cardiovascular implants show the highest potential growth prospects. Nevertheless, the commonly applied metallic implants possess relatively poor surface properties caused by the lack of total chemical stability in human body environment<sup>1</sup>. Therefore, even the corrosion resistant metals may cause adverse biological response via release of the degradation products<sup>1</sup>. As a result, the growing interest is given to the surface modifications of metallic implants enhancing the biological response of the human body towards the surface of the implant. One of the most extensively researched solutions include the application of diamond-like carbon (DLC) coatings, which exhibit a combination of highly desirable properties in the context of biomedical applications<sup>2</sup>. Moreover, different properties of carbon coatings, including cell behaviour and body reaction towards the DLC surface, can be further improved by the incorporation of different elements into the carbon matrix<sup>3</sup>. As a consequence, the modified DLC coatings are nowadays extensively studied in terms of their possible medical applications.

As far as cardiovascular implants are concerned, one of the most promising dopants is silicon (Si), which not only favours the proliferation of endothelial cells, but also acts as an antithrombogenic agent. The increasing concentration of Si is associated with lower number of adhering platelets and decreased platelet activation level, and hence higher hemocompatibility<sup>4</sup>. At the same time, Si favours the attachment of human endothelial cells and does not induce cytotoxicity<sup>5</sup>. In the case of orthopaedic implants the enhancement of the osseointegration process is highly desirable in order to assure the proper bone-healing, what may be achieved by the addition of either titanium (Ti) or silicon. The incorporation of Ti into the DLC matrix not only promotes the bone marrow cells proliferation, but also simultaneously reduces the activity of the osteoclast-like cells<sup>6</sup>. Silicon in turn is considered to play an important role in bone calcification process and to increase the bone density<sup>7</sup>.

However, despite the numerous studies considering the biological properties of Si- and Ti-incorporated DLC coatings, there is lack of conclusive reports in terms of biological behaviour of coatings manufactured by a magnetron sputtering method. Moreover, the existing reports do not directly indicate the possible medical applications of the modified carbon coatings. Taking this into consideration, a complex biological evaluation of Si-DLC and Ti-DLC coatings followed by their surface characteristics was performed, since surface properties have a direct role in different post-implantation reactions including protein adsorption and cell proliferation<sup>1</sup>. The examined coatings were deposited on two commonly applied metallic biomaterials (AISI 316 LVM steel and Ti6Al7Nb alloy) using a magnetron sputtering method. The surface characteristics involved the analysis of surface morphology (SEM), chemical composition and structure (XPS, FTIR) as well as surface wettability and surface free energy. The biological assessment of the deposited coatings was based on two complementary cell proliferation and viability assays (LIVE/DEAD and XTT test) performed on two different cell lines, i.e. endothelial cells line EA.hy926 and osteoblast-like cells line Saos-2. The obtained results allowed to check the influence of both dopants on the biological response towards the modified carbon coatings as well as to correlate the obtained results with the surface properties of the investigated coatings.

**Acknowledgements:** This research has been supported by the National Centre for Research and Development under the grant no. LIDER/040/707/L-4/12/NCBR/2013 entitled „MOBIOMED: Modified BIOMaterials – MEDicine future”.

1. Y. Okazaki, E. Gotoh, T. Manabe, K. Kobayashi, Comparison of metal concentrations in rat tibia tissues with various metallic implants, *Biomaterials* 25(28), 5913-5920 (2004);
2. R. Hauert, K. Thorwarth, G. Thorwarth, An overview on diamond-like carbon coatings in medical applications, *Surface and Coatings Technology* 233, 119–130 (2013);
3. R. Hauert, A review of modified DLC coatings for biological applications, *Diamond and Related Materials* 12, 583–589 (2003);
4. S.E. Ong, S. Zhang, H. Du, H.C. Too, K.N. Aung, Influence of silicon concentration on the haemocompatibility of amorphous carbon, *Biomaterials* 28, 4033–4038 (2007);
5. A.A. Ogwu, T.I. Okpalugo, N. Ali, P.D. Maguire, J.A. McLaughlin, Endothelial cell growth on silicon modified hydrogenated amorphous carbon thin films, *Journal of Biomedical Materials Research Part B: Applied Biomaterials* 85(1), 105-113 (2008);
6. A. Shroeder, G. Francz, A. Bruinink, R. Hauert, J. Mayer, E. Wintermantel, Titanium containing amorphous hydrogenated carbon films (a-C:H/Ti): surface analysis and evaluation of cellular reactions using bone marrow cell cultures in vitro, *Biomaterials* 21, 449-456 (2000);
7. M.R. Calomme, J.B. Sindambiwe, P. Cos, C. Vyncke, P. Geusens, D.A. Van den Berghe, Effect of choline stabilized orthosilicic acid on bone density in ovariectomized rats, *Journal of Bone and Mineral Research* 19, 449-458 (2004).

# Compositional analyses of aerosols via laser-induced breakdown spectroscopy in helium

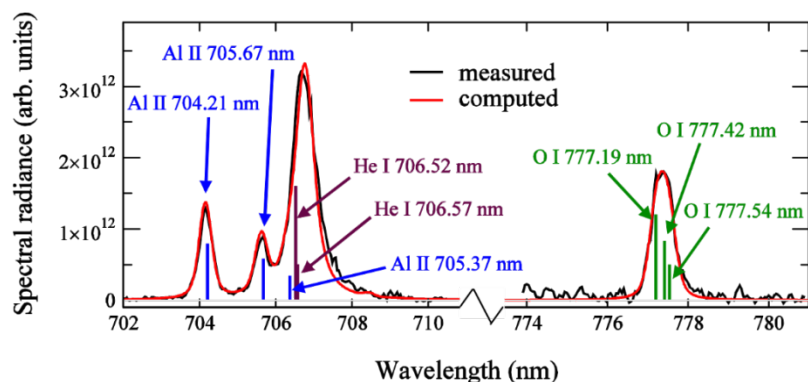
M. Boudhib<sup>1</sup>, J. Hermann<sup>2</sup>, C. Dutouquet<sup>1</sup>

<sup>1</sup>Institut National de l'Environnement Industriel et des Risques/DRC/CARA/NOVA, 60550 Verneuil-en-Halatte, France

<sup>2</sup>LP3, CNRS/Aix-Marseille Université, 163 av. Luminy, 13288 Marseille, France

hermann@lp3.univ-mrs.fr

The detection and the characterization of particles in the air and in water are major challenges in the field of environmental survey. Recently, particular efforts have been dedicated to the development of in situ real-time measurements of size and composition of particles in gaseous or liquid suspensions.<sup>1,2</sup> Laser-induced breakdown spectroscopy (LIBS) is a promising technique for such type of analyses. However, the variability of particle size and density make the measurement calibration difficult.<sup>3</sup> To overcome this problem, we have developed a calibration-free LIBS measurement procedure. Based on modeling of the laser-induced plasma, the composition of aerosols is deduced by comparing the measured emission spectrum to a spectrum computed for plasma in local thermal equilibrium. To illustrate the feasibility, the breakdown was produced in helium at atmospheric pressure. Due to the high initial temperature and the large thermal conductivity, breakdown in helium leads to rapid aerosol vaporisation and a more uniform plasma, compared to breakdown in air or argon. We demonstrate that the plasma can be described by a partial thermodynamic equilibrium. Thus, the population number densities of all plasma species follow the Boltzmann equilibrium distributions, except of helium atomic and ionic number densities. By recording spectra at different delays with respect to the laser pulse, we show that accurate analyses of the aerosol composition are only



possible for  $t \leq 1 \mu\text{s}$ , when the electron density is large enough to ensure the collisional equilibrium for the aerosol species.<sup>4</sup> In agreement with recent LIBS analyses of solid glass and alumina, the present results encourage compositional measurements of aerosols via laser-induced breakdown spectroscopy.

Figure 1: Emission spectrum of laser-induced breakdown in helium charged with alumina aerosols. The simulation based on a partial local thermodynamic equilibrium enables the compositional analysis of aerosols.<sup>5</sup>

1. D. W. Hahn, M. M. Lunden, Detection and Analysis of Aerosol Particles by Laser-Induced Breakdown Spectroscopy, *Aerosol Sci. Technol.*, 33,30–48 (2000);
2. C. B. Faye, T. Amodeo, E. Frejafon, N. Delepine-Gilon, C. Dutouquet, Sampling considerations when analyzing micrometric-sized particles in a liquid jet using laser induced breakdown spectroscopy, *Spectrochim. Acta Part B*, 91, 5–11 (2014);
3. V. Hohreiter, D. W. Hahn, Plasma-particle interactions in a laser-induced plasma: implications for laser-induced breakdown spectroscopy, *Anal. Chem.*, 78, 1509–1514 (2006);
4. M. Boudhib, J. Hermann, C. Dutouquet, Compositional analysis of aerosols using calibration-free laser-induced breakdown spectroscopy, *Anal. Chem.*, 88, 4029–4035 (2016).

## PLD and MAPLE deposited WO<sub>3</sub> thin films for gas sensors

S. Boyadjiev<sup>1,2</sup>, V. Georgieva<sup>1</sup>, N. Stefan<sup>3</sup>, N. Mihailescu<sup>3</sup>, A. Visan<sup>3</sup>, I. N. Mihailescu<sup>3</sup>, K. A. Gesheva<sup>4</sup>, I. M. Szilágyi<sup>2,5</sup>

<sup>1</sup>“Georgi Nadjakov” Institute of Solid State Physics, Bulgarian Academy of Sciences, 72 Tzarigradsko chaussee Blvd., 1784 Sofia, Bulgaria

<sup>2</sup>MTA-BME Technical Analytical Chemistry Research Group, Szent Gellért tér 4, Budapest, H-1111, Hungary

<sup>3</sup>National Institute for Lasers, Plasma and Radiation Physics, 409 Atomistilor St., RO-77125, Bucharest-Magurele, Romania

<sup>4</sup>Central Laboratory of Solar Energy and New Energy Sources, Bulgarian Academy of Sciences, Sofia, Bulgaria

<sup>5</sup>Budapest University of Technology and Economics, Department of Inorganic and Analytical Chemistry, Hungary  
boiajiev@gmail.com

Tungsten trioxide (WO<sub>3</sub>) thin films were grown by pulsed laser deposition (PLD) and matrix assisted pulsed laser evaporation (MAPLE) with the aim to be applied in gas sensors. The films were studied by atomic force microscopy (AFM), scanning electron microscopy coupled with energy-dispersive X-ray spectroscopy (SEMEDX), X-ray diffraction (XRD), UV-Vis and FTIR spectroscopies. The research was focused on the gas sensing behaviour of these WO<sub>3</sub> films. They were deposited on quartz resonators and the quartz crystal microbalance (QCM) method was applied to analyze their gas sensitivity. This way, highly sensitive gas sensors could be produced capable to detect changes in the molecular range. Such prototype QCM sensors were tested for sensing NO<sub>2</sub>. These PLD and MAPLE grown WO<sub>3</sub> thin films even in as-deposited state show good sensitivity and fast reaction at room temperature. With the presented technology the manufacturing of QCM gas sensors is simple, fast and cost-effective, and it is also suitable for energy-effective portable equipment for on-line monitoring the environment.

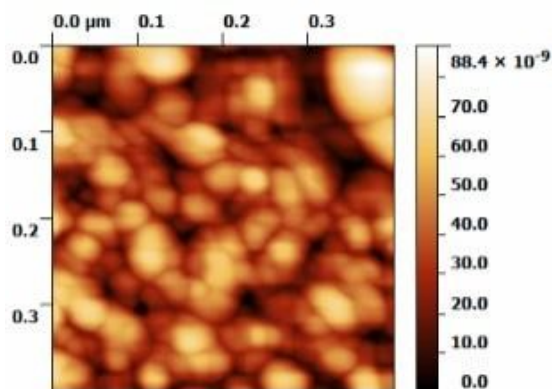


Figure 1: AFM image of a MAPLE grown WO<sub>3</sub> thin film.

## Copolymer PLCL-PEG-PLCL functional bio-coating obtained by Matrix Assisted Pulsed Laser Evaporation: a deposition parametric study

S. Brajnicov<sup>1,2</sup>, V. Marascu<sup>1,3</sup>, L. Rusen<sup>1</sup>, A. Moldovan<sup>1</sup>, V. Dinca<sup>1</sup> and M. Dinescu<sup>1</sup>

<sup>1</sup>National Institute for Lasers, Plasma and Radiation Physics, 409 Atomistilor Street, PO Box MG-16, RO-077125, Magurele, Bucharest, Romania

<sup>2</sup>University of Craiova, Faculty of Mathematics and Natural Sciences, RO-200585, Craiova, Romania

<sup>3</sup>University of Bucharest, Faculty of Physics, RO-077125, Magurele, Romania

valentina.dinca@inflpr.ro

An important aspect in the field of biomedical research and tissue engineering is given by the biological reactions which occur at proteins and cell-surface interfaces. Poly(lactide-co-caprolactone)-block-poly(ethyleneglycol)-block-poly(lactide-co-caprolactone) PLCL-PEG-PLCL co-polymers are studied extensively for their applicability in drug delivery and like ligament-bone interface applications. In this work, a parametric study on the optimization of the synthetic biodegradable PLCL-PEG-PLCL co-polymer thin films by using matrix-assisted pulsed laser evaporation (MAPLE) is presented. The evaporation process of the copolymer was carried out using an Nd:YAG pulsed laser, operating at different fluences (0.3–0.9 J/cm<sup>2</sup>) with a wavelength of 266 nm and a repetition rate of 10 Hz. The main functional groups in the MAPLE-deposited thin films were determined by Fourier transform infrared spectroscopy. The results of the Fourier transform infrared spectroscopy revealed the similarity between the molecular structures of the transferred material and of the initial material. The morphological characteristics of the samples were analyzed by Atomic force microscopy (AFM) technique and correlated with the deposition parameters. The ability to control the morphology and chemistry of the deposited material through MAPLE technique is an important step in creating functional biointerfaces.

**Acknowledgments:** This work was supported by Romanian National Authority for Scientific Research (CNCS – UEFISCDI), under the projects PNII-PT-PCCA-2013-4-199, PN-II-RU-TE-2014-4-2434 and PN09-39

# Laser polarization effects in laser-assisted electron-hydrogen inelastic collisions

G. Buica

Institute of Space Sciences-INFLPR, P.O. Box MG-23, Ro 77125, Bucharest-Magurele, Romania  
buica@space-science.ro

The purpose of this work is to study the laser polarization effects in *inelastic* scattering of fast electrons by hydrogen atoms in the presence of a circularly polarized (CP) laser field. We consider the excitation of hydrogen to an arbitrary state accompanied by one- and two-photon absorption. It is important to evaluate the contribution of the laser-assisted *inelastic* electron-atom scattering to the total electron energy spectrum since in experimental studies it might be quite difficult to separate the signal of elastic and inelastic scattering channels.<sup>1</sup>

Because the scattering process under investigation is a very complex problem, the theoretical approach presents considerable difficulties and several assumptions are made. (i) Moderate field strengths below  $10^7$  V/cm and fast projectile electrons are considered in order to safely neglect the second-order Born approximation in the scattering potential as well the exchange scattering.<sup>2</sup> (ii) The interaction between the projectile electrons and the laser field is described by a Gordon-Volkov wave function. (iii) The dressing of the hydrogen atom by the laser field, i.e., the modification of the target atom in the laser field, is described within the first-order time-dependent perturbation theory in the field.<sup>3</sup> Using the approach described for linearly polarized (LP) fields<sup>4,5</sup> we have obtained an *analytical formula* for the differential cross section (DCS) in the laser-assisted inelastic e-H( $1s$ ) scattering that is valid for both circular and linear polarization. We analyze the angular distributions and the resonance structure of the DCSs for the excitation of the  $n = 2$  and  $n = 4$  subshells and we discuss the influence of the laser polarization on the angular distribution of the scattered electrons.

We focus our discussion on three particular laser field polarizations denoted as: (a)  $CP_x$ , where the laser beam is circularly polarized in the  $(y,z)$ -scattering plane and the laser beam propagates in the  $x$ -axis direction,  $\epsilon_{CPx} = (\epsilon_y + i\epsilon_z)/\sqrt{2}$ ,

(b)  $LP_q$ , where the laser beam is linearly polarized and the polarization vector is parallel the momentum transfer vector  $\mathbf{q}$ ,  $\epsilon_{LPq} \parallel \mathbf{q}$ , and (c)  $LP_z$ , where the laser beam is linearly polarized with the polarization vector is parallel to the  $z$ -axis,  $\epsilon_{LPz} = \epsilon_z$ . A comparison between the linear and circular polarizations of the laser field is made for the excitation of the  $2l$  subshells and important differences appear between the angular distributions of DCSs depending on the type of polarization. In Figure 1 we show the ratios of the DCSs with excitation of the  $2s$  and  $2p$  subshells by the LP and CP fields for one- and two-photon absorption as a function of the scattering angle  $\theta$ . The DCSs are calculated at the incident projectile energy of 200 eV, the laser field strength  $E_0 = 10^7$  V/cm, the photon energy 2 eV, and the azimuthal angle  $\varphi = 90^\circ$ . Depending of the laser parameters, projectile energies, and scattering geometry the CP scattering signal can be larger than the LP signal.

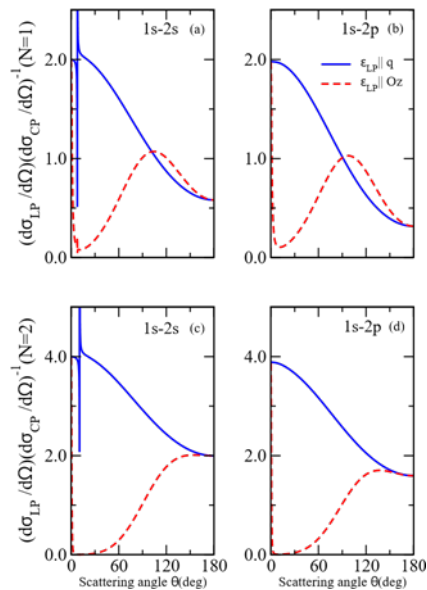


Figure 1: Ratios of the DCSs by the  $LP_{z(q)}$  and  $CP_x$  fields for inelastic laser assisted scattering,  $e(E_i)+H(1s) + N\omega \rightarrow e(E_f)+H(2l)$ , with the excitation of the  $2l$  subshells as a function of the scattering angle for  $N = 1$  in (a) and (b), and  $N = 2$  in (c) and (d). The full lines represent the results for  $LP_q$ , while the dashed lines denote the  $LP_z$  fields.

1. C. J. Joachain, N. J. Kylstra, and R. M. Potvliege, *Atoms in Intense Laser Fields* (Cambridge University Press, UK) (2012);
2. F. W. Byron Jr. and C. J. Joachain, *Electron-atom collisions in a strong laser field*, *J. Phys. B*, 17, L295 (1984);
3. V. Florescu and T. Marian, *First-order perturbed wave functions for the hydrogen atom in a harmonic uniform external electric field*, *Phys. Rev. A*, 34, 4641 (1986);
4. A. Cionga and V. Florescu, *One-photon excitation in the e-H collision in the presence of a laser field*, *Phys. Rev. A*, 45, 5282 (1992);
5. G. Buica, *Inelastic scattering of electrons by metastable hydrogen atoms in a laser field*, *Phys. Rev. A*, 92, 033421 (2015).

# Laser-induced damage thresholds of gold, silver and their alloys in air and water

A.V. Bulgakov, S.V. Starinskiy, Yu.G. Shukhov

S.S. Kutateladze Institute of Thermophysics SB RAS, 1 Lavrentyev Ave., 630090 Novosibirsk, Russia  
bulgakov@itp.nsc.ru

Pulsed laser ablation in liquids (PLAL) is an efficient and flexible technique for synthesis of nanoparticles of various materials, in particular of noble metals. In recent years, colloidal metal alloy nanoparticles attract much attention as new multifunctional nanosystems combining functional properties of individual metals.<sup>1,2</sup> However, in contrast to laser ablation in ambient gases, little is still known about the PLAL mechanisms and the available data are sometimes contradictory and rather poorly understood.

In this work, we have systematically investigated the laser-induced single-shot damage thresholds of gold, silver and gold-silver alloys (50 and 75% Au molar fraction) in air and water. The thresholds were determined by measuring the damaged area induced on the surface by a Nd:YAG laser (1064 nm, 7 ns) as a function of laser fluence. The experimental results are analyzed theoretically by solving the heat flow equation for the samples irradiated in air and in water taking into account vapor formation at the solid-water interface. The damage thresholds of Au-Ag alloys are systematically lower than those for pure metals, both in air and water, by a factor of  $\sim 1.4$  (Fig. 1), that is explained by lower thermal conductivities of the alloys. The thresholds measured in air agree well with the calculated melting thresholds for all samples. The damage thresholds in water are found to be considerably, also by a factor of  $\sim 1.4$ , higher than the corresponding thresholds in air (Fig. 1). This cannot be explained, in the frames of the used model, neither by the conductive heat transfer to water nor by the vapor pressure effect. In this context, such critical phenomena in the superheated water as critical opalescence and anomalous heat transport due to the piston effect are discussed as possible reasons for the high damage thresholds in water.

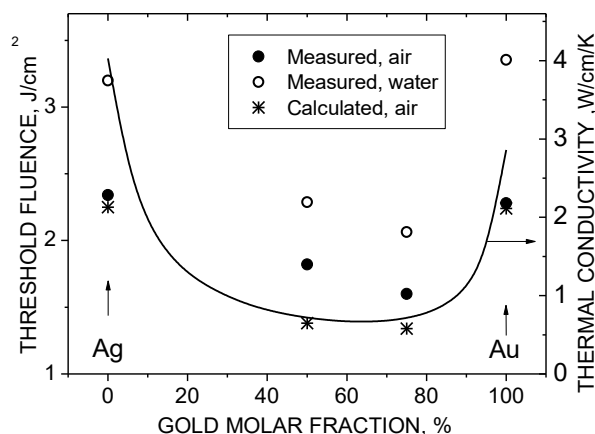


Figure 1: Measured laser-induced damage thresholds of gold, silver and their alloys in air (closed circles) and water (open circles) and calculated melting thresholds in air (stars) as a function of the gold molar fraction. The solid line shows the thermal conductivity of gold-silver alloys.<sup>3</sup>

**Acknowledgements:** This work was supported by the Russian Science Foundation (Project 16-19-10506).

1. S. Besner, M. Meunier, Femtosecond laser synthesis of AuAg nanoalloys: Photoinduced oxidation and ions release, *J. Phys. Chem. C* **114**, 10403-10409 (2010);
2. S. Grade, J. Eberhard, J. Jakobi, A. Winkel, M. Stiesch, S. Barcikowski, Alloying colloidal silver nanoparticles with gold disproportionally controls antibacterial and toxic effects, *Gold Bull.* **47**, 89-93 (2014);
3. C.Y. Ho, M.W. Ackerman, K.Y. Wu, S.G. Oh, T.N. Havill, Thermal conductivity of ten selected binary alloy systems, *J. Phys. Chem. Ref Data* **7**, 959-1177 (1978).

# Interaction of femtosecond doughnut-shaped laser pulses with glasses

N.M. Bulgakova<sup>1,2</sup>, V.P. Zhukov<sup>3,4</sup>, M.P. Fedoruk<sup>3,5</sup>, A.M. Rubenchik<sup>6</sup>

<sup>1</sup>HiLASE Centre, Institute of Physics ASCR, Za Radnici 828, 25241 Dolní Břežany, Czech Republic

<sup>2</sup>Institute of Thermophysics SB RAS, 1 Lavrentyev Ave., 630090 Novosibirsk, Russia

<sup>3</sup>Institute of Computational Technologies SB RAS, 6 Lavrentyev Ave., 630090 Novosibirsk, Russia

<sup>4</sup>Novosibirsk State Technical University, 20 Karl Marx ave., 630073, Novosibirsk, Russia

<sup>5</sup>Novosibirsk State University, 1 Koptug Ave., 630090 Novosibirsk, Russia

<sup>6</sup>Lawrence Livermore National Laboratory, Livermore, California 94550, USA

bulgakova@fzu.cz

Interaction of femtosecond laser pulses with bulk glass (fused silica as an example) has been studied numerically based on Maxwell's equations supplemented by the hydrodynamics-type equations for free electron plasma for the cases of Gaussian linearly-polarized and doughnut-shaped radially-polarized pulses. For Gaussian pulses focused inside glass (800 nm wavelength, 50 – 100 fs duration, numerical aperture < 0.3), the maxima of laser intensity, free electron density, and absorbed laser energy density do not considerably change with the beam energy (clamping effect). At pulse energies of 200 nJ – 2  $\mu$ J, the free electron density in the laser-excited region remains subcritical while the locally absorbed energy density does not exceed  $\sim 4000$  J/cm<sup>3</sup>. Increasing pulse energy results mainly in increased laser-excited volume.

For doughnut-shaped pulses, the initial high-intensity ring of light shrinks upon focusing. For relatively low beam energies, the internal and external radii of the light ring are decreasing with almost the same rate, creating a subcritical electron plasma of annual spatial distribution. With increasing energy, dynamics of beam focusing can be divided into two stages. At the first stage, the laser beam evolves similarly to the cases of low beam energy and the maximum electron density is similar to that obtained for Gaussian pulses. At the second stage, the light ring separates into two branches, one of which shrinks swiftly toward the beam axis well before the geometrical focus, leading to supercritical free electron density generation. The second branch is the laser light scattered by the electron plasma away from the beam axis, which tends to focus closer to geometrical focus. The near-axis laser-excited volume represents a tube of 0.5–1  $\mu$ m in radius and 10–15  $\mu$ m long. The local maximum of absorbed energy can be up to 10 times higher compared to the case of Gaussian beams of the same energy. The tube-like shape of the deposited energy should lead to implosion of material that can be used for improving the direct writing of high-refractive index optical structures inside glass.

Calculated spectra of light transmitted through the sample and scattered to large angles have demonstrated spectral broadening with blue shift. The spectra are considerably different for the two studied pulse shapes that can be used for diagnostics of laser-glass interaction processes.

*Acknowledgements:* This research is supported by the Russian Foundation for Basic Research (RFBR project No. 15-01-02432). The work of M.P. Fedoruk is supported by Russian Science Foundation (Project No. 1204 14-21-00110). The work of A. Rubenchik was performed under the auspices of the U.S. Department of Energy by Lawrence Livermore National Laboratory under contract DE-AC52-07NA27344. We thank S.K. Turitsyn for fruitful discussions.

## Modeling of multipulse ultrashort laser irradiation of fused silica: Accumulation effects

N.M. Bulgakova<sup>1,2</sup>, V.P. Zhukov<sup>3,4</sup>, Y. Morova<sup>5</sup>, S. Aktürk<sup>5</sup>

<sup>1</sup>HiLASE Centre, Institute of Physics ASCR, Za Radnici 828, 25241 Dolní Břežany, Czech Republic

<sup>2</sup>Institute of Thermophysics SB RAS, 1 Lavrentyev Ave., 630090 Novosibirsk, Russia

<sup>3</sup>Institute of Computational Technologies SB RAS, 6 Lavrentyev Ave., 630090 Novosibirsk, Russia

<sup>4</sup>Novosibirsk State Technical University, 20 Karl Marx ave., 630073, Novosibirsk, Russia

<sup>5</sup>Department of Physics, Istanbul Technical University, Maslak 34469 Istanbul, Turkey

bulgakova@fzu.cz

The results of modeling of irradiation of fused silica by a sequence of laser pulses are presented. The model is based on Maxwell's equations supplemented by the hydrodynamic equations for generated free electron plasma in two geometries, cylindrical and 2D ("laser knife") ones. It is assumed that repetition rate is of order or smaller than 100 kHz and, hence, excited matter relaxes to each subsequent pulse with keeping memory about previous irradiations. The memory effect of fused silica glass is linked to accumulation of defects (E' centers) which (i) provide more effective photoionization for each subsequent pulse<sup>1</sup> and (ii) can affect refractive index in the laser-excited zone. The model reproduces the experimental evidences that the accumulation effects result in gradual increasing of laser-affected zone, changing of the peak absorbed energy, and a decrease of transmitted energy. Based on 2D geometry, effects of nonreciprocal laser writing by laser pulses with spatiotemporal coupling are discussed.

*Acknowledgements:* This research is supported jointly by the Russian Foundation for Basic Research (RFBR project No. 15-5146007) and TUBITAK (The Scientific and Technological Research Council of Turkey, Grant 114F502).

1. N.M. Bulgakova, V.P. Zhukov, Y.P. Meshcheryakov, L. Gemini, J. Brajer, D. Rostohar, T. Mocek, Pulsed laser modification of transparent dielectrics: what can be foreseen and predicted by numerical simulations? J. Opt. Soc. Am. B **31**, C8-C14 (2014).

# Evanescent Optical Trapping Method for Localization and Decontamination of Viruses and Microorganisms

N. Ciobanu<sup>1,2</sup>, I. N. Mihailescu<sup>3</sup>, C. Ristoscu<sup>3</sup>, M. Turcan<sup>2</sup>, T. Pislari<sup>2</sup>, N. Enaki<sup>2</sup>

<sup>1</sup>Department of Human Physiology and Biophysics, State University of Medicine and Pharmacy "Nicolae Testemitanu", Chisinau, Moldova

<sup>2</sup>Institute of Applied Physics, Academy of Sciences of Moldova, Chisinau, Moldova

<sup>3</sup>National Institute for Lasers, Plasma and Radiation Physics, Bucharest, Romania  
cnellu@gmail.com

Optical trapping techniques play an important role for localization of nanometers and submicron's particles<sup>1</sup>. Such kind of methods based on optical metamaterials, e.g., photonic crystals, optical fibres or cavities, where the penetration of evanescent field in the contaminated zone is primordial, can be used as an efficient decontamination procedure for viruses and microorganisms<sup>2</sup>. Recently, a new novel type of photonic crystal fiber setup was proposed, where the radiation can be efficiently coupled to the biological liquid integrated in the hollow core of the fiber<sup>3</sup>. It well known that most viruses vary in diameter from 20 nm to 400 nm and can be trapped using electromagnetic radiation sources. In the following we discuss a theoretical method for localization of nono-particles (viruses) using ultraviolet (UV) radiation. When UV or light is propagated through a fibre (or sphere) significant quantity of radiation is spread outside of the fibre as an evanescent field that interacts with surrounding medium. In case of many fibres or spheres (see Figure 1) an evanescent standing wave (ESW) system can be created. If the surrounding medium consists from an infected biological medium, the localization of nano-particles via the evanescent standing wave is produced. The dependence of intensity of the standing wave on the positions and distance of nano-particles in the evanescence field is discussed. The influence of optical force that pulls viruses into regions of evanescence standing wave with high intensity is investigated.

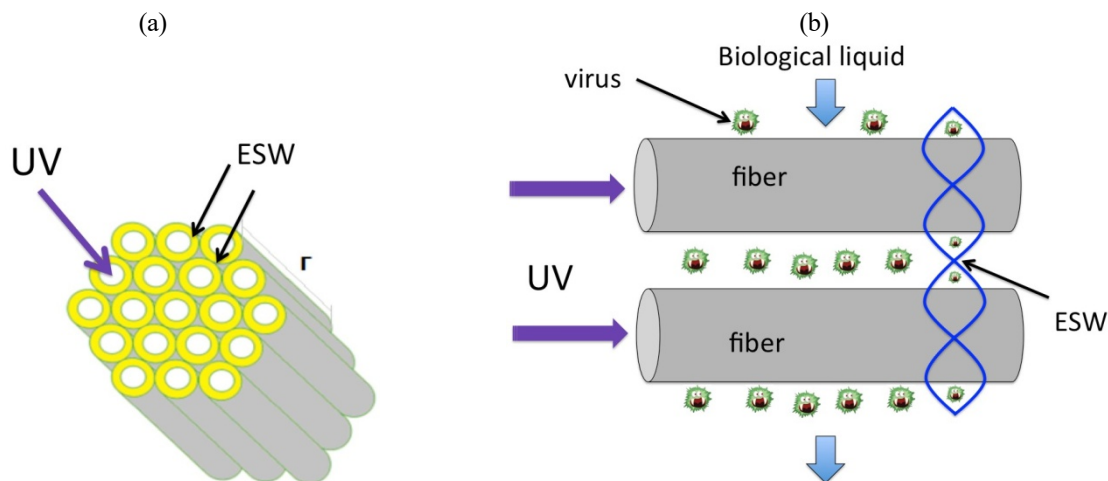


Figure 1: Model setup consists from (a) multiple fibres equivalently separate through which a biological liquid is propagated. The propagation of UV radiation via the fibre creates an evanescent standing wave (b), where the viruses can be trapped.

1. M. Daly, M. Sergides, S. Nic Chormaic, Optical trapping and manipulation of micrometer and submicrometer particles, *Laser Photon. Rev.* **9**, pp. 309–329 (2015);
2. S. Bazgan, C. Ristoscu, I. Negut, C. Hapenciu, M. Turcan, N. Ciobanu, I. N. Mihailescu, N. Enaki, Propagation of UV radiation through meta-material and its application in bio decontamination, *Romanian Reports in Physics*, **67** (4), pp. 1602–1607 (2015);
3. A. M. Cubillas, S. Unterkofler, T. G. Euser, B. J. M. Etzold, A. C. Jones, P. J. Sadler, P. Wasserscheid and P. St. J. Russell, Photonic crystal fibres for chemical sensing and photochemistry., *Chem. Soc. Rev.* **42**, pp. 8629–8648 (2013)



# Effects of the Deposition Geometry on Structure and Stoichiometry of PLD Grown Films

D. Craciun<sup>1</sup>, O. Fufa<sup>1</sup>, G. Socol<sup>1</sup>, D. Cristea<sup>2</sup>, D. Pantelica<sup>3</sup>, P. Ionescu<sup>3</sup>,  
R. Trusca<sup>4</sup>, E. Lambers<sup>5</sup>, and V. Craciun<sup>1</sup>

<sup>1</sup>National Institute for Lasers, Plasma and Radiation Physics, Măgurele, Romania

<sup>2</sup>Materials Science Department, Transilvania University, Brasov, Romania

<sup>3</sup>Horia Hulubei National Institute for Physics and Nuclear Engineering, Magurele, Romania

<sup>4</sup>Polytechnic University of Bucharest, Bucharest, Romania.

<sup>5</sup>MAIC, University of Florida, Gainesville, USA

doina.craciun@infirpl.ro

The pulsed laser deposition (PLD) technique is very useful to grow thin films to investigate the interdependence between structure, composition and properties. A simple control of the deposition conditions (substrate temperature, nature and pressure of the gaseous atmosphere, laser fluence, repetition rate, laser wavelength and deposition geometry) will result in the growth of films having different stoichiometry, crystalline grain sizes, texture, stress levels and properties. However, it has been known for many years that, besides the non-uniform thickness profile of the PLD grown films, there might be lateral compositional variations, which will influence the film properties. Such lateral variations will mainly depend on the mass of the ablated atoms, laser fluence and nature and pressure of the gaseous atmosphere. We investigated using grazing incidence X-ray diffraction, X-ray reflectivity, X-ray diffuse scattering, nanoindentation, X-ray photoelectron spectroscopy, scanning electron microscopy and Rutherford backscattering spectrometry the lateral variations of the structure, chemical composition and properties of PLD grown thin films. Several transition metal nitrides and carbides such as ZrC, TiC, ZrN, TiN as well as indium zinc oxide films were investigated as typical examples of compounds containing atoms with rather different masses. In addition, since these compounds are deposited under various reactive gases we also investigated the role of the deposition nature and pressure and target-substrate distance on the film composition and properties.

## Pulsed Laser Deposition of Nanocrystalline and Amorphous Biocompatible Protective Coatings

V. Craciun<sup>1</sup>, G. Socol<sup>1</sup>, G. Dorcioman<sup>1</sup>, C. Radu<sup>1</sup>, O. Fufa<sup>1</sup>, D. Craciun<sup>1</sup>, D. Cristea<sup>2</sup>, L. Floroian<sup>2</sup>,  
M. Badea<sup>2</sup>, D. Pantelica<sup>3</sup>, P. Ionescu<sup>3</sup>, R.C. Popescu<sup>3</sup>, B. S. Vasile<sup>4</sup>, R. Trusca<sup>4</sup>

<sup>1</sup>National Institute for Lasers, Plasma and Radiation Physics, Măgurele, Romania

<sup>2</sup>Materials Science Department, Transilvania University, Brasov, Romania

<sup>3</sup>Horia Hulubei National Institute for Physics and Nuclear Engineering, Magurele, Romania

<sup>4</sup>Polytechnic University of Bucharest, Bucharest, Romania.

valentin.craciun@infpr.ro

Many problems associated with Ti implants failure occur at the metal-body interface. In order to reduce them and improve the mechanical and chemical stability of this interface, the Ti surface is usually coated with a biocompatible thin film. We deposited mixtures of ZrN, ZrC, TiN, TiC and SiC films on highly polished Ti samples by a combinatorial pulsed laser deposition technique to investigate the role of structure and composition on their properties. The structural properties of the deposited films were investigated using the grazing incidence X-ray diffraction and X-ray reflectivity measurements (XRR) performed in several locations. The chemical composition, density and thickness were extracted by modelling Rutherford backscattering spectra acquired with 2.2 MeV alpha particles. The results were compared with the density values extracted from simulations of the XRR curves. The adhesion and mechanical properties of the films were investigated by nanoindentation, scratch and wear tests. Electrochemical measurements involving corrosion and electrochemical impedance spectroscopy studies were carried out in physiological solutions at room temperature to evaluate the chemical stability of the titanium, bare or covered with the PLD grown films and to compare their performance. The results showed that the deposition of protective coatings improved the stability of the Ti surface, which was less affected by corrosion. Also, the coated surfaces exhibited better mechanical properties than bare Ti. The biocompatibility of the deposited thin films was confirmed after 24 hours of treatments on osteoblast-like cells, by considering *in vitro* viability assay (MTS). The morphology and behavior of human-derived osteoblasts in presence of the experimental coatings were investigated by performing SEM analysis and immunofluorescence evaluations, which confirmed the auspicious circumstances for cellular attachment and proliferation. The biological data suggests the successful fabrication of protective coatings with potential osseous tissue applications.

# Isoflavonoid Thin Films Fabricated By MAPLE For Improved Resistance of Biomedical Surfaces to Microbial Colonization

R. Cristescu<sup>1</sup>, V. Grumezescu<sup>1,2</sup>, G. Socol<sup>1</sup>, A.M. Holban<sup>3</sup>, R. Trusca<sup>4</sup>, F. Iordache<sup>5</sup>, M.C. Chifiriuc<sup>6</sup>, R. Narayan<sup>7</sup>, D.B. Chrisey<sup>8</sup>

<sup>1</sup>National Institute for Lasers, Plasma & Radiation Physics, Lasers Department, Bucharest-Magurele, Romania

<sup>2</sup>Faculty of Applied Chemistry and Materials Science, Department of Science and Engineering of Oxidic Materials and Nanomaterials, University Politehnica of Bucharest, Bucharest, Romania

<sup>3</sup>Faculty of Biology, Microbiology Immunology Department, University of Bucharest, Bucharest, Romania

<sup>4</sup>S.C. Metav-CD S.A., Bucharest, Romania

<sup>5</sup>“Nicolae Simionescu” Institute of Cellular Biology and Pathology of Romanian Academy, Department of Fetal and Adult Stem Cell Therapy, Bucharest, Romania

<sup>6</sup>Faculty of Biology, Microbiology Immunology Department, Research Institute of the University of Bucharest— ICUB, Bucharest, Romania

<sup>7</sup>Biomedical Engineering, University of North Carolina, Chapel Hill, NC, USA

<sup>8</sup>Department of Physics and Engineering Physics, Tulane University, New Orleans, LA, USA  
rodica.cristescu@infpr.ro

*Staphylococcus aureus* and *Pseudomonas aeruginosa* are two major microbial threats in the hospital environment, because of their widespread and significant antibiotic resistance. This study reports on the deposition of polyvinylpyrrolidone/antibiotic/isoflavonoid thin films by Matrix Assisted Pulsed Laser Evaporation (MAPLE). Scanning Electron Microscopy (SEM), Infrared Microscopy (IRM) and X-ray Diffraction were used to characterize the films. In addition, *in vitro* biological assays were performed in order to assess the dynamics of biofilms formed by the Gram-positive and Gram-negative strains on the thin films. Furthermore, the *in vitro* biocompatibility of the thin films for up to five days of incubation with human endothelial cells was investigated. SEM micrographs revealed the uniform morphology of the prepared films; IRM demonstrated both the integrity of the functional groups and the homogeneity of MAPLE-deposited thin films. The microbiological assay results evidenced that the thin films efficiently inhibited *S. aureus* and *P. aeruginosa* adherence as well as biofilm formation at all of the tested time points. These results demonstrated that the MAPLE-functionalized surfaces can successfully act as anti-adherent coatings on biomedical device surfaces.

## Personalized Hip Implants Manufacturing and Testing

S.M. Croitoru<sup>1</sup>, A. Pacioga<sup>1</sup>, S. Comşa<sup>2</sup>

<sup>1</sup>POLITEHNICA University of Bucharest, Faculty of Engineering and Management of Technological Systems, Machines and Manufacturing Systems Dept., 313 Spl. Independenței, Sector 6, 060042, Bucharest, Romania

<sup>2</sup>National Institute of Research and Development in Mechatronics and Measurement Technique, 6-8 Pantelimon Road, Sector 2, Bucharest, Romania  
sorin.croitoru@gmail.com

Multiple experimental studies<sup>1,2</sup> have shown that in total hip arthroplasty, adaptation of geometric shape of the uncemented implant stem to the inner contour of the cortical bone of the proximal femur is essential for optimizing load takeover and for a better mechanical stability. Taking in account these studies and also the characteristic trabecular structure of the proximal end of the femur and using the idea to reproduce (at a macroscopic scale) this natural bone structure<sup>3</sup>, two models of customized femoral stems for hip replacements were designed. These have a fenestrated architecture that mimics the natural bone structure, providing postoperative bone ingrowth and final implant fixation, enhancing the elasticity of the entire structure, thus approaching much more to the natural elasticity of the healthy bone. The two models of implants were provided with two different sizes of fenestrations, the mechanical tests that followed aiming to determine which of the two models withstands better the loading occurring during normal use.

The design was based on the CT images from a patient requiring a surgery for hip arthroplasty, their manufacture was made using biocompatible titanium alloy powder (Ti6Al4V) by 3D additive manufacturing (see. Figure 1.a), selective laser sintering being already known as a technology that ensures the fastest path from the idea of product it's market launch. The manufactured endoprostheses are shown in Figure 1.b.



Figure 1: (a) 3D additive manufacturing (b) The manufactured endoprostheses

The endoprostheses were statically and dynamically tested to determine the fatigue limit. Endurance tests were performed according to ISO 7206: 2010, parts 4<sup>4</sup> and 8<sup>5</sup>, in order to determine the fatigue limit using the Locati method. The tests were conducted with the endoprostheses immersed in distilled water salted solution with a concentration of 0.91% (9.1g NaCl in 1000ml distilled water) whose temperature was maintained at  $37^{\circ} \pm 1^{\circ} \text{C}$ . The results of the tests were the fatigue limit of the implants which were: 3376N for the model with large fenestrations and 4682N for the model with small fenestrations.

Mechanical tests findings may be summarized as follows:

- The characteristic curves (for the static test) of the two customized fenestrated implants reveal elastic behaviour by their nonlinear appearance;
- Large fenestrations conferred the desired elasticity to the implant, but contributed life service reduction;
- Reduction of the fenestrations size contributed to an increase with 38.7% of the fatigue limit;
- The fatigue limit for both implants was much above the minimum value specified by ISO 7602: 2010 (2300N), so we can conclude that both models can be safely used in the medical practice.

1. Darrell, L., Moulton, Ronald, W., Lindsey: Proximal Femur Size and Geometry in Cementless Total Hip Arthroplasty Patients, <http://f1000research.com/articles/4-161/v1>, (last accessed 27 apr 2016);
2. M.L.Z. Ridzwan, Solehuddin Shuib, A.Y. Hassan, A.A. Shokri and M.N. Mohamad Ibrahim, 2007. Problem of Stress Shielding and Improvement to the Hip Implant Designs: A Review. *Journal of Medical Sciences*, 7: 460-467;
3. Orban, H., Bunea, D., Moldovan, L., Antoniac, I., Gheorghiu, D., Semenescu, A.: Componentă femurală pentru proteză totală de șold, Brevet de invenție RO 117890 B, Oficiul de stat pentru invenții și mărci, 30 Sept. 2002;
4. ISO 7206-4:2002: Implants for surgery - Partial and total hip prostheses, Part 4-Determination of endurance properties of stemmed femoral components;
5. ISO 7206-8:2002: Implants for surgery - Partial and total hip prostheses, Part 8- Endurance performances of stemmed femoral components.

## R&D on Dental Implants Breakage

S.M. Croitoru<sup>1</sup>, I.A. Popovici<sup>2</sup>

<sup>1</sup>*POLITEHNICA University of Bucharest, Faculty of Engineering and Management of Technological Systems, Machines and Manufacturing Systems Dept. 313 Spl. Independentei, Sector 6, Bucharest, Romania*

<sup>2</sup>*University of Medicine and Pharmacy "Carol Davila", Faculty of Dentistry, 19 Calea Plevnei, Sector 1, Bucharest, Romania  
sorin.croitoru@gmail.com*

Most used dental implants for human dental prostheses are of two steps type: first step means implantation and, after several months healing and osseointegration, second step is prosthesis fixture. For sure, dental implants and prostheses are meant to last for a lifetime. Still, there are unfortunate cases when dental implants break. This paper studies two steps dental implants breakage and proposes a set of instruments for replacement and restoration of the broken implant. First part of the paper sets the input data of the study: structure of the studied two steps dental implants based on two Romanian patents<sup>1,2</sup>, values of the masticatory forces found in speciality papers<sup>3-6</sup> and most defavourable loading case. In the second part of the paper, using DEFORM 2D™ FEM simulation software<sup>7</sup>, loading dental implants is studied in order to determine which zones and components of the dental implant kit are affected (broken). Last part of the paper is dedicated to design and presentation of a set for extracting and cutting tools used to replace the broken implant kit.

**Authors' opinion:** Mechanical engineering applied on human body will develop extensively in this 21-st century. It will use at least the knowledge acquired up to present.

1. Gh. Ștefan, I.A. Popovici, F. Popovici, F., S.M. Croitoru, Patent No. 121362: Implant. Set of instruments for insertion and endosseal implant made by their use, Romania, 2007;
2. R. Stanciu, B. Stanciu, I.A. Popovici, F. Popovici, S.M. Croitoru, L. Popovici, Patent No 125886, Threaded dental implant made of ceramics, Romania, 2014;
3. D.N. Mancuso, M.C. Goiato, H.G. Filho, É.A. Gomes, Bite Force and Masticatory Efficiency in Implant-Retained Dentures. Literature Review, Dentistry Today, Department of Continuing Education, 100 Passaic Avenue, Fairfield, NJ 07004, Course Number 104.2, september 2008;
4. M. Rismanchian, F. Bajoghli, Z. Mostajeran, A. Fazel, P. sadr Eshkevari, Effect of implants on maximum bite force in edentulous patients, *Journal of Oral Implantology*, Vol. XXXV/No. Four/2009, pp. 196-200;
5. K. Tokmakidis, B. Wessing, K. Papouliia, H. Spiekermann, Belastungsverteilung und Belastungskonzepte auf Zähnen und Implantaten, © Deutscher Ärzte-Verlag | zzi | *Z Zahnärztl Impl* | 2009; 25 (1), pp. 44-52;
6. A. Mahajan, K.N. Kadam, The Influence of Mechanical Loads on the Biomechanics of Dental Implant, *International Journal of Science and Research (IJSR)*, [www.ijsr.net](http://www.ijsr.net), ISSN (Online): 2319-7064, Volume 3 Issue 11, November 2014, Paper ID: 03111402, pp.1085-1090;
7. DEFORM 2D™ v.9.0 perpetual license, POLITEHNICA University of Bucharest, National Research Center for Performances of Technological Systems OPTIMUM, Romania, 2008.

# Production and photo-excitation of nuclear isomers at ELI-NP

L. D'Alessi<sup>1</sup>, Y. Xu<sup>1</sup>, M. Zeng<sup>1</sup>, S. Aogaki<sup>1</sup>, O. Tesileanu<sup>1</sup>, K. Homma<sup>2,3</sup>, H. Utsunomiya<sup>4</sup>

<sup>1</sup>ELI-NP, "Horia Hulubei" National Institute for Physics and Nuclear Engineering, 30 Reactorului Street, RO-077125, Magurele, Romania

<sup>2</sup>Graduate School of Science, Hiroshima University, Higashihiroshima, Hiroshima, Japan

<sup>3</sup>International Center for Zetta-Exawatt Science and Technology, Ecole Polytechnique, France

<sup>4</sup>Department of Physics, Konan University, 8-9-1, Okamoto, Higashi-nada, Kobe, Hyogo, 658-8501, Japan  
loris.dalessi@eli-np.ro

In the stellar environment, because of the extremely high temperature in the stellar interior, a significant contribution to photonuclear reactions comes both from the ground state level of the nuclei, as well as from the thermally populated excited levels. The photonuclear reactions currently studied in laboratories on Earth take place from the ground state levels, therefore no information is available on the cross sections for the production of photoneutrons from the excited ones. In ELI-NP we intend to produce nuclear isomers and induce photoneutron emissions by exciting the isomers with gamma photons coming from the Gamma Beam System (GBS), taking advantage from the highly monochromatic  $\gamma$ -ray beam. The details on the proposed experiments have been presented in a Technical Design Report (TDR).<sup>1</sup> In order to obtain a significant yield of photoneutrons, a key role is played by the preparation of the isomeric sample, which can be obtained by bombarding a specimen with a high flux of bremsstrahlung photons. In this work we present the results of numerical simulations where a beam of electrons produced by Laser Wake-Field Acceleration mechanism<sup>2</sup> is used to generate bremsstrahlung radiation by irradiating a tungsten target. The LWFA electron beam is derived from PIC simulations by using EPOCH software and imported in a GEANT4 code for the computation of the corresponding bremsstrahlung photon distribution. In Figure 1 are shown the properties of the LWFA electron beam obtained from EPOCH simulations (panel a) and the corresponding photon energy spectrum (panel b). By using the TALYS software for the calculation of the photonuclear cross sections, the production and decay yields are then calculated. The results of our simulations carried for different isomers proposed for the first experiments, suggest that, depending on the formation cross sections and lifetimes, several production strategies may be adopted at ELI-NP based on the available beams.

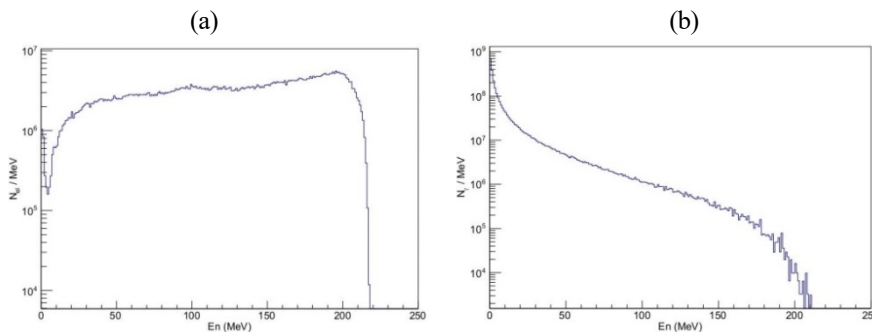


Figure 1: Energy spectrum of the LWFA electron beam entering the tungsten target (a) and the corresponding exiting bremsstrahlung photons (b).

1. K. Homma et al, Romanian Reports in Physics, Vol. 68, Supplement, S233–S274 (2016);

2. T. Tajima and J. M. Dawson, Laser Electron Accelerator, Physical Review Letters, 43, 267-270 (1979).

## Titanium oxide/graphene oxide spin coated composite material for photocatalytic applications

A. Datcu,<sup>1,2</sup> M. L. Mendoza,<sup>2</sup> A. Pérez del Pino,<sup>3</sup> C. Logofatu,<sup>4</sup> C. Luculescu,<sup>5</sup> and E. György<sup>1,3</sup>

<sup>1</sup>National Institute for Lasers, Plasma and Radiation Physics, P. O. Box MG 36, 77125 Bucharest, Romania

<sup>2</sup>Departamento de Ciencias Químicas y Ambientales, FCNM, ESPOL, Ecuador

<sup>3</sup>Instituto de Ciencia de Materiales de Barcelona, Consejo Superior de Investigaciones Científicas, ICMAB-CSIC, Campus UAB, 08193 Bellaterra, Spain

<sup>4</sup>National Institute for Materials Physics, P. O. Box MG 7, 77125 Bucharest, Romania

datcu.angela@inflpr.ro

Titanium oxide ( $\text{TiO}_2$ ) is a fascinating oxide semiconductor material with several industrial applications such as solar energy conversion, medical devices and food preparation equipment disinfection, photocatalytic water splitting, etc. To date, many examples of  $\text{TiO}_2$  based materials with photocatalytic properties, in particular for organic pollutants degradation have been reported.

In the last decades several methods have been used to enhance the photocatalytic properties of  $\text{TiO}_2$ . In this sense, it was found that the combination of graphene oxide (GO) platelets with  $\text{TiO}_2$  nanoparticles (NPs) creates composites with outstanding functions improving the photocatalytic properties.<sup>1</sup> Possessing oxygen functional groups, high electron mobility and high surface area, GO contributes to the separation and transport of the photogenerated charge carriers.<sup>2</sup> Moreover, it contributes to the reduction of the band gap, as compared to pure

TiO<sub>2</sub>. The absorption range of commercial transition metal oxide semiconductor catalysts is limited to the UV spectral range, which represents only about 4% of the solar light. Through the addition of reduced GO (rGO) the optical absorption can be extended towards the visible region, about 42% of the solar spectrum.

In the present work, we study the effect of GO concentration on the surface morphology, structure, chemical composition and photoactive properties of TiO<sub>2</sub> NPs/GO composite films deposited by spin coating.

In case of TiO<sub>2</sub>/GO composite films the partial reduction of GO platelets was observed. The relative number of oxygen functional groups was determined from X-ray photoelectron spectrometry (XPS) data (Fig. 1) through the calculation of the ratio between C-O single and C=O double bonds (lines II-III in the XPS spectra) and *sp*<sup>2</sup> C from C=C bonds (line I) (Fig. 1b) and was found to decrease significantly as compared to reference drop-cast GO sample (Fig. 1a).

Photoactive properties of the spin coated composite layers were investigated by the decomposition of organic methylene blue dye solutions under UV and visible light irradiation conditions. The photoefficiency of the spin coated immobilized composites can be controlled and enhanced through the GO concentration of the TiO<sub>2</sub>/GO nanocomposite samples.

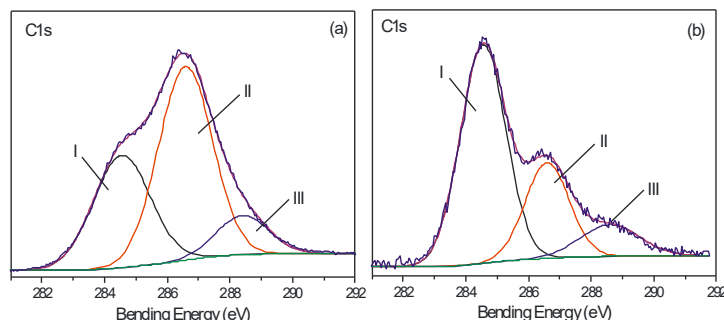


Figure 1: C1s XPS spectra of (a) reference drop-cast GO sample and (b) TiO<sub>2</sub>/GO composite films obtained by spin coating method from the 5% TiO<sub>2</sub> and 2%GO in water/acetone dispersion.

1. W-K. Jo, N. C. Sagaya Selvam, Synthesis of GO supported Fe<sub>2</sub>O<sub>3</sub>-TiO<sub>2</sub> nanocomposites for enhanced visible-light photocatalytic applications, Dalton Trans., **44**, 16024–16035 (2015);
2. Y. Zhang, C.Pan, TiO<sub>2</sub>/graphene composite from thermal reaction of graphene oxide and its photocatalytic activity in visible light. J. Mater. Sci., **46**(8), 2622–2626 (2011).

## Morphological and structural study of the laser-induced diamond to graphite transformation

M. De Feudis<sup>1,2</sup>, A.P. Caricato<sup>1,2</sup>, E. Broitman<sup>3</sup>, A. Taurino<sup>4</sup>, P. M. Ossi<sup>5</sup>, C. Castiglioni<sup>6</sup>,  
L. Brambilla<sup>6</sup>, G. Chiodini<sup>2</sup>, M. Martino<sup>1,2</sup>

<sup>1</sup>Department of Mathematics and Physics, University of Salento, 73100 Lecce, Italy

<sup>2</sup>INFN National Institute of Nuclear Physics, 73100 Lecce, Italy

<sup>3</sup>IFM, Linköping University, SE58183 Linköping, Sweden

<sup>4</sup>CNR-IMM, Institute for Microelectronics and Microsystem, 73100 Lecce, Italy

<sup>5</sup>Dipartimento di Energia, Politecnico di Milano, 20133 Milan, Italy

<sup>6</sup>Dipartimento di Chimica, Materiali, Ingegneria Chimica, Politecnico di Milano, 20133 Milan, Italy

In the last a few years, there has been an increasing interest in the laser-induced diamond graphitization process. The process allows to produce graphitic layers on diamond for several applications, such as dosimeters, detectors and new black diamond materials whose properties are tailored to optically and electrically interact with solar radiation.

In this work, we aim at studying and better understanding how the diamond-graphite transition occurs by following step by step the physical evolution of the graphitization process. Spot-like graphitic structures were produced on CVD diamond surface, with different values of laser energy density and number of laser shots, thereafter performing several characterizations. In particular, nano-indentation was useful to check how hardness values change from typical of a very hard material to a very soft material with increasing number of laser shots. Similarly, a change of the elastic modulus was observed which is related to the carbon-bonding. Next, Scanning Electron Microscopy was performed on the same graphitic structures to study the morphological evolution due to the laser ablation associated to the graphitization.

Micro-Raman Spectroscopy analysis was carried out on strip-like graphitic structures produced on the same diamond sample, with different values of laser energy density and number of laser scans. The structural information in addition to morphological ones (obtained by nano-indentation maps and SEM analyses) give us the instruments to design the best combination of laser parameters to create more homogeneous graphitic layers on diamond, useful for applications as full-carbon dosimeters, detectors and absorbers and converters of solar energy.



study as well as other larger investigation will be able to contribute with new insights in the role of combination of SD-OCT with hyperspectral imaging in the non-invasive diagnosis of tissues.

1. Calin M.A., Parasca S.V., Savastru R., Calin M.R., Dontu S. (2013) Optical techniques for the non-invasive diagnosis of skin cancer. *J. Cancer Res. Clin.*, Vol.139, Iss.7, pp: 1083-1104, DOI: 10.1007/s00432-013-1423-3;
2. Savastru D., Miclos S., Chang E.W., Preda D., Iftimia N. (2014) Feasibility of Breast Surgical Margins Analysis with Fluorescence-guided Optical Coherence Tomography Imaging. *CLEO: QELS Fundamental Science San Jose, California United States June 8-13, 2014*, ISBN: 978-1-55752-999-2, [http://dx.doi.org/10.1364/CLEO\\_AT.2014.JTu4A.130](http://dx.doi.org/10.1364/CLEO_AT.2014.JTu4A.130);
3. Guolan, L. and Baowei F. (2014). Medical hyperspectral imaging: a review. *J. Biomed. Opt.* 19(1): 010901.

## Microscopical and Raman investigations of periodical surface structures fabricated by picosecond visible laser irradiation of carbon thin films

G. Dorcioman<sup>1</sup>, C. Popescu<sup>1</sup>, B. Bită<sup>2,3</sup>, C. Besleaga<sup>4</sup>, I. Zgura<sup>4</sup>, C. Himcinschi<sup>5</sup>, A. C. Popescu<sup>1</sup>

<sup>1</sup>National Institute for Lasers, Plasma and Radiation Physics, 409 Atomistilor Street, Magurele RO-077125, Romania

<sup>2</sup>National Institute for Research and Development in Microtechnologies, 126A Erou Iancu Nicolae Street, Voluntari RO-077190, Romania

<sup>3</sup>Faculty of Physics, 405 Atomistilor Street, Magurele RO-077125, Romania

<sup>4</sup>National Institute of Materials Physics, 105bis Atomistilor Street, Magurele RO-077125, Romania

<sup>5</sup>Institute of Theoretical Physics, TU Bergakademie Freiberg, Freiberg D-09596, Germany

*gabriela.dorcioman@infpr.ro*

Diamond-like carbon thin films possess valuable mechanical properties that recommend them to be used in engineering fields, especially as protective coatings for metal machining tools, in view of increasing their lifetime. We have synthesized hard carbon thin films by pulsed laser deposition and further irradiated them with laser sources. The objective was to obtain on their surface periodical structures that will reduce their friction coefficient. As laser induced periodical surface structures on carbon films, generated with ps laser sources emitting in visible were not reported in literature, we conducted a thorough study of their morphology, structure and chemistry. Optical microscopy, scanning electron microscopy and atomic force microscopy investigations were conducted on films synthesized in various experimental conditions, in order to identify the energy and focusing regimes for producing surface structures on large areas. Peculiarities of surface structures such as dimensions, shapes, distances between structures and depths were investigated and 3d profiles of the irradiated surfaces were generated. Structural and chemical modifications induced by the laser radiation were studied by X-ray diffraction, micro-Raman and micro-FTIR, in order to identify crystallinity modifications or types of bonds between carbon atoms in the irradiated areas.

## Properties of tungsten, magnesium and carbon composite thin films deposited by PLD

L.N. Dumitrescu<sup>1,2</sup>, V.Ion<sup>1</sup>, A.Moldovan<sup>1</sup>, A. Bercea<sup>1,3</sup>, D. Colceag<sup>1</sup>, M. Dinescu<sup>1</sup>

<sup>1</sup>National Institute for Lasers, Plasma and Radiation, Magurele, Bucharest, Romania

<sup>2</sup>University of Craiova, Faculty of Sciences, Craiova, Romania

<sup>3</sup>University of Bucharest, Faculty of Physics, Bucharest, Romania

*nicoleta.dumitrescu@infpr.ro, ln\_dumitrescu@yahoo.com*

The first wall and the divertor of the International Tokamak Experimental Thermonuclear Reactor (ITER) are supposed to be made of special materials resistant to high temperatures and erosion: tungsten is such a material. Their behavior when exposed to tokamak plasma, resulting in redeposition and contamination with impurities becomes relevant for further experiments and cleaning processes. Thus, studies regarding properties of ternary systems based on tungsten and carbon and containing nitrogen as intrinsic impurity are of paramount importance.

In this work, we report preliminary results on the morphological, structural, optical, and compositional properties of C/W/Mg composite as thin films obtained by Pulsed Laser Deposition (PLD), in correlation with their respective deposition parameters. The samples were deposited sequentially on Si substrates, at temperatures between 200 °C and 600°C, using a rotation-translation system with three different targets. The composition of the gas mixture (Ar, H<sub>2</sub>, N<sub>2</sub>), the substrate temperature and the number of pulses were varied in order to find the optimal growth conditions.

The deposited layers were characterized in terms of morphology, structure, composition and optical properties by atomic force microscopy (AFM), X-ray diffraction (XRD), secondary ion mass spectrometry (SIMS) and spectroellipsometry (SE) respectively. We obtained C/W/Mg composite thin films having low roughness values (in nanometers range) and thicknesses between 20 and 50 nm.

*Acknowledgement: EURATOM, Consortiu EUROFUSION 1EU-12/01.01.2016 (WPEDU-RO).*

# Polyvinylidene fluoride thin films deposited by MAPLE

L.N.Dumitrescu<sup>1,2</sup>, I.Tirca<sup>1,2</sup>, V.Ion<sup>1</sup>, A. Moldovan<sup>1</sup>, V.Marascu<sup>1,3</sup>, V.Dinca<sup>1</sup>, M. Dinescu<sup>1</sup>

<sup>1</sup>National Institute for Laser, Plasma and Radiation, Bucharest, Magurele, Romania.

<sup>2</sup>University of Craiova, Faculty of Sciences, Craiova, Romania.

<sup>3</sup>University of Bucharest, Faculty of Physics, Bucharest, Romania

nicoleta.dumitrescu@inflpr.ro, ln\_dumitrescu@yahoo.com

Poly(vinylidene fluoride)(PVDF) is a highly non-reactive thermoplastic fluoropolymer, with more than one crystalline structure, which possess interesting piezoelectric characteristics, making it very attractive for a wide range of applications. In this paper, we report preliminary results on optical and morphological properties correlated with deposition parameters of PVDF thin films grown by Matrix Assisted by Pulsed Laser Evaporation (MAPLE). The samples were deposited on various substrates as Si, Pt/Si, SiO<sub>2</sub> using a frozen target with different concentrations of polymer in di-methyl sulfoxide (DMSO) matrix solvent. A parametric study was carried out based on target composition, laser fluence and number of pulses in order to find the optimal deposition parameters for obtaining low roughness continuous layers.

The resulted coatings were investigated in terms of morphology, chemical structure, and optical properties by atomic force microscopy (AFM), Fourier Transform Infrared Spectroscopy (FTIR), ultraviolet–visible spectroscopy (UV-VIS) and spectroellipsometry (SE). PVDF thin films with optical and structural characteristics resembling to the pristine material and in agreement with the literature<sup>1</sup>, appropriate for different applications have been obtained.

**Acknowledgement:** PCCA 239

1. Ajay Pal Indolia& M. S. Gaur, Optical properties of solution grown PVDF-ZnO nanocomposite thin films, JOURNAL OF POLYMER RESEARCH, DOI 10.1007/s10965-012-0043-y, DECEMBER 2012.

## Laser techniques for deposition and microstructuring of layered double hydroxides and organo-modified layered double hydroxides

M. Dumitru<sup>1</sup>, R. Birjega<sup>1</sup>, A.Vlad<sup>1</sup>, S. Brajnicov<sup>1</sup>, R.Zavoianu<sup>2</sup>, M.C. Corobea<sup>3</sup>, M. Dinescu<sup>1</sup>

<sup>1</sup>National Institute for Lasers, Plasma and Radiation Physics, 409 Atomistilor Str., 077125 Bucharest, Magurele, Romania

<sup>2</sup>University of Bucharest, Faculty of Chemistry, Department of Chemical Technology and Catalysis, 4-12 Regina Elisabeta Bd., Bucharest, Romania

<sup>3</sup>National R.&S. Institute for Chemistry and Petrochemistry, ICECHIM, 202 Splaiul Independentei Str., 060021, Bucharest, Romania  
marius.dumitru@inflpr.ro

Pulsed laser deposition (PLD), is used for the deposition of various thin films and laser induced forward transfer (LIFT), allows the transfer of materials, usually in the form of thin films, from a substrate, the donor, to an acceptor substrate (possibly a device in various stages of construction), with high precision and millimeter to micron size. This single-step direct printing technique offers the possibility to obtain surface micro patterning and localized deposition of almost materials from biomaterials, polymers, nanotubes, metals, inks etc. Our study aims to explore the ability of LIFT to transfer hybrid nanocomposite structures such as organo-modified layered double hydroxides. Layered double hydroxides (LDHs) are a class of layered materials consisting of positively charged brucite-like layers and exchangeable interlayer anions, which have received increasing attention in the last years due to their chemical versatility and potential applications in different field such as catalysis, biomedicine, water purification, anticorrosive coating etc. Curcumine, a functional food colorant material was used to obtain an organo-modified LDH. Donor substrates were made by depositing thin films of LDHs using PLD and spin coating, respectively. The donor substrates were used for the transfer of LDHs and curcumine-modified LDH in the form of pixels on silicon and glass substrates. The as prepared donors and the transferred pixels were characterized through X-ray diffraction and atomic force microscopy (AFM) and FT IR spectroscopy.



# Surface modification of PVC for biomedical applications

O. C. Duta<sup>1</sup>, D. Ficai<sup>1</sup>, A. Ficai<sup>1</sup>, M. C. Chifiriuc<sup>2</sup>, E. Andronescu<sup>1</sup>

<sup>1</sup>University POLITEHNICA of Bucharest, Faculty of Applied Chemistry and Material Science; 1-7 Polizu St., Bucharest, Romania

<sup>2</sup>Department of Microbiology, Faculty of Biology, University of Bucharest, 1-3 Aleea Portocalelor, Bucharest 060101, Romania  
oana\_cristina\_duta@yahoo.com

Cardiovascular diseases are responsible for a large number of deaths among older people and it is estimated that this number will increase in the next years. Therefore, it is necessary to obtain cardiovascular devices, including vascular bypass, catheters, stents, heart valves, which provide the desired interactions between material and blood. Thrombogenicity due to incompatibility of the material surface and the modification of dynamics flow at the site of implantation are some of the most common causes that lead to failure of functions for which the device it was implanted<sup>1</sup>.

The aim of this work is to modify the surface of the polyvinyl chloride (PVC) (standard flat samples or catheters) in order to assure a more inert surface. A method used for modifying the material surface for obtaining improved properties in order to use the material in biomedical applications is to cover the material with a polymeric film that should be uniform and to ensure a smooth non-thrombogenic surface. The method used is called spin coating and consists in applying a PVC film containing an anticoagulant substance, such as dicoumarol or warfarin, in order to prevent blood clot and thus preventing the blocking of the device for which was used. The substrate to be coated is secured to a rotary part using a vacuum pump, and then the coating solution is poured on the surface. Due to centrifugation, the liquid flows radially, and the excess is discharged outside the substrate. The film continues to thin gently until thick deposition reaches equilibrium or until it hardens due to increased viscosity that occurs after solvent evaporation<sup>2</sup>. The surface modification of PVC by depositing a uniform and smooth thin film of PVC that contains dicoumarol and respectively warfarin was confirmed by FT-IR microscopy. The drug delivery was analyzed by HPLC. Microbiological analysis will be conducted to determine whether the surface is non-thrombogenic and whether bacteria or enzymes adhere or not onto the surface of the modified material.

**Acknowledgement:** This work was supported by the Romanian National Authority for Scientific Research, CNCS-UEFISCDI, # 94/2012.

1. A. de Mel, A. M. Seifalian, *Surface Modification of Biomaterials: A Quest for Blood Compatibility*. International Journal of Biomaterials, p. 1-8, 2012;

2. A. Niemczyk, M. El Fray, *Spin-coated chitosan on copolyester substrates*. Progress on Chemistry and Application of Chitin and its Derivatives, **XX**: p. 236-245, 2015.

## ***In vitro* assessment of reinforced biological hydroxyapatite thin films for implantology applications**

L. Duta<sup>1</sup>, A.C. Popescu<sup>1</sup>, G.E. Stan<sup>2</sup>, G. Popescu-Pelin<sup>1</sup>, I.N. Mihailescu<sup>1</sup>, P.E. Florian<sup>3</sup>, L.E. Sima<sup>3</sup>,  
A. Roseanu<sup>3</sup>, F.N. Oktar<sup>4,5,6</sup>

<sup>1</sup>National Institute for Lasers, Plasma and Radiation Physics, Magurele, Romania

<sup>2</sup>National Institute of Materials Physics, Magurele, Romania

<sup>3</sup>Institute of Biochemistry of the Romanian Academy, Bucharest, Romania

<sup>4</sup>Department of Bioengineering, Faculty of Engineering, Marmara University, Istanbul, Turkey

<sup>5</sup>Department of Medical Imaging Techniques, School of Health Related Professions, Marmara University, Istanbul, Turkey

<sup>6</sup>Nanotechnology and Biomaterials Application & Research Centre, Marmara University, Istanbul, Turkey

liviu.duta@infpr.ro

We report on the Pulsed Laser Deposition of biological-origin hydroxyapatite (HA) thin films. The HA powders were calcinated according to a protocol which guarantees the full security against disease transmission and contamination. The role of reinforcement agents (e.g., Li<sub>2</sub>O, Li<sub>2</sub>CO<sub>3</sub> or Li<sub>3</sub>PO<sub>4</sub>), in different concentrations, on the structure, bonding strength and cytocompatibility of the films was investigated.

The morphological, structural, compositional, and mechanical properties of the films were evidenced by Scanning Electron Microscopy (SEM), X-Ray Diffraction (XRD), Energy Dispersive X-Ray Spectroscopy (EDS) and pull-out tests, respectively. *In vitro* biological tests for viability of human mesenchymal stem cells (hMSC) on the thin films in the presence of reinforcement elements were assessed using calcein AM/ethidium homodimer method.

SEM images revealed a granular morphology consisting of spheroidal particles with ~ 2–3 μm in diameter. XRD analyses demonstrated that the synthesized structures consisted of a pure HA phase, with different degrees of crystallinity mainly influenced by the reinforcement agents. EDS spectra indicated the purity of the films, apart from the healthy human bone main constituents, no elemental impurities being detected. We emphasize that the

bonding strength values of the biological HA structures were superior to the ones imposed by the International Standards that regulate the fabrication of implant coatings for biomedical applications.

Interestingly, viability tests revealed that high concentrations of  $\text{Li}_2\text{O}$  within HA thin films are very toxic for hMSC *in vitro*, whilst deposition of  $\text{Li}_2\text{CO}_3$  led to promotion of hMSC growth on all thin films, irrespective of the reinforcement agent concentrations used.

Due to their improved performances, low cost fabrication from renewable resources and good biocompatibility, these new coating materials could represent a prospective competitor to synthetic HA for implantology applications.

*Acknowledgments:* LD, ACP, GPP and INM acknowledge with thanks the support of the Romanian National Authority for Scientific Research and Innovation, CNCS-UEFISCDI, under project number PN-II-RU-TE-2014-1570 (TE 108/2015).

## 2D Direct laser writing of polymer graphene composites

G. Epurescu<sup>1</sup>, A. Chibac<sup>2</sup>, A. Matei<sup>1</sup>, I. Ion<sup>3</sup>, E.C. Buruiana<sup>2</sup>, F. Stokker<sup>1</sup>, T. Buruiana<sup>2</sup>

<sup>1</sup>National Institute for Lasers, Plasma and Radiation Physics, 409 Atomistilor St, 077125 Magurele, Ilfov, Romania

<sup>2</sup>Petru Poni Institute of Macromolecular Chemistry, 41 A Gr. Ghica Voda Alley, 700487 Iasi, Romania

<sup>3</sup>National Institute for Electrical Engineering - ICPE CA, Adv Mat Dept, 313 Splaiul Unirii St, 030138 Bucharest, Romania.  
george.epurescu@inflpr.ro

Graphene has emerged as a subject of enormous scientific interest due to its exceptional electron transport, mechanical properties, and high surface area, has attracted large attention as a reinforcement for polymers due to its ability to modify electrical and thermal conductivity and mechanical properties of host polymers. Graphene films and composites have attractive electronic and optical properties, making them ideal for photonics and optoelectronics. At large scale graphene-polymers composites can be easily obtained. At micrometric scale the incorporation of graphene into the polymer matrix it's a complicated task. For this purpose, Direct Laser Writing by Two-Photon Polymerization technique is used to obtain graphene-polymer composite. With an IR femtosecond laser 2D graphene-polymer composites microstructures can be produce. Graphene with 1-5 layers were obtained by exfoliation, as Raman and HR-TEM investigations revealed.

A series of photopolymerizable urethane mono(dimethacrylates) containing different functionalities capable to interact with the inorganic component for producing polymer/graphene hybrid materials synthesized. Different mixtures of graphene and monomers solutions are prepared for concentrations ranging from 0.05% to 0.2% graphene. Graphene dispersion is chemically controlled. Two sets of graphene with different sheet sizes were used. The influence of the graphene sheet size and concentration, the monomer type and the laser power on the 2D composite structures properties were investigated.

## Laser processing of ferrocene thin films patterns for sensor application

M. Filipescu, A. Palla Papavlu, A. Matei, V. Marascu, M. Dinescu

National Institute for Lasers, Plasma, and Radiation Physics, 409 Atomistilor Street, PO Box MG-16, 077125 Magurele, Romania  
andreea.purice@inflpr.ro

The micro-devices fabrication and their integration onto large-area, flexible and low cost substrates represent a challenge for microelectronics. Devices based on ferrocene –  $\text{Fe}(\text{C}_5\text{H}_5)_2$  can be used in sensors as active membrane. Ferrocene –  $\text{Fe}(\text{C}_5\text{H}_5)_2$  is a type of organometallic chemical compound consisting of two cyclopentadienyl rings bound on opposite sides of a central iron atom. Thin films of ferrocene were obtained on quartz substrates by MAPLE (matrix assisted pulse laser evaporation) using toluene as matrix. These films are used as donors (targets) for LIFT (laser induced laser transfer) experiments in order to obtain different micro-patterns of ferrocene on flexible substrates (PDMS). Spectroscopic-ellipsometry, Fourier transform infrared spectroscopy, scanning electron microscopy and atomic force microscopy techniques were used to investigate the structure, morphology and optical properties of the films and transferred pixels.

# Dielectric thin films obtained by laser-plasma methods for high power laser optics

M. Filipescu<sup>1</sup>, A. Bercea<sup>1</sup>, S. Nistor<sup>2</sup>, L. C. Nistor<sup>2</sup>, V. Ion<sup>1</sup>, M. Dinescu<sup>1</sup>

<sup>1</sup>National Institute for Lasers, Plasma and Radiation Physics, 409 Atomistilor St, RO-077125, Magurele, Romania

<sup>2</sup>National Institute of Materials Physics, 077125 Magurele, Ilfov, Romania  
mihaela.filipescu@gmail.com

In this paper we report the progress on growing and characterization of antireflection coatings from dielectric oxides for high power laser optics. The combination of dielectric materials with low and high refractive index used as thin films and/or heterostructures with antireflection properties was studied. Starting from metal oxide targets ( $\text{Ta}_2\text{O}_5$ ,  $\text{Al}_2\text{O}_3$ ,  $\text{SiO}_2$ , and  $\text{HfO}_2$ ) in a controllable oxygen atmosphere, thin layers were grown at different temperatures (24-600°C) by pulsed laser deposition (PLD). Also, a hybrid deposition technique was implemented; this combines the advantages of PLD in gaseous atmosphere (in particular oxygen) with the enhanced reactivity associated to a beam of excited and ionized atoms and molecules produced by a radiofrequency (RF) discharge in oxygen and impinging on the substrate. This allows better oxygen embedding in the layers.

The experimental set-up consists in a laser, a reactive chamber, a pumping system, a heater acting as substrate holder and a rotation-translation system of the target, mass flow controllers for gas admission. A RF discharge generator working at 13.56 MHz and a maximum power of 1000 W is added to the classic PLD system for RF-PLD set-up. For laser ablation experiments different wavelengths ( $\lambda=1064$ , 532, 355, 266 nm) supplied by a Nd:YAG laser or  $\lambda=193$  nm from an excimer (ArF) laser were used.

The antireflection coatings with low roughness, uniform thickness, and high dielectric constant were obtained by selecting the best deposition parameters such as: wavelength, laser fluence, oxygen pressure and substrate temperature. In order to obtain heterostructures of  $\text{HfO}_2/\text{SiO}_2$ ,  $\text{Al}_2\text{O}_3/\text{SiO}_2$ ,  $\text{Ta}_2\text{O}_5/\text{SiO}_2$ , all the oxide layers were investigated from morphological, structural and optical point of view.

*Acknowledgements:* This work has been financed by the National Authority for Research and Innovation in the frame of Nucleus programme - contract 4N/2016 and the project PCCA 38/2014.

# Antimicrobial thin films based on ayurvedic plants extracts embedded in a polymeric matrix

L. Floroian<sup>1</sup>, C. Ristoscu<sup>2</sup>, N. Mihailescu<sup>2</sup>, M. Badea<sup>1</sup>, E. Pozna<sup>1</sup>, M. Galca<sup>3</sup>, M. Moscatelli<sup>4</sup>, N. Pastori<sup>4</sup>, G. Candiani<sup>4</sup>, R. Chiesa<sup>4</sup>, I.N. Mihailescu<sup>2</sup>

<sup>1</sup>Transilvania University of Brasov, 29 Eroilor Blvd, 500036, Brasov, Romania

<sup>2</sup>National Institute for Lasers, Plasma and Radiation Physics, Măgurele, Romania

<sup>3</sup>"Carol Davila" University of Medicine and Pharmaceutics, 8 Eroilor Sanitari Blvd, 50471, Bucharest

<sup>4</sup>Politecnico di Milano, 7 Via Mancinelli, 20131, Milano, Italy  
lauraf@unitbv.ro

Ayurvedic medicine is one of the world's oldest medical systems. It is an example of a coherent traditional system which have a time tested and precise algorithm for medicinal plant selection, based on several ethnopharmacophore descriptors whose knowledge endows the user to adequately choose the optimal medicinal plant for the treatment of certain pathology.

This work tries to link traditional knowledge with biomedical science by using traditional ayurvedic plants with antimicrobial effect in manufacture of thin films for implant protection.

We report on the transfer of novel polymer-antimicrobial plants extract-bioactive glass composites by matrix-assisted pulsed laser evaporation to uniform thin layers onto stainless steel implant surfaces. Influence of the deposition process on the structure of nanomaterials was studied. The targets were prepared by freezing in liquid nitrogen of mixtures containing polymer and plants extract reinforced with bioglass powders. The cryogenic targets were submitted to multipulse ablation with an UV KrF\* ( $\lambda=248$  nm,  $\tau \sim 25$  ns) excimer laser source. The main advantages with this coating are multiple: stopping any leakage of metal and metal oxides to the biological fluids and eventually to inner organs (by polymer use), speeding up osteointegration (by bioactive glass use), antimicrobial effect (by ayurvedic plants extracts use) and decreasing of the implant price (by cheaper stainless steel use).

*Acknowledgements:* LF and MB hereby acknowledge the structural funds project PRO-DD (POS-CCE, O.2.2.1., ID 123, SMIS 2637, ctr. No 11/2009) and "Bursa universitatii 2016" for providing the infrastructure used in this work.

# Compositional analyses of steel via laser-induced breakdown spectroscopy

O. Fufa<sup>1</sup>, E. Axente<sup>1</sup>, G. Socol<sup>1</sup>, A. Stancalie<sup>1</sup>, D. E. Mihaiescu<sup>2</sup>, R. Trusca<sup>2</sup>, D. Sporea<sup>1</sup>, A. Bodea<sup>3</sup>,  
B. Verdes<sup>3</sup>, V. Craciun<sup>1</sup> and J. Hermann<sup>4</sup>

<sup>1</sup>Laser-Surface-Plasma Interactions Laboratory, Lasers Department, National Institute for Lasers, Plasma and Radiation Physics, RO-077125, Măgurele, Ilfov, Romania.

<sup>2</sup>Faculty of Applied Chemistry and Material Science, Polytechnic University of Bucharest, RO-011061, Bucharest, Romania.

<sup>3</sup>ADREM Invest, Bucharest, Romania.

<sup>4</sup>LP3, CNRS – Aix-Marseille University, 163 Av. de Luminy, 13288 Marseille, France.

emanuel.axente@inflpr.ro, valentin.craciun@inflpr.ro

The refining of liquid steel composition in separate ladles is referred to as secondary metallurgy. To control composition, current practice is to remove a sample of molten material for elemental analysis. There are two major problems: first, by sampling the material off-line, the process comes to a halt while the sample is analyzed. Secondly, if alloying materials were added and the melt was not sufficiently mixed, the composition may be inhomogeneous and changes made on the basis of the analysis of one particular sample may not bring the processed steel into specification. These issues lead to excessive melting time, quality control problems, wasted feedstock, increased energy use and CO<sub>2</sub> emissions.

The goal of this study is the testing and optimizing the performances of Calibration-Free Laser-induced breakdown spectroscopy<sup>1</sup> (LIBS) technique as a potential tool for implementing real time and in-situ analysis of steel composition. Usually, the most common approach for the investigation of elemental composition of materials by LIBS is usually performed using calibration curves, generated after measurements on standard samples with certified composition. Calibration-Free LIBS, is an alternative approach for multi-elemental quantitative analysis, based on the modeling of the plasma emission spectrum.

The main difficulty of steels analyses rely on their complicated composition, consisting of minor and major elements. The later (e.g. Fe, Ni, Cr) exhibits very rich spectra with many intense and thus self-absorbed lines, which are not suited for calibration-free approach. Moreover, the lack of knowledge of the Stark broadening parameters of the transitions selected for analyses and the imprecision of the spectroscopic databases may influence the accuracy of the results. Here we present the results achieved after analyses of several unknown and standard steel samples when compared with complementary measurements by ICP-OES and EDX.

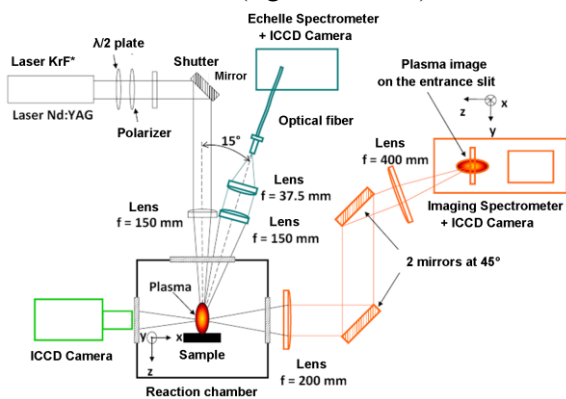


Figure 1: Schematic representation of the plasma diagnostics setup available at LP3 Laboratory.

1. J. Hermann, (WO/2010/052380), E. Axente *et al.*, *J. Anal. At. Spectrom.*, **29** (2014), 553.;
2. J. Hermann *et al.*, *Spectrochim. Acta B*, **100** (2014), 189;
3. A. De Giacomo *et al.*, *Spectrochim. Acta B*, **98** (2014), 19.

# Biocompatible HAp–Ag nanostructured coatings for titanium implants

O. Fufa<sup>1,2</sup>, G. Socol<sup>2</sup>, A.M. Grumezescu<sup>1</sup>, E. Andronescu<sup>1</sup>, M. Socol<sup>3</sup>, R.C. Popescu<sup>1,4</sup>, A.M. Holban<sup>1,5</sup>

<sup>1</sup>Department of Science and Engineering of Oxide Materials and Nanomaterials, Faculty of Applied Chemistry and Materials Science, Politehnica University of Bucharest, Bucharest, Romania

<sup>2</sup>Lasers Department, National Institute for Laser, Plasma and Radiation Physics, Magurele, Bucharest, Romania

<sup>3</sup>National Institute of Materials Physics, Magurele, Bucharest, Romania

<sup>4</sup>Life and Environmental Physics Department, Horia Hulubei National Institute of Physics and Nuclear Engineering, Magurele, Bucharest, Romania

<sup>5</sup>Microbiology and Immunology Department, Faculty of Biology, University of Bucharest, Bucharest, Romania  
oana.fufa@infllpr.ro

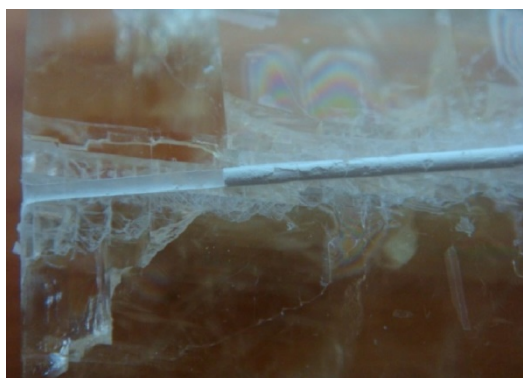
The aim of our experimental study was to produce bioactive coatings consisting in hydroxyapatite (HAp) and silver nanoparticles (AgNPs) for titanium implants, by means of a laser-assisted deposition technique. In this respect, we firstly synthesized AgNPs functionalized with essential oils by using a facile and efficient wet chemistry route, employing both the classical chemical reduction strategy and the ultrasound-assisted synthesis. The as-obtained nanopowder samples were physicochemically investigated in terms of composition and microstructure by TGA, FT-IR, XRD and TEM. Furthermore, the biodistribution of the synthesized AgNPs was evaluated in terms of the histological aspects of vital organs after performing *in vivo* assays on a mouse animal model. Subsequently, the obtained AgNPs were mixed with commercial HAp in order to produce composite coatings onto the titanium substrates by matrix assisted pulsed laser evaporation (MAPLE) technique. The compositional and microstructural features of the resulted coatings were investigated by means of the IRM, XRD, SEM and AFM techniques. The biocompatibility of the deposited coatings was evaluated by considering the cellular viability results obtained after the *in vitro* treatment of osteoblast-like cells. Also, relevant data regarding the morphology and behaviour of cells in the presence of the produced coatings were obtained by performing immunofluorescence and SEM analysis. The anti-adherent potential of HAp-AgNPs coatings against microbial contamination was *in vitro* assessed, against both Gram-positive and Gram-negative bacterial pathogens.

## High-aspect ratio channels by self-guiding and filamentation of high-power CW CO<sub>2</sub> laser beam in solids

M. Ganciu, C. Luculescu, C. Diplasu, C. Ticos

National Institute for Laser, Plasma and Radiation Physics, PO Box MG-36, 077125, Magurele, Bucharest, Romania  
mihai.ganciu@infllpr.ro

Laser techniques are more and more required for the solid material processing, in particular for cutting or drilling. In order to achieve larger aspect-ratio of holes, new techniques are developed, based on laser beam filamentation and self-guiding in material, by using fs pulsed laser beams and adapted optics<sup>1,2</sup>. In this paper we



report drilling in the range of few cm, generating channels with inner diameter of 400  $\mu\text{m}$  in certain rocks (carbonates, phosphates) through the phenomenon of self-channelling of a high power CW CO<sub>2</sub> laser beam (10.6  $\mu\text{m}$ , 1kW) focused with an f/30 lens onto the target surface. A calcite crystal drilled by this process, with a remarkable aspect-ratio of the resulted capillary, is illustrated in Figure 1. The structure modification of the internal walls of the channel ensures the laser beam propagation like in a hollow fiber. The paper will present the relevant physical and photo-chemical processes and possible applications in mining, destruction of small asteroids, etc.

Figure 1: A high aspect ratio capillary drilled in a natural calcite crystal

1. S. Abbas Hosseini, Method and apparatus for machining diamonds and gemstones using fillamentation by burst, ultrafast laser pulses, US Patent Appl. 0121960 A1 (2015);
2. Chen Xie, Vytautas Jukna, Carles Milián, Remo Giust, Ismail Ouadghiri-Idrissi, Tatiana Itina, John M. Dudley, Arnaud Couairon, Francois Courvoisic, Tubular filamentation for laser material processing, Scientific Reports 5, 8914 (2015)

# Optical arrangement of gold nanoparticles by array of Bessel-like beams

M. Garliauskas, E. Stankevičius, G. Račiukaitis

Center for Physical Sciences and Technology, Savanoriu Ave. 231, LT-02300, Vilnius, Lithuania  
mantas.garliauskas@ftmc.lt

Over the past decade, gold nanoparticles gained the significant attention of researchers due to their unique size- and shape-dependent optical properties, large surface-to-volume ratio, excellent biocompatibility and low toxicity<sup>1,2</sup>. The combination of precise spatial control and plasmonic properties of gold nanoparticles paves the way for development of plasmonic sensors for detection of pollutants, analytes or biological markers in the environment<sup>3</sup>, surface plasmon circuits<sup>4</sup> or even cancer detection and photothermal therapy<sup>5</sup>. The focused laser beam is applied as an optical tweezer to manipulate nanoparticles on a surface. However, stable optical manipulation of metallic nanoparticles is proven to be difficult due to the strong gradient forces needed to overcome the scattering and absorption of nanoparticles using tightly focused Gaussian beams<sup>6</sup>. Therefore, in order to trap particles with laser wavelengths close to their plasmonic resonance, the special beam shapes, such as Laguerre-Gaussian<sup>3</sup> or Bessel beams<sup>7</sup>, should be utilized.

In this presentation, we introduce optical arrangement of gold nanoparticles by the array of Bessel-like beams which was generated by illumination of polymeric microstructure arrays fabricated via laser interference lithography<sup>8</sup>. The intensity distribution of each generated Bessel-like beam consists of intensive central maximum surrounded by series of concentric rings (Fig. 1a). Measured transverse intensity distribution shows a good agreement with an approximation of the theoretical Bessel beam.

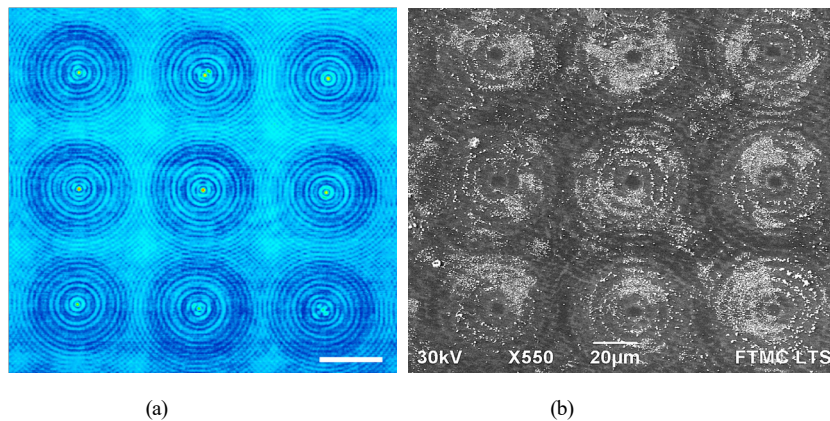


Figure 1: (a) Intensity distribution of the generated Bessel-like beam array. The scale bar corresponds to 30  $\mu\text{m}$ . (b) Distribution of gold nanoparticles on the soda-lime glass substrate after irradiation with an array of Bessel-like beams.

Experiments have demonstrated that a short exposure of gold nanoparticles, uniformly spread on the soda-lime glass substrate, with such intensity distribution, using the laser wavelength corresponding their plasmonic resonance, results in scattering forces leading to an arrangement of the nanoparticles in circles of intensity minima. Compared to the optical trapping by tightly focused Gaussian beam, the advantage of this approach is a rapid, single exposure optical arrangement of nanoparticles in the array of concentric circles over the relatively large ( $\sim 0.25 \text{ mm}^2$ ) area.

1. Y. C. Yeh, B. Creran, V. M. Rotello, Gold nanoparticles: preparation, properties, and applications in bionanotechnology, *Nanoscale* **4**, 1871-1880 (2012).
2. A. Tomar, G. Garg, Short review on application of gold nanoparticles, *Glob. J. Pharmacol.* **7**, 34-38 (2013);
3. A. S. Urban, S. Carretero-Palacios, A. A. Lutich, T. Lohmüller, J. Feldmann, F. Jäckel, Optical trapping and manipulation of plasmonic nanoparticles: fundamentals, applications, and perspectives, *Nanoscale* **6**, 4458-4474 (2014);
4. S. Hashimoto, D. Werner, T. Uwada, Studies on the interaction of pulsed lasers with plasmonic gold nanoparticles toward light manipulation, heat management, and nanofabrication, *J. Photochem. Photobiol. C Photochem. Rev.* **13**, 28-54 (2012);
5. X. Huang, M. A. El-Sayed, Gold nanoparticles: Optical properties and implementations in cancer diagnosis and photothermal therapy, *J. Adv. Res.* **1**, 13-28 (2010);
6. K. Wang, E. Schonbrun, K. B. Crozier, Propulsion of Gold Nanoparticles with Surface Plasmon Polaritons: Evidence of Enhanced Optical Force from Near-Field Coupling between Gold Particle and Gold Film, *Nano Lett.* **9**, 2623-2629 (2009);
7. P. Zemanek, A. Jonas, L. Sramek, M. Liska, Optical trapping of nanoparticles and quantum dots, *Opt. Lett.* **24**, 1448-1450 (1999);
8. E. Stankevičius, M. Garliauskas, M. Gedvilas, G. Račiukaitis, Bessel-like beam array formation by periodical arrangement of the polymeric round-tip microstructures, *Opt. Express* **23**, 28557 (2015).

# Vanadium dioxide: thermochromic properties of nanoparticle stacks versus dense thin film

M. Gaudin<sup>1</sup>, F. Dumas-Bouchiat<sup>1</sup>, P. Carles<sup>1</sup>, E. Laborde<sup>1</sup>, V. Coudert<sup>1</sup>, C. Champeaux<sup>1</sup>

<sup>1</sup> Univ. Limoges, CNRS, SPCTS, UMR 7315, 12, rue Atlantis, F-87000 Limoges, France  
michael.gaudin@yahoo.fr

Vanadium dioxide (VO<sub>2</sub>) is particularly interesting due to its first order metal to insulator transition (MIT) at 68°C. This MIT is characterized by abrupt changes in resistivity and near-IR optical transmission when submitted to external stimuli such as heating, strain, electrical voltage or current. As we already showed, these amazing properties render VO<sub>2</sub> thin films ideal smart material for integration in specific electronic devices.<sup>1-2</sup>

Recently, we have developed a free nanoparticles (NPs) generator coupled to a Pulsed Laser Deposition (PLD) set-up. Based on laser sputtering and plasma condensation, this complex process offers the possibility to realize a large number of new exotic nanocomposite materials. Using separately, simultaneously or sequentially the generator and/or the PLD, the deposition process leads respectively to NP-stacks, nanocomposite thin films with embedded NPs or multilayers NPs/thin films.

In this paper, metallic vanadium nanoparticles (V-NPs) were synthesized. These V-NPs are crystallized at room temperature and TEM-statistical analyses reveal a very narrow size distribution (2.7 nm ± 0.5 nm). Furthermore, V-NPs are synthesized in flight and keep their shape after impact on the substrate. Due to the well-known high reactivity of such small objects, VO<sub>2</sub> majority phase were obtained after annealing of NPs stacks during 10 min at 300°C and 3.3x10<sup>-2</sup> mbar oxygen pressure. This relatively low temperature allows deposition on various substrates such as Al<sub>2</sub>O<sub>3</sub>, MgO and mostly amorphous glass substrates. Both electrical and optical behaviors of these VO<sub>2</sub>-NP-stacks present a lower transition temperature (~50°C) and a larger hysteresis width (~10-20°C) compared to VO<sub>2</sub> conventional PLD thin films (deposited at ~700°C). These properties can be explained partially by the individual/collective effect of the NP-stacks presenting a high porosity (around 50%)

leading to a modified propagation of the transition.

Taking benefit of differences and complementarities between VO<sub>2</sub>-NP-stacks and VO<sub>2</sub>-PLD thin films, we made films combinations of the two elements. Also, the MIT characteristic occurs by steps (see Fig.1, (c), steps 0, 1, 2)) controlled by the size of NPs and texture of stacks, allowing, as example, the modulation of the transmission in a visible-IR range.

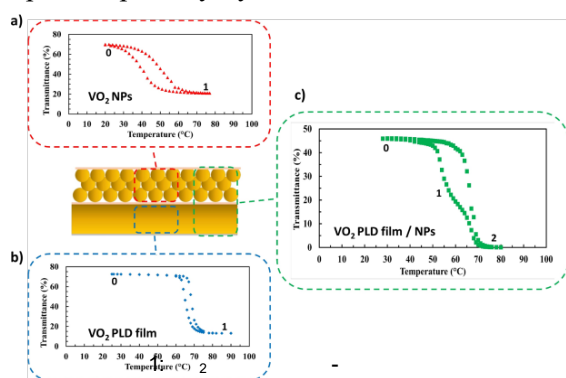


Figure 1: VO<sub>2</sub> PLD film/NPs-a step behavior

1. F. Dumas-Bouchiat et al., APL 91(22) (2007) ;
2. J. Leroy et al., APL 100(21) (2012).

## Method of nano titanium dioxide synthesis by laser pyrolysis targeting photocatalytic applications

L. Gavrilă-Florescu<sup>1</sup>, E. Popovici<sup>1</sup>, I. Morjan<sup>1</sup>, E. Dutu<sup>1</sup>, A. D. Badoi<sup>1</sup>, G. Demian<sup>2</sup>, M. Demian<sup>2</sup>, M. Iliescu<sup>3</sup>, E. M. Stanciu<sup>3</sup>, L. C. Diamandescu<sup>4</sup>, V. Raditoiu<sup>5</sup>, A. Raditoiu<sup>5</sup>, L. E. Wagner<sup>5</sup>

<sup>1</sup>National Institute for Laser, Plasma and Radiation Physics, Laser Department, Laser Photochemistry Laboratory, Magurele, Romania

<sup>2</sup>University of Craiova, 13 A. I. Cuza, Craiova, Romania

<sup>3</sup>OPTOELECTRONICA - 2001 SA Atomistilor 409 st. R 077125, Magurele, Romania

<sup>4</sup>Institutul National de Cercetare - Dezvoltare pentru Fizica Materialelor, Magurele, Romania

<sup>5</sup>Institutul National de Cercetare - Dezvoltare pentru Chimie si Petrochimie - ICECHIM, Bucharest  
lavinia.gavrila@inflpr.ro

It shows a method of obtaining at an enlarged scale of a wide range of NP / NS TiO<sub>2</sub>. The targeted applications are in the field of photocatalytic. This method is based on the TTIP as main precursor source of Ti and partial / total of the oxygen, which has special physical properties with respect to melting point of 17-19°C, boiling point of 239-242°C. Considering the properties of TiO P25 AEROXIDE® product as an accepted reference in the field, all those properties and method provide additional advantages that lie in product purity and flexibility in controlling parameters. As noticed in the thermogravimetric analysis carried out on samples obtained by laser pyrolysis and P25 in air atmosphere is similar, both featuring a weight gain of 1.34% and 1.37% due to absorption of oxygen air, is deficient in oxygen compounds. According to literature this behavior is closely related to the presence of OH

groups on the surface of TiO<sub>2</sub> particles in correlation with photocatalytic properties of the products. The method utilizes the principle of separation of phase transformations by nonduplication natural chemical reactions between elements cleavage. Physical transformation phase liquid / vapor and that vapor / gas are separated from the interaction laser - matter, where a form very tightly controlled occurring physical transformation as generic energy transfer (laser radiation) - matter and chemical reactions decomposition and recombination of basic substances. Phase transformations are achieved through convective heat transfer about the major advantages stability vaporization process, reaction speed, temperature control, essential in ensuring the reproducibility of the process - and control the temporal dynamics of the process of vaporization. About convective energy transfer system has advantages over infrared energy source that requires automation IR complex is influenced by the thermal inertia of the system and is characterized by inhomogeneity of the vaporization process.

## High-speed processing of CIGS thin film solar cells

P. Gečys<sup>1</sup>, E. Markauskas<sup>1</sup>, S. Nishiwaki<sup>2</sup>, S. Buecheler<sup>2</sup>, R. De Loor<sup>3</sup>, G. Račiukaitis<sup>1</sup>

<sup>1</sup>Center for Physical Sciences and Technology, Savanoriu Ave. 231, LT-02300, Vilnius, Lithuania

<sup>2</sup>Laboratory for Thin Films and Photovoltaics, Swiss Federal Laboratories for Materials Science and Technology EMPA, Ueberlandstrasse 129, CH-8600 Dübendorf, Switzerland

<sup>3</sup>Next Scan Technology, Noorwegenstraat 29, 9940 Evergem, Belgium  
p.gecys@fmc.lt

High CIGS thin-film solar cell efficiency, flexibility and light weight make this technology attractive for future developments. In order to preserve small cell efficiency over the large area, structuring of large-scale devices is needed. The module is divided into small cells interconnected in series by the tree-step laser scribing<sup>1</sup>. P1 laser process patterns the back-contact forming the stripe-shaped molybdenum grid. P2 is used for the series interconnect formation between the adjacent cells after the TCO deposition. The P3 process is used for isolation of neighboring cells (see figure 1 a). The Cu-chalcopyrite layer is thermally sensitive material, and laser modification can induce local structural changes followed by device shunting<sup>2</sup>. That is undesirable for the P3 scribing since the device shunting can lead to significant efficiency losses. For this, it is necessary to validate the CIGS scribing at high-speed regime.

In this work, we investigate high-speed laser processing of the CIGS thin-film solar cells. The modern ultrashort high pulse repetition rate (up to 1 MHz) laser was used for solar cell processing. Two main P3 scribing approaches were investigated – ablation of the full layer stack to expose the molybdenum back-contact (P3 “type 1”), and removal of the front-contact only (P3 “type 2”). The scribing was evaluated visually followed by electrical testing. We used a linear laser scribing technique to validate the scribe conductivity<sup>3</sup>. We found, that high laser pulse repetition rate induced severe shunting of the CIGS solar cells (see figure 1 b). On the other hand, the P3 “type 2” process showed promising results. It was possible to scribe at the relatively high speed of 1.7 m/s with minimal device degradation. Also, we demonstrated the P3 processing in the ultra-high speed regime with novel polygon scanner system, where the scribing speed of 50 m/s was obtained. Overall, we conclude, that the top-contact layer lift-off processing is the only reliable solution for high-speed P3 laser scribing, which can be implemented in the future TW production facilities.

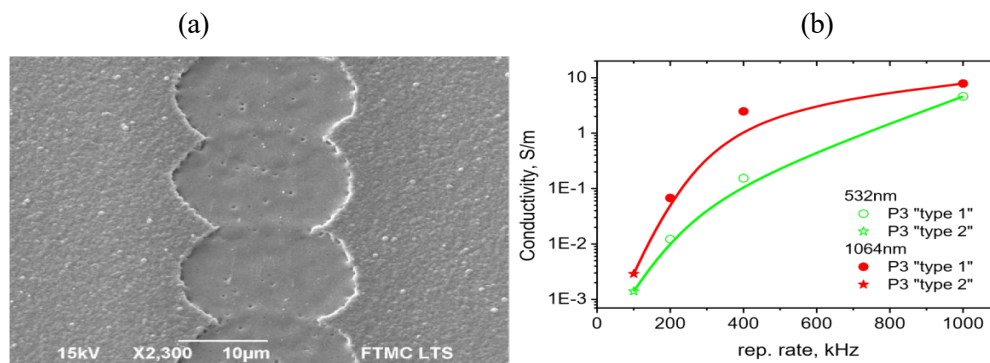


Figure 1: (a) P3 “type 2” pattern in CIGS thin-film solar cell structure. (b) Laser scribe conductivity versus laser repetition rate.

1. C. Dunsky, F. Colville, Solid state laser applications in photovoltaics manufacturing, Proc. SPIE, 6871 (2008);
2. P. Gečys, E. Markauskas, A. Žemaitis, G. Račiukaitis, Variation of P2 series interconnects electrical conductivity in the CIGS solar cells by picosecond laser-induced modification, Sol. Energy, **132**, 493–502 (2016);
3. E. Markauskas, P. Gečys, A. Žemaitis, M. Gedvilas, G. Račiukaitis, Validation of monolithic interconnection conductivity in laser scribed CIGS thin-film solar cells, Sol. Energy, **120**, 35–43 (2015).



# Oxide thin film transistors made by pulsed electron beam deposition

F. Gherendi<sup>1</sup>, N.B. Mandache<sup>1</sup>, M. Nistor<sup>1</sup>

<sup>1</sup>National Institute for Lasers, Plasma and Radiation Physics (NILPRP), Plasma Physics and Nuclear Fusion Laboratory (L 22), Magurele-Bucharest, Romania  
florin.gherendi@infim.ro

Transparent conducting oxide thin films are widely used for the fabrication of thin film transistors due to their very good optical transparency in the visible spectrum and high tunability of their electrical properties. In this work we report on the use of pulsed electron beam deposition technique (PED) with shadow masks for the fabrication of thin film field effect transistors (TFTs) with various oxides, structures and geometries. PED is a technique similar to pulsed laser deposition (PLD), where the target ablation is done by a pulsed electron beam produced in a channel-spark discharge. Typically used substrates were glass and paper, for transparent, respectively flexible and disposable (low cost) transistors. The working gas for the PED device was Ar or O<sub>2</sub> at typically 10<sup>-2</sup> mbar range pressure.

The source and drain contacts (In<sub>2</sub>O<sub>3</sub> or ZnO films) were patterned with shadow mask during the film deposition process at room temperature. The conductivity of the films made of these oxides can be increased by increasing the concentration of oxygen vacancies, which can be done by lowering the working gas pressure. In a classical approach of TFT fabrication, the oxide channel film, less conductive, was grown in oxygen at higher pressure (2x10<sup>-2</sup> mbar) on top of the source and drain contact films with a different shadow mask, obtaining a multi-layer structure.

In a second approach, self-assembled source-channel-drain structures were also made<sup>1</sup>, by placing the sourcedrain shadow mask (100µm diameter wire) at 50µm distance from the substrate and letting the oxide channel layer grow between the source and drain by plasma scattering behind the mask in the same time when the source and drain films are grown. Using O<sub>2</sub> as working gas, the film in the shadowed region is enriched in oxygen, therefore less conductive, even up to four orders of magnitude less than in the source and drain regions of the same film<sup>1</sup>.

Y<sub>2</sub>O<sub>3</sub> thin films grown by RF magnetron deposition on top of the channel film were used as gate insulators for the transistors made on glass in the top gate – bottom contacts geometry, while the paper transistors use the substrate itself as gate insulator<sup>2</sup>.

A comparative electrical characterization of multi-layer and self-assembled TFTs fabricated with different transparent oxides will be presented and discussed. The best performances were obtained for In<sub>2</sub>O<sub>3</sub> selfassembled TFTs on glass, having a low subthreshold swing (~0.26 V/decade), I<sub>on</sub>/I<sub>off</sub> of 10<sup>6</sup>-10<sup>7</sup>, a threshold voltage of +1.06 V and a saturation channel carriers mobility of ~40 cm<sup>2</sup>/Vs. The present work goes further by investigating the role of the shadow mask as a mechanical obstacle in the ablation plasma path, for changing the electrical properties of an oxide thin film grown in the obstacle shadow compared to the non-shadowed regions. By scaling the shadow mask, the film properties can be gradually tuned, opening a path to a convenient way to obtain thin films for small scale applications using ablation deposition methods such as PED, due to the simplicity of the setup and low costs.

1. F. Gherendi, M. Nistor, S. Antohe, L. Ion, I. Enculescu, N.B. Mandache, Self-assembled homojunction In<sub>2</sub>O<sub>3</sub> transparent thin-film transistors, *Semicond. Sci. Technol.* **28** (8), 085002 (2013);

2. F. Gherendi, M.Nistor, N.B.Mandache, In<sub>2</sub>O<sub>3</sub> Thin Film Paper Transistors, *J.Displ.Tech* **9** (9), 760-763 (2013).

## MAPLE fabricated thin coatings based on magnetite nanoparticles embedded into biopolymeric spheres with resistance to microbial colonization

V. Grumezescu<sup>1,2</sup>, A.M. Holban<sup>3,6</sup>, M.C. Chifiriuc<sup>3,6</sup>, A.M. Grumezescu<sup>2</sup>, R. Trusca<sup>4</sup>, F.Iordache<sup>5</sup>, M. Patachia<sup>1</sup>, G. Socol<sup>1</sup>

<sup>1</sup>National Institute for Lasers, Plasma & Radiation Physics, Magurele, Bucharest, Romania

<sup>2</sup> Faculty of Applied Chemistry and Materials Science Politehnica University of Bucharest, Bucharest, Romania

<sup>3</sup>Faculty of Biology, University of Bucharest, Bucharest, Romania

<sup>4</sup>S.C. Metav-CD S.A., Bucharest, Romania

<sup>5</sup>Institute of Cellular Biology and Pathology of Romanian Academy, "Nicolae Simionescu", Romania

<sup>6</sup>Research Institute of the University of Bucharest, Bucharest, Romania

valentina.grumezescu@inflpr.ro

The aim of this study was to obtain improved coatings for surfaces with increased biocompatibility and resistance to microbial colonization and biofilm formation. The prepared magnetite nanoparticles functionalized with gentamicin (Fe<sub>3</sub>O<sub>4</sub>@G) have been embedded into poly(lactic-co-glycolic acid) (PLGA) spheres by oil-in-water emulsion. The PLGA- Fe<sub>3</sub>O<sub>4</sub>@G spheres were deposited on the surface of glass and silicone samples by Matrix Assisted Pulsed Laser Evaporation (MAPLE).

The thin coatings were analysed by High Resolution Transmission Electron Microscopy (HR-TEM), Scanning Electron Microscopy (SEM) and Infrared Microscopy (IRM). The antimicrobial and antibiofilm efficiency of the thin coatings was tested on Gram-positive (*Staphylococcus aureus*) and Gram-negative (*Pseudomonas aeruginosa*) clinical strains by viable cells counts assay performed at different time intervals. The obtained results proved that the thin coatings based on PLGA-Fe<sub>3</sub>O<sub>4</sub>@G spheres exhibited an efficient antimicrobial activity against both adherent and sessile bacterial cells.

Besides their excellent anti-adherence and antibiofilm effect, the obtained MAPLE-deposited thin films were highly biocompatible, allowing the normal development and growth of cultured human endothelial cells. This approach could be successfully applied for the optimization of medical implants surfaces in order to control and prevent microbial colonization and further development of biofilm associated infections.

## Femtosecond time-resolved ellipsometry for measuring the ultrafast excitation dynamics in dielectric materials

L. Haahr-Lillevang, T. B. Reynisson, P. Balling

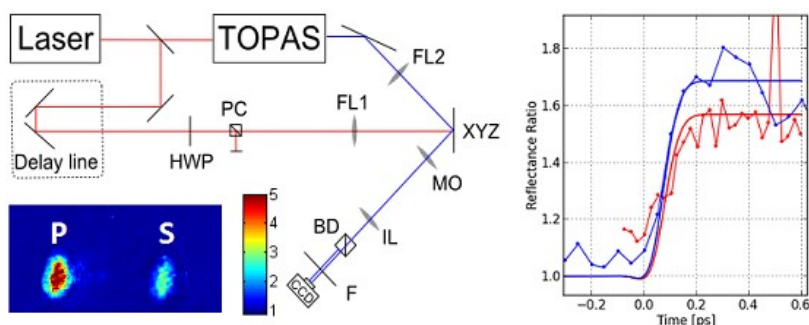
Department of Physics and Astronomy, Aarhus University, DK-8000 Aarhus C, Denmark  
lassehl@phys.au.dk

The ultrafast absorption of laser pulses in large-band-gap materials provides a window into the life of extremely hot and dense plasmas. During a strong femtosecond pulse, the material changes from being a transparent medium with no free electrons to a metallic, highly reflective hot electron plasma, but with a cold lattice; for a recent review of modelling and applications, see<sup>1</sup>. In the current presentation, the basic nature of this ultrafast change is investigated experimentally using ultrafast ellipsometry and the results are understood through numerical simulations.

We use a pump-probe setup employing 100 fs pulses impinging on the surface of a dielectric material at fixed angle as illustrated in figure 1. By simultaneously measuring the surface reflectance of the probe at two polarizations of the probe light and varying both the pump-probe delay and the probe wavelength, we obtain a comprehensive time-resolved map of the optical properties of the material.

From a theoretical point of view, during this ultrafast transition many fundamental physical processes must simultaneously be included in a description, e.g. strong field excitation, collisional excitation (potentially causing avalanche processes) and the ultrafast change of the optical properties; this is done numerically using a multiple-rate equation model as originally proposed by Rethfeld<sup>2</sup> and later modified by us<sup>3-5</sup>.

Similar pump-probe techniques, e.g. single probe wavelength reflectance combined with spectral interference measurements of the transmitted probe through the full depth of the irradiated area, provide ample information of the optical properties. These combined observations can generally be understood well through numerical models<sup>3,4</sup>, but there are some indications that the optical properties of the surface, the sub-surface and the bulk exhibit different transient response to the pump laser, especially when self-trapped excitons are added to the mix, as required for e.g. fused silica<sup>5</sup>. At the conference, the initial results of the time-resolved ellipsometry investigations and their comparison with theoretical modeling will be presented. The goal is that a detailed investigation of the surface-optical properties will clarify the model in this regard.



properties will clarify the model in this regard.

Figure 1: Experimental setup. Pump laser @ 800 nm. Bottom left: An example of raw single shot reflectance data on sapphire (normalized to Fresnel reflectance) at peak pump fluence 10 J/cm<sup>2</sup>, pump-probe delay 600 fs, and probe wavelength 480 nm. Right: Reflectance ratio of p- to s-polarized light versus pump-probe delay for constant pump fluence. Probe light at 480 nm (red) and 532 nm (blue).

1. P. Balling and J. Schou, *Femtosecond laser ablation dynamics of dielectrics: Basics and applications for thin films*, Reports on Progress in Physics, **76**, 036502 (2013);
2. B. Rethfeld, Phys. Rev. Lett., **92**, 187401 (2004); B. Rethfeld, Phys. Rev. B, **73**, 035101 (2006);
3. K. Wædegaard, D. B. Sandkamm, A. Mouskeftaras, S. Guizard, and P. Balling, *Probing ultrashort-pulse laser excitation of sapphire: From the initial carrier creation to material ablation*, Europhysics Letters **105**, 47001 (2014);
4. L. Haahr-Lillevang, K. Wædegaard, D. B. Sandkamm, A. Mouskeftaras, S. Guizard and P. Balling, *Short-pulse laser excitation of quartz: Experiments and modeling of transient optical properties and ablation*, Applied Physics A **120** (4) p. 1221-1227 (2015);
5. M. Garcia-Lechuga, L. Haahr-Lillevang, J. Siegel, P. Balling, S. Guizard, and J. Solis, *Simultaneous time-and-space resolved reflectivity and interferometric measurements of dielectrics excited with femtosecond laser pulses*, in preparation (2016).

# Selection of antimicrobial Silver-doped Carbon structures by combinatorial pulsed laser deposition

C. Hapenciuc<sup>1</sup>, I. N. Mihailescu<sup>1</sup>, D. Bociaga<sup>2</sup>, G. Socol<sup>1</sup>, G. E. Stan<sup>3</sup>, M. C. Chifiriuc<sup>4,5</sup>, C. Bleotu<sup>6</sup>, M. A. Husanu<sup>2</sup>,  
C. Luculescu<sup>1</sup>, G. Popescu-Pelin<sup>1,7</sup>, L. Duta<sup>1</sup>, I. Negut<sup>1,7</sup>, C. Besleaga<sup>3</sup>, I. Zgura<sup>3</sup>, F. Miculescu<sup>8</sup>

<sup>1</sup>National Institute for Lasers, Plasma and Radiation Physics, 077125 Magurele-Ilf, Romania

<sup>2</sup>Division of Biomedical Engineering and Functional Materials, Lodz University of Technology, Institute of Materials Science and Engineering, 1/15  
Stefanowskiego St., 90-924 Lodz, Poland

<sup>3</sup>National Institute of Materials Physics, 077125 Magurele-Ilf, Romania

<sup>4</sup>Department of Microbiology, Faculty of Biology, University of Bucharest, 060101 Bucharest, Romania

<sup>5</sup>Earth, Environmental and Life Sciences Section, Research Institute of the University of Bucharest, 050107 Bucharest, Romania

<sup>6</sup>“Stefan S. Nicolau” Institute of Virology, 030304 Bucharest, Romania

<sup>7</sup>Faculty of Physics, University of Bucharest, 077125 Magurele-Ilf, Romania

<sup>8</sup>Politehnica University of Bucharest, Faculty of Materials Science and Engineering, 060042 Bucharest, Romania  
hapenciuc.claudiu@inflpr.ro

We report on the selection by combinatorial pulsed laser deposition of Silver-doped Carbon structures with reliable physical-chemical characteristics and high efficiency against microbial biofilms. The films investigation was performed by scanning electron microscopy, high resolution atomic force microscopy, energy dispersive X-Ray Spectroscopy, Rutherford backscattering spectrometry, X-ray diffraction, Raman spectroscopy, bonding strength „pull-out” tests, and surface energy measurements.

*In vitro* biological assays were carried out using a large spectrum of bacterial and fungal strains, *i.e.*, *Staphylococcus aureus*, *S. epidermidis*, *Pseudomonas aeruginosa*, *Enterococcus faecalis* and *Candida albicans*. The biocompatibility of the obtained films was evaluated on MG63 mammalian cell cultures.

The optimal combination with reasonable physical-chemical properties, efficient protection against microbial colonization and benign effects on human cells was found for Silver-doped Carbon films containing 2 to 7 at.% silver. These mixtures can be used for the fabrication of safe and efficient coatings of metallic implants, with the goal of decreasing the risk of implant associated biofilm infections which are difficult to treat and often responsible for implants failure.

## Material analyses via calibration-free laser-induced breakdown spectroscopy: influence of plasma nonuniformity on measurement accuracy

J. Hermann<sup>1</sup>, E. Axente<sup>2</sup>, C. Gerhard<sup>3</sup>, C. Dutouquet<sup>4</sup>

<sup>1</sup>LP3, CNRS/Aix-Marseille Université, 163 av. Luminy, 13288 Marseille, France

<sup>2</sup>Laser-Surface-Plasma Interactions Laboratory, National Institute for Lasers, Plasma and Radiation Physics, 077125 Magurele, Romania

<sup>3</sup>HAWK-University of Applied Sciences, Laboratory for Laser and Plasma Technologies, 37085 Göttingen, Germany

<sup>4</sup>INERIS /DRC/CARA/NOVA, 60550 Verneuil-en-Halatte, France

hermann@lp3.univ-mrs.fr

Laser-induced breakdown spectroscopy (LIBS) is an emerging technique for compositional analyses of materials. Although the analytical performance was demonstrated for several types of materials, the technique remains mostly qualitative or semi-quantitative. The low measurement accuracy is due to the difficulties of calibrating the LIBS measurements. Thus, calibration-free LIBS measurement procedures have been developed. Based on modeling of the laser-produced plasma, the elemental composition is deduced from the best agreement between computed and measured plasma emission spectra. The first calibration-free LIBS measurement procedure was proposed by Ciucci et al.<sup>1</sup> It was based on four hypotheses: (i) laser ablation is stoichiometric, (ii) the plasma is in local thermodynamic equilibrium, (iii) the plasma is optically thin and, (iv) the plasma is spatially uniform. Several improvements have been proposed, most of them concern the last two hypotheses. Among them, we proposed an approach based on the calculation of the spectral radiance of a plasma in local thermodynamic equilibrium.<sup>2,3</sup> It accounts for self-absorption and may consider possible gradients of temperature and density. In addition, the method benefits from the calculation of the spectral shape of lines that is used as feedback to verify the model validity.<sup>4</sup>

In the present paper, we investigate the influence of the spatial distributions of temperature and densities on the accuracy of LIBS measurements based on modeling. In particular, we illustrate the benefit of LIBS analyses in argon. Compared to the plasma produced by laser ablation in ambient air, the plume generated in argon appears almost uniform. This simplifies the plasma model and increases the measurement accuracy.

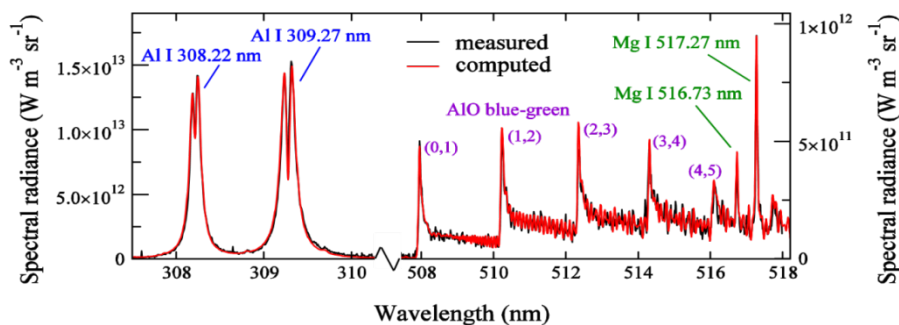


Figure 1: Plasma emission spectrum recorded during laser ablation of aluminum in air. Comparison to the spectral radiance of a nonuniform plasma in local thermodynamic equilibrium. The simulation shows that the atomic lines originate from the hot plasma core whereas the molecular emission comes from the cold periphery, where the aluminum resonance lines were re-absorbed.<sup>5</sup>

1. A. Ciucci, M. Corsi, V. Palleschi, S. Rastelli, A. Salvetti, E. Tognoni, Appl. Spectrosc., 53, 960-964 (1999);
2. C. Gerhard, J. Hermann, L. Mercadier, L. Loewenthal, E. Axente, C.R. Luculescu, T. Sarnet, M. Sentis, W. Viöl, Spectrochim. Acta Part B, 101, 32-45 (2014);
3. E. Axente, J. Hermann, G. Socol, L. Mercadier, S. Beldjilali, M. Cirisan, C. R. Luculescu, C. Ristoscu, I. N. Mihailescu, V. Craciun, J. Anal. At. Spectrom., 29, 553-564 (2014);
4. J. Hermann, C. Gerhard, E. Axente, C. Dutouquet, Spectrochim. Acta Part B, 100, 189-196 (2014);
5. J. Hermann, A. Lorusso, A. Perrone, F. Strafella, C. Dutouquet, B. Torralba, Phys. Rev. E, 92, 053103 1-15 (2015).

## Magnetite nanoparticles functionalized with $\beta$ -pinene modulate virulence, attachment and biofilm formation of opportunistic pathogens

A.M. Holban<sup>1,2</sup>, E. Andronescu<sup>2</sup>, A.M. Grumezescu<sup>2</sup>, L.M. Ditu<sup>1</sup>, C. Curutiu<sup>1</sup>, V. Lazar<sup>1</sup>, V. Grumezescu<sup>2,3</sup>, B. Vasile<sup>2</sup>, C.M. Chifiriuc<sup>1</sup>

<sup>1</sup>Faculty of Biology, Department of Microbiology and Immunology, University of Bucharest & Research Institute of the University of Bucharest,

<sup>2</sup>Department of Science and Engineering of Oxidic Materials and Nanomaterials, University Politehnica of Bucharest,

<sup>3</sup>Lasers Department, National Institute for Lasers, Plasma & Radiation Physics, Magurele, Romania

alina\_m\_h@yahoo.com

The purpose of this study was to obtain, characterize and evaluate the antimicrobial effect of an optimized iron oxide nanosystem that succeeded the efficient stabilization and delivery of the natural volatile compound  $\beta$ -pinene by using two opportunistic pathogens bacterial models: the Gram positive *Staphylococcus aureus* and the Gram negative *Pseudomonas aeruginosa*.

*P. aeruginosa* ATCC 27853 and *S. aureus* ATCC 25923 strains were obtained from American Type Culture Collection (ATCC, USA). Magnetite nanoparticles ( $\text{Fe}_3\text{O}_4@$ ) have been synthesized by coprecipitation, functionalized with the plant derived compound  $\beta$ -pinene ( $\beta\text{P}$ ) and characterized by infrared spectroscopy (IR), XRD (X ray diffraction), Thermogravimetric (TG) analysis, high resolution transmission electron microscopy (HR TEM) and selected area electron diffraction (SAED). Minimum inhibitory concentrations and attachment to the inert substrata were established by a broth microdilution method, while biofilm formation was assessed by viable counts at different periods of time. Attachment to cellular substrata was established by an adapted Cravioto method, using HeLa cells as sensitive substrata and virulence was revealed by spotting fresh cultures on specific media containing different enzyme substrata for highlighting the production of soluble virulence factors. Cytotoxicity against diploid human cells was assessed by fluorescence microscopy and the reduction of tetrazolium salt (MTT) assay.

The results revealed that the obtained magnetic nanosystem can inhibit bacterial multiplication, attachment and biofilm formation in a time and dose dependent manner. The minimum inhibitory concentration of the nanosystem was different among the Gram negative and Gram positive tested bacteria, being of about  $5\mu\text{g/mL}$  for *S. aureus* and  $10\mu\text{g/mL}$  for *P. aeruginosa* in planktonic cultures, while the minimum concentration needed to interfere with biofilm formation or to disrupt biofilm maturation was at least three folds higher for both strains. Moreover,  $\text{Fe}_3\text{O}_4@$  $\beta\text{P}$  nanoparticles altered microbial attachment to the cellular substrata, favouring a diffuse attachment pattern, while reducing the production of soluble virulence factors such as toxin pore forming enzymes. Despite the antimicrobial and antibiofilm effects,  $\text{Fe}_3\text{O}_4@$  $\beta\text{P}$  nanoparticles showed a good biocompatibility to human diploid cells, allowing the normal development and proliferation of the treated cells.

In conclusion, our data demonstrate that magnetite nanoparticles functionalized with the plant-derived compound  $\beta$ -pinene represent a successful alternative to improve the treatment of difficult to treat infections caused by opportunistic pathogens able to produce biofilms and may contribute to the development of personalized and ecologic anti-infectious therapies.

**Acknowledgments:** This work was supported by Romanian National Authority for Scientific Research (CNCS – UEFISCDI), under the projects PN-II-RU-TE-2014-4-2269.

# Laser-Driven Broadband Fibre Source with Spectral Compensation using a High-Voltage Pulse LED

M. W. Hung, W.-T. Hsiao, K.-C. Huang, Y.-H. Lin

Instrument Technology Research Center, National Applied Research Laboratories, Hsinchu 30076, Taiwan  
marklin@narlabs.org.tw

Laser-driven light source is a broadband, high brightness and collimation source that has been widely applied in optical imaging and spectroscopy applications, such as advanced materials analysis, super-continuum optics and bio-medical inspection<sup>1,2</sup>. Traditionally, the broadband white light source such as a light bulb or LED is energy-divergent, therefore the achievement of collimation must use a large lenses, concave mirror or diffractive device, even though the coupling efficiency is limited. The laser-driven light source is native collimated. It use a CW laser to heat directly the plasma in the light bulb or the phosphor of LED<sup>2,3</sup>. Due to the high collimation characteristic of the excitation laser, an ultra small light spot could be therefore generated. A second lenses would be further used to create a parallel ray that is broadband and will spread minimally as it propagates. In this study, a LED-based laser-driven broadband fibre source was developed. As shown in Fig.1, YAG phosphor layer generates a broadband light point after being focused by a blue laser with power of 5 mW and wavelength of 473 nm. A filter cube that contains filter, attenuator and beam splitter was used precisely to perform the spectrum modification. The broadband light excited from the phosphor was collected by an objective lens (Nikon, 20X, N.A=0.5) and finally coupled into a fiber (core diameter=625  $\mu\text{m}$ ). The fiber provides an ultrasmall light spot and could be easily re-collimated. However, the spectral distribution of the output light is very similar with that of the general white light LED. In order to further improve the uniformity of spectrum, a green light LED with wavelength of 505 nm was chosen to be the base of the YAG phosphor for the brightness compensation in the green regimen. Nevertheless, the contribution of the green light in this system is very small because the coupling efficiency of the LED is relatively poor. To solve this problem, an instantaneous pulse of high-voltage acted on the LED is necessary. The high-output green light of LED could effectively compensate the regional lack of the laser-driven source spectrum. In the

experiment, various light power of the blue laser, green LED and fibre source was measured by the power meter (Thorlabs, PM204), and the spectrum of the laser-driven broadband fibre emission was analysed by the spectrometer (BWTEK, BRC642). The result shows that the uniform broadband fibre source could be successfully generated, and the relationships of the coupling efficiency, filter cube condition, pulse time and LED voltage were established. This study developed a novel solution for broadband light source technology and related applications.

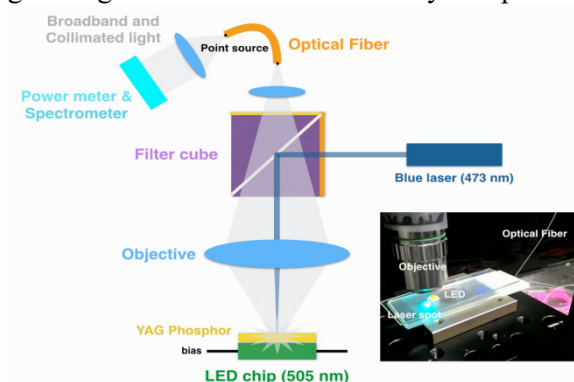


Figure 1.: Schematic diagram of LED-based laser-driven broadband fibre source.

1. D. K. Smith, J. A. Casey, Laser-driven light source, US patent, 7989786 B2;
2. M. -T. Tsai, J. -J. Hung, M. -C. Chan, Ultrahigh-Resolution Optical Coherence Tomography with LED-Phosphor-Based Broadband Light Source, Applied Physics Express, 6, 122502 (2013);
3. K.A. Denault, M. Cantore, S. Nakamura, S. P. DenBaars, R. Seshadri, Efficient and stable laser-driven white lighting, AIP ADVANCES, 3, 072107(2013).

# ***In vitro* degradability and bioactivity of hybrid coatings containing Lactoferrin and Hydroxyapatite embedded in a copolymer matrix**

M. Icriverzi<sup>1,2</sup>, L. E. Sima<sup>1</sup>, L. Rusen<sup>3</sup>, S. Brajnicov<sup>3,4</sup>, V. Ion<sup>3</sup>, A. Bonciu<sup>3,5</sup>, L.N. Dumitrescu<sup>3,4</sup>,  
M. Dinescu<sup>3</sup>, A. Cimpean<sup>2</sup>, A. Roseanu<sup>1</sup>, V. Dinca<sup>3</sup>

<sup>1</sup>Institute of Biochemistry, Romanian Academy, 296 Spl. Independentei, Bucharest, Romania

<sup>2</sup>University of Bucharest – Faculty of Biology, Department of Biochemistry and Molecular Biology, Bucharest Splaiul Independentei 90-94, Romania

<sup>3</sup>National Institute for Lasers, Plasma and Radiation Physics, Atomistilor 409, 077125, Magurele, Bucharest, Romania

<sup>4</sup>University of Craiova, Faculty of Mathematics and Natural Sciences, RO-200585, Craiova, Romania

<sup>5</sup>University of Bucharest, Faculty of Physics, RO-077125, Magurele, Romania

valentina.dinca@inflpr.ro

In most of the cases of implanted material in orthopedic clinics, local host defense mechanisms will be initiated and in a case of persistent inflammatory response will end up with the destruction of bone or encapsulation / loosening of the implant. That is why, providing an active functional biomodulating interface based on a combination of bioactive molecules, such as natural components of bone and osteogenic factors, represent a strategic key approach for implants applications. In this work, we used Matrix Assisted Pulsed Laser Evaporation (MAPLE) methods to obtain hybrid coatings of lactoferrin (Lf) and hydroxyapatite (HA) embedded in a Polycaprolactone-Polyethylene-Glycol copolymer matrix.

Surface characterization by scanning electron microscopy (SEM), Atomic Force Microscopy (AFM), and qualitative method Fourier Transform Infrared (FTIR) demonstrated successful deposition of hybrid coatings and the maintaining of the integrity of functional groups in the MAPLE-deposited coatings.

*In vitro* evaluation of biomimetic compounds degradation was tested by Spectro-ellipsometry (SE) and AFM measurements. The changes in coating thickness and roughness during immersion time revealed the degradation trend for each component of the hybrid coating, respectively the complex hybrid coating.

The potential inflammatory response of biomimetic coated biomaterial was assessed using an *in vitro* model of inflammation based on stimulation of the human leukemic monocytic THP-1 cells differentiated to macrophages with bacterial endotoxin.

A promising early cellular and immunomodulatory response was obtained on the novel biohybrid coatings which could be a strategy for future biomedical bone applications.

**Acknowledgments:** This work was supported by Romanian National Authority for Scientific Research (CNCS – UEFISCDI), under the projects PNII- PT-PCCA-2013-4-199, PN-II-RU-TE-2014-4-2434, PN09-39 and Romanian Academy project 1/2015-2016.

## **Principal Component Analysis of Raman spectra for Nanoparticle Auto-Classification**

Alina G. Ilie<sup>1,2</sup>, Monica Scarisoreanu<sup>1</sup>, Ion Morjan<sup>1</sup>, Elena Dutu<sup>1</sup>

<sup>1</sup>National Institute for Lasers, Plasma and Radiation Physics, Magurele, Romania,

<sup>2</sup>University of Bucharest, Faculty of Physics, Bucharest, Romania

ilie.georgiana@inflpr.ro

The Raman spectrum of Sn doped TiO<sub>2</sub> nanoparticles was processed with a self-written software that applies Principal Component Analysis (PCA) on the measured spectrum to verify the possibility of objective auto-classification of nanoparticles from their vibrational modes. The photo-excited process of Raman scattering is very sensible to the materials properties, especially in the case of nanomaterials, where more properties become relevant for the vibrational behavior. We used PCA, a statistical procedure that performs eigenvalue decomposition of descriptive data covariance, to automatically analyze the sample's measured Raman spectrum, and obtained a good correlation between nanoparticle dimensions, tin and carbon concentration, and their vibrational modes. This type of application can allow an approximation of the crystallite size, or tin concentration, only by measuring the Raman spectrum of the sample. The study of the loadings of the principal components gives information of the way the vibrational modes are affected by the nanoparticle features and which spectral area is relevant for the classification.

# Biocompatibility studies on $(\text{Ba}_{1-x}\text{Ca}_x)(\text{Zr}_y\text{Ti}_{1-y})\text{O}_3$ thin films obtained by laser deposition methods

V. Ion<sup>1</sup>, N.D. Scarisoreanu<sup>1</sup>, F. Craciun<sup>2</sup>, R. Birjega<sup>1</sup>, A. Bercea<sup>1</sup>, A. Bonciu<sup>1</sup>, A. Moldovan<sup>1</sup>, V. Dinca<sup>1</sup>, M. Dinescu<sup>1</sup>, L.E. Sima<sup>3</sup>, M. Icriverzi<sup>3</sup>, A. Roseanu<sup>3</sup>

<sup>1</sup>National Institute for Laser, Plasma and Radiation Physics, 077125 Magurele, Romania

<sup>2</sup>CNR-ISC, Istituto dei Sistemi Complessi, Area della Ricerca di Roma-Tor Vergata, Via del Fosso del Cavaliere 100, I-00133 Roma, Italy

<sup>3</sup>Institute of Biochemistry of the Romanian Academy, 296 Splaiul Independentei, 060031, Bucharest, Romania

valentin.ion@inflpr.ro

Bulk lead-free  $(\text{Ba}_{1-x}\text{Ca}_x)(\text{Zr}_y\text{Ti}_{1-y})\text{O}_3$  (BCZT) materials have attracted a lot of attention in the last period for replacing piezoelectric and ferroelectric materials containing toxic elements in different applications.

Laser based approaches to obtain BCZT as biomaterials which supports cellular adhesion, proliferation and differentiation can have important impact to their exploitation in a variety of biomedical applications. In this paper we investigate the biocompatibility properties of BCTZ materials in form of thin films.

The BCTZ thin films have been obtained using Matrix Assisted Pulsed Laser Evaporation method: its (the method) allows the use of different types of substrates from flexible kapton to biocompatible metallic alloys, due to low deposition temperature. Starting from a frozen target of nanopowders of BCTZ 45 composition, thin films of BCTZ 45 have been obtained on Pt-coated kapton substrates. The cell proliferation studies have been made using epithelial embryonic kidney HEK 293 cells and malignant melanoma A 375 cells which were seeded onto the deposited layers. The results suggest that BCTZ 45 material led to an increased proliferation level compared to borosilicate glass coverslip irrespective of the cell line tested. The immunofluorescence study shows that the both cell lines used in our experiment adhere on BCTZ45 material and display normal morphology on glass coverslip and BCTZ45 material respectively.

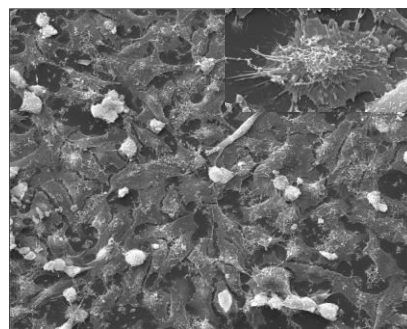
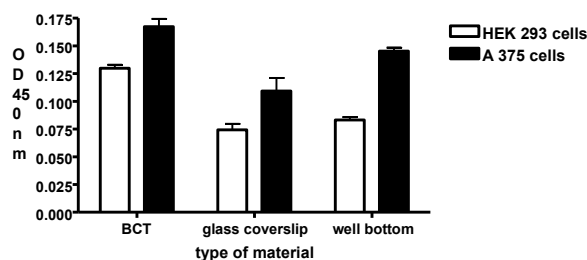


Figure 1: Diagram and SEM results of the HEK 293 and A 375 cells attached on the BCTZ 45 material and cover glass surface after 48 hours post seeding at a magnification of 1000x (with insert pictures of 5000x). Scale bar 50 $\mu\text{m}$

## Ultrafast time-resolved pump-probe investigation of LIPSS formation by multiple femtosecond laser pulses

L. Ionel<sup>1</sup>, I. Dumitrache<sup>1</sup>, I. Anghel<sup>1</sup>, S. Sandel<sup>1</sup>, M. Zamfirescu<sup>2</sup>

<sup>1</sup>National Institute for Lasers, Plasma and Radiation Physics, Atomistilor 409, RO-077125, Măgurele, Romania

<sup>2</sup>Center for Advanced Laser Technologies - CETAL, National Institute for Lasers, Plasma and Radiation Physics, Atomistilor 409, RO-077125, Măgurele, Romania  
marian.zamfirescu@inflpr.ro

In this work we report the determination of the build-up time of periodic structures induced by laser effect (LIPSS) on solid materials using a pump and probe experimental configuration. The periodic nanostructures produced by linearly polarized 775-nm, 200-fs pump laser pulse behave as a diffraction grating at the arrival time of the probe pulse. Thus, the formation time of the periodic structures is given by the diffraction signal from the sample which depends on the delay between the two pulses. This dynamic process of LIPSS formation is investigated in multiple pulse regime. In the proposed pump-probe method the formation of the LIPSS is temporally characterized at hundreds of picoseconds time scale after each pump pulse. The time domain available for LIPSS build-up time measurements is 0.1-2000 ps corresponding to the delay line which tunes the delay between the two pulses. These delays are at the order of the melting time and re-solidification time of the investigated materials (stainless steel, titanium and nickel). The LIPSS are observed to form after a delay between pump and probe pulse of 250 ps for stainless steel, 290 ps for titanium and 320 ps for nickel. This combination of

fs-laser and the pump probe technique provides an accurate and fast tool for high precision measurements of ultrafast processes induced in material by ultrashort laser pulses.

1. R. D. Murphy, B. Torralva, D. P. Adams, S. M. Yalisove, "Pump-probe imaging of laser-induced periodic surface structures after ultrafast irradiation of Si," *Appl. Phys. Lett.* 103, 141104 (2013);
2. X. Jia, T. Q. Jia, N. N. Peng, D. H. Feng, S. A. Zhang, Z. R. Sun, "Dynamics of femtosecond laser-induced periodic surface structures on silicon by high spatial and temporal resolution imaging," *J. Appl. Phys.* 115, 143102 (2014);
3. K. R. P. Kafka, D. R. Austin, H. Li, A. Y. Yi, J. Cheng, E. A. Chowdhury, "Time-resolved measurement of single pulse femtosecond laser-induced periodic surface structure formation induced by a pre-fabricated surface groove," *Optics Express*, 23(15), 19432-19441 (2015);
4. R. Wagner, J. Gottmann, "Sub-wavelength ripple formation on various materials induced by tightly focused femtosecond laser radiation", *J. Phys.: Conf. Ser.* 59, 333-337, (2007);
5. D. Dufft, A. Rosenfeld, S. K. Das, R. Grunwald, J. Bonse, "Femtosecond laser-induced periodic surface structures revisited: A comparative study on ZnO", *J. Appl. Phys.* 105 (3), 034908/1-9 (2009).

## Surface modification on medical grade PDMS by fs-laser irradiation

E. Iordanova<sup>1</sup>, G. Yankov<sup>1</sup>, N. E. Stankova<sup>2</sup>, Ru.G. Nikov<sup>2</sup>, R.G. Nikov<sup>2</sup>, P.A. Atanasov<sup>2</sup>,  
K.N. Kolev<sup>3</sup>, Dr. M. Tatchev<sup>3</sup>, M. Grozeva<sup>1</sup>

<sup>1</sup>*Institute of Solid State Physics, Bulgarian Academy of Sciences, 72 Tsarigradsko Chaussee Blvd., 1784 Sofia, Bulgaria*

<sup>2</sup>*Institute of Electronics, Bulgarian Academy of Sciences, 72 Tsarigradsko chaussee Blvd., Sofia 1784, Bulgaria*

<sup>3</sup>*Rostislav Kaischew Institute of Physical Chemistry, Bulgarian Academy of Sciences, Acad. G. Bonchev Str., block 11, Sofia 1113  
eiordanova@issp.bas.bg*

The present work concerns investigation on medical grade polydimethyl siloxane (PDMS) elastomer irradiated by fs-laser. The motivation of the research is based on the wide use of the PDMS material in medicine and medical devices. The application in the medical field is due to some of the main properties of the PDMS. Thus its high biocompatibility and biostability, mechanical flexibility and chemical stability, optical transparency from UV to near IR spectral region.

The experimental setup includes fs-laser system, optical parametric amplifier, optical elements and XYZ translating stage. The regenerative Ti:Sapphire amplified laser system emits at 800 nm central wavelength with a pulse duration of 35fs and 1 kHz repetition rate. The working parameters as laser fluence and number of pulses are varied. Specifically, the laser fluence applied is between 0.16 and 0.5 J.cm<sup>-2</sup> and the number of consecutive pulses is from 10<sup>2</sup> to 10<sup>4</sup>. Additionally, the wavelengths used in the experiments are 266, 355 and 532 nm.

Tranches on the PDMS-elastomer MED 4860 surface are produced by the fs-laser processing and the material inside them is modified. Optical properties and morphology of the tranches are investigated in terms of the laser beam parameters. Despite the low optical absorption of the native PDMS for UV, VIS and NIR wavelengths, successful laser treatment is accomplished due to the chemical transformations occurring below the polymer surface. The optical absorption and thus saturation caused by the incubation process is observed with the increase of the number of pulses. Such process increases significantly the efficiency of the laser ablation. The ablation depth measured is in the range of 4 ÷ 10 μm for UV light and in the range of 10 ÷ 40 μm for VIS laser treatment, respectively. Furthermore, a successful electroless plating of the tranches by Ni and Pt is achieved. A DC resistance between 0.2 and 5.0 Ω/mm is measured.



# Effect of ZrO<sub>2</sub> coating on the electrochemical behavior and surface properties of 316L stainless steel

M. Iordoc, P. Barbu, A. Teisanu, M.V. Lungu, I. Iordache

National Institute for Research and Development in Electrical Engineering ICPE-CA,  
Department of Efficiency in Energy Conversion and Consumption, 313 Splaiul Unirii Street, 030138, District 3, Bucharest, Romania  
mihai.iordoc@icpe-ca.ro

The coating of metallic surfaces is achieved due to the need of improving the surface properties, such as corrosion resistance, mechanical and tribological properties and, last but not least, the biocompatibility. Nor can we overlook the economic aspect, which involves maintaining cheap and easily processed materials technologies in manufacturing medical devices, improving their surface properties. An example would be to cover the stainless steel with ceramics, while maintaining the properties of stainless steel in the volume and, at the same time, replacing them on the surface with the superior ones of ceramics materials. The aim of this work is to study the influence of ZrO<sub>2</sub> coating on the electrochemical and mechanical behavior of 316L stainless steel. Due to its higher biocompatibility, corrosion resistance and excellent mechanical properties, ZrO<sub>2</sub> is the favorable non-allergenic protective coating in attempt to create higher biocompatible medical devices. On 316L stainless steel samples were made several attempts to deposit films of Zr, ranging deposition time and voltage of the magnetron. It has been found that an optimum Zr coating film on 316L stainless steel substrate occurs after 15 minutes of exposure, and a voltage of 600V. Zr targets were produced from metal powder of high purity by pressing in a circular mold at 400 kgf/cm<sup>2</sup> for 5 minutes. The heat treatment of the Zr coating proceeds at room temperature with an increase in the temperature of 80<sup>0</sup>C/h up to 500<sup>0</sup>C, where the temperature is kept constant for 3 h. Is followed by a gradual cooling for 15 h with a decrease in the temperature of 20<sup>0</sup>C/h. During the heat treatment, oxygen from the atmosphere diffuses into the sample to a depth of tens of microns and reacts with Zr, turning it into a very adherent dense layer of black ZrO<sub>2</sub>, with excellent mechanical properties and very high corrosion resistance. This coating protects the 316L stainless steel from further oxidation and increases the hardness and the fatigue resistance. As electrochemical techniques we used potentiodynamic polarization and electrochemical impedance spectroscopy (EIS), and as complementary technique we used contact angle, tribological and mechanical measurements, to study the influence of ZrO<sub>2</sub> coating on 316L stainless steel. Electrochemical measurements were carried out in Ringer solution at 37<sup>0</sup>C. The results indicated that the ZrO<sub>2</sub> coating improves the corrosion resistance and mechanical characteristics of 316L stainless steel.

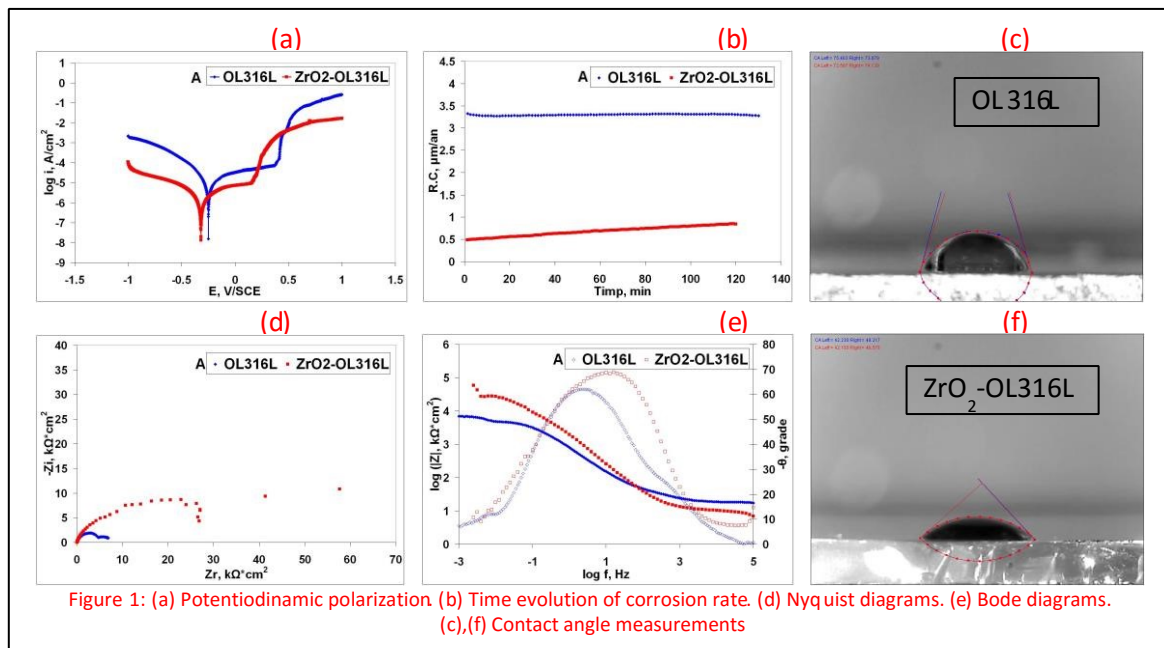


Figure 1: (a) Potentiodynamic polarization. (b) Time evolution of corrosion rate. (d) Nyquist diagrams. (e) Bode diagrams. (c),(f) Contact angle measurements

**Acknowledgements:** This research is supported by Ministry of National Education and Scientific Research (MENCS) - Executive Unit for Financing Higher Education, Research, Development and Innovation (UEFISCDI), Romania, and cosupported by SC MGM STAR CONSTRUCT SRL, Romania, through the program Partnerships in priority areas, project number PN-II-PT-PCCA-2013-4-1292, contract number 215/2014.

# Time-resolved electrical investigations of transient plasmas generated by femtosecond laser ablation of various metallic targets

S.A. Irimiciuc<sup>1,2</sup>, S. Gurlui<sup>2</sup>, P. Nica<sup>3</sup>, M. Agop<sup>3</sup>, C. Focsa<sup>1</sup>

<sup>1</sup>Laboratoire de Physique des Lasers, Atomes et Molécules, Université Lille 1, 59655 Villeneuve d'Ascq, France

<sup>2</sup>Faculty of Physics, Alexandru Ioan Cuza University, 700506 Iasi, Romania

<sup>3</sup>Department of Physics, Gh. Asachi Technical University, 700050 Iasi, Romania  
stefan.irimiciuc@yahoo.com

Time-resolved electrical diagnosis of laser induced plasmas generated by femtosecond laser ablations on several metals (W, Te, In, Mn, Ni, Cu, Al) was performed in order to comprehend the effect of the target physical properties on the dynamics of the plasma plumes. The experiments were performed in same conditions of background pressure ( $p = 10^{-5}$  Torr), target biases and probe-target axial distances. By collecting probe plasma current for different biases and reconstructing the I-V characteristics at different evolution times we were able to obtain the temporal evolution of various plasma parameters. Also the probe current is discussed in terms of a shifted Maxwell-Boltzmann distribution function which allowed us to determine parameters such as the drift velocity and the ion average temperature.

The nature of the targets and their physical properties (electrical and thermal conductivities, melting and boiling points) proved to have an important influence over the plumes dynamics. The changes in expansion velocity, electron temperature and plasma potential were correlated to target characteristics through material removal mechanisms involved in femtosecond laser ablation

## A study on micro hydroforming using shock wave of 355nm UV-pulsed laser

G.J. Je<sup>1</sup>, H.S. Kim<sup>1</sup>, B.S. Shin<sup>2</sup>

<sup>1</sup> Department of Cogno-mechatronics Engineering, Pusan National University, Pusan 609-735, Korea

<sup>2</sup>CRC of 3D Laser-aided Innovative Manufacturing Technology, Pusan National University, Pusan 46239, Korea  
jmandu333@naver.com

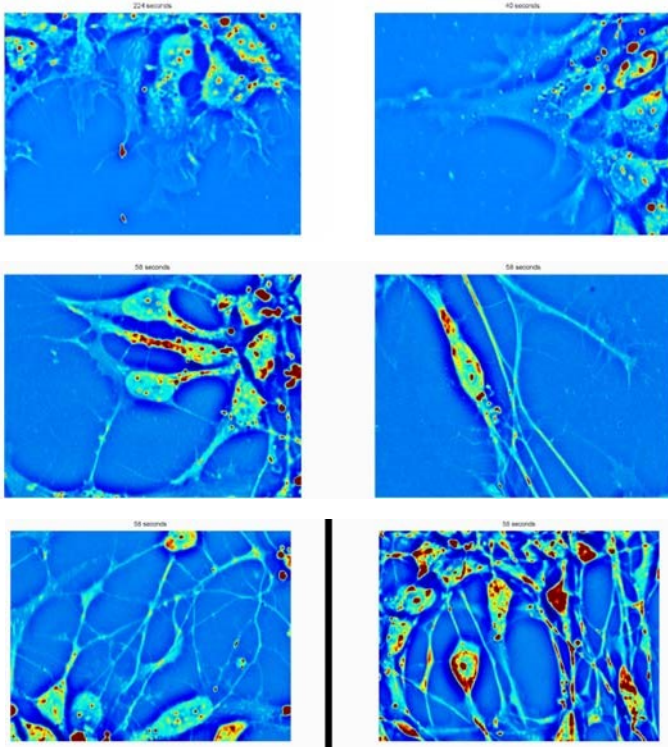
In this paper, we proposed a new manufacturing method of micro hydroforming using 355nm UV-pulsed laser and conduct experiment. Microforming is a well suited technology to manufacture very small metallic parts, in particular for mass production, as they are required in many industrial products resulting from microtechnology. When the material exposed to laser, photochemical and photothermal, photomechanical phenomena are multiply occurred. Some of light reflected, the other is transmitted and the rest is absorbed in material and these seriously affect nano size material. Because of increase of surface area, photothermal effect have expand and hard to control the manufacturing. To resolve this problem, laser exposed to water and induced pressure wave and use this. Go through the water photothermal effect reduced and the pressure wave is created. And then we use this wave to manufacturing materials and to confirm this process using computer aided engineering to demonstrate it. Compared with conventional direct manufacturing method, this new method provided more stable and do not change the properties of material.

# Quantitative phase imaging of live cells

M. Kandell, T. Nguyen, H. Majeed, M. Mir, G. Popescu

Quantitative Light Imaging Laboratory, Department of Electrical and Computer Engineering  
Beckman Institute for Advanced Science & Technology, University of Illinois at Urbana-Champaign, Urbana, IL 61801  
gpopescu@illinois.edu | <http://light.ece.illinois.edu/>

Most living cells do not absorb or scatter light significantly, i.e. they are essentially transparent, or phase objects. Phase contrast microscopy proposed by Zernike in the 1930's represents a major advance in intrinsic contrast imaging, as it reveals inner details of transparent structures without staining or tagging. While phase contrast is sensitive to minute optical path-length changes in the cell, down to the nanoscale, the information retrieved is only *qualitative*. *Quantifying* cell-induced shifts in the optical path-lengths permits nanometer scale measurements of structures and motions in a non-contact, non-invasive manner. Thus, quantitative phase imaging (QPI) has recently become an active field of study and various experimental approaches have been proposed.



Recently, we have developed Spatial Light Interference microscopy (SLIM) as a highly sensitive QPI method. Due to its nanometer pathlength sensitivity, SLIM enables interesting structure and dynamics studies over broad spatial (nanometers-centimeters) and temporal (milliseconds-weeks) scales. I will review our recent results on applying SLIM to basic cell studies, such as intracellular transport, cell growth, and single cell tomography. Recently, we have demonstrated that SLIM is a valuable tool for cancer diagnosis and prognosis in unlabeled biopsies. This capability is particularly valuable in prostate pathology.

Recently, we have demonstrated that SLIM is a valuable tool for cancer diagnosis and prognosis in unlabeled biopsies. This capability is particularly valuable in prostate pathology.

Figure 1: Quantitative phase imaging of the neuronal differentiation process over 13 days: from stem cells (top left) to fully functional neurons (bottom right)

## Selective carbonized patterning on the surface of polyimide film using a 355nm UV laser

H.S. Kim<sup>1</sup>, G.J. Je<sup>1</sup>, B.S. Shin<sup>1,2</sup>

<sup>1</sup>Department of Cogno-Mechatronics Engineering, Pusan National University, Busan 46239, Korea

<sup>2</sup>CRC/3D\_LIMIT, Pusan National University, Busan 46239, Korea  
heysukim@pusan.ac.kr

A general polymer film is flexible but has low electrical conductivity. This paper proposed the method of conductivity improvement of polyimide (PI) film.

A polyimide film was successfully formed by pre-curing at 130°C in an oven after spin coating N-methyl-2pyrrolidone (NMP) on the glass. And then when selective part of PI film was irradiated by using a 355nm UV laser, that part was carbonized. Finally, we can make carbonized patterning on the surface of polyimide film.

The carbonized polyimide film made this way has advantages compare to other polymer film which is not carbonized. The carbonized part on the polyimide film can be made into a various shape and size, the position of carbonized part can be arranged as we want, the polyimide film has characteristics that flexible and high electric conductivity for general polymer film at the same time.

# Molecular Dynamics Simulations of Laser Ablation in Silicon and Germanium: the Influence of Electron-Temperature dependent Interactions

A. Kiselev, J. Roth

*Institute for Functional Materials and Quantum Technologies, University of Stuttgart, Germany  
alexander.kiselev@fmq.uni-stuttgart.de*

The well-known continuum two-temperature model for solids with highly excited electrons is extended from metals to semiconductors. It is combined with classical molecular dynamics simulations to study laser ablation in semiconductors where the charge carriers are created by the absorption of the laser light. The model is further enhanced by extending the static modified Tersoff<sup>1</sup> potential to a dynamical interaction which depends on the electron temperature of the material.

At the opposite side of the irradiated surface<sup>2</sup> pressure-transmitting boundary conditions are applied to prevent reflections of the laser-induced pressure waves. Results are presented for single and multiple pulses in Silicon and Germanium films at different laser fluences.

1. T. Kumagai, S. Izumi, S. Hara and S. Sakai, *Comput. Mater. Sci.* **39**, 457-464 (2007);

2. L.V. Zhigilei, B.J. Garrison, *Mater. Res. Soc. Symp. Proc.* **538**, 491-496 (1999).

## Biocompatible Diamond-Like Carbon layers modified by ion bombardment during grow

T. Kocourek<sup>1,2</sup>, M. Jelínek<sup>1,2</sup>, P. Písařík<sup>1,2</sup>, J. Remsa<sup>1,2</sup>, M. Janovská<sup>3</sup>, M. Landa<sup>3</sup>, J. Zemek<sup>1</sup>, V. Havránek<sup>4</sup>

<sup>1</sup>*Institute of Physics of the Czech Academy of Sciences, Na Slovance 2, 182 21 Praha 8, Czech Republic*

<sup>2</sup>*Czech Technical University, Faculty of Biomedical Engineering, nám. Sítná 3105, 27201 Kladno, Czech Republic*

<sup>3</sup>*Institute of Thermomechanics of the Czech Academy of Sciences, Dolejškova 1402/5, 182 00 Praha 8, Czech Republic*

<sup>4</sup>*Nuclear Physics Institute of the Czech Academy of Sciences, Řež 130, 250 68 Řež, Czech Republic  
kocourek@fzu.cz*

The biocompatible Diamond-Like Carbon (DLC) films were prepared by Pulsed Laser Deposition technique using the laser energy density on the graphite target of  $10 \text{ Jcm}^{-2}$ . The surface of grown film was modified during the deposition by bombardment<sup>1</sup> with Argon, Xenon, Nitrogen or Oxygen ions. Energy of ions (up to 150 eV) was changed by gun voltage and by ionic current. The films with high and low diamond/graphite content were prepared. Physical and mechanical properties of biocompatible DLC thin layers prepared by hybrid laser technology were studied. The content of  $sp^2$  and  $sp^3$  bonds was measured using X-ray Photoelectron Spectroscopy. For different energy ions of Argon and Oxygen the maximum of  $sp^3$  bonds content was found (83.63% of  $sp^3$  bonds for Argon ions). All films were smooth, which confirmed by profilometric and AFM measurements. Maximum roughness Ra and RMS was not higher than 1 nm. The Young's and Shear Modulus were studied by Resonant Ultrasound Spectroscopy<sup>2,3</sup>. Young Modulus achieved the value 601 GPa and Shear Modulus achieved the value 253 GPa at energy of 30 eV of Ar ions. The influence of ion bombardment and DLC film properties are discussed.

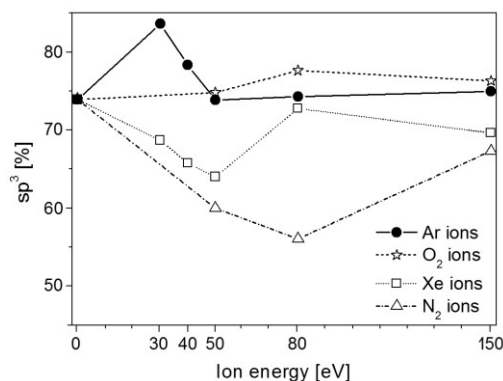


Figure 1: The graph of values of  $sp^3$  bonds of DLC films depending on the energy of Ar, O<sub>2</sub>, Xe, and N<sub>2</sub> ions.

1. M. Jelínek, P. Písařík, T. Kocourek, J. Zemek, J. Lukeš, Influence of ion bombardment on growth and properties of PLD created DLC films. *Appl. Phys. A* **110**, 943-947 (2013);
2. M. Růžek, P. Sedlák, H. Seiner, A. Kruisová, M. Landa, Linearized forward and inverse problems of the resonant ultrasound spectroscopy for the evaluation of thin surface layers, *Acoust. Soc. Am.* **128**, 3426-3437 (2010);
3. M. Janovská, P. Sedlák, H. Seiner, M. Landa, P. Marton, P. Ondrejko, J. Hlinka, Anisotropic elasticity of DyScO<sub>3</sub> substrates, *J. Phys. Condens. Matter* **24**, 385404 (2012).

# Inducing subwavelength periodic nanostructures on multilayer NiPd thin film by low-fluence femtosecond laser beam

A. G. Kovačević<sup>1</sup>, S. Petrović<sup>2</sup>, V. Lazović<sup>1</sup>, D. Peruško<sup>2</sup>, D. Pantelić<sup>1</sup>, B. M. Jelenković<sup>1</sup>

<sup>1</sup>Institute of Physics, University of Belgrade, Pregrevica 118, 11080 Belgrade, Serbia

<sup>2</sup>Institute of Nuclear Sciences "Vinča", University of Belgrade, PO Box 522, 11000 Belgrade, Serbia

Aleksander.Kovacevic@ipb.ac.rs

The applications of thin films play an important role in many fields, like semiconductor technology, optics, chemistry, mechanics, magnetism, electricity. Various types of coatings for protection, diffusion barriers, filtering, reflection/antireflection, sensing, waveguiding, decorative and other purposes are just some to mention. Structuring of thin films can enhance their characteristics. The interaction of femtosecond laser beam with thin films can generate surface subwavelength periodic nanostructures (laser-induced periodic surface structures, LIPSS), which gain more interest.<sup>1-2</sup> Thin films and alloys based on Ni and Pd possess specific physico-chemical as well as mechanical characteristics, like high corrosion resistance, durability and high tensile strength. Due to its mechanical characteristics and the catalytic activity, the applications range from catalyst and hydrogen storage material to holography. During femtosecond interaction with surfaces, the processes of liquid and solid-state dewetting could be responsible for the generation and regrouping of nanoparticles and nanoparticle clusters. The occurrence of surface plasmon polariton most probably induces the LIPSS arrangement. Using low-fluence beam, below ablation threshold, enables the generation of higher quality LIPSS. We have used low-fluence scanning femtosecond beam ( $\lambda=880$  nm) to generate periodic structures on multilayer Ni/Pd thin films on Si. The presence of the sublayer, depending on its optical characteristics, strongly influences both the shape and the quality of the LIPSS.

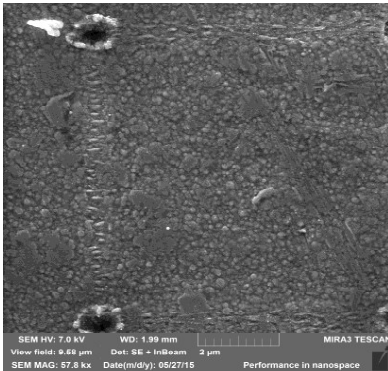


Figure 1: The SEM micrograph of LIPSS on multi-layer Ni/Pd thin films upon irradiation by scanning low-fluence fs beam.

**Acknowledgements.** This work has been supported by the Ministry of Science of the Republic of Serbia with projects and OI171005 and III45016.

1. A. Kovačević, S. Petrović et al., Surface nanopatterning of Al/Ti multilayer thin films and Al single layer by a low-fluence UV femtosecond laser beam, *Appl. Surf. Sci.* **326**, 91–98 (2015);
2. A. Beltaos, A. Kovačević et al., Femtosecond laser induced periodic surface structures on multi-layer graphene, *J. Appl. Phys.* **116** 204306 (2014).

## Synthesis of Ti-based nano-particles for photocatalytic reaction by laser ablation in water

S. Kurumi<sup>1</sup>, S. Kigawa<sup>1</sup>, K. -i. Matsuda,<sup>1</sup> K. Suzuki<sup>1</sup>

<sup>1</sup>Department of Electrical Engineering, College of Science and Technology, Nihon University, 1-8-14, Kanda-Surugadai, Chiyoda-ku, Tokyo 101-8308, Japan  
kurumi.satoshi@nihon-u.ac.jp

Titanium (Ti) based photocatalytic fine particles were synthesized by utilizing a milli-second (MS) pulsed laser ablation (PLA) method (wavelength: 1064 nm, pulse width: 0.4 ms, power: 0.1 J/pulse) in a liquid water<sup>1,2</sup>. Images taken by a high-speed camera revealed that bubbles and Ti particles were generated from a bar-shaped Ti target by a focused laser beam irradiation. Generated bubbles and particles were rapidly heated to high temperatures during one-pulse laser beam irradiation. This phenomenon implied that Ti particles were oxidized with oxygens in the bubbles due to thermal oxidation accelerated by MS laser beam irradiation. Just after the ablation, a drop of water containing fine particles was casted onto a metal grid plate for transmission electron microscope observation. As shown in Fig. 1 we have observed the existence of many nano-particles (diameter: below  $\sim 50$  nm). In order to evaluate the efficiency of the photocatalytic reaction, we have prepared a methylene blue (MB) solution containing produced nano-particles because photocatalytic reactions of TiO<sub>2</sub> based materials show chemical transfer from MB solution to leuco MB solution<sup>3</sup>. Photocatalytic reactions of produced particles in MB solution were induced by ultraviolet (UV) fluorescent light irradiation (peak wavelength: 360 nm, power: 10 mW). After UV fluorescent light irradiation for 3 hours, we have measured transmittance spectra of solutions (Fig. 2). Transmittance values around 650 nm due to a MB-absorption were increased about 20 % to 70 % by UV light irradiation. This means that MB was transferred to leuco MB by photocatalytic reaction of produced particles.

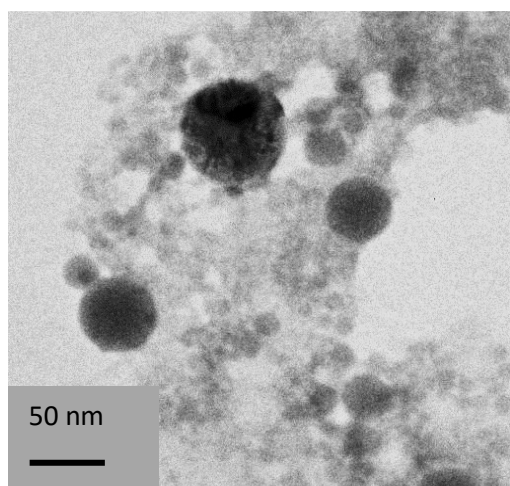


Figure 1: Ti nano particles produced by a pulsed laser ablation method in a liquid water

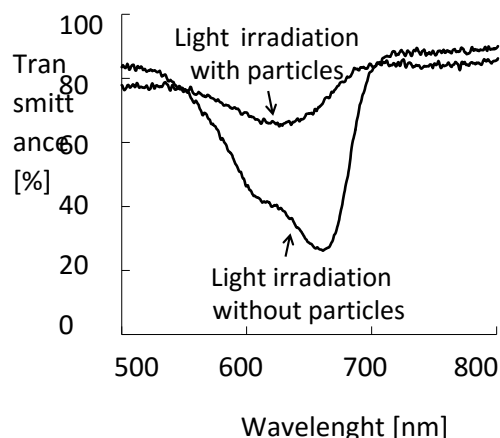


Figure 2: Transmittance spectra of MB solutions containing produced particles to evaluate a photocatalytic reaction

1. A. M. Morales et al., *Science*, **279**, 208 (1998) ;
2. R. Ishihara et al., *IEEEJ Trans. EIS*, **135**, 1060 (2015);
3. K. Tennakone et al., *Sol. Energy. Mater. Sol. Cells*, **29**, 109 (1993).

## Zinc oxide - a material for the future

L.N. Leonat<sup>1</sup>, A. Vlad<sup>2</sup>, A. Bratulescu<sup>1</sup>, M. Lungu<sup>1</sup>

<sup>1</sup>The National Institute for Electrical Engineering, ICPE-CA, [www.icpe-ca.ro](http://www.icpe-ca.ro)

<sup>2</sup>The National Institute for Laser, Plasma and Radiation Physics, [www.inflpr.ro](http://www.inflpr.ro)  
[lucia.leonat@icpe-ca.ro](mailto:lucia.leonat@icpe-ca.ro)

Zinc oxide is a very complex and versatile material with piezoelectric and semiconducting properties. Because it is environmentally friendly, low-cost and shows high photocatalytic efficiency, it is nowadays one of the most studied material. Having a wide range of morphologies, from nanoparticles with different shapes to thin films, enabling broad functionality, in optoelectronic applications such as transparent conductive electrodes for photovoltaics, short wavelength emission media for UV lasers and diodes, active semiconductor layer for thin film field effect transistors, hydrophobic substrates for surface enhanced Raman spectroscopy (SERS) and biomedical applications due to its antibacterial properties. In this paper we summarize some of the most important applications of ZnO, properties and fabrication methods, focusing on silver doped ZnO thin films.

**Acknowledgements.** This research is supported by Ministry of National Education and Scientific Research (MENCS) - Executive Unit for Financing Higher Education, Research, Development and Innovation (UEFISCDI), Romania, and cosupported by SC MGM STAR CONSTRUCT SRL, Romania, through the program Partnerships in priority areas, project number PN-II-PT-PCCA-2013-4-1292, contract number 215/2014.

# Laser-induced Coloring of Titanium Alloy Using Nanosecond Pulses Scanning Technology

Y. C. Lin, C.-C. Yang, Y. H. Lin, K. C. Huang, W. T. Hsiao

Instrument Technology Research Center, National Applied Research Laboratories, Hsinchu 30076, Taiwan  
wentse@narlabs.org.tw

Titanium alloys has been widely applied in various fields, including the automotive, medical, electrical, electronics, and aerospace industries due to its variety of useful physical properties. The titanium oxide films could present a range of colors for art, painting, jewelry, advertising, and security identification<sup>1,2</sup>. Some techniques can be used to obtain the different colors, includes deposition, oxidation<sup>3</sup>, and marking<sup>4</sup>. Nowadays, the colorful changes on the metal surface are made by printing, coating, or oxidation. This paper presents the laser-induced coloring on titanium alloy (Grade 5) using nanosecond pulses ultraviolet scanning technology as shown in Fig. 1 (a) and Fig. (b). It was determined the different laser process parameters, such as laser fluence, pulse repetition frequency, and the scanning speed that affect the repeatability of the colors created analysis. The experiment tests were carried out on plates made of the most commonly used type of titanium alloy (Grade 5) with chemical composition: Ti = 89.2 %, Fe = 0.4 %, C = 0.08 %, N = 0.04 %, H = 0.003 %, O = 0.2 %, Al = 6%, V = 3.7%) with dimensions of 10 mm<sup>2</sup> and thickness of 1 mm for each laser-induced coloring specimen. Before the laser-induced coloring experiment, the plates were washed with alcohol in an ultrasonic cleaner, then, the samples were marked in atmospheric air. To discuss the effect of the color change, the characteristics of the laser-induced surface are systemically examined using a three-dimensional confocal laser scanning microscope (KEYENCE, VK-9700), field-emission scanning electron microscope (Hitachi, H-4300), energy-dispersive spectroscopy are used to measure the surface micrograph, roughness of the patterns, and chemical composition, respectively. In addition, to characterize the color of the samples, reflectance spectra in the range 300-800 nm were measured with a spectrophotometer (OtO, SE1220). From the spectra evaluation, the standard CIE 1931 chromaticity coordinates of the different colors were calculated as shown in Fig. 1 (c). The experimental results using different laser scan speed and spacing shown in Fig. 1 (d). The chromacity coefficient for each color change of the laser-induced surface that depended on the temperature, laser fluence, scan speeds, and machining time.

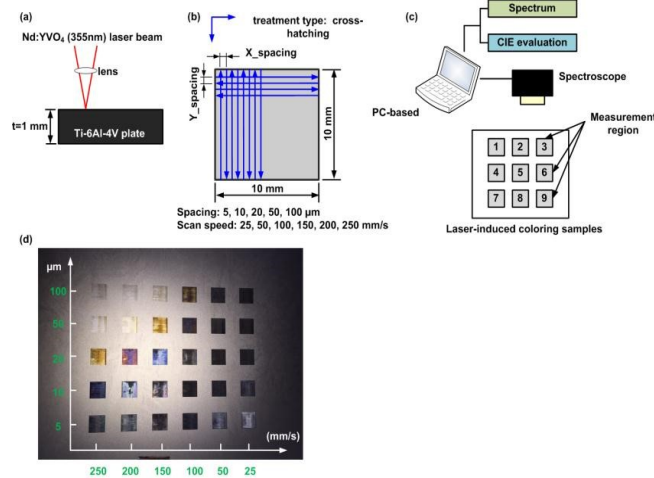


Figure 1: (a) Experiment set-up. (b) laser-induced coloring parameters, (c) reflectance spectra and CIE 1931 chromaticity coordinates evaluation. (d) laser-induced coloring results for different laser conditions.

1. M.V. Diamanti, B.D. Curto, M.P. Pedferri, Interference colors of thin oxide layers on titanium. *Color Research & Application*, **33**, 221228 (2008);
2. S. ÓHana, A.J. Pinkerton, K. Shoba, A.W. Gale, L. Li, Laser surface colouring of titanium for contemporary jewelry. *Surface Engineering*, **24**, 147-153 (2008);
3. V. Veiko, G. Odintsova, E. Gorbunova, E. Ageev, A. Shimko, Y. Karlagina, Y. Andreeva, Development of complete color palette based on spectrophotometric measurements of steel oxidation results for enhancement of color laser marking technology, *Materials and Design* **89**, 684-688 (2016);
4. A.J. Antończak, D. Koczoł, M. Nowak, P. Kozioł, K.M. Abramski, Laser-induced colour marking—Sensitivity scaling for a stainless steel, *Applied Surface Science*, **264**, 229-236 (2013).

# Diffusion in thermoelectric multilayers observed by SIMS

J. Lorincik<sup>1</sup>, D. Veselá<sup>1</sup>, J. Remsa<sup>2</sup>, T. Kocourek<sup>2</sup>, M. Jelínek<sup>2</sup>

<sup>1</sup>Research Centre Rez, Husinec-Rez, Czech Republic

<sup>2</sup>Institute of Physics of the Czech Academy of Sciences v.v.i.  
jremsa@gmail.com

Improving the electricity generation is never ending goal of our civilization. If we take into account the requirements that emerged in last decades like, mobility, flexibility and low carbon footprint, then thermoelectric devices may become a solution not only for portable devices, but also for industrial scale applications. Skutterudites are a class of materials based on cage-like structure (e.g.  $\text{Bi}_2\text{Te}_3$ ,  $\text{CoSb}_3$ ) filled by an additional element. This element causes phonon scattering and the material achieves low lattice thermal conductivity while still maintaining good electric conductivity.

In this paper we focus on characterisation of multilayers composed of  $\text{FeSb}_2\text{Te}$  and  $\text{Ce}_{0.1}\text{Fe}_{0.7}\text{Co}_{3.3}\text{Sb}_{12}$  materials by the Secondary Ion Mass Spectrometry (SIMS). The multilayers were prepared by pulsed laser deposition from two different targets in modified off-axis configuration with following conditions: 15 Pa argon ambient, fluence of  $2 \text{ J}\cdot\text{cm}^{-2}$ , target-substrate distance 30 mm, 10 Hz repetition frequency. The multilayers were then annealed in rapid thermal processing device (Solaris 75, *Surface Science Integration*) with different temperature (100/150/200/250°C) for 15 minutes. Although the results of electric and thermoelectric measurement<sup>1</sup> were already published, we were not successful in imaging the individual layers via scanning electron microscopy in cross-section and the XRD results suggested very small shift in crystal lattice<sup>1</sup> compared to  $\text{CoSb}_4$  structure. Therefore additional analysis was needed to determine the composition. The calculated thicknesses (from the growth rate and the system thickness) were 58 nm for  $\text{FeSb}_2\text{Te}$  and 48 nm for

$\text{Ce}_{0.1}\text{Fe}_{0.7}\text{Co}_{3.3}\text{Sb}_{12}$ .

The SIMS measurements were performed in the 3D retrospective-analysis mode with a Cameca IMS 7f magnetic-sector instrument. A  $\text{Cs}^+$  primary ion beam (10 keV, 2 nA) at an impact angle of  $\sim 46^\circ$  from the surface normal was raster-scanned over an area of  $150 \text{ }\mu\text{m} \times 150 \text{ }\mu\text{m}$ . That setup resulted in a sputter rate of  $\sim 0.1 \text{ nm/s}$  and the depth resolution of  $\sim 5 \text{ nm/decade}$ . Properly chosen positively charged secondary ions for the elements O, Si, Fe, Co, Sb, Te, Ce were monitored. The depth scale of the SIMS craters was calibrated using a stylus profilometer.

The SIMS data revealed substantial differences in the depth profiles of Te for the non-annealed (Fig. 1a) and the annealed samples (Fig. 1b). The amount of Te in the  $\text{Ce}_{0.1}\text{Fe}_{0.7}\text{Co}_{3.3}\text{Sb}_{12}$  layer went up from a trace level concentration by a factor of  $\sim 20$ , which is an indication of a thermally-induced Te diffusion from the  $\text{FeSb}_2\text{Te}$  layers. Another observation is the oxygen diffusion from the  $\text{Ce}_{0.1}\text{Fe}_{0.7}\text{Co}_{3.3}\text{Sb}_{12}$  layers to the  $\text{FeSb}_2\text{Te}$  layers in the sample annealed at the highest temperature of 250°C used in our experiments.

Using SIMS, the migration of Te and O was observed, showing important merits of this technique. SIMS depth profiles had high dynamic range and high depth resolution, which we utilized in the optimization of the thin film deposition technology of the thermoelectric layers.

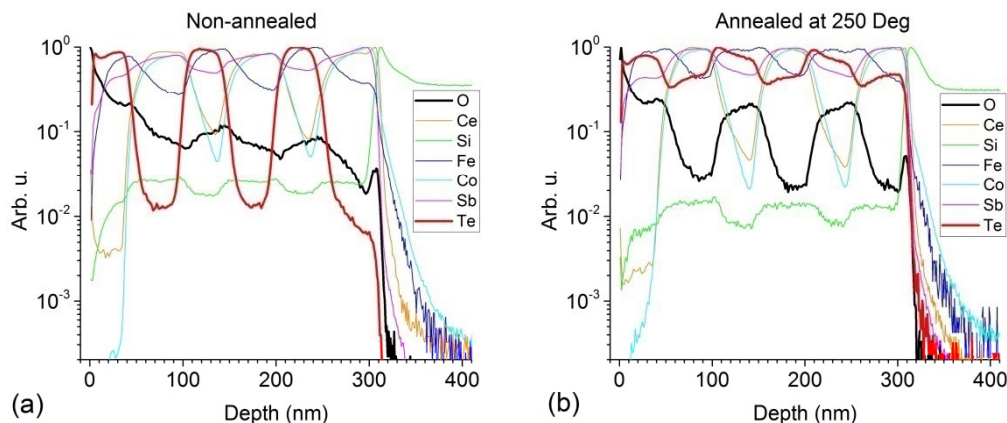


Figure 1: SIMS depth profiles of  $\text{FeSb}_2\text{Te}/\text{Ce}_{0.1}\text{Fe}_{0.7}\text{Co}_{3.3}\text{Sb}_{12}$  multilayered structure of (a) the non-annealed sample and (b) the sample annealed at 250 °C.

**Acknowledgement:** This work has been supported by the SUSEN Project CZ.1.05/2.1.00/03.0108 (ERDF) and by MEYS grant LO1409.

1) J. Remsa, M. Jelínek, T. Kocourek, R. Zeipl, J. Navrátil, Very Smooth  $\text{FeSb}_2\text{Te}$  and  $\text{Ce}_{0.1}\text{Fe}_{0.7}\text{Co}_{3.3}\text{Sb}_{12}$  Layers Prepared by Modified PLD, *Journal of Electronic Materials* 45(3), 1921-1926 (2016) DOI: 10.1007/s11664-015-4295-2



# High Power Laser Irradiation of Pure and Mixed Be/C/W Films Prepared by TVA Method

C. P. Lungu<sup>1</sup>, C. Porosnicu<sup>1</sup>, I. Jepu<sup>1</sup>, O.Pompilian<sup>1</sup>, P. Dinca<sup>1,3</sup>, P. Chiru<sup>1</sup>, A. Marcu<sup>1</sup>, M. Lungu<sup>1,3</sup>, I. Tiseanu<sup>1</sup>, C. Luculescu<sup>1</sup>, G. Cojocaru<sup>1</sup>, G. R. Ungureanu<sup>1</sup>, D.Sporea<sup>1</sup>, C.E.A. Grigorescu<sup>2</sup>, D. Savastru<sup>2</sup>

<sup>1</sup>National Institute for Laser, Plasma and Radiation Physics, 077125 Bucharest, Romania

<sup>2</sup>National Institute R&D for Optoelectronics INOE 2000, 077125 Bucharest, Romania

<sup>3</sup>Doctoral School, Bucharest University, Faculty of Physics  
aurelian.marcu@infpr.ro

Beryllium, carbon and tungsten are the only elements in contact with fusion plasma in the ITER (International Thermonuclear Experimental Reactor), under construction at Cadarache, France<sup>1</sup>. These materials, proposed to cover the walls of the fusion device are intensely bombarded by ionized particles, neutrons, photons and support the thermal action of the plasma. Beryllium, covering the most part of the first wall of the fusion device is influenced by the powerful thermal shocks and an intense bombardment of hydrogen isotopes ions and as a result is sputtered and transported toward the divertor tiles. Also, Be is bombarded by neutrons that change its network characteristics (become more brittle) as well as the adherence to the Inconel, carbon, and copper used to transmit the heat to the external circuit. Concerning tungsten, which are used to fabricate divertor tiles, is exposed to the high level of thermal shocks and is covered by the sputtered beryllium of the first wall of the fusion device and transported by an X point of the magnetic field. W has a high thermal resistance, a low sputtering yield and a quite high thermal conductivity. W is coated by carbon transported by plasma from the wall part protected with carbon fiber composite (CFC). W and C can form the tungsten carbide which lowers the resistance qualities to the plasma actions. The mentioned elements were coated on Si wafers and fine grain graphite substrates using thermionic vacuum arc method (TVA)<sup>2</sup>. Be/W and Be/C films morphologies are shown in Figs 1 and 2.

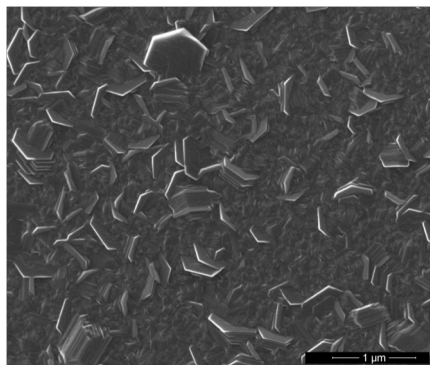


Figure 1: SEM image of Be/W film prepared by TVA

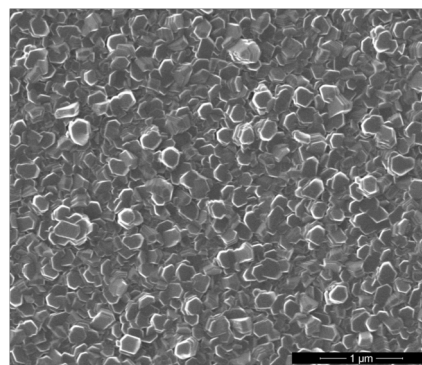


Figure 2: SEM image of Be/C film prepared by TVA

The peculiar conditions during fusion plasma influence of the 3 elements and their combinations are simulated by plasma produced in air and deuterium gas ( $10^2$ - $10^4$  Pa) in interaction with high power lasers. One of the used lasers is a single or multiple ultra short pulsed laser beams produced by the TEWALAS facility. This is a multi-terawatt laser amplifier system,  $0.025 - 360 \times 10^{-12}$  s pulse duration, up to 400 mJ pulse energy, 10 Hz maximum repetition rate,  $10^{12} - 10^{14}$  W/cm<sup>2</sup> power density. The laser pulses were programmed to have durations and power densities compared to the fusion plasma instabilities. The relative concentration distribution on the samples, the morphology and the structure of the as prepared and irradiated films were studied using XRF, SEM, XRD, XPS and Raman techniques. The deuterium gas retained into the pure and mixed materials was studied by thermal desorption spectroscopy method, showing the great influence of the W concentration.

**Acknowledgements.** This work was supported by a grant of the Romanian National Authority for Scientific Research, CNCS – UEFISCDI, project number PN-II-IDPCE-2011-3-0522.

1. Lorne Horton, JET EFDA Contributors, Operation of JET with an ITER-like Wall Fusion Engineering and Design, **96-97**, 28-33 (2015);
2. I. Jepu, R.P. Doerner, M.J. Baldwin, C. Porosnicu, C.P. Lungu, Temperature influence on deuterium retention for Be-W mixed thin films prepared by Thermionic Vacuum Arc method exposed to PISCES B plasma, Journal of Nuclear Materials, **463**, 983-988 (2015)

# Enhanced ZnO and Ag-ZnO Nanostructured Coatings Grown on Stainless Steel for Medical Applications

M. V. Lungu<sup>1</sup>, A. Sobetkii<sup>2</sup>, A.A. Sobetkii<sup>2</sup>, N. Mihăilescu<sup>3</sup>, D. Pătroi<sup>1</sup>, L. Leonat<sup>1</sup>, E. M. Lungulescu<sup>1</sup>, M. Iordoc<sup>1</sup>, L. E. Radu<sup>1</sup>, N. Stancu<sup>1</sup>, M. Lucaci<sup>1</sup>, C. D. Cîrstea<sup>1</sup>, I. Ion<sup>1</sup>, V. Tsakiris<sup>1</sup>, M. C. Chifiriuc<sup>4,5</sup>

<sup>1</sup>National Institute for Research and Development in Electrical Engineering ICPE-CA, Advanced Materials Department, 313 Splaiul Unirii Street, 030138 Bucharest, Romania

<sup>2</sup>SC MGM STAR CONSTRUCT SRL, 7 Pâncota Street, 022773 Bucharest, Romania

<sup>3</sup>National Institute for Lasers, Plasma and Radiation Physics, 77125 Măgurele, Ilfov, Romania

<sup>4</sup>University of Bucharest, Faculty of Biology, Microbiology Department, 36-46 Mihail Kogălniceanu Street, 050107 Bucharest, Romania;

<sup>5</sup>Research Institute of the University of Bucharest – ICUB, Life, Environment and Earth Sciences Division, Splaiul Independentei 91-95, 050095 Bucharest, Romania  
magdalena.lungu@icpe-ca.ro

In this study, ZnO and Ag-ZnO nanostructured coatings having 0...0.71 wt. % Ag were efficiently grown on 316L stainless steel substrate by electron-beam gun evaporation method. After deposition, the samples were annealed in air at 500°C for 1 h. The influence of an Inconel 600 interlayer deposited on steel substrate on structural, optical, tribological, mechanical, electrochemical and antimicrobial properties of the synthesized coatings was investigated. ZnO and Ag-ZnO nanostructured coatings without Inconel interlayer were manufactured for comparison, too. XRD analysis, ATR-FTIR spectroscopy, UV-Vis spectroscopy, SEM with EDAX, AFM analysis, as well as tribological and electrochemical tests were carried out, comparatively with steel substrate and Inconel coating. The failure mechanisms of the coatings was determined by microscratch tests. XRD study revealed for ZnO and Ag-ZnO coatings hexagonal wurtzite structure with (002) preferential orientation. ATR-FTIR analysis confirmed the absorption bands ranging 750-400 cm<sup>-1</sup> assigned to metal oxide bond arising from inter-atomic vibrations. Optical measurements in visible spectral region shown that all the Ag-ZnO deposited layers exhibit single surface plasmon absorption band of silver nanoparticles (Ag NPs) ranging 453-497 nm. The deposition method proved to be an efficient one since all the coatings have smooth surfaces with high uniformity and homogeneity over the substrate surface as SEM and AFM analyses showed. The samples exhibited good adhesion with optical critical loads of 7-15 N suggesting the detachment of the coating from the stainless steel substrate with exposing the substrate, average friction coefficient of 0.2-0.9, wear rate of 1-58 x 10<sup>-5</sup> mm<sup>3</sup>/Nm and corrosion rate of 2-5 μm/year determined in Ringer's solution. It was found that the heat treatment of the Ag-ZnO nanostructured coatings improved significantly the light absorption in the visible region, wear rate and corrosion resistance. Moreover the experimental results demonstrate that the nanostructured coatings have enhanced properties due to the Inconel interlayer existence over steel substrate. The all coatings inhibited totally the development of bacterial biofilm formed by Gram-positive (*Staphylococcus aureus*) and Gram-negative (*Pseudomonas aeruginosa*) strains but yielded lower antifungal activity against *Candida albicans*. Consequently, it is expected that the synthesized antimicrobial nanostructured coatings can be used in medical applications to functionalize stainless steel instruments for reducing surgical site infections.

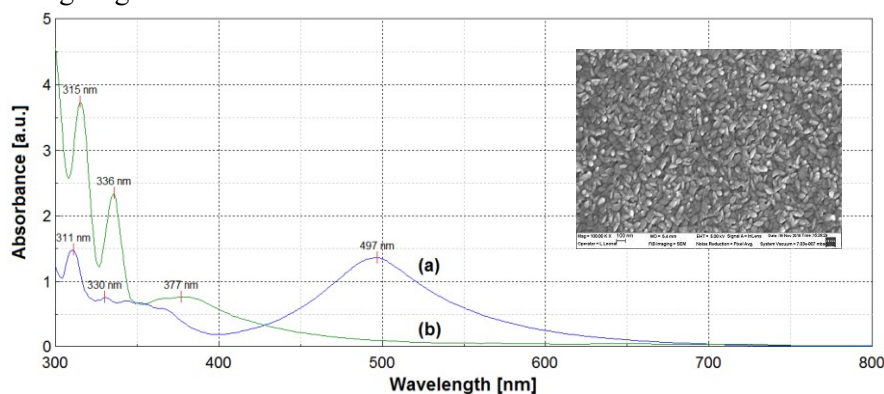


Figure 1: Absorbance spectra in UV-Vis of (a) Ag-ZnO with 0.71 wt.% Ag and (b) ZnO coatings (500 nm in thickness) containing Inconel interlayer and annealed at 500°C for 1 h; the inset is the SEM image of the Ag-ZnO coating (scale bar: 100 nm).

**Acknowledgements:** This research is supported by Ministry of National Education and Scientific Research (MENCS) - Executive Unit for Financing Higher Education, Research, Development and Innovation (UEFISCDI), Romania, and co-supported by SC MGM STAR CONSTRUCT SRL, Romania, through the program Partnerships in priority areas, project number PN-II-PT-PCCA-2013-4-1292, contract number 215/2014.

# Synthesis and Characterization of Hydrophobic Fe<sub>3</sub>O<sub>4</sub> Nanoparticles Functionalized with Triphenylphosphine

T. Malaeru<sup>1</sup>, G. Georgescu<sup>1</sup>, E. A. Patroi<sup>1</sup>, M. Eugen<sup>1</sup>, C. Morari<sup>1</sup>

<sup>1</sup>National Institute for Research and Development in Electrical Engineering INCIE ICPE-CA  
teodora.malaeru@icpe-ca.ro

Among various nanoparticles, iron oxides nanoparticles represent one of the most attractive nanomaterials for various magnetic applications<sup>1-4</sup>.

This paper reports the synthesis of magnetite (Fe<sub>3</sub>O<sub>4</sub>) nanoparticles with a hydrophobic surface functionalized with organic molecules (triphenylphosphine) through a simple technique of the hydrothermal method<sup>5</sup>. Structural, compositional, morphological and magnetic characterizations of the nanoparticles were performed by X-Ray Diffractometer (XRD), energy dispersive X-ray spectrometry (EDX), infrared spectroscopy (FTIR), scanning electron microscopy (SEM) and vibrating sample magnetometer (VSM).

The X-ray diffraction analysis demonstrated the crystalline structure of Fe<sub>3</sub>O<sub>4</sub> with an average crystallite size of 9.91 nm for the unfunctionalized nanoparticles and 10.55 nm for nanoparticles functionalized with triphenylphosphine. Absorption peaks in the FTIR spectrum confirmed the binding of triphenylphosphine on the surface of magnetite nanoparticles. SEM micrographs show a morphological difference before and after the functionalization of nanoparticles, namely, there is a film on the particles surface which is relatively homogeneously distributed over the entire surface of the nanoparticles. Magnetic properties investigation revealed a ferromagnetic behavior at room temperature with a value of the saturation magnetization (M<sub>s</sub>) of 33.43 emu/g for unfunctionalized nanoparticles and M<sub>s</sub> = 27.13 nm for the nanoparticles functionalized with triphenylphosphine.

1. D. Ling, N. Lee and T. Hyeon, Chemical Synthesis and Assembly of Uniformly Sized Iron Oxide Nanoparticles for Medical Applications, ACC. Chem. Res., 48(5), pp.1276-1285 (2015);
2. D. Shi, Y.P. Cheng, F. Liu and X.B. Zhang, Controlling the size and size distribution of magnetite nanoparticles on carbon nanotubes, Journal of Alloys and Compounds, 502(2), pp.365-370(2010);
3. C.Y. Wang, Y.M.Hong, G. Chen, Y. Zhang and N. Gu, Facile method to synthesize oleic acid- capped magnetite nanoparticles, Chinese Chem. Lett., 21, pp.179-182 (2010);
4. R. Hao, R. Xing, Z. Xu, Y. Hou, S. Goo and S. Sun, Synthesis, functionalization, and biomedical applications of multifunctional magnetic nanoparticles, Advanced Materials, 22(25), pp. 2729-2742 (2010);
5. J. Wang, J. Sun, Q. Sun and Q. Chen, One-step hydrothermal process to prepare highly crystalline Fe<sub>3</sub>O<sub>4</sub> nanoparticles with improved magnetic properties, Materials Research Bulletin, 38(7), pp.1113- 1118 (2003).

## Surface Diffusion in PLD/VLS Growing

A. Marcu<sup>1</sup>, B. Calin<sup>1</sup>, C.P. Lungu<sup>1</sup>

<sup>1</sup>National Institute for Laser, Plasma and Radiation Physics, 077125 Bucharest, Romania  
aurelian.marcu@inflpr.ro

Vapor-Liquid-Solid (VLS) grow is one of the most popular techniques for Bottom-Up nanostructures fabrication, and particularly for oxide nanowires. The technique is known as being consisted of several elementary processes as: absorption and desorption into catalyst, surface diffusion and nucleation (Fig. 1). In spite of the very good efficiency of the chemical-vapor-deposition approach (particularly for industrial application) laser ablation is still giving in many cases better performances in terms of nanostructure morphostructural properties. Furthermore, investigations using pulsed laser ablation was giving interesting insides about absorption and desorption processes

control of the nanowire growing through the critical saturation level within the catalyst droplet<sup>1</sup> and on the catalyst size limitations<sup>2</sup>. Among the VLS elementary processes, surface diffusion is still known as a fundamental process but very few experimental investigation were performed to clarify it's influence on the nanostructure growing process and the corresponding key parameters.

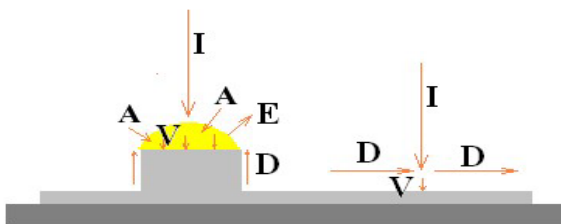


Figure 1: VLS elementary processes: I-impinging particles, D-diffused particles, A catalyst absorbed particles, E catalyst desorbed particles, V deposited particles

In the present work, oxide nanowires were grown using VLS technique in a PLD system using gold as liquid catalyst. Special system geometries (as plume reflection) were used as the experimental setups for plume filtering purpose but also for elementary processes investigations through plume propagation control. Also laser patterned

masks were fabricated for catalyst surface positioning, in order to investigate VLS elementary processes through the nanowire morphology control but with a particular interest for surface diffusion in particular. Catalyst properties and surface disposal together with the particle flux seems to control the grown nanostructure morphology. Observed influences of this process over the nanostructure growing and their properties are summarized and discussed.

*Acknowledgements.* Financial support from the Romanian National Authority for Scientific Research - ANCS, through project LAPLAS 3, cod PN 09 39 is acknowledged.

1. A. Marcu, T. Yanagida, K. Nagashima, H. Tanaka and T. Kawai, "Effect of ablated particle flux on MgO nanowire growth by pulsed laser deposition", *J. Appl. Phys.*, **102** (2007) pp.016102;

2. A. Marcu, L. Trupina, R. Zamani, J. Arbiol, C. Grigoriu and J. R. Morante, *Thin. Solid Films* **520** (2012), pp. 4626 – 4631

## The selection of optimal deposition conditions for producing thin films of Mg-Al LDH using laser techniques

A. Marinescu<sup>1</sup>, A. Matei<sup>1</sup>, A. Vlad<sup>1</sup>, R. Birjega<sup>1</sup>, M. Filipescu<sup>1</sup>, V. Marascu<sup>1</sup>, M. Dinescu<sup>1</sup>, I. Tirca<sup>1</sup>, R. Zavoianu<sup>2</sup>, O. D. Pavel<sup>2</sup>, C. Corobea<sup>3</sup>

<sup>1</sup>National Institute for Lasers, Plasma and Radiation Physics, Bucharest - Magurele, Romania

<sup>2</sup>University of Bucharest, Faculty of Chemistry, Bucharest, Romania

<sup>3</sup>National R.&S. Institute for Chemistry and Petrochemistry, Bucharest, Romania  
anca.nedelcea@inflpr.ro

Layered double hydroxides (LDHs) are a class of materials with the general formula  $M^{(II)}_{1-x}M^{(III)}_x(OH)_2 \cdot (A^n/n)_m H_2O$ , where  $M^{(II)}$  is a divalent cation ( $Mg^{2+}$ ,  $Ni^{2+}$ ,  $Zn^{2+}$ ,  $Cu^{2+}$  or  $Co^{2+}$ ) and  $M^{(III)}$  is a trivalent cation ( $Al^{3+}$ ,  $Cr^{3+}$ ,  $Fe^{3+}$ , or  $Ga^{3+}$ ).  $A^n$  is commonly an inorganic like  $OH^-$ ,  $CO_3^{2-}$ ,  $Cl^-$ ,  $NO_3^-$  or an organic anion<sup>1</sup>. Due to the large variety of elements, functional materials can be produced leading to a large area of applications like catalysis, drug delivery, sensoristics, optoelectronics etc.

Until now, the techniques reported for the deposition of oriented LDH films are sol-gel methods using hot water treatment, spin coating, hydrolysis, ultrasonification, exfoliation in organic solvents, decarbonation based methods, anionic exchange and delamination. We have previously demonstrated the capability of laser techniques for the deposition of LDH films or their derived mixed oxides<sup>2</sup>.

In this paper is presented the optimized conditions for the deposition via Pulsed Laser Deposition (PLD) and Matrix assisted pulsed laser evaporation (MAPLE) of thin films of Mg-Al based LDHs with different Mg/Al ratios (Mg/Al varies from 2 to 5 molar ratios).

The deposition parameters as number of pulses, laser wavelength, substrate temperature, radiofrequency power were varied. The morphological and structural characterizations were performed to investigate the deposited films were: X-ray diffraction (XRD), atomic force microscopy (AFM), scanning electron microscopy (SEM) coupled with energy dispersive X-ray analysis (EDX) and Fourier Transform Infra-Red Spectroscopy (FTIR).

*Acknowledgements:* This work was supported by Romanian National Authority for Scientific Research, CNCS – UEFISCDI, project number PN-II-RU-TE-2014-4-0976 (contract TE 270/2015) — "DESIRE".

1. Umberto Costantino, Valeria Ambrogi, Morena Nocchetti, Luana Perioli, "Hydrotalcite-like compounds: Versatile layered hosts of molecular anions with biological activity", *Microporous Mesoporous Mater* **107**, 149– 160 (2008);

2. A. Matei, R. Birjega, A. Nedelcea, A. Vlad, D. Colceag, M.D. Ionita, C. Luculescu, M. Dinescu, R. Zavoianu, O.D. Pavel, *Appl. Surf. Sci.*, **257** (2011) 5308-5311

# Nonlinear optical studies on 1,2,3,4,5,6,7,8-octahydro-9-hydroxiacridine-10-oxide thin films deposited by matrix-assisted pulsed laser evaporation (MAPLE)

M. Marinescu<sup>1</sup>, C. Constantinescu<sup>2,3</sup>, A. Matei<sup>2</sup>, I. Ionita<sup>4</sup>, F. Potmischil<sup>1</sup>, V. Ion<sup>2</sup>, M. Dinescu<sup>2</sup>, A. Emandi<sup>1</sup>

<sup>1</sup>UB-University of Bucharest, Faculty of Chemistry, 90-92 Pandurilor, Sector 5, RO-010184, Bucharest, Romania

<sup>2</sup>INFLPR, National Institute for Laser, Plasma and Radiation, Physics, 409 Atomistilor, Magurele, RO-077125, Bucharest, Romania

<sup>3</sup>University of Limoges, CNRS, ENSCI, SPCTS, UMR 7315, F-87000 Limoges, France

<sup>4</sup>UB - University of Bucharest, Faculty of Physics, 405 Atomistilor, Magurele RO-077125, Bucharest, Romania  
maria.marinescu@chimie.unibuc.ro

Thin films of 1,2,3,4,5,6,7,8-octahydro-9-hydroxiacridine-10-oxide (Figure 1) are deposited by matrix-assisted pulsed laser evaporation (MAPLE), on quartz and silicon substrates, with the aim of evaluating the nonlinear optical properties for potential optoelectronic applications<sup>1,2</sup>. The frozen target is irradiated by using a Nd:YAG laser (4 $\omega$ /266 nm, 7 ns pulse duration, 10 Hz repetition rate), at low fluences ranging from 0.1 to 1 J/cm<sup>2</sup>. Spectroscopic-ellipsometry (SE), Fourier transform infrared spectroscopy (FTIR), scanning electron microscopy (SEM) and atomic force microscopy (AFM) techniques were used to investigate the structure, morphology and optical properties of the films. The second harmonic generation (SHG) potential is assessed by using a femtosecond Ti:sapphire laser (~800 nm, 60–100 fs pulse duration, 80 MHz repetition rate), at 500 mW maximum output power, revealing that the SHG signal intensity is strongly influenced by the films' thickness.

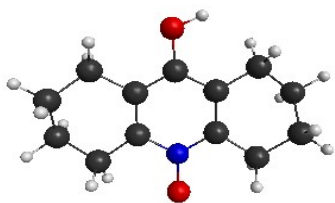


Figure 1: The structure of 1,2,3,4,5,6,7,8-octahydro-9-hydroxiacridine-10-oxide.

1. F. Potmischil, M. Marinescu, T. Loloiu, Hydroacridines XXVIII. Syntheses of New 9-Substituted 1,2,3,4,5,6,7,8-octahydroacridine Derivatives and their N(10)-Oxides, *Revista de Chimie (București)*, **58**, 795-798 (2007);

2. A. Matei, C. Constantinescu, M. Marinescu, B. Mitu, V. Ion, I. Ionita, M. Dinescu, A. Emandi, Nonlinear optical studies on 4(ferrocenylmethylimino)-2-hydroxybenzoic acid thin films deposited by matrix-assisted pulsed laser evaporation (MAPLE), *Applied Surface Science*, **374**, 206-212 (2016)

# 9-(2-Furyl)-1,2,3,4,5,6,7,8-octahydro-10-oxide thin films grown by matrix-assisted pulsed laser evaporation for nonlinear optical applications

M. Marinescu<sup>1</sup>, C. Constantinescu<sup>2,3</sup>, A. Matei<sup>2</sup>, I. Ionita<sup>4</sup>, F. Potmischil<sup>1</sup>, V. Ion<sup>2</sup>, M. Dinescu<sup>2</sup>, A. Emandi<sup>1</sup>

<sup>1</sup>UB-University of Bucharest, Faculty of Chemistry, 90-92 Pandurilor, Sector 5, RO-010184, Bucharest, Romania

<sup>2</sup>INFLPR, National Institute for Laser, Plasma and Radiation, Physics, 409 Atomistilor, Magurele, RO-077125, Bucharest, Romania

<sup>3</sup>University of Limoges, CNRS, ENSCI, SPCTS, UMR 7315, F-87000 Limoges, France

<sup>4</sup>UB - University of Bucharest, Faculty of Physics, 405 Atomistilor, Magurele RO-077125, Bucharest, Romania  
maria.marinescu@chimie.unibuc.ro; catalin.constantinescu@inflpr.ro; catalin.constantinescu@unilim.fr

We study the growth of high quality, nanometric-sized 9-(2-furyl)-1,2,3,4,5,6,7,8-octahydro-10-oxide thin films by a non-conventional technique, *i.e.* matrix-assisted pulsed laser evaporation (MAPLE), on silicon or quartz substrates by using a Nd:YAG pulsed laser device (4 $\omega$ /266 nm, 7 ns pulse duration, 10 Hz repetition rate). This compound (Fig. 1) has a chemical structure that indicates potential nonlinear optical response (NLO)<sup>1,2</sup>. The surface morphology of the films are probed using atomic force microscopy (AFM) and scanning electron microscopy (SEM). The structures of the thin film material and starting material were compared by Fourier transform infrared (FTIR) and Raman spectroscopy. The optical properties of the thin films are investigated by spectroscopic-ellipsometry (SE), and the refractive index dependence with respect to temperature is studied<sup>3</sup>. The second harmonic generation (SHG) potential is assessed by using a femtosecond Ti:sapphire laser (~800 nm, 60–100 fs pulse duration, 80 MHz repetition rate), at 200 mW maximum output power, revealing that the SHG signal intensity is strongly influenced by the films' thickness.

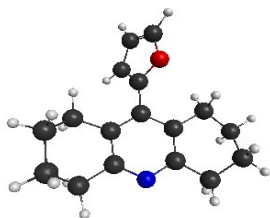


Figure 1: The structure of 9-(2-furyl)-1,2,3,4,5,6,7,8-octahydro-10-oxide.

1. F. Potmischil, M. Marinescu, A. Nicolescu, C. Deleanu, M. Hillebrand, Hydroacridines: part 29. <sup>15</sup>N NMR chemical shifts of 9substituted 1,2,3,4,5,6,7,8-octahydroacridines and their N-oxides – Taft, Swain-Lupton, and other types of linear correlations, *Magnetic Resonance in Chemistry*, **46**, 1141-1147 (2008);

2. M. Marinescu, A. Emandi, G. Marton, L.O. Cinteza, C. Constantinescu, Structural studies and optical nonlinear response of some pyrazole-5-ones, *Nanoscience and Nanotechnology Letters*, **7**, 846-854 (2015);

3. A. Matei, C. Constantinescu, M. Marinescu, B. Mitu, V. Ion, I. Ionita, M. Dinescu, A. Emandi, Nonlinear optical studies on 4(ferrocenylmethylimino)-2-hydroxybenzoic acid thin films deposited by matrix-assisted pulsed laser evaporation (MAPLE), *Applied Surface Science*, **374**, 206-212 (2016).

# Nonlinear optical properties studied on thin films of 2-(2,4-dibromophenyl)-1H-benzo[d]imidazole by matrix-assisted pulsed laser (MAPLE) evaporation

M. Marinescu<sup>1</sup>, C. Constantinescu<sup>2,3</sup>, A. Matei<sup>2</sup>, I. Ionita<sup>4</sup>, V. Ion<sup>2</sup>, M. Dinescu<sup>2</sup>, A. Emandi<sup>1</sup>

<sup>1</sup>UB-University of Bucharest, Faculty of Chemistry, 90-92 Pandurilor, Sector 5, RO-010184, Bucharest, Romania

<sup>2</sup>INFLPR, National Institute for Laser, Plasma and Radiation, Physics, 409 Atomistilor, Magurele, RO-077125, Bucharest, Romania

<sup>3</sup>University of Limoges, CNRS, ENSCI, SPCTS, UMR 7315, F-87000 Limoges, France

<sup>4</sup>UB - University of Bucharest, Faculty of Physics, 405 Atomistilor, Magurele RO-077125, Bucharest, Romania  
maria.marinescu@chimie.unibuc.ro; catalin.constantinescu@inflpr.ro; catalin.constantinescu@unilim.fr

A newly synthesized compound (Fig. 1), namely 2-(2,4-dibromophenyl)-1H-benzo[d]imidazole, has a suitable structure for nonlinear optical response (NLO)<sup>1-2</sup>. Thin films with controlled thickness are deposited by matrix-assisted pulsed laser evaporation (MAPLE), on quartz and silicon substrates, with the aim of evaluating the NLO for potential optoelectronic applications. The frozen target is irradiated by using a Nd:YAG laser (4 $\omega$ /266 nm, 7 ns pulse duration, 10 Hz repetition rate), at low fluences ranging from 0.1 to 1 J/cm<sup>2</sup>. Spectroscopic-ellipsometry (SE), Fourier transform infrared spectroscopy (FTIR), scanning electron microscopy (SEM) and atomic force microscopy (AFM) techniques were used to investigate the structure, morphology and optical properties of the films. The second harmonic generation (SHG) potential is assessed by using a femtosecond Ti:sapphire laser (~800 nm, 60–100 fs pulse duration, 80 MHz repetition rate), at 140 mW maximum output power, revealing that the SHG signal intensity is strongly influenced by the films' thickness.

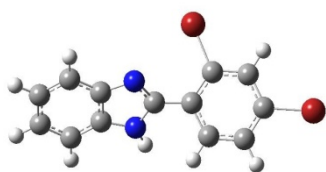


Figure 1. The structure of 2-(2,4-dibromophenyl)-1H-benzo[d]imidazole.

1. M. Marinescu, A. Emandi, G. Marton, L.O. Cinteza, C. Constantinescu, Structural studies and optical nonlinear response of some pyrazole-5-ones, *Nanoscience and Nanotechnology Letters*, **7**, 846-854 (2015);

2. A. Matei, C. Constantinescu, M. Marinescu, B. Mitu, V. Ion, I. Ionita, M. Dinescu, A. Emandi, Nonlinear optical studies on 4(ferrocenylmethylimino)-2-hydroxybenzoic acid thin films deposited by matrix-assisted pulsed laser evaporation (MAPLE), *Applied Surface Science*, **374**, 206-212 (2016).

## Layered double hydroxides thin films grown by laser techniques for food additives detection

A. Matei<sup>1</sup>, R. Birjega<sup>1</sup>, A. Vlad<sup>1</sup>, A. Palla Papavlu<sup>1</sup>, M. Filipescu<sup>1</sup>, V. Marascu<sup>1</sup>, R. Zavoianu<sup>2</sup>, O.D. Pavel<sup>2</sup>, M.C. Corobea<sup>3</sup>, M. Dinescu<sup>1</sup>

<sup>1</sup>National Institute for Lasers, Plasma and Radiation Physics, 409 Atomistilor Str., 077125 Bucharest, Magurele, Romania

<sup>2</sup>University of Bucharest, Faculty of Chemistry, Department of Chemical Technology and Catalysis, 4-12 Regina Elisabeta Bd., Bucharest, Romania

<sup>3</sup>National R.&S. Institute for Chemistry and Petrochemistry, ICECHIM, 202 Splaiul Independentei Str., CP-35-274, 060021, Bucharest, Romania  
andreea.purice@inflpr.ro

$[M^{2+}_{1-x}M^{3+}_x(OH)_2]^{x+}(A^r)_{x/n} \cdot mH_2O$ , where  $M^{2+}$  is Mg, Ni, Zn, Cu or Co and  $M^{3+}$  is Al, Cr, Fe, or Ga is the general formula characteristic to layered double hydroxides (LDH) materials. Because of their unique layered structure, large surface areas, high anion-exchange capacities LDHs received considerable attention as promising materials for a widespread applications as: anion exchangers and adsorbents, catalysts and catalysts supports, electroactive and photoactive materials, polymer stabilizers and fillers etc. The techniques reported until now for the deposition of oriented LDH films are sol-gel methods using hot water treatment, spin coating, hydrolysis, ultrasonification, exfoliation in organic solvents, decarbonation based methods, anionic exchange and delamination. We have previously demonstrated the capability of the laser techniques for the deposition of LDH films or their derived mixed oxides.

Here in we report on the properties of the Ni-Al and Co-Al LDHs films deposited on different substrates via laser techniques as potential materials to be used in sensing devices. A Nd:YAG laser with 3 harmonics (1064, 532, 266 nm) was used in PLD experiments to irradiate the LDH pressed targets with a fluence between 1.5 and 3 J/cm<sup>2</sup> and the ablated material was deposited onto Si and ITO/glass substrates placed at 4 cm in front of the target. Ni-Al based LDH was homogeneously dispersed in water, frozen and used as targets for MAPLE experiments.

All the depositions took place in vacuum, at room temperature and the films were the result of 20.000-90.000 pulses.

X-ray diffraction (XRD), atomic force microscopy (AFM), scanning electron microscopy (SEM) combined with energy dispersive X-ray analysis (EDX) and Fourier Transform Infra-Red Spectroscopy (FTIR) were the techniques used to characterize the as prepared films. Cyclic voltammetry was performed in order to test the detection capabilities of the as deposited films. Solutions of monosodium glutamate (MSG) were used as test food additive.

# Dual Imaging System for Tumor Assessment: Diffuse Optical Tomography and Hyperspectral Fluorescence

C.E. Matei<sup>1</sup>, M. Patachia<sup>1</sup>, S. Banita, M. Petrus, C. Achim, D.C. Dumitras

<sup>1</sup>Laser Department, National Institute for Laser, Plasma and Radiation Physics, Magurele, Romania  
consuela.matei@inflpr.ro

Health is one of the high impact dimensions of the society in terms of quality of life and incapacitation of active population. The high rate of social expenses related to the treatment of malignant diseases could be decreased by a sustained development of the fundamental research on both directions of prophylactic screening for early detection of tumoral formations and improvement of the treatment techniques.

Since the 1990s, hybrid imaging by means of software and hardware image fusion alike allows the intrinsic combination of functional and anatomical image information. Combined imaging has revolutionized the medical diagnosis, increasing the chances of early diagnosis, improving the accuracy of the anato-metabolic collected data, or allowing the precise monitoring of interventional procedures, while the patients avoid multiple examinations and radiation exposure. For oncology, the interest resides in several directions as non-invasively monitoring the tumor evolution following radiation therapy, improving the discrimination rate between benign and malign nature of tumors in the diagnostic process, or helping the surgeon to assess the tumor spreading during resection procedures.

We present such a system, based on the duality of Diffuse Optical Tomography (DOT) and Hyperspectral Fluorescence Spectroscopy, which was developed and improved in our laboratory. The system includes a self-developed DOT arm and a commercial available hyperspectral imaging module. The DOT system is equipped with two laser diodes (780 nm and 830nm) as light sources, and is built on a 16 optical fiber circular configuration, using two fast 1x8 fiber switches as multiplexors, and a performant detection chain. The hyperspectral imaging module is working in the spectral range 400 - 1000 nm, with a nominal spectral resolution of 2.73 nm. The CCD camera has a monochrome 2/3" sensor, being able to acquire 1.5 Mega pixel images at 11 fps. For data acquisition and basic processing of the hyperspectral images, the producer's company software SP-SpectralDAQ is used.

The construction of the system will be presented in our paper, covering both optical and technical aspects, presenting calibration and test measurements, and also including few considerations on the implementation of reconstruction algorithms.

*Acknowledgements:* This work has been funded by a grant of the Romanian Ministry of Education, CNCS-UEFISCDI, project number PN-II-PT-PCCA-2013-4-2098.

## Experimental thin film coatings for engineering super lens tuned in UV and Visible

V. R. Medianu, M. Oane

National Institute for Laser, Plasma and Radiation Physics, Str. Atomistilor 409,  
077125 Magurele - Bucharest, Romania  
mihai.oane@yahoo.com; vrmlaser@gmail.com

A new class of materials, with negative index of refraction (NIM), will be engineered to overcome the diffraction limit. We propose to design & develop a NIM processed for UV and visible spectrum using transparent metal-dielectric photonic band gap technology coupled with a graphene far-field super lens grating. The technologies using active surfaces induced by functional new thin films or functionalized surfaces and interfaces represent a great development of scientific activities in the field, from new artificial materials designed in photonics (display & visual devices, super lens/flat lens, metamirrors, plasmonic cavity, solar cells, photonic components for very high laser fluency) to surface treatment (control of wetting, adhesion, catalysis, processing and Nano structuring) represent the genuine technological trends in the domain of photonic components using thin films for active material production. The new coating technology will be able to build new materials, new metasurfaces and new Nano-multifunctional periodic structure capable to design the most sophisticated optical components up to photonic crystals. Using dedicated technology (Ion Beam processed Radio Frequency Magnetron Sputtering/IBRFMS-Coating and Laser Lithography Processing Fresnel Super-Lens/LLPFS) we propose a concept of super-lens.

# Numerical Analysis of Long Period Grating Fiber Sensor Fabrication Using Thermal Processing

S. Miclos<sup>1</sup>, D. Savastru<sup>1</sup>, R. Savastru<sup>1</sup>, I. Lancranjan<sup>1</sup>

<sup>1</sup>The National Institute of Research and Development for Optoelectronics - INOE 2000  
409 Atomistilor Street, Magurele, Ilfov, RO-077125, Romania  
miclos@inoe.ro

In the last over thirty years of laser physics, important efforts have been made in studying and designing grating fiber sensor applications in various research, industrial, medical and military fields. These efforts are part of the main activity having as the purpose the development of all-fiber devices, because of their evident advantages versus other types such as electronic or optoelectronic devices. All-fiber devices perform a function on the light (e.g. by modulating, amplifying, routing, and coupling optical signals) without extracting it from the fiber. As a logical consequence, aiming to improved design of all-fiber devices, the simulation of techniques used for manufacturing such devices as a whole or of their components is of great interest. The purpose of this article consists in presenting results obtained in simulation of manufacturing a component of all-fiber devices, namely Long Period Grating Fiber Sensors (LPGFS). LPGFS form a basic component of all-fiber devices. LPGFS are operated by coupling of optical power from the guided mode into co-propagating cladding modes by a longperiod grating formed in optical fiber core. A LPGFS is formed by writing over a length  $L$ , commonly of 5-50 mm, a modulated, usually approximated as sinusoidal, alteration of refractive index in the core of a single mode (SM) optical fiber with 10-1000  $\mu\text{m}$  spatial wavelength (period) along the optical fiber axis. It is a common practice to manufacture LPGFS in silicate communication SM optical fiber with a core of 4-8  $\mu\text{m}$  and a cladding of 125  $\mu\text{m}$  diameters such as Corning SM 28. LPGFSs are extremely sensitive to small variation of refractive index of the surrounding medium, being used as chemical sensors for detection of pathogen bacteria, as to give an example among others.

Basically, the LPG's can be written in the core of an optical fiber by using two main technologies: by UV laser irradiation (190-250 nm) or by localized thermal processing of the fiber<sup>1-4</sup>. The first technique consists in altering the core refractive index in a periodic manner by inducing color center defects in the silicate glass of the core. Such color centers are slowly fading over long periods, longer than several years, and/or more rapidly being exposed at temperatures of 200-300 °C. The first technique may require photosensitization of optical fiber by doping with hydrogen. The second technique used for manufacturing of LPGFS consists in slightly physically deform the fiber to create the required optical modulation<sup>1-4</sup>. The physically deformation of the optical fiber is accomplished in several ways: by irradiation from a carbon dioxide laser, with femtosecond laser pulses, writing by electric discharge, ion implantation, by periodic ablation and annealing, by dopant diffusion into the fiber core, corrugation of the cladding or by micro-structuring of tapered fibers previously thermally processed. More specifically, the purpose of this paper consists in presenting results obtained in simulation of LPGFS fabrication by using the most financially effective (cheapest) of the mentioned ways of optic fiber deformation: irradiation from a carbon dioxide laser, writing by electric discharge from a commercial fiber fusion splice machine and periodic ablation and annealing. The simulation of the thermal processes used for optic fiber deformation is performed for improving LPGFS design. In this sense, several specific tasks are on pursuit, e.g. the optical fiber asymmetry observed in the case of using irradiation from a carbon dioxide laser and the possible reduction of it and/or beneficial use in sensing applications. These specific simulation tasks have a major common base: the as most as possible accurate definition of longitudinal and transverse distribution of temperature in the optical fiber during and after thermal processing. The obtained simulation results are compared with reported in literature ones indicating a fairly good agreement.

1. V. Bhatia and A.N. Vengsarkar, *Optics Letters*, **21**, 692-694 (1996);

2. S.W. James, R.P. Tatam, R.P., *Measurement Science and Technology*, **14**, R49-R61 (2003);

3. A.N. Vengsarkar, P.J.Lemaire, J.B. Judkins, V. Bhatia, T. Erdogan, and J.E. Sipe, *Journal of Lightwave Technology*, **14**, 58-65 (1996);

4. D. Savastru, S. Miclos, R. Savastru, I. Lancranjan, *Romanian Reports in Physics*, **67**, 1586-1596 (2015).



# Nanostructured bioactive glass thin films synthesized by pulsed laser deposition onto biodegradable metallic implants

N. Mihailescu<sup>1</sup>, A. Fica<sup>2</sup>, C. Ristoscu<sup>1</sup>, F. Sima<sup>1</sup>, C.N. Mihailescu<sup>1</sup>, Laura Floroian<sup>3</sup>, M. Sopronyi<sup>1</sup>,  
M. C. Chifiriuc<sup>4</sup>, I. Negut<sup>1</sup>, C. Bleotu<sup>5</sup>, I. N. Mihailescu<sup>1</sup>

<sup>1</sup>National Institute for Lasers, Plasma and Radiation Physics, 409 Atomistilor Street, Magurele, Ilfov, RO-77125, Romania;

<sup>2</sup>Politehnica University of Bucharest, Faculty of Applied Chemistry and Material Science; 1-7 Polizu Str., 011061 Bucharest, Romania;

<sup>3</sup>Romania Transilvania University of Brasov, 29 Eroilor Blvd, 500036 Brasov, Romania;

<sup>4</sup>Faculty of Biology, University of Bucharest, Research Institute of the University of Bucharest – ICUB, Spl. Independentei 91-95, 050095 Bucharest, Romania

<sup>5</sup>“Stefan S. Nicolau” Institute of Virology, 285 Mihai Bravu Avenue, Bucharest, Romania  
natalia.serban@inflpr.ro

Nowadays, intense research is focused on the development of “*smart implants*” based on biodegradable metallic materials. Corrosion of metallic materials is critical because it can affect the bioactivity, biocompatibility and the mechanical integrity<sup>1-3</sup>. Corrosion and surface film dissolution are the responsible mechanisms for introducing unwanted ions in the body from implants. Extensive release in the body of metal ions from implants can cause adverse biological reactions and lead to mechanical failure of the device<sup>4</sup>. Moreover, imperfect shielding can cause supplementary tensions which may lead to major difficulties such as implant loosening, delay in the healing process and consequently damaged bone growth. Bioactive materials play an increasingly important role in the biomaterials industry, and are extensively used in a range of applications, including biodegradable metallic implants<sup>5</sup>.

We report on thin films deposition of Bioactive Glasses (BG) by pulsed laser techniques onto biodegradable metallic substrates. The coatings were obtained using a KrF\* excimer laser source ( $\lambda = 248$  nm,  $\tau_{FWHM} \leq 25$  ns). The obtained coatings preserved their initial composition, as demonstrated by physical-chemical analyses: Infrared Spectroscopy, Scanning Electron Microscopy, Energy Dispersive X-ray Spectroscopy and XRay Diffraction. Electrochemical measurements, impedance spectroscopy and *in vitro* immersion tests were conducted to evaluate the corrosion resistance of the uncovered and covered biodegradable metallic substrates into physiological fluids. The *in vitro* assay revealed that the obtained thin films are non-cytotoxic. The antimicrobial effect of the covering layers was tested against *S. aureus* and *E. coli* strains, involved implant associated infections. The results proved that the applied method allow for the fabrication of efficient shield barriers against corrosion, biofilm formation and contamination with bacteria.

1. T. Kokubo and H. Takadama, *Biomaterials* **27** 2907, (2006);

2. Mark P. Staiger, Alexis M. Pietak, Jerawala Huadmai and George Dias, *Biomaterials* **27** 1728–1734, (2006);

3. J.J. Jacobs, J.L. Gilbert and R.M. Urban, *J. Bone Joint Surg.* **80** 268, (1998);

4. S. Torgerson, N.R. Gjerdet and J. Mater. Sci.: Mater. Med. **5** 256, (1994);

5. Zhao X., J.M. Courtney and H. Qian, Ed. Woodhead Publishing Series in Biomaterials, ISBN 10: 1845696247, (2011).

## Low transition temperature in strain-free VO<sub>2</sub>/TiO<sub>2</sub> epitaxial thin films

C. N. Mihailescu<sup>1,2</sup>, E. Symeou<sup>1</sup>, E. Svoukis<sup>1</sup>, R. F. Negrea<sup>3</sup>, C. Ghica<sup>3</sup>, V. Teodorescu<sup>3</sup>, C. Negrila<sup>3</sup>, J. Giapintzakis<sup>1</sup>

<sup>1</sup>Nanotechnology Research Center and Department of Mechanical and Manufacturing Engineering, University of Cyprus,  
75 Kallipoleos Avenue, PO Box 20537, 1678 Nicosia, Cyprus

<sup>2</sup>National Institute for Laser, Plasma and Radiation Physics, 409 Atomistilor Street, PO Box MG-36, 077125 Magurele, Romania

<sup>3</sup>National Institute of Materials Physics, RO-077125 Magurele, Romania  
giapintz@ucy.ac.cy

Within the study of the semiconductor-metal transition of vanadium dioxide, controlling its transition temperature through strain-induced lattice distortion in epitaxial thin films is an interesting issue in terms of fundamental physics, but also the practical application. In this research by investigating the effects of the substrate temperature on the structure, chemical composition, interface coherency and electrical characteristics across the phase transition boundary of phase-pure vanadium dioxide epitaxial films, we have found that that the thermal expansion/contraction of the TiO<sub>2</sub> substrate leads to an increase of the transition temperature as a function of growing temperature which opposite to current belief is accompanied by a net decrease of the V<sup>4+</sup>-V<sup>4+</sup> bond length in the metallic state. Additionally, we show that by using a low deposition temperature the obtained thin films exhibit a relaxed state and a transition temperature close to room temperature. The presented results suggest the existence of an interfacial oxygen exchange mechanism, but also highlight the difficulty to deduce the intrinsic material response to strain when the exact contribution of all strain sources cannot be effectively determined.

# Maple Deposition of Complex Hybrid Fe<sub>3</sub>O<sub>4</sub>-PEDOT:PSS-PLGA Coatings

F. M. Miroiu<sup>1</sup>, N. Stefan<sup>1</sup>, A. I. Visan<sup>1</sup>, C. Luculescu<sup>1</sup>, V. Grumezescu<sup>1</sup>, C. Radu<sup>1</sup>, R. Cristescu, M. Socol<sup>2</sup>, R. C. Popescu<sup>3</sup>, D. Savu<sup>3</sup>, M. Temelie<sup>3</sup>, G. Socol<sup>1</sup>

<sup>1</sup>National Institute for Lasers, Plasma and Radiation Physics, 409 Atomistilor Street, Magurele, Ilfov, Romania

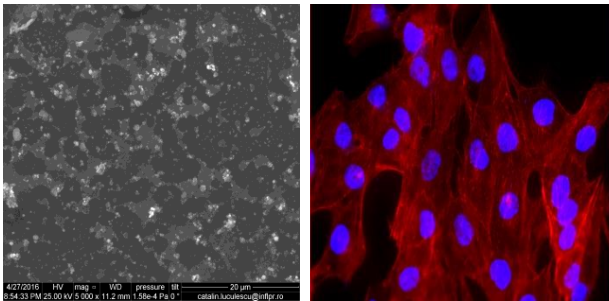
<sup>2</sup>National Institute of Materials Physics, 105 bis Atomistilor Street, Magurele, Ilfov, Romania

<sup>3</sup>Horia Hulubei National Institute of Physics and Nuclear Engineering, Magurele, 30 Reactor Street, Ilfov, Romania  
marimona.miroiu@infpr.ro

Hybrid coatings of PEDOT:PSS and Fe<sub>3</sub>O<sub>4</sub> nanoparticles embedded into biodegradable PLGA polymeric matrix have been deposited by Matrix Assisted Pulsed Laser Evaporation (MAPLE) for a study of optimized drug administration, related to the application of external stimuli in order to adjust the release rate of drugs, when specific, inconstant dosing is required. While Fe<sub>3</sub>O<sub>4</sub> nanoparticles makes targeting possible by external magnetic field application and the PEDOT:PSS nanoparticles under electric activation, the PLGA acts as a vehicle for the active therapeutic agent.

Local and sustained release may be thus electromagnetically controlled. Hybrid Fe<sub>3</sub>O<sub>4</sub>-PLGA-PEDOT:PSS and Fe<sub>3</sub>O<sub>4</sub>-PLGA-PEDOT:PSS-Cypress coatings, with Cypress essential oil as active agent, were synthesized on titanium, silicon and glass substrates. FTIR, XRD, SEM, AFM, electrochemical spectrometry, RF magnetical stimulation and *in vitro* biological assays were performed to characterize the obtained coatings in terms of stoichiometry, morphology, magnetic properties, biocompatibility, and response to external stimuli.

FTIR and XRD analyses confirmed the stoichiometric transfer, while SEM and AFM showed specific



morphology of the obtained coatings. The electrochemical corrosion potential increased when aspirin was entrapped in the coatings. The Fe<sub>3</sub>O<sub>4</sub>-PLGA and Fe<sub>3</sub>O<sub>4</sub>-PLGA-PEDOT:PSS films revealed enhanced cellular viability, superior to glass or titanium controls, when cultured with Mg63-cells. Selected coatings were further subjected to advanced *in vitro* tests.

Figure 1: SEM on a Fe<sub>3</sub>O<sub>4</sub>-PLGA coating, 5000 x (left). Immunofluorescence of osteoblast-like Mg 63 cells on a Fe<sub>3</sub>O<sub>4</sub>-PEDOT:PSS-PLGA after 48 h, 20 x (right)

**Acknowledgements:** This work was supported under the contract TE 188 /2015 – UEFISCDI.

## Mapping the optical near field of metallic nanoparticles: applications for high-efficiency photovoltaics

S. H. Møller<sup>1</sup>, P. L. Tønning<sup>1</sup>, and P. Balling<sup>1</sup>

<sup>1</sup>Department of Physics and Astronomy, Aarhus University, Ny Munkegade 120, DK-8000 Aarhus C, Denmark  
soerenhm@phys.au.dk

Much current research is focused on producing cost-effective photovoltaic (PV) devices (or solar cells) for harvesting the solar energy. Various approaches for utilizing plasmonics to enhance the efficiency of the PV devices at low additional cost have been proposed<sup>1</sup>. The current investigation is part of a new research project, SunTune, in which the overall goal is the increase of the PV efficiency by upconverting a fraction of the near-infrared solar spectrum, centered around 1550 nm, which is usually not absorbed in conventional cells based on e.g. silicon due to the band gap. A primary idea of the design is to improve the upconversion process by using optimally designed plasmonic nanoparticles to enhance the local electric field of infrared sunlight. The design optimization will in part be based on numerical solutions of Maxwell's equations, so experimental verification of the calculations is crucial.

In this presentation, preliminary investigations of the optical near field around metallic nanoparticles will be presented. The technique is based on mapping the near field directly onto a thin film of the well-known phase-change material Ge<sub>2</sub>Sb<sub>2</sub>Te<sub>5</sub> (GST); by irradiating the sample with a femtosecond laser pulse, the thin film will switch locally from a crystalline to an amorphous state wherever a certain threshold fluence is reached, thus allowing a quantitative mapping of the near field that can be viewed directly in optical and scanning-electron microscopy (SEM)<sup>2,3</sup>. Figure 1 shows one of our first SEM pictures of such near-field mapping. The use of a tunable femtosecond light source allows the near fields to be measured at a range of wavelengths, thus permitting a more detailed comparison with theory. Modelling of the material excitation in the GST film during the short-pulse

excitation is carried out by extending previous models in our group<sup>4,5</sup>, which in turn is based on the multiple-rate equation model, originally proposed by Rethfeld<sup>6</sup>.

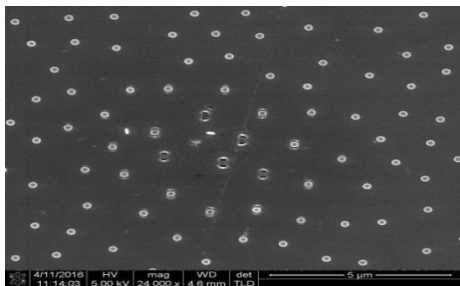


Figure 1: SEM picture of randomly distributed gold nanoparticles on Ge<sub>2</sub>Sb<sub>2</sub>Te<sub>5</sub> after irradiation with a 40 fs laser pulse at 1500 nm central wavelength focused to a spot size of 10 μm. The crystalline/amorphous phases cannot be distinguished in this picture, however, ablation craters due to near-field enhancement are clearly visible around the most intensely irradiated nanoparticles.

1. H. Atwater, and A. Polman, *Plasmonics for improved photovoltaic devices*, Nature Mater. **9**, 205 (2010)
2. P. Kühler, et al., *Quantitative imaging of the optical near field*, Opt. Expr. **20**, 22063 (2012)
3. C. David, P. Kühler, F. J. García de Abajo, and J. Siegel, *Near-field nanoimprinting using colloidal monolayers*, Opt. Expr. **22**, 8226 (2014)
4. B. H. Christensen and P. Balling, *Modeling short-pulse laser ablation of dielectric materials*, Phys. Rev. B **79**, 155424 (2009).
5. K. Wædegaard, D. B. Sandkamm, L. Haahr-Lillevang, K. G. Bay, and P. Balling, *Modeling short-pulse laser excitation of dielectric materials*, Applied Physics A **117**, 7 (2014).
6. B. Rethfeld, Phys. Rev. Lett., **92**, 187401 (2004); B. Rethfeld, Phys. Rev. B, **73**, 035101 (2006).

## Investigation of the efficiency of Pt/Rd, Pt/Ru and Pt/Co multilayer catalysts in Polymer Electrode Membrane fuel cells

W. Mróz<sup>1</sup>, B. Budner<sup>1</sup>, S. Grigoriev<sup>2</sup>, V. Fateev<sup>3</sup>, M. L. Korwin-Pawłowski<sup>4</sup>, Y. Suda<sup>5</sup>, Z. Szymański<sup>6</sup>

<sup>1</sup>Institute of Optoelectronics, Military University of Technology, 2 Kaliskiego Street, 00-908 Warsaw, Poland

<sup>2</sup>National Research University "Moscow Power Engineering Institute", Krasnokazarmennaya str., 14, Moscow, 111250, Russia

<sup>3</sup>National Research Centre "Kurchatov Institute", Kurchatov sq., 1, Moscow, 123182, Russia

<sup>4</sup>Université du Québec en Outaouais, Département d'informatique et d'ingénierie, 101 rue Saint-Jean-Bosco, Gatineau, (Québec), Canada

<sup>5</sup>Department of Electrical and Electronic Information Engineering, Toyohashi University of Technology, Toyohashi, Aichi 441-8580, Japan

<sup>6</sup>Laser Technology Application, Institute of Fundamental Technological Research, Pawinskiego 5B, PL-02-106 Warsaw, Poland  
waldemar.mroz@wat.edu.pl

In this work will be presented results of electrochemical investigations of thin catalyst films deposited in high vacuum at room temperature by the PLD method using a pulsed ArF ( $\lambda=193$  nm) laser. Pt/Pd, Pt/Ru and Pt/Co structures of nanometric thicknesses were deposited on the surface of gas diffusion electrodes fabricated from the porous carbon fabric ELAT LT 2500W (E-Tek) and were, alternatively, performing the functions of the cathode and the anode of a polymer fuel cell. As the counter-electrode was used a carbon fabric covered with platinum black deposited by painting on the surface of the gas diffusion layer from a Nafion suspension. Membrane-electrode assemblies (MEA) with catalyst layers containing different proportions of Pt to Rd, Ru and Co and different amounts of the noble metals were fabricated and investigated. The total surface specific weights of metals deposited on the electrodes were 4.76 to 9.50  $\mu\text{g cm}^{-2}$  in the case of Pt/Pd structures, 3.23 to 5.43  $\mu\text{g cm}^{-2}$  for Pt/Ru and 3.81 to 5.23  $\mu\text{g cm}^{-2}$  for Pt/Co. The electrocatalytic properties of the catalyst layers were investigated in the MEA of a fuel cell fed with H<sub>2</sub>/O<sub>2</sub>. Basing on the results of the electrochemical investigations were determined the current efficiencies of the electrodes and the degrees of utilization of the catalyst. It was established that among the investigated groups the highest efficiencies were shown by the electrodes with Pt/Pd catalyst. Those electrodes also showed more than twice higher effectiveness of utilization of the bi-metallic catalyst by specific surface weight compared with pure Pt.

# Quantitative phase imaging of neuronal networks with programmable illumination

V. Nastasa<sup>1,5</sup>, T. Kim<sup>1</sup>, H. Majeed<sup>1</sup>, M. Shan<sup>1</sup>, P. Sengupta<sup>2,3</sup>, M. U. Gillette<sup>3,4</sup>, M.L. Pascu<sup>5</sup>, and G. Popescu<sup>1,3</sup>

<sup>1</sup>Quantitative Light Imaging Laboratory, Department of Electrical and Computer Engineering, Beckman Institute for Advanced Science and Technology, University of Illinois at Urbana-Champaign, Urbana, IL 61801, USA

<sup>2</sup>Opto Neuro Technology Laboratory, Beckman Institute for Advanced Science and Technology, University of Illinois at Urbana-Champaign, Urbana, IL 61801, USA

<sup>3</sup>Department of Bioengineering, University of Illinois at Urbana-Champaign, Urbana, IL 61801, USA

<sup>4</sup>Department of Cell & Developmental Biology, University of Illinois at Urbana-Champaign, Urbana, IL 61801, USA <sup>5</sup>National Institute for Laser Plasma and Radiation Physics, Magurele, IL, 077125, Romania

Current technology for measuring electrical activity in neurons requires physical contact, either by patch clamping or, more recently, by electrode arrays placed on the substrate. While extremely valuable, these approaches are limited in terms of the spatiotemporal scales on which they can report electrical activity. It is therefore clear that novel, ultrasensitive, label-free imaging methods are highly desirable. The development and

implementation of novel neurotechnologies that will enable a non-invasively control, measure, and analyze spatial and temporal neural network dynamics is required. To evaluate the phase shift induced by the optical stimulation of optogenetically-modified neuronal networks with light pulses a quantitative phase imaging (QPI) with programmable light stimulation setup was developed.

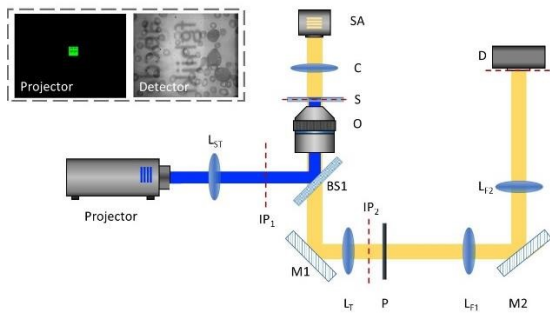


Figure 1: Quantitative phase imaging (QPI) with programmable light stimulation. The yellow light path shows a regular SLIM light path, and the blue light path is the projector illumination onto the sample plane. A pattern from the projector is imaged onto the sample plane, as shown in the inset.

One benefit from this setup is that, when the projector illumination is focused on the sample plane, a selective illumination can be applied onto the same plane. For example, when measuring a cell culture, one can select certain cells and illuminate only the selected cells. Combined with the high sensitivity and resolution of spatial light interference microscopy (SLIM)<sup>1</sup>, this idea can be used for a measurement of neurons that are genetically engineered to be sensitive to light. These optogenetic neurons respond to a certain wavelength and send signals when they are stimulated by light. These signals are generated through the ion channels on the plasma membrane, when the membrane potential increases and surpasses the threshold. This subtle and rapid event occurs at millisecond timescale, which makes it extremely difficult to detect them without an expensive electrophysiology system. These systems also require a highly accurate control during its operation and are limited to single point measurements. The standard method for measuring these signals implies the use of electrophysiology systems based on electrodes or MEMS devices. However, it is still difficult to do wide-field imaging of these cells in action because of the required imaging speed and sensitivity<sup>2</sup>.

**Acknowledgements:** This work was supported by the National Science Foundation (CBET-0939511 STC, IIP-1353368). For more information, visit <http://light.ece.illinois.edu/>. Mingguang Shan was supported by National Natural Science Foundation of China (61377009), China Scholarship Council (201506685053) and Fundamental Research Funds for the Central Universities of China. Viorel Nastasa was supported by the Fulbright Senior Postdoctoral Program 2015-2016.

1. Z. Wang, L. J. Millet, M. Mir, H. Ding, S. Unarunotai, J. A. Rogers, M. U. Gillette and G. Popescu, Spatial light interference microscopy (SLIM), *Opt. Exp.*, 19, 1016 (2011);

2. T. Kim, R. Zhou, L. L. Goddard and G. Popescu, Quantitative phase imaging (QPI): Metrology meets biology, *Photonics Journal, IEEE*, 6 (2), 1 (2014).

# *In vitro* biological performance of multifunctional composite coatings

P. Neacsu<sup>1</sup>, V. Dinca<sup>2</sup>, S. Brajnicov<sup>2,3</sup>, V. Marascu<sup>2,4</sup>, L. Rusen<sup>2</sup>, L.N. Dumitrescu<sup>2,3</sup>, M. Dinescu<sup>2</sup> and A. Cimpean<sup>1</sup>

<sup>1</sup>University of Bucharest, Department of Biochemistry and Molecular Biology, 91-95 Spl. Independentei, 050095, Bucharest, Romania

<sup>2</sup>National Institute for Lasers, Plasma and Radiation Physics, Atomistilor 409, 077125, Magurele, Bucharest, Romania

<sup>3</sup>University of Craiova, Faculty of Mathematics and Natural Sciences, RO-200585, Craiova, Romania

<sup>4</sup>University of Bucharest, Faculty of Physics, RO-077125, Magurele, Romania  
anisoara.cimpean@bio.unibuc.ro valentina.dinca@inflpr.ro

The surface characteristics of materials surface in terms of topography, surface energy or chemistry, play an important role in cell behavior having implications over long term cell-substrate interactions both *in vitro* and *in vivo*<sup>1</sup>.

The objective of our study was to evaluate the *in vitro* response of MC3T3-E1 pre-osteoblasts to multifunctional poly(ethylene glycol)-block-poly( $\epsilon$ -caprolactone) methyl ether-hydroxyapatite (PEG-PCL-HA) coatings deposited by Matrix Assisted Pulsed Laser Evaporation technique. These coatings were combined with lactoferrin (PEG-PCL-HA-LF) which was reported to stimulate osteoblast proliferation and inhibit osteoclast activity in bone cell culture. These two substrates were compared with deposited polymer (PEG-PCL), hydroxyapatite (HA) and lactoferrin (LF), and tissue culture plates (TCPS) as usual substrates for cell cultures. The cell culture-based studies have been performed in terms of cell viability/proliferation, cell adhesion and morphology and osteoblast differentiation (extracellular matrix mineralization, alkaline phosphatase activity and expression levels of collagen). Lactate dehydrogenase activity, assessed in cell culture media as a relevant toxicity marker, recorded an almost constant low level over 1-, 3- and 5-day culture periods for all analyzed coatings, suggesting that they are biocompatible. Moreover, these coatings promoted cell proliferation in similar extent as established by MTT assay. Fluorescent staining of actin cytoskeleton and vinculin at 4h post-seeding demonstrated that MC3T3-E1 cells equally spread on all coatings excepting HA coating where they were less spread. However, at 24h post-seeding the cells adopted typical osteoblast morphologies with well-defined stress fibers and almost similar cell density (Fig. 1).

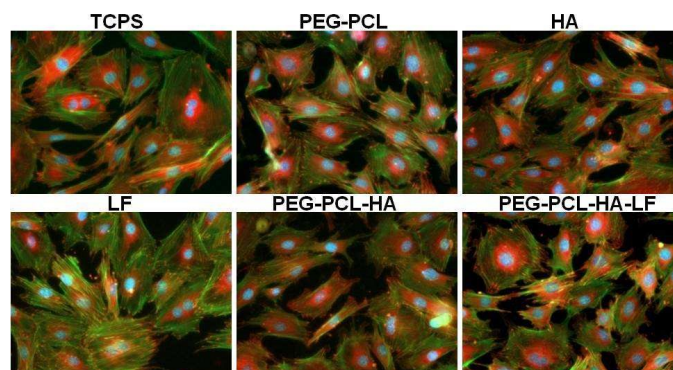


Figure 1: Fluorescent microscopy images of MC3T3-E1 pre-osteoblasts cultured for 24 h on TCPS, PEG-PCL, HA, LF, PEG-PCL-HA and PEG-PCL-HA-LF substrates. Actin (green); Vinculin (red).

An essential requirement for a candidate material to significantly improve the speed of bone formation on its surface is the ability to promote bone matrix maturation and mineralization. In this work, the extracellular matrix mineralization was quantified by Alizarin red staining at 2 and 4 weeks after cell seeding both in standard and pro-osteogenic (stimulation with ascorbic acid and  $\beta$ -glycerophosphate) culture conditions. Notably at 4 weeks post-seeding the PEG-PCL-HA-LF coating promoted extracellular matrix mineralization at cell-material interface to the highest extent. Furthermore, the alkaline phosphatase activity recorded significant increased levels after 10 days of culture in pro-osteogenic culture conditions in preosteoblasts grown on LF, PEG-PCL-HA and PEG-PCL-HA-LF coatings. Collagen secretion was quantified by Sirius red staining. The results obtained at 4 weeks post-seeding in pro-osteogenic culture conditions have shown that on all studied coatings were expressed higher levels of collagen than on TCPS substrate. Our *in vitro* findings indicate that the multifunctional PEG-PCL-HA coatings elicit a positive osteoblast response showing promise for future biomedical applications.

**Acknowledgments:** This work was supported by Romanian National Authority for Scientific Research (CNCS – UEFISCDI), under the projects PNII-PT-PCCA-2013-4-199, PN-II-RU-TE-2014-4-2434 and Nucleus programme-contract 4N/2016

1. Klaus Gottfredsen, Implant Surfaces and their Biological and Clinical Impact (Springer-Verlag Berlin Heidelberg), Implant Coating and Its Application in Clinical Reality (2015).

# Functionalized Graphene Oxide nanoscale thin films for melanoma therapy

I. Negut<sup>1</sup>, V. Grumezescu<sup>1</sup>, C. Hapenciu<sup>1</sup>, C.R. Luculescu<sup>1</sup>, F. Sima<sup>1</sup>, L.E. Sima<sup>2\*</sup> and E. Axente<sup>1,\*</sup>

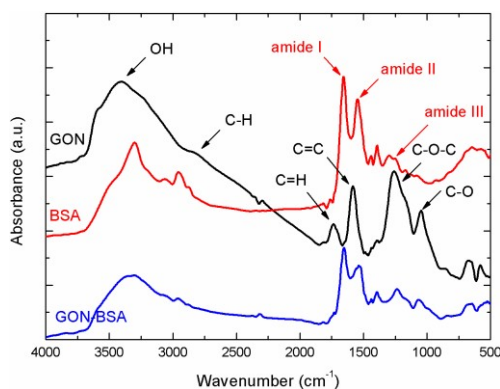
<sup>1</sup>Laser-Surface-Plasma Interactions Laboratory, National Institute for Lasers, Plasma and Radiation Physics, 077125 Măgurele, Romania

<sup>2</sup>Department of Molecular Cell Biology, Institute of Biochemistry, Romanian Academy, 296 Splaiul Independentei, 060031, Bucharest 17, Romania  
lsima@biochim.ro, emmanuel.axente@inflpr.ro

Melanoma, the most dangerous skin cancer, is caused by the transformation of melanocytes (pigment-producing cells) that suffered genetic alterations, thus leading to abnormal proliferation and dissemination.<sup>1</sup> All major cancer therapies, including chemo-, immuno-, and radio-therapies failed to increase patients' survival rates.<sup>2</sup> This failure is attributed to different resistance mechanisms, the tumor cells developing a drug-resistant subpopulation, behaving as a "moving target".<sup>3</sup>

On the other hand, Graphene Oxide Nanomaterials (GON) have proven fascinating properties, several applications being actively explored by the scientific community.<sup>4</sup> However, the merging of graphene and graphene oxide with biotechnology is still in its infancy, many challenges remaining unexplored. Potential applications are related to biosensors, drug delivery or gene therapy and cells imaging.<sup>5</sup> One major advantage is their high specific surface area, which allows high-density drug loading. The cytotoxicity of graphene and its derivatives is highly dependent on surface functionalization.

Here we report on the noncovalent GON surface conjugation with Bovine Serum Albumin (BSA) followed by thin films assembling by Matrix-Assisted Pulsed Laser Evaporation (MAPLE) technique. In a first step, aqueous solutions consisting of serial dilutions of both GON and GON-BSA (GONB) conjugates were submitted to cytotoxicity tests. Safe concentration windows were identified against different melanoma cell lines, while melanocytes and human dermal fibroblasts were used as normality controls. A parametric study was devoted then to thin films synthesis by MAPLE. Optimal deposition conditions were found and used for nanomaterials



assembling on glass and silicon substrates. Surface characteristics were evaluated by optical, atomic force and scanning electron microscopies. Fourier Transform Infrared (FTIR) Spectroscopy was used to monitor the composition of GON, BSA and their mixtures (Figure 1). *In vitro* assays did not evidence a cytotoxic effect of all cell lines due to MAPLE transfer and assembling.

Figure 1: FTIR spectra of GON, BSA and GON-BSA nanomaterials collected on Silicon substrates.

1. A. Vultur and M. Herlyn, *Cancer Cell*, **23**, Issue 5, p706–706, (2013);
2. A. Roesch *et al.*, *Cancer Cell* **23**, 811–825, (2013);
3. H. Hoag, *Nature*, **515**, S118–S120, (2014);
4. A.K. Geim, *Science* **324**, 1530–1534 (2009);
5. V.C. Sanchez *et al.*, *Chem Res Toxicol.* **25**(1): 15–34 (2012).

## MAPLE deposition of Fe<sub>3</sub>O<sub>4</sub> nanoparticles functionalized with *Nigella sativa* for antimicrobial applications

I. Negut<sup>1,2</sup>, V. Grumezescu<sup>2,3</sup>, A.M. Holban<sup>4</sup>, F. Iordache<sup>5</sup>, R. Trusca<sup>6</sup>, M. Petrus<sup>2</sup>, G. Socol<sup>2</sup>

<sup>1</sup> Faculty of Physics, University of Bucharest, Magurele, Ilfov, Romania, 077125

<sup>2</sup> National Institute for Lasers, Plasma, and Radiation Physics, 409 Atomistilor Street, RO-77125, MG-36, Magurele - Ilfov, Romania

<sup>3</sup> Faculty of Applied Chemistry and Materials Science, Politehnica University of Bucharest, Polizu Street, No. 1–7, Bucharest, Romania

<sup>4</sup> Faculty of Biology, University of Bucharest, Microbiology Immunology Department, Aleea Portocalelor 1-3, Sector 5, 77206 Bucharest, Romania

<sup>5</sup> Institute of Cellular Biology and Pathology of Romanian Academy, "Nicolae Simionescu", Department of Fetal and Adult Stem Cell Therapy, 8, B.P. Hasdeu, Bucharest 050568, Romania

<sup>6</sup> S.C. Metav-CD S.A., 31 Rosetti Str., 020015 Bucharest, Romania  
negut.irina@inflpr.ro

*Nigella sativa* is a plant commonly used in various alternative medicine systems like Ayurveda, Siddha, Unani and Tibb. Numerous scientific studies on *Nigella sativa* revealed its pharmacological actions like antimicrobial, analgesic, spasmolytic, anti-inflammatory, hepato-protective, etc.

The aim of this study was to fabricate novel biocompatible assemblies containing iron oxide nanoparticles functionalised with *Nigella sativa* oil (Fe<sub>3</sub>O<sub>4</sub>@*Nigella sativa*) and Fe<sub>3</sub>O<sub>4</sub>@*Nigella sativa* embedded into poly(lactic-co-glycolic acid) (Fe<sub>3</sub>O<sub>4</sub>@*Nigella sativa*-nPLGA) capsules used in form of coatings grown by Matrix-Assisted Pulsed Laser Evaporation (MAPLE) technique.

The obtained samples were physico-chemically evaluated by Fourier Transform Infrared Spectroscopy and Infrared Mapping Spectroscopy, Scanning Electron Microscopy, Transmission Electron Microscopy and X-ray Diffraction.

The biological response of coatings was evaluated by *in vitro* assays while the antimicrobial activity was tested with respect to *Gram positive* and *Gram negative* microbial strains.

## Photocatalytic degradation of methylene blue by a combination of TiO<sub>2</sub> and charcoal

N. Popa<sup>1</sup>, M. Visa<sup>1</sup>

<sup>1</sup>R&D Center Renewable Energy Systems and Recycling, Transilvania University of Brasov, Eroilor 29, 500036, Brasov, Romania.  
popanicol@yahoo.com

Colored wastewater is released in textile effluents and poses a potential environmental hazard. Moreover, a variety of organic chemicals are produced during the dyeing process, and some have been shown to be carcinogenic.

The goal of this paper is to develop a new material (composite) from charcoal and TiO<sub>2</sub> Degussa P25 which was further used for the advanced treatment of wastewaters with pollutants load. The investigation of the effectiveness of the removal of one dye (methylene blue - MB) from synthetic wastewaters was studied. The photodegradation of organic pollutants by composite TiO<sub>2</sub>/MRDSD was studied under irradiation with UV. The composite used as a substrate in adsorption processes and as a photocatalyst (under UV radiation) was synthesized through sonication method from activated charcoal (obtained from forest waste by distillation without air) and Degussa P25. Surface characterization included micro-porosity and BET surface area measurements (Autosorb-IQ-MP, Quantachrome Instruments), roughness and macro-pores size distribution using AFM (Ntegra Spectra, NT-MDT model BL222RNTE, in semi-contact mode with Golden silicon cantilever, NCSG10, at constant force 0.15 N/m, with a 10nm tip radius) and morphology using scanning electron microscopy before and after adsorption (SEM, S-3400N- Hitachi, accelerating voltage of 20 KV) Fig. 1a. The surface elemental composition was evaluated using energy dispersive X-ray spectroscopy (EDS Thermo Scientific Ultra Dry).

The crystallinity of the material was evaluated with X-ray diffraction (XRD) for phase and crystalline analysis and the optical band gap was estimated based UV-VIS spectroscopy.

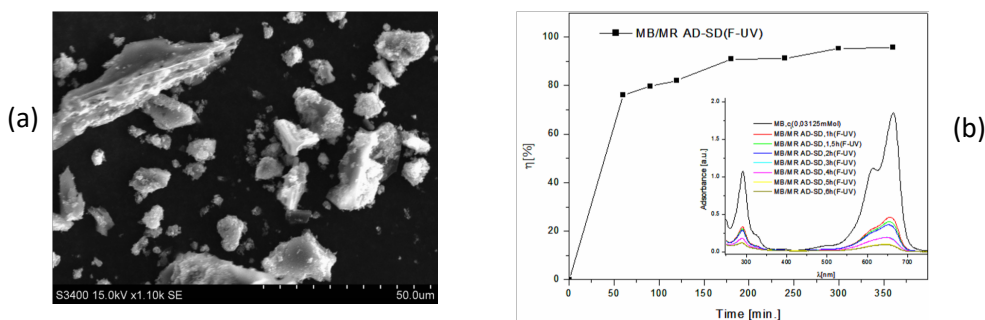


Figure 1: (a) SEM image for MRDSD material. (b) Efficiency of photodegradation of Methylene Blue

The results show that this composite is as a viable, low cost, up-scalable and sustainable technology along with the parallel process involving the photodegradation and adsorption of dye. For obtaining a maximum efficiency during the photocatalytic processes some parameters such as pH, the contact time, the amount of substrate and the initial concentration of pollutants were optimized. The dye quantitative analysis was done by UV-VIS spectroscopy (Perkin Elmer Lambda 25). These parameters were further used in thermodynamic and kinetic studies. The results show, that MB removal runs with the highest efficiency and the effect of irradiation is major on this pollutant (95.68%), in adsorption in dark (54.74%) and in photocatalytic conditions. The kinetic studies indicate that the removal of MB pollutant follows the pseudo-second order equation.

*Acknowledgments:* This work was supported by a grant Transilvania University of Brasov, Doctoral Programme

# Structural and morphological characterization of MAPLEdeposited thin films from TiO<sub>2</sub>-SnO<sub>2</sub> NPs obtained by different methods

A. M. Niculescu<sup>1,2</sup>, C. T. Fleaca<sup>1</sup>, M. Scarisoreanu<sup>1</sup>, M. Dumitru<sup>1</sup>, C. Luculescu<sup>1</sup>, M. Dinescu<sup>1</sup>, I. Morjan<sup>1</sup>

<sup>1</sup>National Institute for Lasers, Plasma and Radiation Physics, 409 Atomistilor Str., 77125 Bucharest- Magurele, Romania

<sup>2</sup>University of Craiova, Faculty of Mathematics and Natural Sciences, RO-200585, Craiova, Romania  
niculescu.anam@gmail.com

The aim of this work is to compare different methods of ZnO nanoparticles synthesis regarding their structure and morphology in order to decide which of them is better for specific applications. We prepared ZnO nanoparticles through: laser pyrolyses technique (LP), laser ablation of a metallic target in aqueous solution using ultrafast and high power lasers (LLA) and solid state combustion (SSC). The as-synthesized powders were investigated with: X-ray diffraction (XRD), Scanning Electron Microscopy (SEM) coupled with Energy Dispersive X-ray Spectroscopy (EDX), Atomic force Microscopy, Raman spectroscopy and Dynamic Light Scattering (DLS), for search the capability of nanopowders to form stable colloids. The resulted informations obtained from samples investigations will be used in the obtaining process of gas sensors using MAPLE (Matrix assisted pulser laser evaporation) method, in which the structure, morphology and stability of dispersions in time are essentials to obtain successfully thin films.

## Investigation of colloidal zinc oxide nanoparticles produced by laser ablation of zinc target in water

R.G. Nikov<sup>1</sup>, N.N. Nedyalkov<sup>1</sup>, P.A. Atanasov<sup>1</sup>, D.B. Karashanova<sup>2</sup>, J.W. Gerlach<sup>3</sup>,  
B. Rauschenbach<sup>3</sup>, I.N. Mihailescu<sup>4</sup>

<sup>1</sup>Institute of Electronics, Bulgarian Academy of Sciences, Tsarigradsko Chaussee 72, Sofia 1784, Bulgaria

<sup>2</sup>Institute of Optical Materials and Technologies, Bulgarian Academy of Sciences, G. Bonchev Street, bl. 109, Sofia 1113, Bulgaria

<sup>3</sup>Leibniz Institute of Surface Modification (IOM), 15 Permoserstrasse, D-04318 Leipzig, Germany

<sup>4</sup>National Institute for Lasers, Plasma and Radiation Physics, PO Box MG-36, RO-77125, Magurele, Ilfov, Romania  
rosen\_nikov@abv.bg

Zinc oxide (ZnO) nanoparticles were synthesized using nanosecond pulsed laser ablation of high purity zinc target immersed in double distilled water. The effect the laser wavelength on the optical properties and structure of the synthesized ZnO nanostructures was studied. For this purpose four different wavelengths: fundamental wavelength (1064 nm), second (532 nm), third (355 nm) and fourth (266 nm) harmonic of a Nd:YAG laser were used in the experiments. The influence of the laser pulse energy on the characteristics of produced nanoparticles was also studied. The produced colloidal nanostructure have been studied using characterization techniques like transmission electron microscopy (TEM), selected area electron diffraction (SAED), X-ray diffraction (XRD) and UV-Vis spectroscopy in order to evaluate their morphology, size distribution, crystalline structure and optical properties. XRD results reveal that in the day of preparation the samples are crystalline and contain both zinc and zinc oxide particles. The optical transmission measurements of the colloids were carried out at different intervals of time after the preparation in order to trace the changes that occur in them. TEM results reveal that the obtained nanoparticles are spherical or spherical-like in shape showing particle sizes less than 100 nm. The presented method can be an efficient alternative for fabrication of metal oxide nanostructures with application in biomedicine, photonics and sensor devices.



# Investigation of Au nanostructures fabricated by laser ablation in air

Ru. Nikov<sup>1</sup>, A. Dikovska<sup>1</sup>, N. Nedyalkov<sup>1</sup>

<sup>1</sup>*Institute of Electronics, Bulgarian Academy of Sciences, Tsarigradsko Chaussee 72, Sofia 1784, Bulgaria  
rumen\_nikov24@abv.bg*

In this paper we demonstrate fabrication of Au nanostructures by direct deposition of Au nanoparticles and aggregates produced by pulsed laser ablation in air at atmospheric pressure. Due to the high density of the ambient atmosphere the plasma plume is strongly confined. At these conditions the nanoparticle formation occurs in the plume by intensive collisions of the species and condensation of the ablated material. The ablation process of Au is performed by nanosecond laser pulses delivered by Nd:YAG laser system as the ablated material is deposited on quartz substrate in air environment. Characteristics of the fabricated structures are studied as a function of the laser wavelength, the laser fluence and the geometry of the deposition process. The complex structure observed in the fabricated samples suggests that they could be successfully used in applications as surface enhanced Raman spectroscopy (SERS) and sensors devices.

## Fabrication of Ag nanoparticle array on different substrates for application in SERS

Ru. Nikov<sup>1</sup>, N. Nedyalkov<sup>1</sup>, P. Atanasov<sup>1</sup>, D. Hirsch<sup>2</sup>, B. Rauschenbach<sup>2</sup>, K. Grochowska<sup>3</sup>,  
G. Sliwinski<sup>3</sup>, I. N. Mihailescu<sup>4</sup>

<sup>1</sup>*Institute of Electronics, Bulgarian Academy of Sciences, Tsarigradsko shousse 72, Sofia 1784, Bulgaria*

<sup>2</sup>*Leibniz Institute of Surface Modification (IOM), 15 Permoserstrasse, D-04318 Leipzig, Germany*

<sup>3</sup>*Centre for Plasma and Laser Engineering, The Szevalski Institute, Polish Academy of Sciences, 14 Fiszerka St., 80-231 Gdansk, Poland*

<sup>4</sup>*National Institute for Lasers, Plasma and Radiation Physics, PO Box MG-36, RO-77125, Magurele, Ilfov, Romania  
rumen\_nikov24@abv.bg*

We present results on laser-assisted fabrication of Ag nanostructured films deposited on different substrates. The thin films are obtained by pulsed laser deposition technology on dielectric and metal substrates. The as deposited films are then annealed by laser pulses delivered by nanosecond Nd:YAG laser system operated at  $\lambda=355$  nm. At certain conditions, the laser processing can result in decomposition of the thin film into array of nanoparticles on the substrate. The characteristics of the obtained film modifications are studied as a function of the annealing conditions – number of the laser pulses and fluence of the laser pulses. The morphology of the samples surface is investigated by means of scanning electron microscopy. The optical properties study based on structure's extinction spectra shows that film decomposition into nanoparticles results in clear peak in the spectra. This effect, called Surface Plasmon Resonance (SPR), is related to efficient excitation of plasmons in the nanostructures. The intensity and the position of the SPR peak are found to depend on both the processing parameters and the type of the substrate. The fabricated structures are covered with Rhodamine 6G and tested as active substrate for Surface Enhanced Raman Spectroscopy (SERS).

## Zn<sub>1-x</sub>Fe<sub>x</sub>O thin films grown by pulsed laser deposition: from transparent Fe-diluted ZnO wurtzite to magnetic Zn-diluted Fe<sub>3</sub>O<sub>4</sub> spinel

M. Nistor<sup>1</sup>, J. Perrière<sup>2,3</sup>, C. Hebert<sup>2,3</sup>, E. Millon<sup>4</sup>, J.J. Ganem<sup>2,3</sup>, N. Jedrecy<sup>2,3</sup>

<sup>1</sup>*National Institute for Lasers, Plasma and Radiation Physics (NILPRP), Plasma Physics and Nuclear Fusion Laboratory (L 22),  
Str. Atomistilor 409, P.O. Box. MG-36, 77125 Bucharest-Magurele, Romania*

<sup>2</sup>*Sorbonne Universités, UPMC Univ. Paris 06, UMR 7588, INSP, F-75005, Paris, France*

<sup>3</sup>*CNRS, UMR 7588, INSP, F-75005, Paris, France*

<sup>4</sup>*GREMI, UMR 7344 CNRS-Université d'Orléans, F-45067 Orléans Cedex 2, France  
mnistor@infim.ro*

Transition metal doped ZnO thin films have been widely studied as a promising diluted magnetic semiconductor with potential applications in spintronics. In particular, the ferromagnetic properties of Fe doped ZnO thin films are controversial and confusing. In this work Zn<sub>1-x</sub>Fe<sub>x</sub>O films (0 < x < 1) were grown on c-cut sapphire substrates by pulsed laser deposition to determine the effects of doping concentration on the structural and physical properties<sup>1</sup>. The phase diagram of Zn<sub>1-x</sub>Fe<sub>x</sub>O films (0 < x < 1) was obtained as well that of the physical properties. For 0 < x < 0.3, epitaxial films with wurtzite (ZnO-like) structure were obtained without noticeable electrical or magnetic properties. For 0.6 < x < 1 spinel (Fe<sub>3</sub>O<sub>4</sub>-like) epitaxial films present room temperature ferromagnetism and spin polarized charge transport

properties. In the intermediate region ( $0.35 < x < 0.65$ ) the phase separation of the  $Zn_{1-x}Fe_xO$  films leads to the formation of nanocomposite oxide films. Indeed, depending upon the conditions (temperature and oxygen pressure) wurtzite and FeO, wurtzite and spinel or FeO and spinel phases were grown, inducing different optical absorption in the visible wavelength domain and limiting the electrical conductivity. These optical, electrical and magnetic properties of the  $Zn_{1-x}Fe_xO$  films are presented and discussed in relation with their structural characteristics.

J. J. Perriere, C. Hebert, M. Nistor, E. Millon, J. J. Ganem and N. Jedrecy,  $Zn_{1-x}Fe_xO$  films: from transparent Fe-diluted ZnO wurtzite to magnetic Zn-diluted  $Fe_3O_4$  spinel, *J. Mater. Chem. C* **3**, 11239 - 11249 (2015).

## Femtosecond laser induced surface structures on silicon: effects of the ambient pressure

J. JJ Nivas<sup>1,2</sup>, Z. Song<sup>1,3</sup>, A. Vecchione<sup>4</sup>, R. Fittipaldi<sup>4</sup>, R. Bruzzese<sup>1,2</sup>, S. Amoruso<sup>1,2</sup>

<sup>1</sup>Dipartimento di Fisica "Ettore Pancini", Università di Napoli "Federico II", Complesso Universitario di Monte S. Angelo, Via Cintia, I-80126 Napoli (Italy)

<sup>2</sup>CNR-SPIN, UOS Napoli, Complesso Universitario di Monte S. Angelo, Via Cintia, I-80126 Napoli (Italy)

<sup>3</sup>School of Science, Tianjin Polytechnic University, Binshuixi Road 399#, Xiqing District, Tianjin, 300387 P. R. China.

<sup>4</sup>CNR-SPIN, UOS Salerno, Via Giovanni Paolo II 132, I-84084 Fisciano (SA), Italy  
 amoruso@na.infn.it; salvatore.amoruso@unina.it

Irradiation of crystalline silicon with femtosecond laser pulses produces a variety of quasi-periodic surface structures, among which subwavelength ripples creation is largely studied. More recently, the seldom considered issue of quasi-periodic, micron-spaced grooves formation is receiving increasing attention.<sup>1-3</sup> Previous studies on surface structures formation on crystalline silicon have been generally carried out in ambient air at atmospheric pressure, while investigations on the effect of the environment pressure on the generated structures remains still scarce. Here we report an experimental investigation on the creation of surface structures on a crystalline silicon (intrinsic) target. The target is irradiated by a sequence of pulses produced by a Nd:glass laser ( $\approx 850$  fs pulse duration, 1054 nm wavelength). Direct femtosecond laser surface structuring is carried out both in ambient air ( $p=1$  atm) and in a vacuum ( $p\sim 10^{-5}$  mbar), while the other experimental parameters remain unchanged. In particular, the morphological evolution of ripples and grooves with the number of pulses  $N$ , and laser pulse energy  $E_L$  is characterized, for different directions of the linear polarization of the laser beam, by Scanning Electron Microscopy (SEM). Our experimental findings evidence striking differences between the characteristics of the surface structures formed in ambient air and in a vacuum, and an intriguing effect of the laser polarization direction on the structured area for the vacuum conditions. Figure 1 reports an example of a typical SEM image of the surface after irradiation in air evidencing that: i) the central area, at higher laser fluence, is characterized by an array of micro-grooves; ii) the typical pattern of quasi-periodic ripples orthogonal to the laser polarization are present in the outer region of the spot, at lower fluence; iii) these two regions are separated by an intermediate annulus where grooves rudiments decorate the underlying ripples; iv) an outer ring of nanoparticles decorating the target surface. The samples irradiated in high vacuum conditions evidence many distinct characteristic morphological features with respect to air conditions, which will be illustrated and discussed in this communication and might help gaining more

knowledge on the intriguing mechanisms involved in surface structures formation by direct femtosecond laser surface processing.

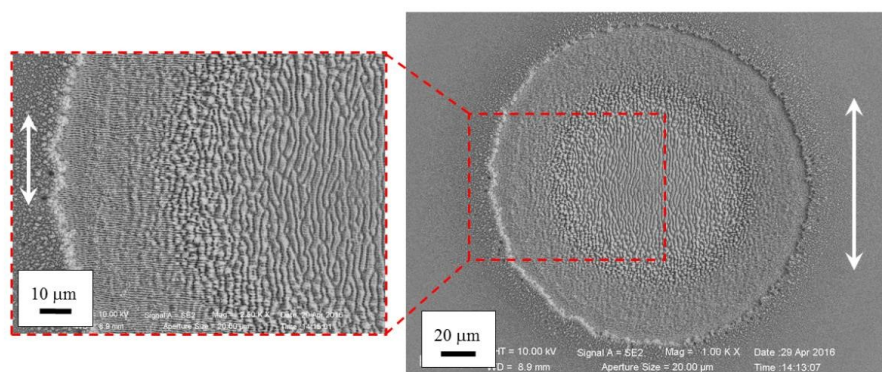


Figure 1: SEM image (right panel) illustrating the typical morphology of the silicon target surface after irradiation with a sequence of  $N=300$  laser pulses, in air, at a laser pulse energy  $E_L \approx 140 \mu J$ . The left panel shows a zoomed area evidencing the characteristic morphology of the various regions. The white double-headed arrow indicates the direction of the incident laser polarization.

1. S. He, J. JJ Nivas, A. Vecchione, M. Hu, S. Amoruso, On the generation of grooves on crystalline silicon irradiated by femtosecond laser pulses, *Opt. Express*, **24**, 3238-3247 (2016);
2. S. He, J. JJ Nivas, K.K. Anoop, A. Vecchione, M. Hu, R. Bruzzese, S. Amoruso, Surface structures induced by ultrashort laser pulses: Formation mechanisms of ripples and grooves, *Appl. Surf. Sci.*, **353**, 1214-1222 (2015);
3. G.D. Tsibidis, C. Fotakis, and E. Stratakis, From ripples to spikes: A hydrodynamical mechanism to interpret femtosecond laser-induced self-assembled structures, *Phys. Rev. B*, **92**, 041405(R) (2015).

# The thermal field in laser – double Nano-particles layered interaction

M. Oane<sup>1</sup>, R. V. Medianu<sup>1</sup>, O. Pacala<sup>2</sup>

<sup>1</sup>National Institute for Lasers, Plasma and Radiation Physics (NILPRP), Magurele, Romania

<sup>2</sup>Institute of Atomic Physics, Magurele, Romania

In the present work we want to figure out the difference between thermal fields in double bulk layered interaction and double nano-particles layered media. We choose the same materials for bulk and nano-particles media, the only reason for the differences being the scale of the irradiated samples. From mathematical point of view we will use the Green function method.

## Experimental analysis and comparison on laser ablations of a cobalt cemented tungsten carbide using various pulse lasers

Kwang H. Oh<sup>1</sup>, D. S. Kim<sup>1</sup>, S. J. Bong<sup>1</sup>, H. S. Hong<sup>1</sup>, J. Y. Oh<sup>1</sup>

<sup>1</sup>Laser Advanced System Industrialization Center, Jeonnam Technopark, Jangseong-gun, Jeollanam-do, 57248, South Korea

twins02@jntp.or.kr

Pulse length and wavelength of lasers are important factors for interaction between lasers and materials. Especially in deep micro-hole drilling, these laser conditions are considered carefully because a large heat affected zone (HAZ) and burr are induced due to accumulated pulse energy in materials. In this study, we apply various pulse lasers such as UV, Visible and IR fs-laser, and also UV, Visible and IR ps-laser to investigate the laser ablation of the cobalt cemented tungsten carbide. With the comparative analysis of the laser ablations for various pulse lasers, we search an optimum condition of deep micro-hole drilling of the cobalt cemented tungsten carbide.

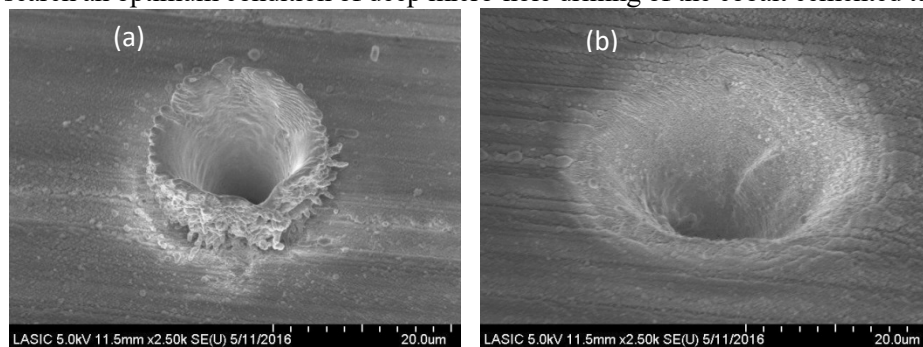


Figure 1: SEM images of the cobalt cemented tungsten carbide surface ablated by (a) IR fs laser, and (b) Visible fs laser.

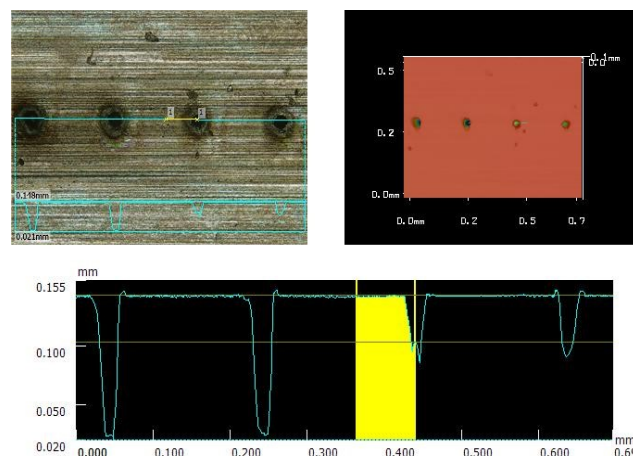


Figure 2: Analysis of ablated depth according to laser fluence and pulse number for deep micro-hole drilling.

1. J.P. Calderon Urbina, C. Daniel, C. Emmelmann, Experimental and analytical investigation of cemented tungsten carbide ultra-short pulse laser ablation, *Physics Procedia*, **41**, 752-758 (2013);
2. G. Dumitru, V. Romano, H.P. Weber, Y. Gerbig, H. Haefke, S. Bruneau, J. Hermann, M. Sentis, Femtosecond laser ablation of cemented carbides: properties and tribological applications, *Applied Physics A*, **79**, 629-632 (2004);
3. Manuel Pfeiffer, Andy Engel, Steffen Weißmantel, Stefan Scholze, Guenter Reisse, Microstructuring of steel and hard metal using femtosecond laser pulses, *Physics Procedia*, **12**, 60-66(2011).

# Three-Dimensional Numerical Simulation of Laser Processing of CFRP

T. Ohkubo, M. Tsukamoto, Y. Sato

<sup>1</sup>Tokyo University of Technology, 1404-1, Katakura-chou, Hachioji-shi, Tokyo, 192-0914, Japan

<sup>2</sup>Smart Beam Processing Research Center, Joining and Welding Research Institute, Osaka University, 11-1 Mihogaoka Ibaraki-shi Osaka, 567-0047, Japan  
ookubotmms@stf.teu.ac.jp

We performed three-dimensional numerical simulation of laser processing of carbon-fiber-reinforced plastic (CFRP) using OpenFOAM<sup>1</sup> as libraries of finite volume method. Although a little theoretical or numerical studies about HAZ formation were performed<sup>2-5</sup>, there is no research considering heat generation of oxidization of materials. It is important to understand the effect of background gas about generation of heat-affected zone (HAZ) in order to improve quality of CFRP cutting by laser.

To develop the new calculation model to consider the effect of combustion and decomposition of each element of CFRP, thermo gravity analysis (TGA) and differential thermal analysis (DTA) was performed about CFRP in the air condition. The results of TG-DTA experiments are shown in Figure 1.

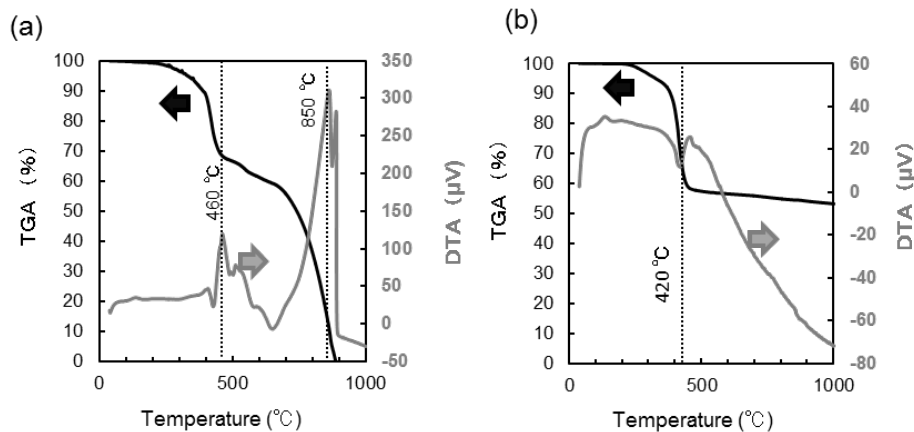


Figure 1: TG-DTA analysis on CFRP (a): in the air (b): Ar gas ambience.

Considering heat generation which is known from the result of TG-DTA analysis, we calculated heat transfer inside CFRP. Results of experiment and calculation are shown in Figure 2. This new model succeeded in simulating HAZ formation qualitatively.

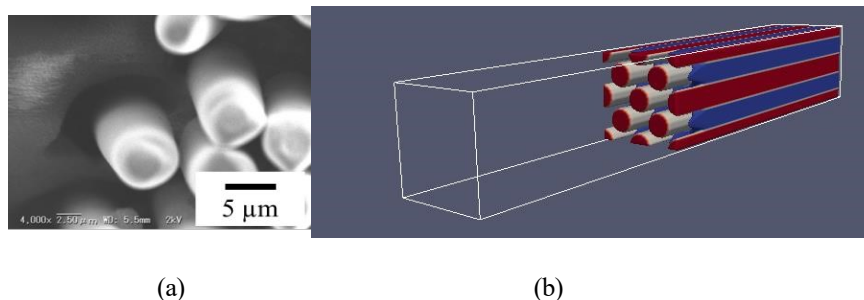


Figure 2: Results of experiment and numerical simulations. (a) Experimental result. (b) Result of numerical simulation. White line is original size. Red and gray region is carbon fiber and blue region is resin. In this report, we discuss this new calculation model and results.

1. OpenFOAM, <http://www.openfoam.org>;
2. Tagliaferri V., Di Ilio A., and Visconti I. C., "Laser cut-ting of fibre-reinforced polyesters". *Composites*, 16(4), 317-325.(1985);
3. Pan C. T. and Hocheng H, "The anisotropic heat-affect zone in the laser grooving of fibre-reinforced composite material", *J.Mater.Process.Technol.*, 62, 54-60(1996);
4. Uhlmann E., Spur G., Hocheng H., Leibelt S. and Pan C. T. "The extent of laser-induced thermal damage of UD and crossply composite laminates", *In.J. Machine Tools Mf.*, 39, 639-650(1999);
5. R. Negarestani, M. Sundar, M. A. Sheikh, P. Mativenga, L. Li, Z. L. Li, P. L. Chu, C. C. Khin, H. Y. Zheng and G. C. Lim, "Numerical simulation of laser machining of carbon-fibre-reinforced composites", *Proc. IMechE Vol. 224 Part B: J. Engineering Manufacture*, pp1017-1027,(2010).

# Analytical expansion of vector complex source vortex beams into vector spherical harmonics and their interaction with a nanoparticle

S. Orlov

Center for Physical Sciences and Technology, Savanoriu Ave. 231, LT-02300, Vilnius, Lithuania  
Sergejus.Orlovas@ftmc.lt

Among the active fields of research in nanosciences are nanoparticles and their properties. The Mie theory was the very first description of light interaction with a particle and it was extended for describing the interaction with highly focused beams. The polarization properties of highly focused electromagnetic beams strongly influence the size and shape of the focal spot of the beams<sup>1</sup>. In recent publications, the interaction between such beams and nanoparticles has been investigated<sup>2</sup>. The optical response of the nanoparticle is strongly dependent both on the particle location in the focal plane and on the polarization state of the beam, and it differs notably from that of the classical Mie theory<sup>2</sup>. An accurate analytical description of highly focused linearly, radially and azimuthally polarized light beams can be obtained via an extension of the so-called complex source beam (CSB) model<sup>3</sup>. Furthermore, the CSB model can be also employed for an accurate and unified vectorial description of highly focused vortex beams of various polarizations that are rigorous solutions of Maxwell's equations<sup>4</sup>.

In this work, I theoretically investigate the interaction of vector complex-source vortices (CSV) with a spherical particle placed in the focal plane. I start by expanding CSVs analytically into vector spherical harmonics (VSHs). Such an expansion is essential for understanding the interaction of light with nano-objects such as atoms, molecules or particles. Those nano-objects locally respond to the various multipole components of the incident field. Normally, the dipole components are dominant, but nano-structures, such as (meta-) atoms are also capable of sensing quadrupole and even higher order excitations<sup>5</sup>. By knowing the expansion of optical beams into multipoles, it is straightforward to study the interaction of a beam with larger objects, which are conveniently described by a T-matrix. Moreover, this multipole approach also provides an efficient method for the exact nanointerferometric amplitude and phase reconstruction of tightly focused vector beams<sup>6</sup>.

I report on the defocusing of highly focused CSVs as they interact with a spherical particle placed in the focal plane. The generalized Mie theory is used to investigate the scattering off a spherical gold particle in detail (Fig. 1).

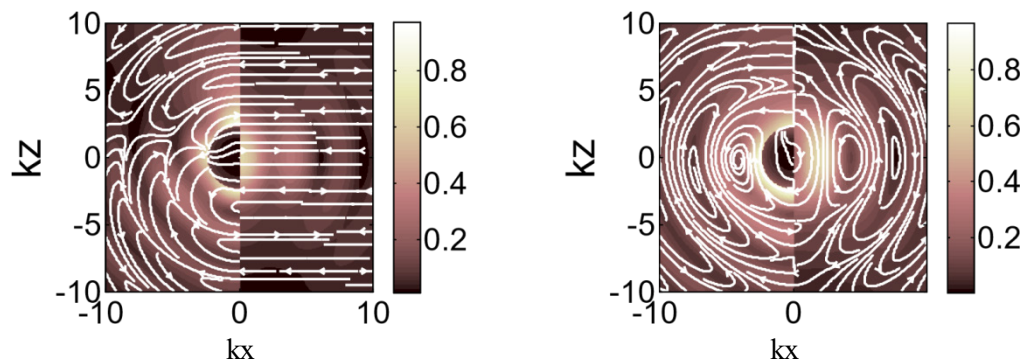


Figure 1: Modulus of the total (left side) and incident (right side) fields for transverse electric  $U_M$  (a) and transverse magnetic  $U_N$  (b) CSV scattered off a gold sphere placed centrally at the waist of the beam. One particular case of CSVs is considered - vector vortex beams with cylindrical symmetry of either electric or magnetic fields<sup>4</sup>. The radius of the sphere is  $R_{sp} = 200$  nm, the wavelength is  $\lambda = 530$  nm and  $kz_0 = 1.5$ , where  $k$  is the wave vector and  $z_0$  is the diffraction length. The white arrows depict of a snapshot of the directions the electric field.

1. S. Quabis, R. Dorn, M. Eberler, O. Glöckl, and G. Leuchs, "Focusing light to a tighter spot", *Opt. Commun.*, **179**, 1 (2000);
2. S. Orlov, U. Peschel, T. Bauer, and P. Banzer, "Analytical expansion of highly focused vector beams into vector spherical harmonics and its application to Mie scattering", *Phys. Rev. A* **85**, 063825 (2012);
3. S. Orlov and U. Peschel, "Complex source beam: A tool to describe highly focused vector beams analytically", *Phys. Rev. A* **82**, 063820 (2010);
4. S. Orlov and P. Banzer, "Vectorial complex-source vortex beams", *Phys. Rev. A* **90**, 023832 (2014);
5. S. Mählig, C. Menzel, C. Rockstuhl, and F. Lederer, "Multipole analysis of meta-atoms", *Metamaterials*, **5**, 64 (2011);
6. T. Bauer, S. Orlov, U. Peschel, P. Banzer, and G. Leuchs, "Nanointerferometric amplitude and phase reconstruction of tightly focused vector beams" *Nature Photonics* **8**, 23 (2014).

# Improved stability of LSCF thin films cathode with Gd-doped ceria interface deposited by PLD on YSZ electrolyte

R. Pascu<sup>1</sup>, G. Epurescu<sup>1</sup>, S. Somacescu<sup>2</sup>, N. Cioatera<sup>3</sup>, S. Brajnicov<sup>1</sup>, R. Birjega<sup>1</sup>, C. Luculescu<sup>1</sup>, B. Mitu<sup>1</sup>

<sup>1</sup>National Institute for Laser, Plasma and Radiation, Magurele, Bucharest, Romania

<sup>2</sup>„Ilie Murgulescu” Institute of Physical Chemistry of the Romanian Academy, Bucharest, Romania

<sup>3</sup> University of Craiova, Craiova, Romania

$\text{La}_{0.5}\text{Sr}_{0.5}\text{Co}_{0.8}\text{Fe}_{0.2}\text{O}_{3-\delta}$  (LSCF) perovskite is limited in the utilization as cathode in ITSOFC because of a relative structural compatibility with 8YSZ electrolyte which generates undesired effects between the materials. The aim of this paper is to add an ionic interface of 10%Gd-doped ceria (10GCO) in order to create a composite cathode while maintaining high thermal and chemical stability of LSCF. LSCF and 10GCO thin layers were deposited at 600C by Pulsed Laser Deposition (PLD) with variable number of pulses onto 8YSZ/Si(100).

The investigations performed on the LSCF/10GCO multilayers evidenced an improved stability of the composite cathode as compared to simple LSCF layer.

## Pulsed Laser Deposition of Thin Catalyst Layers for PEM Fuel Cells

I. Perović<sup>1</sup>, D. Milovanović<sup>1</sup>, S. Maslovara<sup>1</sup>, P. Laušević<sup>1</sup>, C. Ristoscu<sup>2</sup>, G. Socol<sup>2</sup>, I. N. Mihailescu<sup>2</sup>, B. Radak<sup>1</sup>

<sup>1</sup>VINČA Institute of Nuclear Sciences, University of Belgrade, POB 522, 11001 Belgrade, Serbia

<sup>2</sup>National Institute for Lasers, Plasma, and Radiation Physics (INFLPR), Strada Atomistilor, nr. 409, Magurele, Bucuresti, Romania  
bojan.radak@vinca.rs

Fuel cells (FC) with proton exchange membrane (PEM) are devices that transform hydrogen chemical energy to electrical energy and take a very important role within the hydrogen economy concept. Cost and durability are two major factors that delay large-scale production and commercialization of PEMFC's. Reducing platinum content is particularly beneficial in this respect<sup>1</sup>. FC's durability is determined by a number of factors, one of them being catalyst CO poisoning, deactivation of catalyst surface due to strong adsorption of carbon monoxide<sup>1,2</sup>.

The present work is part of a study of obtaining thin metal layers on appropriate supports by pulsed laser deposition (PLD) and electrochemical synthesis as electrocatalysts in PEM fuel cells.

PLD technique has numerous advantages, and one of the most important is stoichiometric deposition of the target to the substrate and excellent adherence of deposited layer to substrate surface<sup>3</sup>.

The composition of the layers varies from pure platinum to platinum/tungsten carbide and molybdenum/platinum combination, Figure 1. The goal was to reduce the necessary amount of platinum without loss in performance and lifetime of fuel cells. The inset in Figure 1 shows the enlarged area of deposited Pt layer on carbon paper. The thickness of uniformly deposited Pt layer is estimated at about 1.15 micrometres.

Membrane electrode assemblies (MEA) were fabricated with different deposited catalyst layers and current-voltage characteristics were measured at various temperatures in the range 30°C to 70°C.

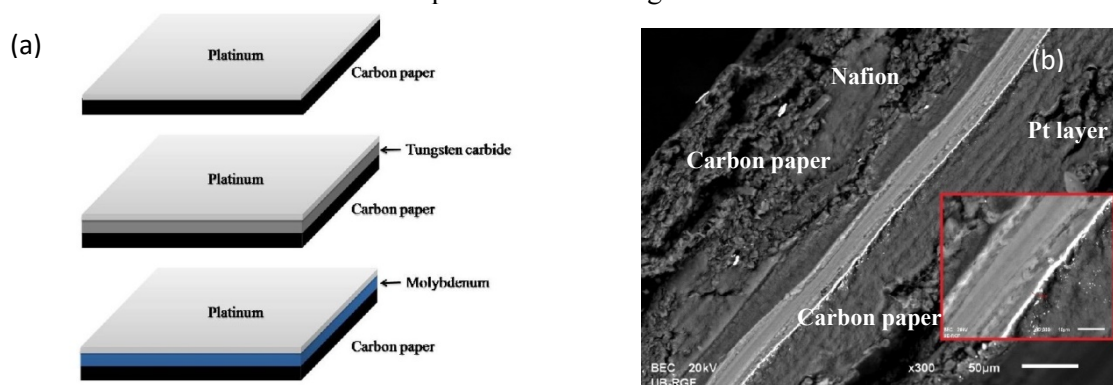


Figure 1: (a) Composition of investigated layers, (b) SEM images of MEAs cross-section with deposited Pt layers.

1. Sridhar, Jae Wook Ihm, Hyung Kyun Yu, and Hojin Ryu, Study of characteristics of the catalytic layer of PEMFC electrode, Journal of the Korean Electrochemical Society, 6, 65 – 67 (2003);
2. Ham DJ, Kim YK, Han SH, Lee J, Pt/WC as an anode catalyst for PEMFC: activity and CO tolerance. Catalysis Today, 132, 117122 (2008);
3. F. Sima, C. Ristoscu, L. Duta, O. Gallet, K. Anselme, I.N. Mihailescu, Laser thin films deposition and characterization for biomedical applications, Book chapter, Elsevier (2016).

# Improving Surface Density of Laser Nanostructuring with Contact Particle Lens Arrays: Two-Color Beams, Resonant Focusing, and Nonspherical Particles

A. Pikulin, N. Mitin, A. Afanasiev, V. Bredikhin, I. Ilyakov, B. Shishkin, R. Akhmedzhanov, N. Biturin

*Institute of Applied Physics of Russian Academy of Sciences, 46, Ul'yanov Str., Nizhniy Novgorod, 603950, Russia  
pikulin@ufp.appl.sci-nnov.ru*

We consider laser nanostructuring of the material surface by means of a colloidal particle lens array. Here, the monolayer of dielectric micro- or nanospheres placed on the surface acts as an array of near-field lenses that focus the laser radiation into the multitude of distinct spots, allowing the formation of many structures in a single stage. In order to be competitive, laser technology should, at least, in principle, be capable of creating nanostructures on large surface areas in a single step. From this point of view, the colloidal particle lens array (CPLA)-mediated laser structuring is very promising, especially when femtosecond laser pulses are used. The improvement of the surface density of nanostructures is constrained by the diffraction that allows for effective focusing by the nanoparticles with diameter about and greater than the wavelength.

Recently, we have experimentally shown that conversion of a small part of the energy of the femtosecond beam into the second harmonic (SH) is an efficient way to increase the surface density of obtained nanostructures. By combining the fundamental frequency and the SH, one benefits both from the power of the former and from the focusing ability of the latter. This method allows improving the structuring surface density without sacrificing the performance.<sup>1</sup>

In this work, we analyze possibilities for the effective focusing by the particles within the contact array while reducing the particle size. The calculations show the possibility for the light focusing by the subwavelength-sized dielectric spheres due to collective resonances not observed for single particles. The monolayers of spheroidal and partially etched spherical particles made of high-refractive-index material (e.g., TiO<sub>2</sub>) also show the benefits for the laser radiation focusing<sup>2</sup> (see Fig. 1).

*Acknowledgements:* This work was financially supported by the Grant No. MK-5858.2016.2 by the President of the Russian Federation and the RFBR Grant No. 16-02-00792.

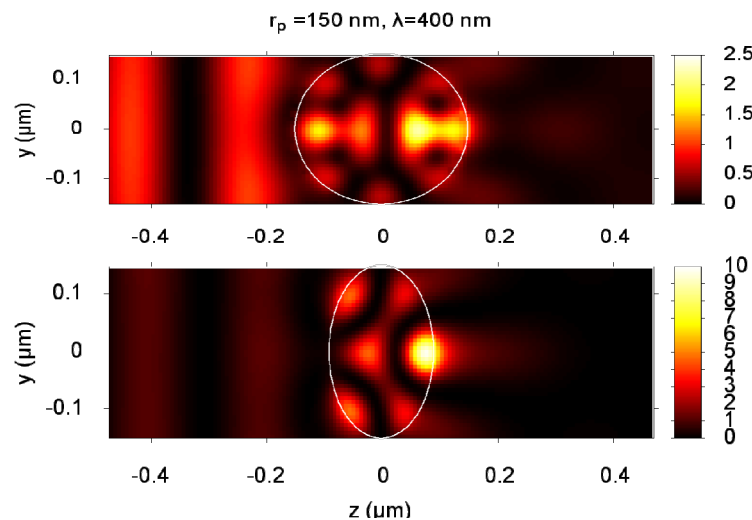


Figure 1: Field (electric field square) enhancement by the monolayer of spherical (top) and spheroidal (bottom) titania particles at PMMA substrate.

1. A. Afanasiev, V. Bredikhin, A. Pikulin, I. Ilyakov, B. Shishkin, R. Akhmedzhanov, and N. Biturin, Two-color beam improvement of the colloidal particle lens array assisted surface nanostructuring, *Appl. Phys. Lett.*, **106**, 183102 (2015);
2. A. V. Afanasiev, V. I. Bredikhin, A. V. Pikulin, N. N. Mitin, I. E. Ilyakov, B. V. Shishkin, R. A. Akhmedzhanov, N. M. Biturin, and E. N. Gorshkova, Increase in the resolution of the method of surface nanostructuring by femtosecond-laser impact through a layer of colloidal microparticles, *Quantum Electron.*, **45**, 467–471 (2015).

# Modeling of Photoinduced Nanoparticle Growth in Inhomogeneous Structured Polymers

A. Pikulin, N. Sapogova, A. Smirnov, N. Biturin

*Institute of Applied Physics of Russian Academy of Sciences, 46, Ul'yanov Str., Nizhniy Novgorod, 603950, Russia  
pikulin@ufp.appl.sci-nnov.ru*

Control over the spatial distribution of nanoparticles in composite polymer materials is a relevant goal for a range of nanotechnology applications. The promising method to produce nanoparticles directly in the polymer matrix relies on their self-assembly from the atoms that are generated due to the photodestruction of the precursor additive. Such materials are known as photoinduced nanocomposites.<sup>1,2</sup> We present the theoretical study of the possibility of producing tailored nanoparticle distributions in such materials by local modification of their physical properties, e.g., by means of laser irradiation. It is shown that the spatial modulation of the diffusivity of the aggregating atoms results in tailored spatial distributions of both nanoparticles and the total number density of the aggregating species. The basic traits of the phenomenon are studied analytically for the simplest case of diffusion-controlled atom dimerization. The nanoparticle generation by means of the first-order phase transition is numerically simulated. It is shown that spatial distribution of nanoparticles can be further enhanced due to the instability of the Lifshitz-Slezov-Wagner coarsening<sup>3</sup> (see Fig. 1).

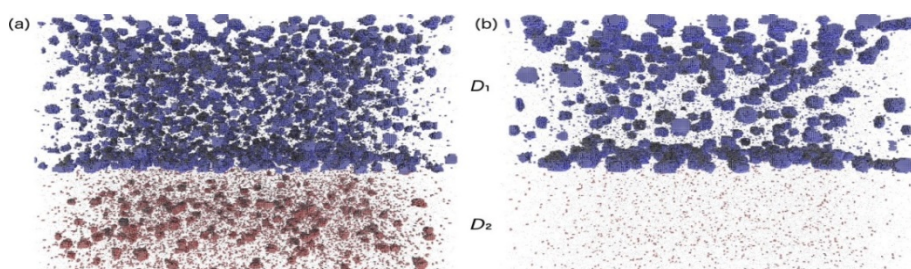


Figure 1: Simulation of the nanoparticle growth in the polymer matrix that comprises layers of different viscosity. The ratio  $D_1/D_2=2$  was taken for the diffusivities of atoms that aggregate into the nanoparticles. Three-dimensional snapshots at at  $4*10^5$  (a) and  $4*10^6$  (b) simulation steps are presented. The nanoparticles in domains of different viscosities are shown in different colors.

**Acknowledgements:** This work was

financially supported by the Russian Scientific Foundation under project No. 14-19-01702.

1. N. Biturin, N. Ermolaev, A. A. Smirnov, A. Afanasiev, N. Agareva, T. Koryukina, V. Bredikhin, V. Kamensky, A. Pikulin, N. Sapogova, Plasmonic and excitonic and exciton-plasmonic photoinduced nanocomposites, *Appl. Phys. A*, **122**, 193 (2016);
2. N. Biturin, A. Alexandrov, A. Afanasiev, N. Agareva, A. Pikulin, N. Sapogova, L. Soustov, E. Salomatina, E. Gorshkova, N. Tsverova, L. Smirnova, Photoinduced nanocomposites—creation, modification, linear and nonlinear optical properties, *Appl. Phys. A*, **112**, 135–138 (2013);
3. V.V. Slezov, *Kinetics of First-order Phase Transitions* (Wiley, 2009).

## Laser Generation of Cavitation Micro- and Nanobubbles near Contact Particle Lens Array: A Prospective to New Optoacoustical Devices

A. Pikulin, A. Reyman, V. Kamensky, N. Biturin

*Institute of Applied Physics of Russian Academy of Sciences, 46, Ul'yanov Str., Nizhniy Novgorod, 603950, Russia  
pikulin@ufp.appl.sci-nnov.ru*

A monolayer of dielectric microspheres placed on the surface acts as an array of near-field lenses that focus the laser radiation into the multitude of distinct spots. We consider such an array deposited on a transparent surface and placed into the water-like medium (see Fig. 1). The field calculation shows that the irradiation of the monolayer of polystyrene microspheres from within the substrate by the laser operating at “surgical” wavelength  $0.97\ \mu\text{m}$  results in the formation of separate field maxima about  $300\ \text{nm}$  in diameter in front of each of the spheres. There, the local heating of the water to about  $300\ ^\circ\text{C}$  can be achieved in reasonable irradiation regimes using single nanosecond pulses.

In this work, the evolution of nanobubbles in a local temperature maximum was modeled, taking into account fast cooling by the heat diffusion. We discuss the possibility of the synchronous cavitation collapse of multiple bubbles produced by separate microlenses in order to magnify and direct the pressure wave. This principle can be employed for the design of new optoacoustical devices, including laser lancets, tools for laser cleaning, etc.

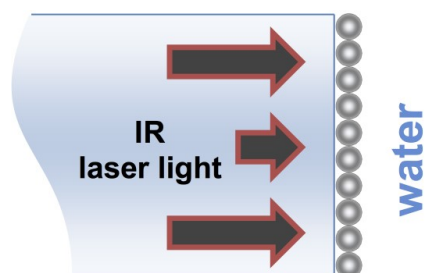


Figure 1: (a) Microspheres deposited on the transparent substrate in the water

**Acknowledgements:** This work was financially supported by the Russian Scientific Foundation under project No. 14-15-00840.



# Experimental set-up for liquid phase monitoring during laser processing of metals

A. C. Popescu<sup>1</sup>, C. Delval<sup>2</sup>, M. Leparoux<sup>2</sup>

<sup>1</sup>National Institute for Lasers, Plasma and Radiation Physics, Atomistilor 409, 077125 Magurele, Romania

<sup>2</sup>Laboratory of Advanced Materials Processing, EMPA, Feuerwerkerstrasse 39, 3602 Thun, Switzerland

The presence of droplets and pores reduce the quality of laser processing. To reduce these deficiencies, high speed imaging, mass spectroscopy and optical emission spectroscopy studies were conducted on molten phase behavior and particles spatter during laser welding of AlMg5 coupons with a Nd:YAG laser source. Experiments were performed under argon shroud. High speed imaging provided info on molten metal dynamics and explanations for spatter generation. By adjusting the laser parameters, liquid can be constrained into the molten pool, thus minimizing the spatter phenomenon and porosity of the welded sample.

The next level of research was to transpose the acquired knowledge to a more complex material: a metal matrix nanocomposite AlMg5/Al<sub>2</sub>O<sub>3</sub> nanoparticles. For this type of material the grains are smaller and more numerous, the heat dispersion is retarded and thus the laser plasma and spatter phenomena are much more violent as compared to casted AlMg5 alloy. We selected three methods for removing expelled particles in situ, during plasma plume expansion: an argon jet that crosses the plasma plume, a silica collector transparent for the laser beam and a mask placed onto the composite surface, in the vicinity of the irradiated area. The efficiency of each method will be discussed during the presentation.

## Solid Target Remote Manipulator System for High Power (PW) Laser Experiments

D. C. Popescu<sup>1,2</sup>, M. O. Cernaianu<sup>1</sup>, L. Tudor<sup>1,2</sup>, Be. De Boisdeffre<sup>1</sup>, D. Dumitrescu<sup>1</sup>, M. Gugiu<sup>1</sup>, F. Rotaru<sup>1</sup>, S. Kisiov<sup>1</sup>, F. Negoita<sup>1</sup>, D. Ursescu<sup>1,3</sup>

<sup>1</sup>ELI-NP, Horia Hulubei National Institute for Physics and Nuclear Engineering 30 Reactorului Street, 077125 Magurele, Ilfov County, Romania

<sup>2</sup>University Politehnica of Bucharest, Bucharest, Romania

<sup>3</sup>National Institute for Lasers, Plasma and Radiation Physics, Măgurele, Romania  
dragos.popescu@eli-np.ro

In this work, a technical solution for a remote manipulator system used with solid targets is presented. The setup was successfully used in experiments focused on producing and accelerating particles using the CETAL High Power (PW) Laser System. It is suitable for high repetition, high power laser experiments where the Interaction Chamber operates under vacuum and equipment is operated remotely due to human radiation safety reasons. This poster covers the design of motorized manipulator and its controllers, remote control system, target layout and alignment procedure for target positioning. Lastly, we approach the problem of electromagnetic pulses (EMP) and their effects on electronic devices close to the interaction point.

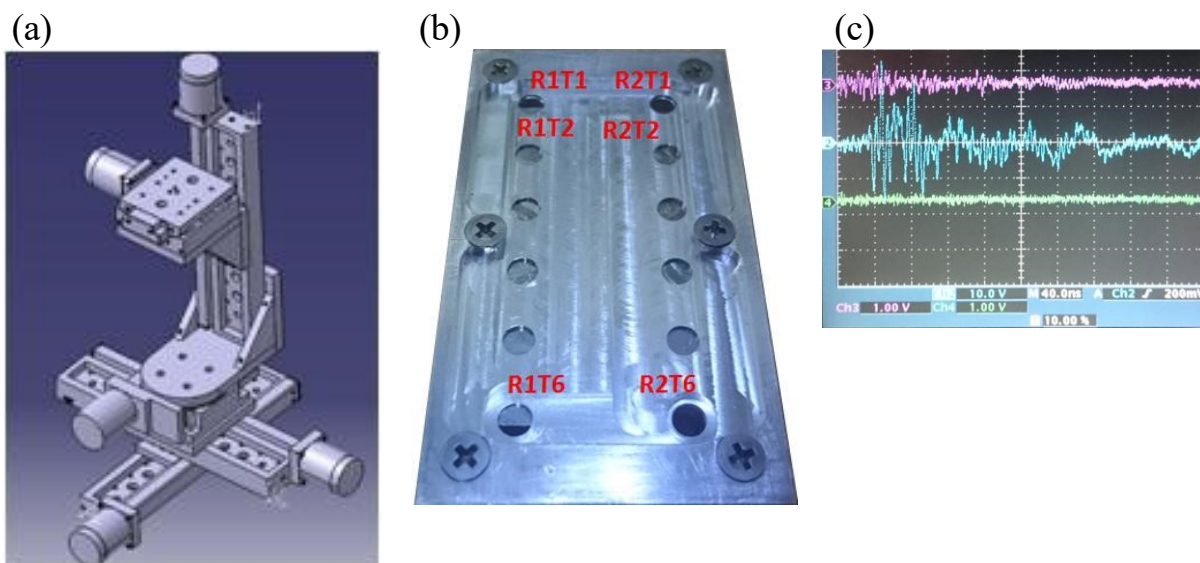


Figure 1: (a) Setup configuration. (b) Target layout. (c) EMP induced electric current in manipulator actuators circuits.

1. N. Booth et al., *Target positioning and alignment on the Astra-Gemini facility*, Proc. SPIE 8850, Target Diagnostics Physics and Engineering for Inertial Confinement Fusion II, 885002 (September 26, 2013); doi:10.1117/12.2023965;

2. D. R. Symes et al., *Investigation into the limitations of target positioning on Astra-Gemini*, CLF Annual Report, (2013-2014).

# Fe<sub>3</sub>O<sub>4</sub>-polyaniline based coatings for biomedical applications

G. Popescu-Pelin<sup>1,2</sup>, M. Socol<sup>3</sup>, R. C. Popescu<sup>4</sup>, D. Savu<sup>4</sup>, M. Temelie<sup>4</sup>, O. Fufa<sup>1</sup>, C. Florica<sup>3</sup>,  
C. Luculescu<sup>1</sup>, I. Zgura<sup>3</sup>, S. Banita<sup>1</sup>, I. N. Mihailescu<sup>1</sup>, G. Socol<sup>1</sup>

<sup>1</sup> National Institute for Lasers, Plasma and Radiation Physics, Magurele, Ilfov, Romania

<sup>2</sup> Faculty of Physics, University of Bucharest, Magurele, Ilfov, Romania

<sup>3</sup> National Institute of Materials Physics, Magurele, Ilfov, Romania

<sup>4</sup> Horia Hulubei National Institute of Physics and Nuclear Engineering, Magurele, Ilfov, Romania  
gianina.popescu@inflpr.ro

Thin films of polyaniline (PANI) and PANI/Fe<sub>3</sub>O<sub>4</sub> were synthesized using matrix assisted pulsed laser evaporation (MAPLE) technique. The experiments were carried out in a vacuum chamber using a KrF\* excimer laser source ( $\lambda=248\text{nm}$ ,  $\tau_{\text{FWHM}}\approx 25\text{ns}$ ), maintaining the same deposition parameters.

The structural, compositional and optical properties of the deposited films were analyzed using the XRay diffraction, wettability investigations, Fourier Transform Infrared and UV-VIS spectrometry. Scanning electron microscopy (SEM) and atomic force microscopy (AFM) investigations were conducted to characterise the films morphology. In order to evaluate the biocompatibility and cytotoxicity of coatings, MTT and immunostaining assays were carried out. The MG63 cells morphology was also examined by SEM analyses, after chemical fixation. Electrochemical measurements showed that PANI based coatings were corrosion resistant.

## CW versus pulsed laser excited emission properties of (Yb<sup>3+</sup>) Ho<sup>3+</sup> (co-) doped CeO<sub>2</sub> nanoparticles

I. Porosnicu<sup>1</sup>, D. Avram<sup>1</sup>, C. Tiseanu<sup>1</sup>

<sup>1</sup> National Institute for Laser, Plasma and Radiation Physics, Bucharest - Magurele, Romania  
ioana.porosnicu@inflpr.ro

We present a detailed study of down (DC) and up - conversion (UPC) properties of 1% Ho<sup>3+</sup> and 1% Ho<sup>3+</sup>, 20% Yb<sup>3+</sup> co - doped CeO<sub>2</sub> nanoparticles (with crystallite size of ~20 nm).<sup>1</sup> The luminescence properties were investigated at room and low temperature over a broad spectral range extending from visible (400 nm) to near - infrared (1200 nm) by use of time - gated emission spectroscopy. The mechanisms involved in DC and UPC are explained in terms of ground state absorption/excited state absorption (GSA/ESA) and ground state absorption/energy transfer up - conversion (GSA/ETU). Color evolution from green to yellow with the increase of pumping power density (~4 to ~48 W/cm<sup>2</sup>) of a cw laser diode operating at 980 nm was observed for Ho, Yb - CeO<sub>2</sub> (Figure 1). We also discuss the impact of CeO<sub>2</sub> structure on the overall emission as well as the role of CeO<sub>2</sub> charge transfer band as a level selective antenna sensitizer.<sup>2</sup>

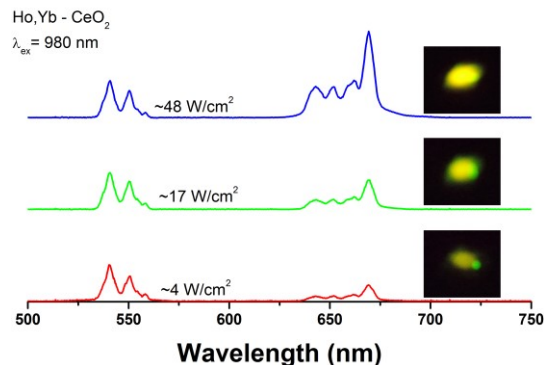


Figure 1: Evolution of the up - conversion emission of Ho, Yb - CeO<sub>2</sub> excited at 980 nm with pumping power density and the corresponding digital photographs of the emitted light.

**Acknowledgements:** The authors acknowledge the Romanian National Authority for Scientific Research (CNCS-UEFISCDI) (Project number PN-II-ID-PCE-2011-3-0534) for the financial support.

1. D. Avram, I. Porosnicu, B. Cojocaru, M. Florea C. Tiseanu, Time-gated down - / up - conversion emission of Ho - CeO<sub>2</sub> and Ho, Yb - CeO<sub>2</sub> nanoparticles – submitted;
2. D. Avram, M. Sanchez-Dominguez, B. Cojocaru, M. Florea, V. Parvulescu, C. Tiseanu, Toward a Unified Description of Luminescence-Local Structure Correlation in Ln Doped CeO<sub>2</sub> Nanoparticles: Roles of Ln Ionic Radius, Ln Concentration, and Oxygen Vacancies, J. Phys. Chem. C, **119** (28), pp 16303–16313, 2015.

# Ultrafast Epitaxial Growth Kinetics in Pulsed Laser Annealed Solution-Derived Functional Oxide Thin Films

A. Queraltó<sup>1</sup>, A. Pérez del Pino<sup>1</sup>, M. de la Mata<sup>1,2</sup>, J. Arbiol<sup>2,3</sup>, M. Tristany<sup>1</sup>, X. Obradors<sup>1</sup>, T. Puig<sup>1</sup>

<sup>1</sup>Institut de Ciència de Materials de Barcelona (ICMAB-CSIC), Campus UAB, 08193 Bellaterra, Catalonia, Spain

<sup>2</sup>Catalan Institute of Nanoscience and Nanotechnology (ICN2), CSIC and The Barcelona Institute of Science and Technology, Campus UAB, 08193 Bellaterra, Catalonia, Spain

<sup>3</sup>Institució Catalana de Recerca i Estudis Avançats (ICREA), 08010 Barcelona, Catalonia, Spain  
albert.queralto.lopez@gmail.com

Functional oxide thin films are an important topic in the field of materials science due to the outstanding physical properties achieved at the nanoscale in fields such as ferromagnetism, ferroelectricity, multiferroicity, superconductivity or photocatalysis. Solution-based methods such as the chemical solution deposition (CSD) have proven to be highly versatile, cost-effective and scalable for the fabrication of highly crystalline and epitaxial thin films with complex compositions. However, they are often limited by the use of slow thermal treatments. In this sense, pulsed laser annealing (PLA) is envisaged as an alternative processing technique to achieve a faster oxide film processing. Thus, it is vital to evaluate the epitaxial crystallization by PLA and understand the mechanisms involved.

We investigated the processed films were also evaluated and compared with equivalent films produced by thermal treatments. epitaxial growth of multiple functional oxide thin films ( $\text{Ce}_{0.9}\text{Zr}_{0.1}\text{O}_{2-y}$ ,  $\text{LaNiO}_3$ ,  $\text{Ba}_{0.8}\text{Sr}_{0.2}\text{TiO}_3$  and  $\text{La}_{0.7}\text{Sr}_{0.3}\text{MnO}_3$ ). A Nd:YAG laser source ( $\lambda=266$  nm, 10 Hz and  $\tau\sim 3$  ns) was used to achieve the crystallization of CSD-derived precursor films on single crystal substrates ( $\text{Y}_2\text{O}_3:\text{ZrO}_2$ ,  $\text{LaAlO}_3$  and  $\text{SrTiO}_3$ ) in atmospheric conditions. The film morphology, structure and the degree of epitaxial crystallization were analyzed by means of atomic force and transmission electron microscopies, and X-ray diffraction. The influence of photochemical and photothermal interactions on the crystallization kinetics from the precursor material was evaluated by varying the laser fluence and applied number of pulses. Theoretical temperature and crystallization models were employed to determine key parameters such as temperature gradients, atomic diffusion coefficients, epitaxial growth rates and activation energies of nucleation and crystallization. The physical properties of laser

1. Queraltó, A.; Pérez del Pino, A.; de la Mata, M.; Arbiol, J.; Obradors, X.; Puig, T., Ultrafast Crystallization of  $\text{Ce}_{0.9}\text{Zr}_{0.1}\text{O}_{2-y}$  Epitaxial Films on Flexible Technical Substrates by Pulsed Laser Irradiation of Chemical Solution Derived Precursor Layers. *Crystal Growth & Design* **2015**, 15, (4), 1957-1967;
2. Queraltó, A.; Pérez del Pino, A.; de la Mata, M.; Arbiol, J.; Tristany, M.; Gómez, A.; Obradors, X.; Puig, T., Growth of ferroelectric  $\text{Ba}_{0.8}\text{Sr}_{0.2}\text{TiO}_3$  epitaxial films by ultraviolet pulsed laser irradiation of chemical solution derived precursor layers. *Applied Physics Letters* **2015**, 106, (26), 262903;
3. Queraltó, A.; Pérez del Pino, A.; de la Mata, M.; Arbiol, J.; Tristany, M.; Obradors, X.; Puig, T., Ultrafast Epitaxial Growth Kinetics in Functional Oxide Thin Films Grown by Pulsed Laser Annealing of Chemical Solutions. *To be published.*

## MAPLE of Graphene Oxide Nanocomposites

A. Queraltó<sup>1</sup>, A. Datcu<sup>1</sup>, A. Pérez del Pino<sup>2</sup>, E. György<sup>1,2</sup>

<sup>1</sup>National Institute for Lasers, Plasma and Radiation Physics, P. O. Box MG 36, 77125 Bucharest, Romania

<sup>2</sup>Institut de Ciència de Materials de Barcelona (ICMAB-CSIC), Campus UAB, 08193 Bellaterra, Catalonia, Spain  
albert.queralto.lopez@gmail.com

Graphene oxide-based nanocomposites have attracted great attention in the last decade due to their remarkable physicochemical properties, for applications in electronics,<sup>1</sup> photocatalysis,<sup>2</sup> energy storage/conversion,<sup>3</sup> etc. The functional properties of graphene oxide highly depend on the amount of oxygen containing groups present in its structure, i.e. the degree of the reduction of the oxygen containing groups<sup>4</sup>. Typically, chemical reduction and thermal treatment of graphene oxide is the most extended approach for the production of reduced graphene oxide. However, these conventional techniques are time consuming, imply toxic chemical substances, and high processing temperatures. Besides chemical composition the unique functional properties of the nanomaterials are determined by their morphological features as size and shape. Laser-based irradiation techniques such as matrix assisted pulsed laser evaporation (MAPLE) could become an alternative of the conventional techniques for the synthesis and deposition of reduced graphene oxide thin films. We have successfully demonstrated the fabrication of reduced graphene oxide thin films with different degrees of reduction, controlled by the irradiation process parameters. We have synthesized nanocomposite graphene-oxide films by MAPLE in argon and nitrogen environments, in order to investigate the reduction process of graphene oxide platelets by doping them with silver and iron oxide nanoparticles. The obtained reduced graphene oxide based films have novel functional properties determined in turn by the concentrations of the silver and iron oxide nanoparticles in the MAPLE target dispersions.

1. A. L. Walter, H. S., J. K., K.-J. Jeon, A. Bostwick, S. Horzum, L. Moreschini, Y. J. Chang, F. M. Peeters, K. Horn, and E. Rotenberg, New family of graphene-based organic semiconductors: An investigation of photon-induced electronic structure manipulation in half-fluorinated graphene, *Phys. Rev. B*, **93**, 075439 (2016);
2. A. Dăcu, L. Duta, A. Pérez del Pino, C. Logofatu, C. Luculescu, A. Duta, D. Pernu and E. György, One-step preparation of nitrogen doped titanium oxide/Au/reduced graphene oxide composite thin films for photocatalytic applications, *RSC Adv.*, **5**, 49771–49779 (2015);
3. Y. Liang, Y. Li, H. Wang, J. Zhou, J. Wang, T. Regier and H. Dai,  $\text{Co}_3\text{O}_4$  nanocrystals on graphene as a synergistic catalyst for oxygen reduction reaction, *Nat. Mater.*, **10**, 780-786 (2011);
4. A. Bagri, C. Mattevi, M. Acik, Y. J. Chabal, M. Chhowalla and V. B. Shenoy, Structural evolution during the reduction of chemically derived graphene oxide, *Nature Chem.*, **7**, 166–170 (2015).

## Plasma generated during underwater laser shock processing

J. Radziejewska<sup>1</sup>, J. Hoffman<sup>2</sup>, Z. Szymanski<sup>2</sup>

<sup>1</sup>Warsaw University of Technology, ul.Narbutta 85, 02-524 Warsaw, Poland

<sup>2</sup>Institute of Fundamental Technological Research, ul.Pawinskiego 5B, 02-106 Warsaw, Poland  
zszym@ippt.pan.pl

Knowledge of the behaviour of materials and their properties under conditions of dynamic deformation is essential for proper designing of machines and equipment and for predicting their behaviour in manufacturing and operating processes. Ultra-high speed deformations occur in the processes of friction and machining of materials, as well as, operation of components used in many fields of technology. Properties of materials under conditions of dynamic deformation significantly differ from those in static conditions. They depend on the speed of deformation, microstructure of the material and temperature. Laser shock processing is regarded as a very promising tool for studying dynamic deformation of materials<sup>1,2</sup>. Pulse laser ablation in water supplies suitable conditions for such studies at relatively low laser fluences. The investigated metallic samples are usually coated with a thin layer of graphite in order to provide full absorption of the laser radiation. Additionally, such a layer isolates the investigated metal from thermal effects connected with interaction of the laser beam. In this paper the ablation of graphite layer is studied to get better insight into underwater laser shock processing. An 10 ns laser pulse of 1064 nm Nd:YAG laser with intensity of  $1.5 \text{ GW}\cdot\text{cm}^{-2}$  was used to produce a shock wave. The induced plasma pressure was about 2 GPa as inferred from measurements with the use of piezoelectric pressure transducers located at the bottom surface of the sample.

The emission spectra of ablated plume consist mainly of continuous radiation. After 50 ns from the laser pulse the absorption spectra of OH ( $\text{A}^2\Sigma^+ - \text{X}^2\Pi_i$ ) system appears. This absorption band results from the absorption of plasma radiation in water and its temperature of about 5000 K reveals the temperature of dissociated water layer, which surrounds the plume. After 100 ns strongly broadened molecular spectra of  $\text{C}_2$  Swan system appear, which become better resolved with longer delay time as the plasma pressure and electron density decrease. Very weak carbon atomic lines are observed after 500 ns from the laser pulse.

Fig. 1a shows the calibrated continuum radiation as a function of wavelength measured 20 ns after the laser pulse. At this moment the experimental intensity fits well to that of blackbody with a temperature of 17000 K. At longer delay times the intensity of plasma radiation deviates significantly from that of blackbody. The temperature can be then obtained from Swan spectra (Fig. 1b).

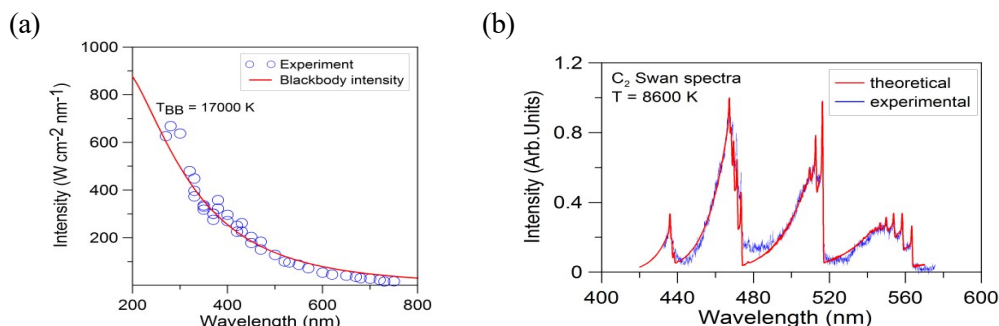


Figure 1: (a) Plasma intensity 20 ns after the laser pulse and blackbody fit.  
(b) Experimental Swan spectra 500 ns after the laser pulse together with theoretical fit.

1. M. Morales, J.L. Ocaña, C. Molpeceres, J.A. Porro, A. García-Beltrán, Model based optimization criteria for the generation of deep compressive residual stress fields in high elastic limit metallic alloys by ns-laser shock processing, *Surface & Coatings Technology* **202**, 2257–2262 (2008);
2. J. Radziejewska, Application of ananosecond laser pulse to evaluate dynamic hardness under ultra-high strain rates, *Optics & LaserTechnology* **78**, 125–133 (2016).

# Structural and biological investigations of pulsed laserdeposited thin films of biocomposites containing HA and foaming agents

C. Ristoscu<sup>1</sup>, N. Mihailescu<sup>1</sup>, M. Sopronyi<sup>1</sup>, I. N. Mihailescu<sup>1</sup>, O. Gingu<sup>2</sup>, G. Sima<sup>3</sup>, C. Teisanu<sup>3</sup>, L. E. Sima<sup>4</sup>

<sup>1</sup>National Institute for Lasers, Plasma and Radiation Physics, POB MG-36, Magurele, Ilfov, Romania

<sup>2</sup>University of Craiova, Department IMST, 1st Calugareni, 220037 Dr. Tr. Severin, Romania

<sup>3</sup>University of Craiova, 13 Al. I. Cuza, 200585, Craiova, Romania

<sup>4</sup>Department of Molecular Cell Biology, Institute of Biochemistry, Romanian Academy, 296 Splaiul Independentei, 060031, Bucharest 17, Romania  
carmen.ristoscu@inflpr.ro

Biocomposites represent a new class of advanced materials for bone reconstruction. Hydroxyapatite (HA) is widely used for bone grafts manufacturing<sup>1</sup>. For this purpose, the biocomposite mixture *1n* consisting of submicronic (< 200 nm) HA particles (> 60 % wt) and titanium hydride powders (20-30 % wt) was used<sup>2</sup>. Apart from this, the mixture *7'n* contained citric acid (1-3 % wt) and foaming agents as CaCO<sub>3</sub> and NH<sub>4</sub>HCO<sub>3</sub>, each of (1-2) %, in order to reach the required density correlated to the grafted cortical trabecular bone tissue. The powders (*1n* and *7'n*), pressed in 1 cm<sup>2</sup> pellets, were pulsed laser deposited onto 12 mm diameter Ti discs or 1cm<sup>2</sup> Si wafers. Both powders and thin films were characterized from morphological, structural, mechanical and biological point of view. The XRD peaks recorded from biocomposite material reveal the phase composition: HA, TiO<sub>2</sub> (rutile), CaCO<sub>3</sub> and Ca<sub>3</sub>(PO<sub>4</sub>)<sub>2</sub>. The morphological aspect is in case of powders rather porous, as expected due to the incorporation of foaming agents. For thin films, the surface is characterised by the presence of micronic and submicronic droplets, a peculiar feature of pulsed laser deposition technique with KrF\* (248 nm, 25 ns) laser pulses. The mechanical behavior of the HA-based biocomposites was strongly dependant on the foaming reactions. For the most rigid biocomposite processed from submicronic HA foamed with 5% CaCO<sub>3</sub> we measured a compression strength, *G*, of 998 MPa.

The presence of TiO<sub>2</sub> (rutile), a biocompatible phase, brings the advantage for further *in vitro* studies. We used mesenchymal stem cells seeded on both biocomposite pellets and thin films. The results proved that our materials are not cytotoxic. The immunofluorescence microscopy evidenced the presence of cells, mostly proliferating on thin films. Their cytoskeleton was well organized, connected to substrates *via* thin dendrites which mediate also the inter-cellular communication (Fig. 1). The quantitative analyses evidenced a 23.91% fraction of proliferating cells of thin films, versus 16.26% on bare Ti and to 4.38% on glass. Our studies demonstrated that the proposed biocomposite materials are biologically active and could be further investigated to be used as bone grafts.

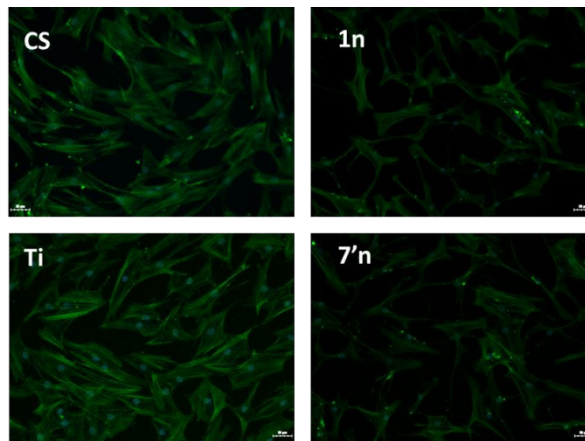


Figure 1: MSC adhesion at 5 days post-seeding on biocomposites thin films (*1n* and *7'n*) and bare titanium (*Ti*) or glass cover slip

1. A. Arifin, A. B. Sulong, N. Muhamad, J. Syarif, M. I. Ramli, Material processing of hydroxyapatite and titanium alloy (HA/Ti) composite as implant materials using powder metallurgy: A review, *Materials and Design*, **55**, 165 (2014);
2. O. Gingu, D. Cojocaru, C. Ristoscu, G. Sima, C. Teisanu, M. Mangra, The influence of the foaming agent on the mechanical properties of the PM hydroxyapatite-based biocomposites processed by two-step sintering route, *JOURNAL OF OPTOELECTRONICS AND ADVANCED MATERIALS*, **17(7-8)**, p. 1044 – 1049 (July – August 2015).

# Effect of aluminum electrode nano-patterning on the properties of the laser prepared arylenevinylene polymer based mixed layer

O. Rasoga<sup>1</sup>, A. Stanculescu<sup>1</sup>, G. Socol<sup>2</sup>, A. M. Catargiu<sup>3</sup>, M. Grigoras<sup>3</sup>, C. Breazu<sup>1,4</sup>, M. Socol<sup>1</sup>, E. Matei<sup>1</sup>, F. Stanculescu<sup>4</sup>, M. Girtan<sup>5</sup>

<sup>1</sup>National Institute of Materials Physics, 405A Atomistilor Street, P.O. Box MG-7, Bucharest-Magurele, 077125 Romania

<sup>2</sup>National Institute for Laser, Plasma and Radiation Physics, Str. Atomistilor, Nr. 409, PO Box MG-36, Magurele, 077125, Romania

<sup>3</sup>P. Poni Institute of Macromolecular Chemistry, 41 A Gr. Ghica Voda Alley, 700487-Iasi, Romania

<sup>4</sup>University of Bucharest, Faculty of Physics, 405 Atomistilor Street, P.O. Box MG-11, Bucharest-Magurele, 077125 Romania

<sup>5</sup>University of Angers, Photonics Laboratory, University 2, Bd. Lavoisier 49045, Angers, France  
sanca@infim.ro

The performances of organic devices depend on many factors such as: the mechanism of charge carriers generation limited by the radiation absorption, charge carriers injection and transport limited by the energetic barriers inside the heterostructure, recombination processes determined by the device structure and extraction of the generated radiation limited by the reflectivity of the metallic electrode. In classical bi-layer organic structure for photovoltaic applications, the limitation induced by the reduced diffusion length of exciton and reduced interfacial contact area between the donor and the acceptor can be overpassed using as active layer blends of two materials known as bulk heterojunctions, which assure an efficient charge carriers transport.

Beside the active layer, the metallic electrode is another very important part of any electronic and optoelectronic devices, including organic devices, such as solar cells, light emitting devices and field-effect transistors. Applying the nano-patterning to the metallic contact in an organic heterostructure it is generated a periodically array (network) of (nano) structures and can be generated both optical effects (improved radiation absorption efficiency by "light trapping") and electrical effects (intense electric field determining an increased mobility of the carriers and enhanced area of the metal-organic contact favoring carriers injection/collection).

This paper presents some studies of the organic structures realized on Si substrates from dichlorobenzene or chloroform by Matrix assisted pulsed laser evaporation (MAPLE) using poly(arylenevinylene)s containing carbazole units substituted at 2,7- and 3,6-positions as p type conduction and two different acceptors as n type conduction acceptor blended in 1:2 ratio. The properties of these mixed layers will be compared with those of the mixed layers deposited by the same method MAPLE based on KrF\* excimer laser Coherent ComplexPro 205 with  $\lambda=248$  nm using the same solvent and following experimental conditions: fluence around 300 mJ/cm<sup>2</sup> and number of pulses=5000-20000.

The mixed layers are composed from the same above mentioned arylenevinylene based polymers as p type conduction donors and [6,6]-phenyl C61 butyric acid butyl ester or perylene tetracarboxydiimide, as acceptor. The Si substrate was firstly covered by a grating of nanostructures (Fig.1) developed in a metallic layer of Al by UV-Nanoimprint Lithography. The 2D periodic structures are characterized by a periodicity around 400 nm with a cylindrical shape with a diameter of few hundreds of nm and depth around 300 nm. The cathode electrode has been deposited on this nanostructured surface by vacuum evaporation.

The effect of the cathode nano-patterning on the morphology of the subsequently deposited organic layer deposited by MAPLE has been evidenced by SEM and AFM measurements. A transparent conductor electrode of ITO has been deposited by sputtering on the top of the heterostructure obtaining an inverted configuration solar cell structure.

I-V measurements in dark and under illumination have confirmed that these mixed layers prepared by MAPLE are adequate for solar cells applications. We have evaluated the parameters for solar cell structure realized with

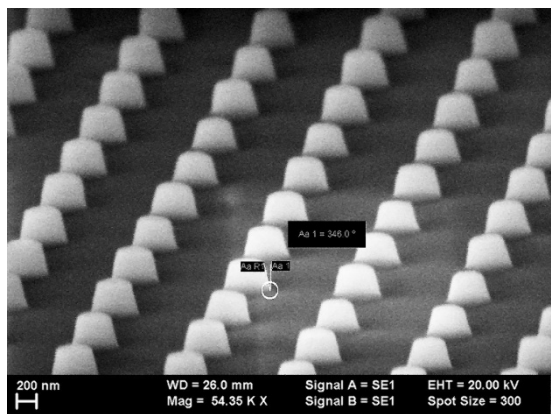


Figure 1: Nano-structured layer on silicon substrate

# Self-organization of single-crystals as ripple patterns through laser ablation of ionic salts solutions

I. Sandu<sup>1</sup>, I. Urzica<sup>1</sup>, A. M. Niculescu<sup>1,2</sup>, C. T. Fleaca<sup>1</sup>, F. Dumitrache<sup>1</sup>, M. Badiceanu<sup>3</sup>

<sup>1</sup>National Institute for Lasers, Plasma and Radiation Physics, P.O. Box MG-36, Bucharest, Romania

<sup>2</sup>University of Craiova, Faculty of Mathematics and Natural Sciences, RO-200585, Craiova, Romania

<sup>3</sup>University of Bucharest, Faculty of Physics  
ionsnd@yahoo.com, ion.sandu@inflpr.ro

Laser-induced periodic surface structures (LIPSSs), also called as ripples, are general phenomenon of laser-matter interaction occurring at a low fluence, around the ablation threshold<sup>1</sup>. Till now, ripples were formed through laser ablation on very diverse materials such as: metals, semiconductors and dielectrics<sup>2</sup>.

In the present work we show for the first time, how by irradiating with a IR pulsed laser (DIAMOND G-Series), (a single shot of  $\sim 2$  J in fluence), a drop ( $V = 1 \mu\text{L}$ .) of aqueous NaCl ( $c = 0.1$  % wt.) deposited onto a microscope glass slide, in the normal conditions of laboratory, we can obtain ripples constituted from NaCl single-crystals (Fig. 1).

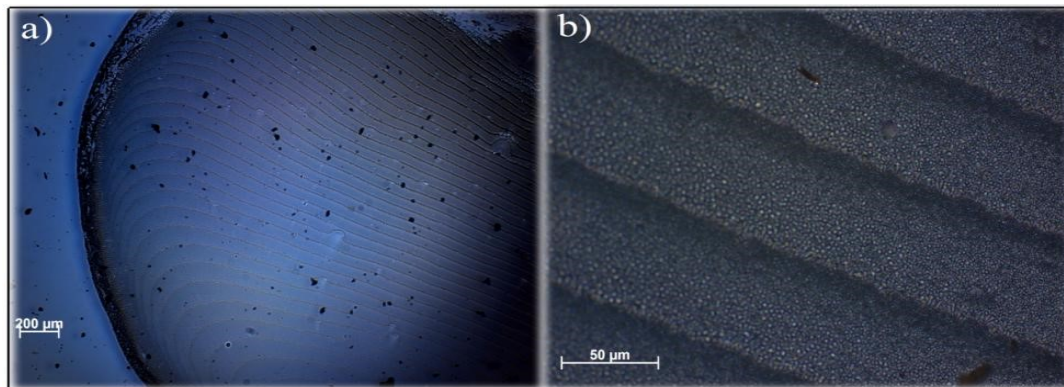


Figure 1: Optical microscopy images of NaCl single-crystal ripples formed through laser ablation

The ripples are of millimetres long, tens of micrometers in width,  $\sim 1$  nm in thickness, and are separated by thin gaps. The large amount of experiments performed on different molecular solutions or colloids show that only the crystallisable materials (such as ionic salts) form ripples during their ablation. This approach may be an interesting one in the domain of crystal nucleation and growth, especially in the protein crystallization for new kind of bio-sensors fabrication or in Nanophotonics as optical active Bragg diffraction grids.

**Acknowledgements:** This work has been financed by the National Authority for Research and Innovation in the frame of Nucleus programme- contract 4N/2016.

1. Y. Tang, J. Yang, B. Zhao, et. al., Control of periodic ripples growth on metals by femtosecond laser ellipticity, *Optics Express*, **23**, 25839, (2012);

2. J. Reif, F. Costache, M. Henyk, and S. V. Pandelov, "Ripples revisited: non-classical morphology at the bottom of femtosecond laser ablation craters in transparent dielectrics," *Appl. Surf. Sci.* **197-198**, 891–895 (2002).

# Development of sputter-less selective laser melting in vacuum for 3D fabrication of titanium alloy

Y. Sato<sup>1</sup>, M. Tsukamoto<sup>1</sup>, Y. Yamashita<sup>2</sup>, S. Masuno<sup>1</sup>, T. Ohkubo<sup>3</sup>, K. Yamashita<sup>4</sup>, N. Abe<sup>1</sup>

<sup>1</sup>Joining and welding research institute, Osaka University (11-1 Mihogaoka, Ibaraki-shi, Osaka, 567-47, Japan)

<sup>2</sup>Industrial Research Institute of Ishikawa, (2-1 Kuratsuki, Kanazawa, Ishikawa 920-8203, Japan)

<sup>3</sup>Graduate School of engineering, Osaka University (1-1 Yamadaoka, Suita-shi, Osaka, 565-0871 Japan)

<sup>4</sup>Tokyo University of Technology (1401-1, Katakura-chou, Hachioji-shi, Tokyo, 192-0914, JAPAN)  
sato@jwri.osaka-u.ac.jp

We demonstrated that a Ti alloy, which is clinically used for artificial bone and hard tissue implant in human body because of their light and biocompatibility, were fabricated by sputter-less selective laser melting (SLM) process in vacuum.

SLM, which is an additive manufacturing technology, is attractive due to its ability to freely form shapes. SLM can fabricate complicated shapes because it builds a 3D material layer-by-layer from a powder. However, some issues have yet to be resolved, including dimensional accuracy, surface finishes, processing time, and mechanical properties such as surface roughness, hardness, and crystal orientation. Especially, in commercial SLM process, splatters were generated when the laser was irradiated to the powder. It was caused to form a fabricated material which had a low relative density to form some pores in samples. Thus, we developed the sputter-less SLM process in vacuum for Ti alloy.

The chamber was evacuated at a pressure of  $5.0 \times 10^{-3}$  Pa to prevent Ti alloy from oxidizing. The single-mode fiber laser irradiated and melted the powder bed to create a molten pool in order to form 2D metallic structures. A 3D fabricated sample was formed by these processes. The scanning strategy of the laser employed a linear raster scan pattern with a scan vector length of 10 mm as shown in Figure 1. The laser scanning speed and baseplate temperature were varied between 5–100 mm/s and 25–150 degree Celsius, respectively. In order to investigate the laser melting and solidification dynamics, a process of Ti 64 plate fabrication was captured by high speed video camera. Figure 2 shows the high speed video camera images when the laser was irradiated to the powder. At the scanning speed of 50mm/s in Fig.2 (b), the sputtering was violently generated from the laser irradiation area, on the other hand, at the scanning speed of 10m/s, no sputtering were generated in Fig. 2 (a). It results that the surface roughness for fabricated sample to 0.6  $\mu$ m from 10-20 $\mu$ m. It was also determined that crystal orientation was evaluated with X-ray diffraction (XRD). It was recorded from the powder peaks of  $\alpha$  (1011),  $\alpha$  (0002),  $\alpha$  (1010), and  $\alpha$  (1012) that the crystal orientation is composed mainly of martensitic alpha by XRD analysis. Diffraction peaks corresponding to  $\beta$  (110) were detected in vacuum SLM processed samples.

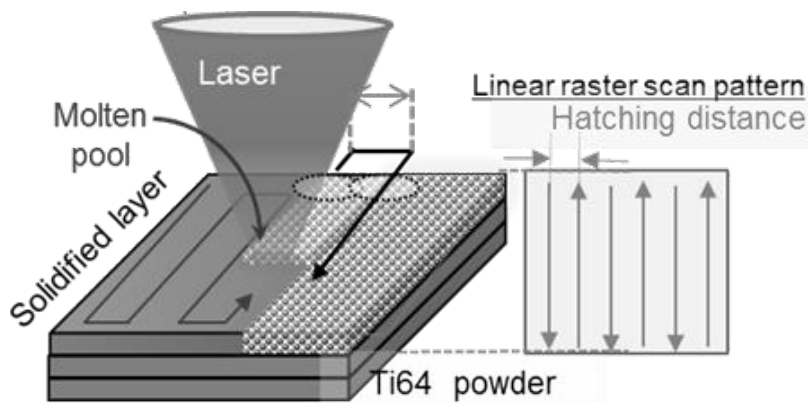


Figure 1: Schematic diagram of laser scanning strategy

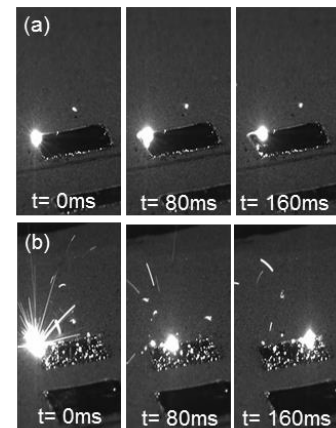


Figure 2: High speed video camera images at laser scanning speed of (a) 10 mm/s and (b) 50 mm/s

1. Y. Sato, M. Tsukamoto, et al. Applied Physics A 122:439 (2016);

2. Y. Sato, M. Tsukamoto, Y. Yamashita, Applied Physics B 119 pp.545-549 (2015)



# Thermal effect on CFRP ablation with 150W class pulse fiber laser using PCF amplifier

Y. Sato<sup>1</sup>, M. Tsukamoto<sup>1</sup>, F. Matsuoka<sup>2</sup>, T. Ohkubo<sup>3</sup>, N. Abe<sup>1</sup>

<sup>1</sup>Joining and welding research institute, Osaka University (11-1 Mihogaoka, Ibaraki-shi, Osaka, 567-47, Japan)

<sup>2</sup>Graduate School of engineering, Osaka University (1-1 Yamadaoka, Suita-shi, Osaka, 565-0871 Japan)

<sup>3</sup>Tokyo University of Technology (1401-1, Katakura-chou, Hachioji-shi, Tokyo, 192-0914, JAPAN)  
sato@jwri.osaka-u.ac.jp

A carbon fiber reinforced plastic (CFRP), which has been employed for many applications such as automobile and aircraft, has light weight, weather resistance and dimensional stability. Due to the current applications and the potential of CFRP as a next –generation material, CFRP processing technology is very important. Laser CFRP processing has recently attracted attention due to characteristics such as stability of the dimensional tolerance because there is no wear of processing parts, specialized environments is not required, and relatively free shapes can be fabricated with a reduction of the processing cost.

Recently, the laser cutting and drilling for CFRP have attracted attention for high speed and high quality processing. By applying the high power CW laser, the matrix resin of CFRP was quickly decomposed before cutting of the carbon fiber. In these processes, formation of a heat affected zone (HAZ) was promoted because of differences in thermal properties and laser absorption of carbon fiber and epoxy resin.

In this study, an experimental study on CFRP processing is presented using a high –power pulsed fiber laser operated at a fundamental wavelength of 1064 nm, an average power of 150W, a repetition rate of 1 MHz and a pulse width of 10ns. A Raman spectroscopy analysis was conducted to measure the heat affected zone quantitatively. Here, the HAZ define as the sum of a matrix evaporation zone (MEZ) and resin alteration zone (RAZ).

As the results, MEZ, RAZ and HAZ in air were 455, over 600 and over 1055  $\mu\text{m}$ , respectively. In case of  $\text{N}_2$  gas flow, the MEZ, RAZ and HAZ were obtained 30, 88 and 118  $\mu\text{m}$ , respectively. The CFRP cutting speed under both ambiances were same, at 0.42 cm/s. From the results, although it was found that cutting speed for CFRP was not depended on processing ambience, the HAZ was depended on processing ambience of oxygen concentration.

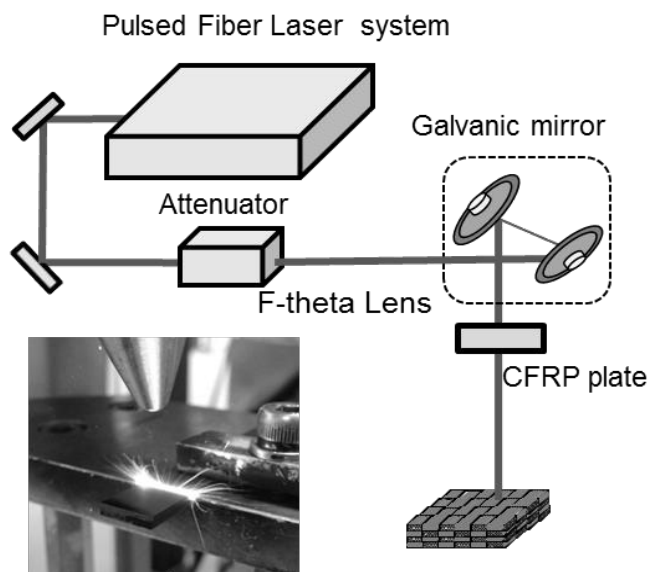


Figure 1: Experimental setup for CFRP processing with high power pulse fiber laser system

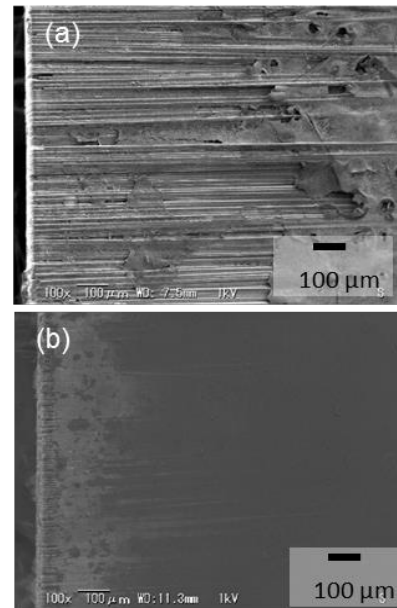


Figure 2: SEM images of CFRP after laser irradiation in (a) air ambient and (b)  $\text{N}_2$  gas Flow

# The influence of addition PbO and MnO on PZT thin films

B.G. Sbarcea<sup>1</sup>, J. Neamtu<sup>1</sup>, A. Dumitru<sup>1</sup>, D. Patroi<sup>1</sup>, V. Marinescu<sup>1</sup>

<sup>1</sup>National Institute for R & D in Electrical Engineering ICPE-CA, Splaiul Unirii  
Street, Nr. 313, District 3, 030138, Bucharest Romania  
gabriela.sbarcea@icpe-ca.ro

Doped PZT thin films are studied to reveal the influence of PbO and MnO upon them. We study the thin films proprieties grown by RF sputtering. The ceramic targets were sintered at 1150°C, 1200°C and 1250°C. These targets were structurally characterized by X-ray diffraction and scanning electron microscopy and the measurements reveal a tetragonal structure. The crystallite size varies in the range of 40-51 nm. Films without thermal treatment shown a thickness of 33 nm, whereas for films treated at 600°C for 30 minutes the thickness was 43 nm and 132 nm for samples treated at 650°C for 30 minutes. PZT doped thin films can be applied to sensor device manufacturing.

I. P. Muralt, PZT Thin Films for Microsensors and Actuators: Where Do We Stand? IEEE Transactions on Ultrasonics, Ferroelectrics, and Frequency Control, vol. 47, no. 4, 903-915, (2000)

# Tungsten bronze $Sr_xBa_{1-x}Nb_2O_6$ and Ca-doped $Sr_xBa_{1-x}Nb_2O_6$ thin films by PLD for electro-optic and pyroelectric devices

N. D. Scarisoreanu<sup>1</sup>, R. Birjega<sup>1</sup>, A. Andrei<sup>1</sup>, V. Ion<sup>1</sup>, G. Stanciu<sup>1</sup>, M. Dinescu<sup>1</sup>

<sup>1</sup>NILPRP, PO Box MG-16, RO-77125, Bucharest, Romania.  
maria.dinescu@inflpr.ro

We report on the optical and electrical properties of epitaxial strontium barium niobate ( $Sr_xBa_{1-x}Nb_2O_6$ -SBN) and Ca-doped SBN thin films obtained by pulsed laser deposition on different substrates. The microstructure, morphology and stoichiometry were studied by XRD, AFM, SIMS, SEM and TEM. The XRD and HR-TEM analysis evidenced the formation of c-oriented SBN and Ca-doped SBN thin films. As a function of Ca doping level, the pyroelectric and the birefringence behavior as well as the electro-optic coefficient ( $r_{33}$ ) of the thin films have been measured by reflection-type spectroscopic ellipsometry method, using coplanar electrodes. The maximum measured change of the refractive index is  $\Delta n = 0.00846$  for  $E_z = 25$  kV/cm, leading to a value for the electro-optic coefficients  $r_{33}$  of about 40.5 pm/V.

# Strain induced nanoscale phase fluctuations for enhanced dielectric behavior of $(1-x)Ba(Zr_{0.2}Ti_{0.8})O_3 - x(Ba_{0.7}Ca_{0.3})TiO_3$ ( $x = 0.45$ ) epitaxial thin films

N.D. Scarisoreanu<sup>1</sup>, V. Ion<sup>1</sup>, A. Bercea<sup>1</sup>, A. Moldovan<sup>1</sup>, A. Andrei<sup>1</sup>, F. Craciun<sup>2</sup>, R. Birjega<sup>1</sup>, M. Dinescu<sup>1</sup>

<sup>1</sup>National Institute for Laser, Plasma and Radiation Physics, 409 Atomistilor St, RO-077125, Magurele, Romania  
<sup>2</sup>CNR-ISC, Istituto Dei Sistemi Complessi, Via del Fosso del Cavaliere 100, I-00133 Rome, Italy  
nicu.scarisoreanu@inflpr.ro

Lead-free  $(1-x)Ba(Zr_{0.2}Ti_{0.8})O_3 - x(Ba_{0.7}Ca_{0.3})TiO_3$  (BCZT) bulk materials are intensively studied in the last period for replacing piezoelectric and ferroelectric materials containing toxic elements in electronic applications. Different properties are targeted, ranging from normal ferroelectrics up to relaxor ferroelectrics by varying the amount of A-site ( $Ca^{2+}$ ) and B-site ( $Ti^{4+}$ ) isovalent substitutions in BCTZ system. The dielectric and piezoelectric properties of the  $(Ba_{1-x}Ca_x)(Zr_yTi_{1-y})O_3$  ceramic system have been reported for bulk form, but the thin films properties are still to be evidenced [1-3].

In this work we make a careful analysis of strain and local lattice distortions in  $(1-x)Ba(Zr_{0.2}Ti_{0.8})O_3 - x(Ba_{0.7}Ca_{0.3})TiO_3$  thin films with high dielectric response and we have identified in the peculiar nanoscale features, the cause of these enhancements. Using Pulsed Laser Deposition (PLD) technique, the role of epitaxial strain and fine stoichiometric changes induced into the BCZT thin films during growth on the enhancement of electrical and electro-optical properties is revealed. X-ray diffraction and high resolution transmission electron microscopy (HRTEM) measurements revealed the epitaxial growth of the films. The out-of-plane and in-plane lattice parameters and their fluctuations at nanoscale level, which are relevant for the existence of nanodomains, have been

evidenced on the BCZT films by Geometric Phase Analysis (GPA) associated with the HRTEM data. High values of dielectric permittivity ( $>3000$ ) combined with low dielectric loss ( $<0.01$ ) are obtained for example in the case of BCZT 45 film deposited on STO substrate, showing nearly constant values between 1 kHz and 10 MHz – Figure 1. The enhanced switching of such nanodomain configuration was probed by piezoforce microscopy, and values up to 230 pm/V has been obtained for  $d_{33}$  piezoelectric coefficient- Figure 1.

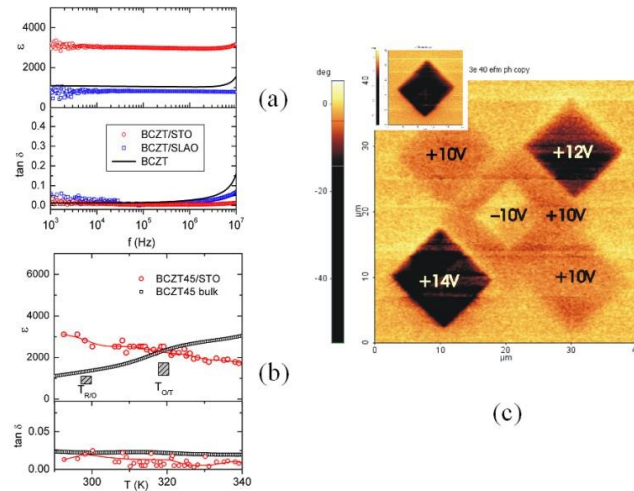


Figure 1. (a) BCZT/STO and BCZT/SLAO dielectric permittivity and loss values dependence on frequency at room temperature; (b) the dielectric permittivity and loss variation with temperature of BCZT/STO films (circle symbols) and bulk BCZT 45 samples (square symbols). The hatched rectangles approximately indicate the R/O and O/T phase transformation regions in the bulk sample; (c) out-of-plane PFM image for BCZT/STO thin films.

1. F. Cordero, F. Craciun, M. Dinescu, N. Scarisoreanu, C. Galassi, W. Schranz, and V. Soprunyuk, *Appl. Phys. Lett.* 105, 232904 (2014);
2. Liu, Z. K.; Li, X.; Zhang, Q. M. *Appl. Phys. Lett.* 101, 082904, (2012);
3. N.D. Scarisoreanu, F. Craciun, A. Moldovan, V. Ion, R. Birjega, C. Ghica, R. F. Negre, M. Dinescu, *ACS Appl. Mater. Interfaces*, 7, 23984–23992 (2015).

## Bi-Based Nanostructures Produced by Laser Ablation in Liquid and Their Functional Properties

N. D. Scarisoreanu<sup>1</sup>, A. Andrei<sup>1</sup>, V. Ion<sup>1</sup>, V. Teodorescu<sup>2</sup>, M. Dinescu<sup>1</sup>

<sup>1</sup>NILPRP, P.O. Box MG-16, RO-77125, Bucharest, Romania.

<sup>2</sup>NIMP-National Institute of Materials Physics, 077125 Bucharest-Magurele, Romania  
nicu.scarisoreanu@inflpr.ro

We report on the synthesis of Bi-based nanostructures by laser ablation in liquids (deionized water, alcohols) of a solid BFO target using lasers working at different wavelengths (193, 266 and 532 nm) and fluences (1.4- 3 J/cm<sup>2</sup>). As a function of laser wavelength different types of Bi nanostructures have been obtained: 2-D single-crystalline sheets of bismuth carbonate (Bi<sub>2</sub>O<sub>2</sub>CO<sub>3</sub>), BiFeO<sub>3</sub>nanoparticles with a narrow mean-size distribution (25-28 nm) or a combination of the two. The average nanostructures size and morphology was estimated by transmission electron microscopy (TEM). To evaluate their functional ferroelectric and ferromagnetic characteristics, the Bi-based nanostructures have been deposited as thin films by MAPLE (Matrix Assisted Pulsed Laser Evaporation).The influence of experimental parameters as solvent type, laser wavelength or thickness of the MAPLE deposited BFO and doped BFO thin films on the local piezoelectric response, optical, multiferoic and photocatalytic properties has been studied using XRD, HRTEM, SE, UV-VIS, PFM or dielectric spectroscopy. A comparison with PLD deposited layers properties was also performed.

# High resolution 2D code marking on PCB using a fiber laser based equipment

M. N. Selagea<sup>1</sup>, B. Lungu<sup>2</sup>, D. Besnea<sup>3</sup>, D. Comeaga<sup>4</sup>, C. I. Ilie<sup>5</sup>, O. Dontu<sup>6</sup>, M. Udrea<sup>7</sup>

<sup>1</sup>University Politehnica of Bucharest, Faculty of Mechanical Engineering and Mechatronics - Precision Mechanics and Nanotechnologies / Apel Laser SRL

<sup>2</sup>University Politehnica of Bucharest, Faculty of Engineering and Management of Technological Systems - Materials Technology and Welding / Apel Laser SRL

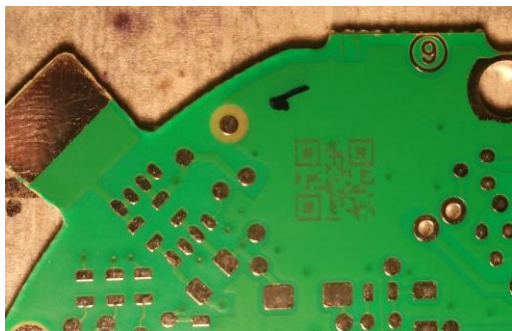
<sup>3,4,6</sup> University Politehnica of Bucharest, Faculty of Mechanical Engineering and Mechatronics- Precision Mechanics and Nanotechnologies

<sup>5</sup>National Institute for Research and Development in Electrical Engineering ICPE-CA

<sup>7</sup>Apel Laser SRL

mihai.selagea@apellaser.ro

Line production marking process of the 2D code on PCB (printed circuit board) is an important process in order to assure the traceability of every single product manufactured by a large scale production factory. In our case thousands of PCB are supposed to be correctly marked daily. The conventional way to accomplish this is to seal an ordinary paper label on every piece of PCB. By using laser marking, the speed of the process is much higher and integrating the system in the line production becomes feasible. We describe here the characteristics of the system that we have developed, in order to be implemented by the end-user (a factory that we are in contract with). A 20 W average power fiber laser is used. The pulse duration is about 15 ns and the repetition rate of the laser pulses may be varied up to 500 kHz. A high speed high accuracy laser scanner was used to control the beam. The focal length of the f-theta lens is 100 mm. Two different lasers which were manufactured by two different companies were used in order to get more information about the influence of the beam characteristics ( $M^2$ ) on the marking resolution. A critical feature of this process is that the laser beam has to evaporate only a certain depth from the soldering mask, until it reaches the copper layer. It is mandatory that the copper layer remains covered by some layer of the soldering mask and also an optimum contrast is needed so that it can be read by any common scanner. An image of the marked PCB is given below.



Satisfactory results have been obtained after this experimental work, in terms of marking depth (copper layer has not been reached) and contrast (the information was read using a conventional laser barcode scanner). Depending on the process parameters, the cycle time can vary from 7.6 sec to 10.85 sec. Future research will be made for establishing the process repeatability if solder mask thickness variations occur or if the PCB is affected, after marking, to different heat inducing processes or comes in contact with different cleaning agents or other aggressive chemical agents.

Also, the bar code reading process repeatability will be checked on a large batch of PCB's, as a last step before this technique is implemented in a large scale production line.

## Optimization of Laser Induced Color Marking on Metals

M. N. Selagea<sup>1</sup>, B. Lungu<sup>2</sup>, D. Besnea<sup>3</sup>, D. Comeaga<sup>4</sup>, C. I. Ilie<sup>5</sup>, O. Dontu<sup>6</sup>, M. Udrea<sup>7</sup>

<sup>1</sup>University Politehnica of Bucharest, Faculty of Mechanical Engineering and Mechatronics - Precision Mechanics and Nanotechnologies / Apel Laser SRL

<sup>2</sup>University Politehnica of Bucharest, Faculty of Engineering and Management of Technological Systems - Materials Technology and Welding / Apel Laser SRL

<sup>3,4,6</sup> University Politehnica of Bucharest, Faculty of Mechanical Engineering and Mechatronics- Precision Mechanics and Nanotechnologies

<sup>5</sup>National Institute for Research and Development in Electrical Engineering ICPE-CA

<sup>7</sup>Apel Laser SRL

mihai.selagea@apellaser.ro

The lasers have established themselves as a reliable tool in the micro-processing of metals. Color marking on stainless steel is a relatively new but very attractive application. The process of coloring of metals by laser induced oxidation is a critical process since the laser parameters have to be very well controlled and stable. We continue our previous study in order to get the best performance, especially for industrial applications. The advantage of metal color marking consists of a better particularization of every object that is marked. Color marking is usually performed by printing or by anodizing techniques. Printing is not time resistant as by anodizing you may not obtain different colors on specific surfaces but on the whole object. The aim is to obtain very visible marking by a specific color, onto a well-defined surface. By using laser irradiation the surface of the metal is not affected significantly. The different colors are obtained by a fine control of the laser power and laser pulse repetition rate. The experiments were performed by using an IPG YLP laser (20 W average power, pulse duration 100 ns, pulse repetition rate 20...200 kHz,  $M^2 = 1.5$ ). The laser beam was directed to a Scanlab scanner and a f-theta lens with 175 mm focal length. The target is placed on a Z-axis adjustable table. By heating a stainless steel surface by laser,

a transparent or semi-transparent oxide film on the metal surface is generated /2, 3/. While illuminating the sample surface, the light is reflected both on the oxide and on the metal surface. As a result of the combining of these beams a colour effect can be obtained. In such a way an external observer can see different colours. The reproducibility of the colors according with some welldefined parameters is still a problem under study /4/. Our study concerns the optimization of the color marking on metal surfaces by using our own fiber laser based device (MARC 20). By heating a stainless steel surface by laser, a transparent or semi-transparent oxide film on the metal surface is generated /1,2/. The values of the parameters which have to be put in order to get a specific color are presented. Also, the influence of an additional source of oxygen directed to the irradiated area is considered.

**Acknowledgements:** This work was performed in the frame of PN-II-PT-PCCA 2013-4-1557, contract PN II 249/2014.

1. Mihai-Nicolae Selagea, Bogdan Lungu, Daniel Besnea, Daniel Comeaga, Cristinel Ioan Ilie, Radu Udrea, Fiber Laser Induced Colour Marking on Stainless Steel, Proc.of 11<sup>th</sup> Int. Conf. "Micro to Nano Photonics", Romopto 2015;
2. Z.L.Li, H.Y.Zheng, K.M.Teh, Y.C.Liu, G.C.Lim, H.L.Seng, N.L.Yakovlev, Analysis of oxide formation induced by UV coloration of stainless steel, Appl.Surf.Sci.256 (2009) 1582-1588;
3. A.Lehmuskerö, V.Kontturi, J.Hiltunen, M.Kuittinen, Modeling of laser-colored stainless steel surfaces by color pixels, Appl.Phys.B 98 (2009) 497 – 500;
4. A.J.Antonczak, D.Kocou, M.Nowak, P.Kozioł, K.M.Abramski, Laser-induced colour marking – Sensitivity scaling for a stainless steel

## Hybrid femtosecond laser processing of biomimetic architectures with lab-on-a-chip devices for cancer cell study

Felix Sima<sup>1,2</sup>, Dong Wu<sup>2</sup>, Jian Xu<sup>2</sup>, Katsumi Midorikawa<sup>2</sup>, Koji Sugioka<sup>2</sup>

<sup>1</sup>Laser Department, National Institute for Lasers, Plasma and Radiation Physics, Magurele, Ilfov, 00175, Romania

<sup>2</sup>RIKEN-SIOM Joint Research Unit, RIKEN Center for Advanced Photonics, 2-1 Hirosawa, Wako, Saitama, 351-0198, Japan  
felix.sima@inflpr.ro; ksugioka@riken.jp

Femtosecond (fs) laser direct writing is a versatile tool for fabricating functional biochips with microscale dimensions. Fs laser induced nonlinear absorption can confine the material modifications at the focal volume inside the transparent materials, so that high resolution movable stages potentiate the fs laser capability of creating complex arrangements in three dimensions (3D). Fs laser irradiation followed by wet chemical etching (FLAE) of photosensitive glasses permitted to fabricate true 3D micro-channels embedded in volume in a manner of subtractive manufacturing. On the other hand, fs lasers can also induce multiphoton absorption to UV-photopolymerizable resins. Thus, two-photon polymerization (TPP) emerged as an additive fabrication technology with much higher precision in order to reduce dimensions from micro to nanoscale of polymeric structures with limit resolution beyond the diffraction frontier to the wavelength used for material processing.

Herein we propose laser fabrication of functional biochips for human cell testing. Hybrid glass and polymeric 3D configurations were designed and innovative biomimetic scaffolds fabricated by fs laser only for study of cancer cells inside glass micro-channels. FLAE of a photosensitive glass followed by TPP of a negative epoxy-resin allowed the lodging of a polymer scaffold with smaller dimensions inside a glass biochip. Time lapse imaging of cancer cell migration was carried out inside biochip during different time intervals. The cells were found responsive to chemo-gradient concentration created through 2  $\mu\text{m}$  diameter channels of the 3D polymeric scaffold (Figure 1).

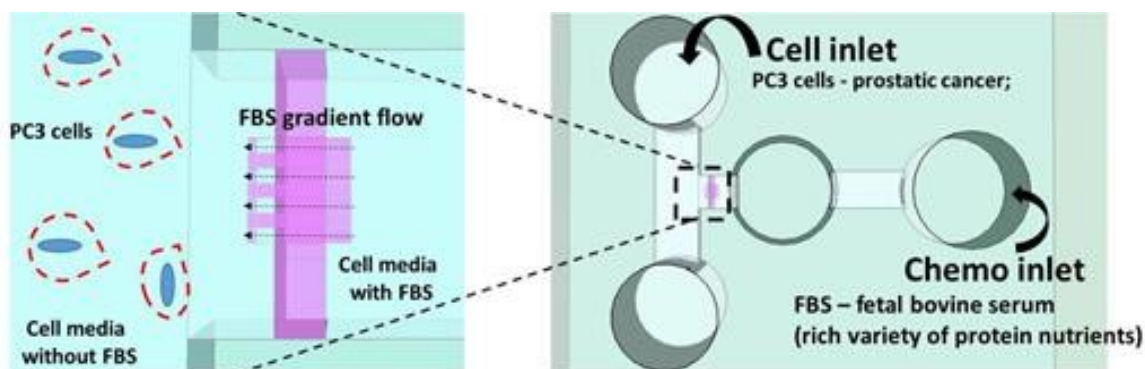


Figure 1: Scheme of a biochip device top view (right), Zoom of area of observation used for time lapse imaging of cancer cells (left).

# Mesenchymal stem cells osteogenic fate on excimer lasersdesigned bone pits topographies

L. E. Sima<sup>1</sup>, M. Icriverzi<sup>1,2</sup>, K. Bohlen<sup>3</sup>, E.C. Siringil<sup>4</sup>, T. Jäger<sup>5</sup>, K. Wasmer<sup>4</sup>, P. Hoffmann<sup>4</sup>,  
M. Dinescu<sup>6</sup>, A. Roseanu<sup>1</sup>, A. Cimpean<sup>2</sup>, V. Dinca<sup>4,6</sup>

<sup>1</sup>Institute of Biochemistry, Romanian Academy, 296 Spl. Independentei, Bucharest, Romania

<sup>2</sup>University of Bucharest – Faculty of Biology, Department of Biochemistry and Molecular Biology, 90-94 Spl. Independentei, Bucharest Romania

<sup>3</sup>Crealas GmbH, Feuerwerkerstrasse 39, CH-3602 Thun, Switzerland

<sup>4</sup>Empa, Laboratory for Advanced Materials Processing, Feuerwerkerstrasse 39 3602 Thun, Switzerland

<sup>5</sup>Empa, Laboratory for Thin Films and Photovoltaics, Ueberlandstrasse 129 8600, Dübendorf, Switzerland

<sup>6</sup>National Institut for Lasers, Plasma and Radiation Physics, Atomistilor 409, 077125, Magurele, Bucharest, Romania  
lsima@biochim.ro

Global increase in life expectancy requires the emergence of new strategies in design of long lasting bone prosthesis. In order to improve implant osseointegration it is crucial to enhance the dynamic formation of new bone at the cells-material interface. Bone tissues are constructed of structures with macro-(osteoids), micro(mineralized extracellular matrix) and nanoscale (collagen fibres and hydroxyapatite crystals) features. Control of mesenchymal stem cells (MSCs) osteogenic fate by implant biomaterials surface features holds great potential for prosthetic design in orthopaedics and dentistry. Micron scale surface topographies have been shown to impact lineage commitment of MSCs.<sup>1-2</sup> However, designing and obtaining highly reproducible and large area polymeric surfaces represent still a challenge in tissue engineering. This work presents large area polymeric microstructured surfaces using excimer laser processing technique. The proposed model surfaces were investigated with a view to understand how anisotropy regulates stem cell behaviour on defined surface microstructures. Bone pits similar to those produced by osteoclast during bone resorption were produced by an ablation process of polycarbonate on a large surface exposure set-up and a consecutive titanium coating process (magnetron sputtering). Microstructured surfaces with various depths (200 nm-7 µm) were put in interaction with either human premonocytic THP-1 cells or MSCs to evaluate their potential to modulate inflammation and osteogenic differentiation, respectively. Cell growth and adhesion were depending on substrate topography depth. MSCs proliferation was apparently not affected for depths below 2 µm after 72 h, but slightly decreased for those in the range of 3-7 µm. The cell shape modifications induced by interaction with microtopography were analysed by SEM and immunofluorescence microscopy following actin filaments labelling. Data were correlated with osteogenic differentiation potential quantitated by mineralization assay. The results indicate that substrate depth features play a key role in hMSCs short-term spreading response and contact guidance, and long-term osteoinduction. Our data support the potential use of laser micropatterned substrates to modulate osteoprogenitor cell fate during bone implantation.

**Acknowledgments:** This work was supported by Sciex project code 11.189-BioAMan and Romanian National Authority for Scientific Research (CNCS – UEFISCDI), under the projects PNII-PT-PCCA-2013-4-199, PN-IIRU-TE-2014-4-2434, PN09-39, and Romanian Academy project I/2015-2016.

1. R. Olivares-Navarrete, S.L. Hyzy, D.L. Hutton, C.P. Erdman, M. Wieland, B.D. Boyan, Z. Schwartz, Direct and indirect effects of microstructured titanium substrates on the induction of mesenchymal stem cell differentiation towards the osteoblast lineage, *Biomaterials*, **31**, 2728-2735 (2010);
2. K. Anselme and M. Biggerelle, Role of materials surface topography on mammalian cell response, *International Materials Reviews*, **56**, 243-266 (2011).

# Spectroscopic investigations of novel pharmaceuticals: stability and laser beam resonant interaction

A. Smarandache<sup>1</sup>, A. Pascu<sup>1</sup>, M. Boni<sup>1,2</sup>, I. Andrei<sup>1</sup>, J. Handzlik<sup>3</sup>, K. Kiec-Kononowicz<sup>3</sup>, A. Staicu<sup>1</sup>, M.-L. Pascu<sup>1</sup>

<sup>1</sup>National Institute for Laser Plasma and Radiation Physics, Str. Atomistilor 409, Magurele 077125, Romania,

<sup>2</sup>Faculty of Physics, University of Bucharest, Str. Atomistilor 405, Magurele 077125, Romania

<sup>3</sup>Medical College, Jagiellonian University, Sw. Anny 12, 31-008 Cracow, Poland  
adriana.smarandache@infpr.ro

This study presents the photophysics of two novel hydantoin derivatives that exhibit promising pharmaceutical properties as antitumoral<sup>1</sup> and antimycobacterial<sup>2</sup> agents. Stability studies are necessary to establish the proper use of drug solutions in different applications. As for their administration, it is imperative to know their shelf life, as well as storage conditions. Time stability studies are usually carried out under constant and variable environmental conditions (e.g. storage temperature, illumination conditions, solvent of utilized medicine solution and its concentration, etc.).

At the same time, laser induced modified properties of the two new compounds are valuable to further investigate their specific interactions with other materials, including biological targets.

The two hydantoin derivatives under generic names SZ2 (C<sub>10</sub>H<sub>7</sub>ClN<sub>2</sub>OS) and SZ7 (C<sub>17</sub>H<sub>14</sub>N<sub>2</sub>O<sub>2</sub>S) were prepared as solutions in dimethyl sulfoxide (DMSO) at different concentrations. They were kept in various light/temperature conditions up to 3 months. Stability assay was conducted based on samples absorption properties measured with a Perkin Elmer UV/VIS absorption spectrophotometer.

Using a specific experimental arrangement, the samples in bulk or droplets were exposed to laser radiation emitted at 266 nm as the fourth harmonic of a Nd:YAG laser for different time intervals.

The UV/VIS absorption spectra of SZ2 and SZ7 solutions in DMSO are characterized by broad bands due to simultaneous electronic and vibrational-rotational excitation. It could be observed the higher magnitude of the peak located in UVA, which is assigned to carbonyl chromophore in position 4 of the imidazolidine ring due to greater delocalization.

As for stability assay, only solutions kept in dark at 4°C have preserved the absorption characteristics, considering the cumulated measuring errors, up to about one week.

The spectral fingerprint of solutions in UV disappeared after 1h of pulsed laser irradiation. A general result of the experiments' analysis is that modifications are induced in molecular structures of hydantoin derivatives by exposure to laser radiation of microdroplets or bulk samples. This fact evidences that in both cases molecules are photoreactive. Changes produced in microdroplet presentation are faster than in bulk exposure. This could be due to higher ratio between the number of photons in the laser beam and the number of molecules in microdroplet comparatively with bulk samples<sup>3</sup> but the resonant interaction of laser beams with molecules in microdroplets has many aspects that need to be further studied.

By comparative analysis of fluorescence emission of the two investigated hydantoin derivatives both in bulk and microdroplet form when exposed to laser beam, it results that in pendant microdroplet the fluorescence signal is amplified and it is possible that lasing emission appears due to the spherical shape of the droplet.<sup>4,5</sup> There are studies asserting that the peak of lasing signal depends on droplet's content, thus creating the opportunity of tuneable microlasers generation for medical applications. Those microlasers effects could be upgraded with the effect of other medicines or micro/nanoparticles which may be simultaneously delivered to the treated tissues without being affected by exposure to pumping laser beam or lasing radiation.<sup>5</sup>

**Acknowledgements:** The authors acknowledge the financial support of the ANCS by projects number PN-II-IDPCE-2011-3-0922 and PN-II-PT-PCCA-2011-3.1-1350, and the PN Nucleu project: 1647/2016.

1. I. Subtelna, D. Atamanyuk, E. Szymanska, K. Kiec-Kononowicz, B. Zimenkovsky, O. Vasylenko, A. Gzella, R. Lesyk, Synthesis of 5-aryliden-2-amino-4-azolones and evaluation of their anticancer activity, *Bioorg. Med. Chem.* 18, 5090-5101 (2010);
2. E. Szymanska, K. Kiec-Kononowicz, A. Bialecka, A.K. Kasproicz, Antimicrobial activity of 5-aryliden aromatic derivatives of hydantoin. Part 2, *Farmaco* 57, 39-44 (2002);
3. I.R. Andrei, T. Tozar, A. Dinache, M. Boni, V. Nastasa, M.L. Pascu, Chlorpromazine Transformation by Exposure to Ultraviolet Laser Beams in Droplet and Bulk, *Eur. J. Pharm. Sci.* 81, 27-35 (2016);
4. H.-M. Tzeng, K. F. Wall, M. B. Long, R. K. Chang, Laser emission from individual droplets at wavelengths corresponding to morphology-dependent resonances, *Opt. Lett.* 9 499-501 (1984);
5. M. Aas, A. Jonas, A. Kiraz, O.Brzobohaty, J. Jezek, Z. Pilat, and P. Zemanek, Spectral tuning of lasing emission from optofluidic droplet microlasers using optical stretching, *Optics Express* 21(18) 21380-21394 (2013).

# UV-LED induced plasmonic and excitonic nanocomposites

A.A. Smirnov<sup>1</sup>, A. Afanasiev<sup>1</sup>, N. Ermolaev<sup>1</sup>, S. Gusev<sup>2</sup>, N. Bityurin<sup>1</sup>

<sup>1</sup>Institute of Applied Physics of Russian Academy of Sciences, 46 Ul'yanov Street, Nizhny Novgorod 603950, Russia

<sup>2</sup>Institute for Physics of Microstructures of Russian Academy of Sciences, GSP-105, Nizhny Novgorod 603950, Russia  
antonsmirnov@uftp.appl.sci-nnov.ru

UV irradiation of materials consisting of a polymer matrix that possesses precursors of different kinds can result in creation of nanoparticles within the irradiated domains. Such photoinduced nanocomposites are promising for photonic applications due to the strong alteration of their optical properties compared to initial non-irradiated materials. We report our results on the synthesis and investigation of plasmonic, excitonic and excitonplasmonic photoinduced nanocomposites. Plasmonic nanocomposites contain metal nanoparticles of noble metals with a pronounced plasmon resonance.<sup>1</sup> Excitonic nanocomposites possess semiconductor nanoclusters (quantum dots).<sup>2</sup> We consider the CdS–Au pair because the luminescent band of CdS nanoparticles enters the plasmon resonance band of gold nanoparticles. The obtaining of such particles within the same composite materials is promising for the creation of media with exciton–plasmon resonance. We demonstrate that it is possible to choose appropriate precursor species to obtain the initially transparent poly(methyl methacrylate)

(PMMA) films containing both types of these molecules either separately or together.<sup>3</sup> Proper irradiation of these materials by a light-emitting diode operating at the wavelength of 365 nm provides material alteration demonstrating light-induced optical absorption and photoluminescent properties typical for the corresponding nanoparticles. Thus, an exciton-plasmonic photoinduced nanocomposite is obtained. It is important that here we use the precursors that are different from those usually employed.<sup>4</sup>

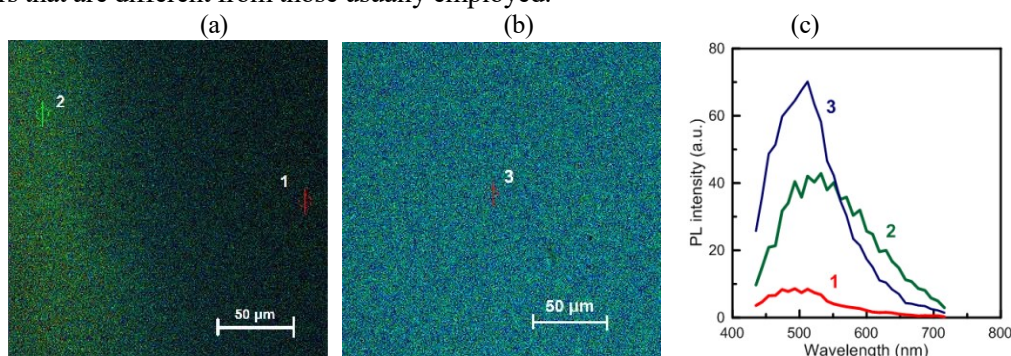


Figure 1: Fluorescent images of  $[Cd(N(SCNEt_2)_2)]/PMMA$  films with weight fraction of precursor 2.5%: (a) the border between LED-irradiated and non-irradiated regions, (b) irradiated region, (c) PL spectra measured in different points. The excitation wavelength is 405 nm.

**Acknowledgements:** The work is supported by Russian Scientific Foundation (Grant No. 14-19-01702).

1. A. Alexandrov, L. Smirnova, N. Yakimovich, N. Sapogova, L. Soustov, A. Kirsanov, N. Bityurin, UV initiated growth of gold nanoparticles in PMMA matrix, *Appl. Surf. Sci.* **248**, 181–184 (2005);

2. A.A. Smirnov, A. Afanasiev, N. Ermolaev and N. Bityurin, LED induced green luminescence in visually transparent PMMA films with CdS precursor, *Opt. Mater. Express.* **6**(1), 290-295 (2016);

3. N. Bityurin, N. Ermolaev, A. A. Smirnov, A. Afanasiev, N. Agareva, T. Koryukina, V. Bredikhin, V. Kamenskiy, A. Pikulin, N. Sapogova, Plasmonic, excitonic and exciton-plasmonic photoinduced nanocomposites. *Appl. Phys. A.* **122**:193 (2016);

4. N. Agareva, A.A. Smirnov, A. Afanasiev, S. Sologubov, A. Markin, E. Salomatina, L. Smirnova, and N. Bityurin, Properties of Cadmium-(bis)dodecylthiolate and Polymeric Composites Based on It, *Materials*, **8**(12), 8691-8700 (2015).



# Plasmonic particle mediated laser alteration of material

A.A. Smirnov, A. Pikulin, N. Sapogova, N. Bityurin

Institute of Applied Physics of Russian Academy of Sciences, 46 Ul'yanov Street, Nizhny Novgorod 603950, Russia  
anton-smirnov@uftp.appl.sci-nnov.ru

We analyze the opportunities provided by the plasmonic nanoparticles inserted into the bulk of a transparent medium to modify the material by laser light irradiation. This study is provoked by the advent of photo-induced nanocomposites consisting of a typical polymer matrix and metal nanoparticles located in the light-irradiated domains of the initially homogeneous material. The subsequent irradiation of these domains by femtosecond laser pulses promotes a further alteration of the material properties. We separately consider two different mechanisms of material alteration. First, we analyze a photochemical reaction initiated by the two-photon absorption of light near the plasmonic nanoparticle within the matrix. We show that the spatial distribution of the products of such a reaction changes the symmetry of the material, resulting in the appearance of anisotropy in the initially isotropic material or even in the loss of the center of symmetry. Second, we analyze the efficiency of a thermally-activated chemical reaction at the surface of a plasmonic particle and the distribution of the product of such a reaction just near the metal nanoparticle irradiated by an ultrashort laser pulse.<sup>1</sup>

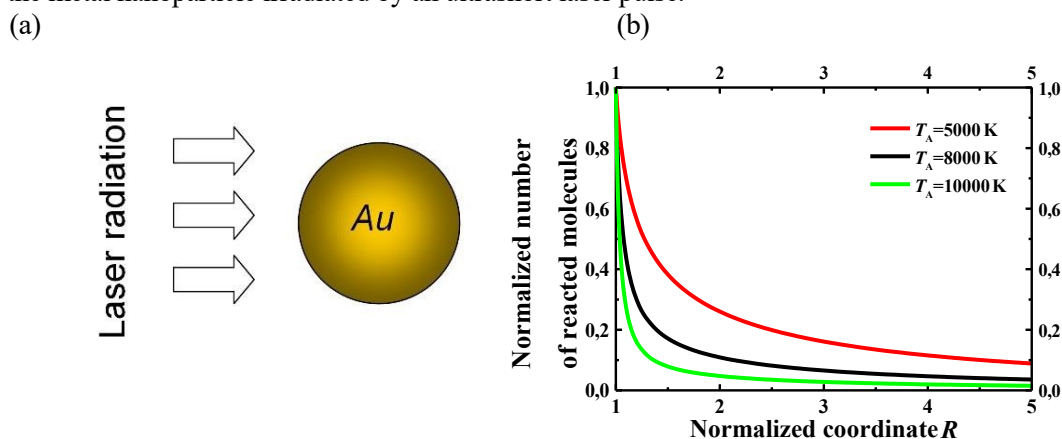


Figure 1: (a) The modeling setup. A spherical gold nanoparticle is irradiated by femtosecond laser pulses. (b) Calculated number of reacted molecules, normalized on its value at the particle surface ( $R=1$ ) as function of the distance from the center of the particle. Temperature increment of the particle after the laser pulse is 100 K, room temperature is 300 K, and different activation temperatures of the reaction are taken:  $T_A = 10000$  K (green line),  $T_A = 8000$  K (black line) and  $T_A = 5000$  K (red line). The distance is normalized on the particle radius

**Acknowledgements:** The work is supported by Russian Scientific Foundation (Grant No. 14-19-01702).

1. A. A. Smirnov, A. Pikulin, N. Sapogova and N. Bityurin, Femtosecond Laser Irradiation of Plasmonic Nanoparticles in Polymer Matrix: Implications for Photothermal and Photochemical Material Alteration, *Micromachines* **5**(4), 1202-1218 (2014).

## Organic heterostructures deposited by MAPLE on AZO substrate

G. Socol<sup>1</sup>, M Socol<sup>2</sup>, N. Preda<sup>2</sup>, A. Stanculescu<sup>2</sup>, C. Breazu<sup>2,3</sup>, F. Stanculescu<sup>3</sup>, M. Girtan<sup>4</sup>

<sup>1</sup>National Institute for Lasers, Plasma and Radiation Physics, 409 Atomistilor Street, 077125, Magurele, Romania

<sup>2</sup>National Institute of Material Physics, 105 bis Atomistilor Street, 077125, Magurele, Romania

<sup>3</sup>University of Bucharest, Faculty of Physics, 405 Atomistilor Street, 077125, Bucharest, Romania

<sup>4</sup>Laboratoire de Photonique d'Angers, Université d'Angers, 2, Bd. Lavoisier, 49045, Angers, France  
gabriel.socol@inflpr.ro

Organic heterostructures thin films based on poly(3-hexylthiophene) (P3HT) and fullerene (C60) were deposited by Matrix-Assisted Pulsed Laser Evaporation (MAPLE) technique on AZO. 3% (wt) Al:ZnO films were deposited by Pulsed Laser Deposition (PLD) on glass substrate in order to replace the classical indium tin oxide (ITO). Optical (UV-VIS, FTIR and PL spectroscopy) and electrical properties of the obtained heterostructures were investigated with respect to the structural (X Ray Diffractions) and morphological (atomic force microscopy and scanning electron microscopy) features. I-V characteristics of (AZO/P3HT/C60/Al multilayer and P3HT:C60 blends) structures were recorded in dark and under the illumination with a solar simulator (AM1.5) to select heterostructures with the optimal features for OPV applications. We found out that the roughness of the organic active layers has a critical role with respect to the electrical behavior of the investigated heterostructures.

# MAPLE fabrication of CaPs: Poly (3-hydroxybutyrate-co-3-hydroxyvalerate)- based coatings as substrate for bone tissue engineering

G. Socol<sup>1</sup>, O. Rasoga<sup>2</sup>, M. Chiritoiu<sup>3</sup>, L. Sima<sup>3</sup>, V. Grumezescu<sup>1</sup>, G. Popescu-Pelin<sup>1</sup>, M. Socol<sup>2</sup>, I. Zgura<sup>2</sup>

<sup>1</sup>National Institute for Lasers, Plasma and Radiation Physics, Magurele, Ilfov, Romania

<sup>2</sup>National Institute of Materials Physics, 405A, Atomistilor Street, Magurele, Ilfov, P.O. Box MG-7, 077125, Romania

<sup>3</sup>Institute of Biochemistry, Splaiul Independentei 296, Bucharest, Romania  
gabriel.socol@inflpr.ro

One of the most used natural biodegradable polymers is Poly(3-hydroxybutyrate-co-3-hydroxyvalerate (PHBV), a poly-3-hydroxybutyrate copolymer with improved mechanical and processability properties, part of the polyhydroxyalkanoates polyester family. Due to their degradation products are non-toxic, encountered like metabolite in human blood with a very slow *in vitro* degradation rate, PHBV is intensively studied in bone tissue engineering, in the preparation of controlled release system, production process like bottles, fibers or clothing. In medical applications, studies were oriented on reinforcing and improving the suitability of the PHBV with various biocompatible materials: natural fibers, bioceramics, natural clays or polymers to enhance the physical and mechanical properties. Among calcium phosphate (CaP) bioceramics, the hydroxyapatite (HA) is the most used in orthopedic treatments due to the fact that is similar to the bone apatite, which is the major mineral component of it. For some applications, the low solubility of HA is considered a drawback of the material. Therefore,  $\beta$ -tricalcium phosphate ( $\beta$ -TCP) seems to be a better choice for bone tissue regeneration, due to its high dissolution rate in the human body environment.

Because the majority of the (bio)organic polymeric applications requires coatings a wide range of methods such as: coaxial electrospinning, electrospinning, meltspinning, Single Emulsion Technique, Alternative Incubation Method, Freezing-Drying Technique, drop cast, Supercritical Fluid Technology or Selective Laser Sintering (SLS) Technology, Laser Induced Forward Transfer (LIFT) and MAPLE Direct Writing (LBW) were used for deposition. Our efforts were focused towards the study of thin films obtained from mixtures of the PHBV copolymer with HA or  $\beta$ -TCP by Matrix Assisted Pulsed Laser Deposition (MAPLE) technique as alternative option to other methods. The physico-chemical properties of the coatings were investigated by Fourier Transform Infrared spectroscopy, Scanning Electron Microscopy and X-Ray Diffraction. We put in evidence, by immunofluorescence microscopy, that the addition of hydroxylapatite (HA) into different PHBV polymeric matrixes induces enhanced bioactivity compared with simple PHBV coatings. The molecular “fingerprints” of the coatings were found to be highly similar to the spectrum of the dropcast, especially at higher fluence, which demonstrate that MAPLE technique is an adequate technique for deposition of biomaterials. By scanning electron microscopy we evidenced a typical morphology of the coatings. Moreover, the X-Ray Diffraction put in evidence that at higher fluences there is a superposition of the PHBV and  $\beta$ -TCP, respectively HA peaks while the addition of the bioceramics increases the cristalinity of the coatings.

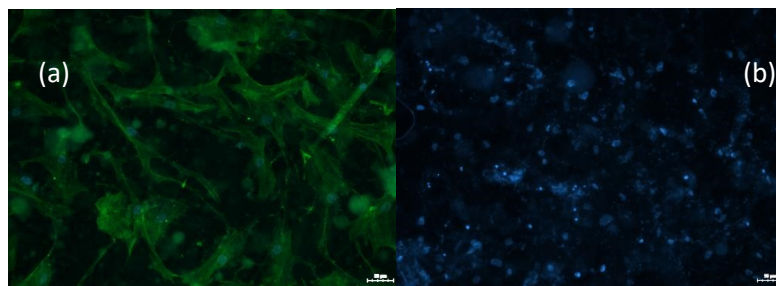


Figure 1: Immunofluorescence microscopy images of mesenchymal stem cells 3 days after adhesion (a) and 28 days post-osteoinduction (b) on PHBV:HA 1:1 MAPLE coating on titanium. Nuclei were stained with Hoechst (blue) and actin filaments were stained using Alexa Fluor 488-conjugated Phalloidin (green).

# Wet chemical synthesis of ZnO-CdS composites with enhanced photocatalytic activity

G. Socol<sup>1</sup>, I. Zgura<sup>2</sup>, N. Preda<sup>2</sup>, L. Frunza<sup>2</sup>, L. Diamandescu<sup>2</sup>, M. Enculescu<sup>2</sup>, L. Nedelcu<sup>2</sup>, C. P. Ganea<sup>2</sup>, S. Frunza<sup>2</sup>

<sup>1</sup>National Institute for Lasers, Plasma and Radiation Physics, 409 Atomistilor Street, Magurele RO-077125, Romania

<sup>2</sup>National Institute of Materials Physics, 405A Atomistilor Street, Magurele RO-077125, Romania  
irina.zgura@infim.ro

In the last years, the composites of various semiconductor micro/nano particles such as ZnO, CdS, TiO<sub>2</sub>, etc. became very attractive for photocatalytic applications<sup>1,2</sup>. The present study is focused on the wet chemical synthesis and the complex characterization of ZnO-CdS composites. The synthesis of ZnO-CdS composites consists in two steps: i) the preparation of CdS nanoparticles by the chemical reaction between Cd(NO<sub>3</sub>)<sub>2</sub> and Na<sub>2</sub>S and ii) the generation of ZnO microparticles from the reaction between Zn(NO<sub>3</sub>)<sub>2</sub> and NaOH, in the presence of different amounts of CdS nanoparticles. The powder samples were investigated by different techniques: scanning electron microscopy (SEM), X-ray diffraction, energy dispersive X-ray analysis, optical spectroscopy, photoluminescence and photocatalytic measurements. SEM image (Fig. 1a) shows flowers like structures for the synthesized ZnO-CdS composites. The UV photocatalytic degradation curves of dyes such as methylene blue for the CdS, ZnO and ZnO-CdS composites (Fig. 2b) prove that the photocatalytic activity of the composites is higher than that of ZnO. In addition, the degradation curves demonstrate that the photoactivity of the ZnO-CdS composites can be tuned by controlling the amounts of CdS nanoparticles added during the chemical synthesis of ZnO. Such simple wet chemical approach can be used for the synthesis of various hybrid composites based on semiconductor structures with enhanced photocatalytic properties, taking into account their advantages such as: the use of inexpensive equipments and easily accessible raw materials and the possibility to control the properties of the final products by changing the experimental parameters.

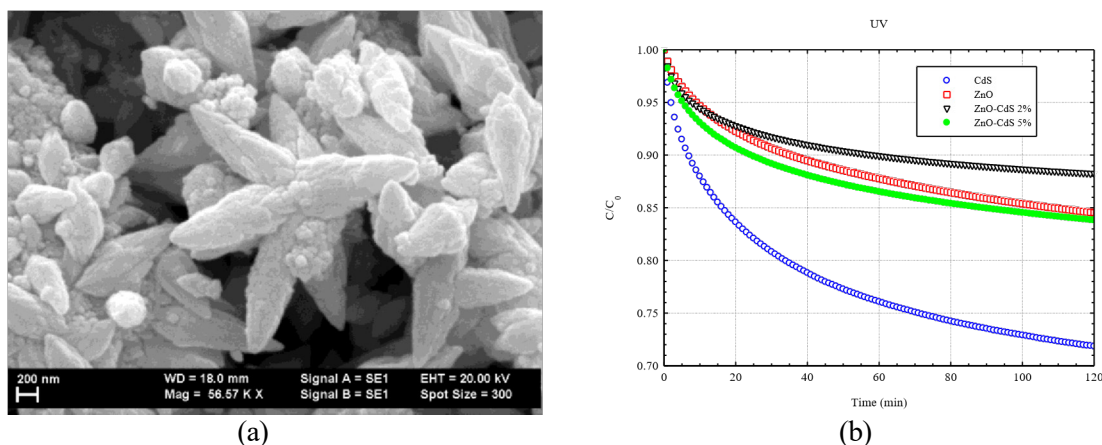


Figure 1: (a) SEM image of ZnO-CdS composites and (b) Photocatalytic degradation curves of methylene blue under UV irradiation of the ZnO, CdS and ZnO-CdS composites samples.

**Acknowledgements:** The authors acknowledge with thanks the funding of this research by the Romanian National Authority for Scientific Research through the Core Program, Project PN16480101.

1. Chun Cheng<sup>1</sup>, Abbas Amini, Chao Zhu, Zuli Xu, Haisheng Song, Ning Wang, Enhanced photocatalytic performance of TiO<sub>2</sub>-ZnO hybrid nanostructures, Title of paper, Scientific Reports, **4**, 4181 (2014);
2. Chienhua Chen, Zhengcao Li, Hehnan Lin, Guojing Wang, Jiecuai Liao, Mingyang Li, Shasha Lv, Wei Li, Enhanced visible light photocatalytic performance of ZnO nanowires integrated with CdS and Ag<sub>2</sub>S, Dalton Trans., **45**, 3750-3758 (2016).

# Mesoporous carbon obtained by light assisted Evaporation induced self-assembly (LA-EISA)

M. Sopronyi<sup>1,2</sup>, F. Sima<sup>1</sup>, L. Vidal<sup>3</sup>, C.M. Ghimbeu<sup>3</sup>

<sup>1</sup>Lasers Department, National Institute for Lasers, Plasma and Radiation Physics, Atomistilor 409 bis, Magurele, Romania

<sup>2</sup>University of Bucharest, Faculty of Physics, Atomistilor 405, Magurele, Romania

<sup>3</sup>Institut de Science des Matériaux de Mulhouse, CNRS UMR 7361, UHA, 15 rue Jean Starcky, 68057 Mulhouse, France  
mihai.sopronyi@inflpr.ro

The interest of mesoporous carbon (MC) has grown in recent years for a wide range of applications, from energy storage and conversion, to sensors and drug release systems. This is related to specific properties of the material, such as high surface area, controllable pore size and geometry, good electric conductivity, and chemical inertness. In order to meet this high demand, optimization of the MC production process is often required.

We report on UV light irradiation of a solution consisting of green phenolic resins (phloroglucinol/glyoxylic acid) and a surfactant agent (Pluronic F127) as a novel approach to obtain mesoporous carbon. The UV-VIS spectra investigation on involved precursors and template showed that each polymer absorbs in the UV regime (from 200 to 300 nm). As a consequence, either a pulsed KrF\* laser ( $\lambda=248$  nm) or UV lamp (254 nm) were used for the solutions irradiation. The laser irradiation allowed to reduce the synthesis time to several minutes compared to one day for the classical evaporation method. Moreover, it was observed that by tailoring the laser irradiation conditions such as energy or pulse repetition rate, the irradiation dose can be increased and the time exposure reduced, resulting in a ordered mesoporous carbon materials with different textural and structural characteristics.

## Photophysics of single wall carbon nanotubes covalently functionalised with porphyrin photosensitizers

A. Staicu<sup>1</sup>, A. Pascu<sup>1</sup>, A. Smarandache<sup>1</sup>, T. Alexandru<sup>1</sup>, M.L. Pascu<sup>1</sup>

<sup>1</sup>National Institute for Laser, Plasma and Radiation Physics, 077125, Magurele, Romania

angela.staicu@inflpr.ro

We report photophysical studies of some compounds of interest in targeted drug delivery as conjugated single walled carbon nanotubes with a photosensitizing agent.

Supramolecular entities porphyrin – single wall carbon nanotubes (CNT) have been synthesized by covalent functionalization and have been analyzed in terms of laser induced fluorescence properties, singlet oxygen generation and photostability.

The fluorescence and singlet oxygen quantum yields were determined. The chemical structure was analyzed by FTIR spectroscopy.

There were highlighted the photophysical characteristics of the conjugated compounds with respect to correspondent mixture of the raw components.

In Fig. 1 there are shown the time-resolved phosphorescence signals (1270 nm) of the photosensitized singlet oxygen for Verteporfin (VP), Methylene Blue (MeB), linked CNT-VP and the mixture of CNT and VP.

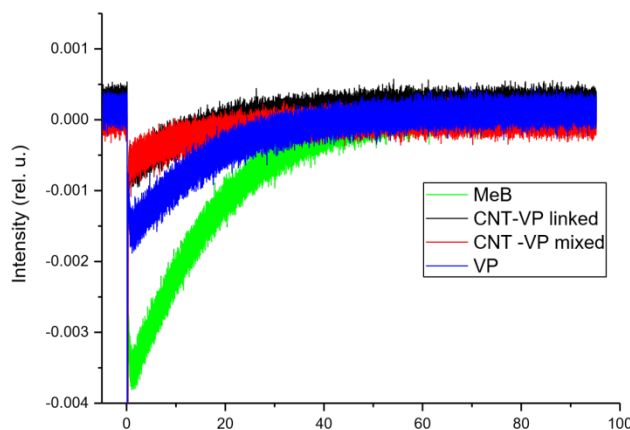


Figure 1: Time-resolved phosphorescence signals (1270 nm) of the photosensitized singlet oxygen for the compounds of interest.

**Acknowledgements:** The authors from INFLPR acknowledge the financial support of the Romanian National Authority for Scientific Research and Innovation, through NUCLEU project PN1647/2016 and CNCSUEFISCDI by project number PN-II-ID-PCE-2011-3-0922.

# Mechanical and *in vitro* biological performance of bioglass coatings deposited by magnetron sputtering on dental implant fixtures

G.E. Stan<sup>1</sup>, A.C. Popa<sup>1,2</sup>, V.M.F. Marques<sup>3</sup>, A.C. Galca<sup>1</sup>, M.A. Husanu<sup>1</sup>, M. Enculescu<sup>1</sup>, C. Tanase<sup>4</sup>, D.U. Tulyaganov<sup>5</sup>, J.M.F. Ferreira<sup>6</sup>

<sup>1</sup>National Institute of Materials Physics, 077125 Magurele, Romania

<sup>2</sup>Army Centre for Medical Research, 020012 Bucharest, Romania

<sup>3</sup>Department of Materials, University of Oxford, Parks Road, Oxford OX1 3PH, United Kingdom

<sup>4</sup>“Victor Babes” National Institute of Pathology, 050096 Bucharest, Romania

<sup>5</sup>Turin Polytechnic University in Tashkent, Tashkent 100174, Uzbekistan

<sup>6</sup>Department of Materials and Ceramics Engineering, CICECO, University of Aveiro, 3810-193 Aveiro, Portugal

Bioactive glasses are currently considered the suitable candidates to stir the quest for a new generation of osseous implants with superior biological/functional performance. In congruence with this vision, this contribution aims to introduce a reliable technological recipe for coating fairly complex 3D-shaped implants (e.g. dental screws) with uniform and mechanical resistant bioactive glass films by the radio-frequency magnetron sputtering method. An exploratory magnetron sputtering (MS) study was employed in the search of the deposition variables capable to imprint suitable chemical, structural, mechanical, and biological properties to the coatings. The prerequisites for reliable implant-type coatings are both their biological and mechanical performances. In congruence with this vision, this contribution introduces for the first time a reliable technological recipe for coating fairly complex 3D-shaped dental implants with uniform and mechanical resistant BG coatings by the MS method. The mechanical reliability of the BG coatings applied to real Ti dental implant fixtures has been evaluated by a procedure comprised of “cold” implantation in pig mandibular bone from a dead animal, followed by immediate tensionfree extraction tests. The effects of the complex mechanical strains occurring during implantation were analysed by SEM-EDS. Extensive biocompatibility assays (MTS, immunofluorescence, Western blot) revealed that the BG coatings stimulated strong cellular adhesion and proliferation of human dental pulp stem cells, without promoting their differentiation. The ability of the BG implant coatings synthesized by MS to conserve a healthy stem cell pool is promising to further endorse the fabrication of new osseointegration implant designs with extended lifetime.

## Investigation of the effect of laser parameters on the target, plume and plasma behavior during and after laser-solid interaction

A. Stancalie<sup>1</sup>, S. Ciobanu<sup>2</sup>, D. Sporea<sup>1</sup>

<sup>1</sup>National Institute for Laser, Plasma and radiation Physics, Atomistilor 409, P.O.Box MG-36, Magurele-Ilfov, 077125 Romania

<sup>2</sup>University Politehnica of Bucharest, Faculty of Applied Sciences, 313 Splaiul Independentei, 060042 Bucharest, Romania  
andrei.stancalie@inflpr.ro

The growing interest on laser-induced plasma has generated a variety of theoretical models and experimental works in order to improve the basic knowledge and determine the best experimental conditions. The laser ablation (LA) of metallic target and the subsequent expansion of the evaporated material plume<sup>1,2</sup>, as well as the laser-induced breakdown spectroscopy (LIBS) techniques<sup>3,4</sup> stand in the use of short laser pulses as the energy source to vaporize samples and excite the emission of electromagnetic radiation from its elements and/or molecular fragments. Although LIBS and LA are based on different mechanisms of detection, the processes occurring during and after laser-solid interaction are quite similar. In the case of metallic target the laser causes heating of the solid target, followed by melting and evaporation of some of the target material. In the present study we report recent both experimental and theoretical characterization of the plume expansion using spectroscopic methods to investigate the time evolution.

We report results on a wide range of laser operating conditions, typical for laser induced breakdown spectroscopy (LIBS) and laser ablation (LA) experiments, which form the basis of further systematically investigation of the effect of laser irradiance, pulse duration and wavelength, on the target, plume and plasma behavior, during and after laser-solid interaction. In order to obtain a better insight in the exact influence of these laser parameters on laser-ablation and laser-plasma formation we present comparatively, recent results obtained from LIBS generated using a commercial instrument, the Applied Photonics LIBS-6, and from LA spectroscopic investigation of a plasma in air produced by the first ( $\lambda=1,064 \mu\text{m}$ , 360 mJ energy), and the second ( $\lambda=0,532 \mu\text{m}$ , 180 mJ energy) harmonics of a Q-switched pulsed Nd: YAG laser, 4.5ns pulse duration, 0.1÷10 Hz repetition frequency. The laser-induced plasma formation conditions to which our investigation is applied are shown in Table 1.

Table1.

Target	Copper
Background gas	Free atmosphere
Laser Irradiance	$10^8 - 10^{10}$ W/cm <sup>2</sup>
Laser pulse duration	0.3 – 10 ns
Laser wavelengths	532nm, 1064 nm

In the LA experiment, the laser beam was focused through a 25 cm focal length convergent lens on a plane copper target in air, at atmospheric pressure. The target was rotated in order to have fresh areas under laser irradiance. In the LIBS experiment, the Applied Photonics LIBS-6 instrument allowed modifying the laser irradiance at the sample surface by changing the pulse energy or the laser focusing distance. The plasma experimental parameters were estimated from spectroscopic data generated by the plasma itself, namely by the line intensities and their ratio which reflect the relative population of neutral or ionic excited species in the plasma. The Saha-Boltzmann plots corresponding to above mentioned two experiments show differences which are explained by the inhomogeneity of the plasmas which leads to a different apparent excitation temperature. The fitting of the Saha-Boltzmann plot to a straight line provides an apparent ionization temperature, whose value depends on the lines used in the plots. For the typical conditions of LA and LIBS, the temperature can be so high that Cu<sup>+</sup> ions are formed. The first –order ionization of Cu (i.e., the ratio of Cu<sup>+</sup>/Cu<sup>0</sup>) is calculated.

1. M.Aden, E. Beyer, G. Herziger, H. Kunze, Laser-induced vaporization of metal surface, *J. Phys. D, Appl Phys* **25**, 57-65(1992);
2. J.R. Ho, C.P. Grigoropoulos, J.A. Humphrey, Computational study of heat transfer and gas dynamics in the pulsed laser evaporation of metals, *J. Appl. Phys.* **78**, 4696-4709(1995);
3. S. Amuroso, M. Armenante, V. Berardi, R. Bruzzese, N. Spinelli, Absorption and saturation mechanisms in aluminium laser ablated plasma, *Appl. Phys. A* **65**, 265-271(1997);
4. J. Hermann, A.L. Thomanhn, C. Boulmer-Leborgne, B. Dubreuil, M.L. De Giogi, A. Perrone, A.Luches, I.N. Mihailescu, Plasma diagnostic in pulsed laser TiN layer deposition, *J. Appl. Phys.* **77**(7) 2928-2936(1995).

## Laser induced break down spectroscopy on soil samples

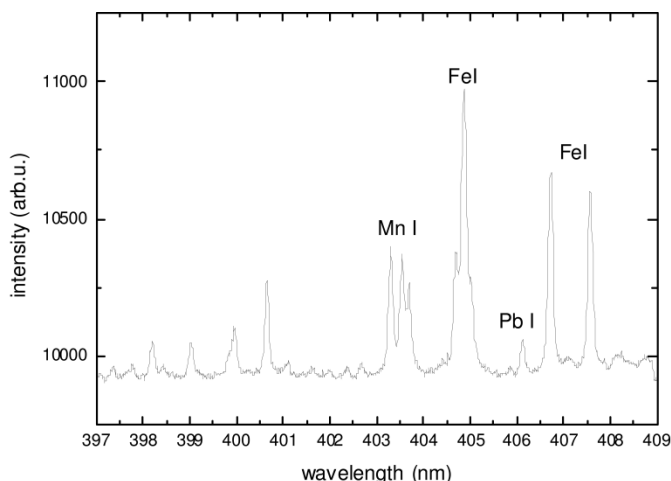
A. Stancalie<sup>1</sup>, A. Neago<sup>2</sup>, V. Iordache<sup>2</sup>, A. Staicu<sup>1</sup>

<sup>1</sup>National Institute for Laser, Plasma and Radiation Physics, 077125, Magurele, Romania,

<sup>2</sup>Faculty of Physics, University of Bucharest, 077125, Magurele, Romania,  
andrei.stancalie@infpr.ro

Laser spectroscopy techniques are modern and competitive methods for environmental analysis. Laser induced break down spectroscopy (LIBS), due to its advantages as noninvasive method, real time monitoring, selectivity, is a promising and suitable tool to measure metals in contaminated soils.

In this respect, based on the well-known spectra of the heavy metals, a study of the pollutants identification in soil was performed by LIBS.



The emission spectrum for a contaminated soil from Zlatna region in the spectral range 397-409 nm is shown in Fig. 1. The emission lines (air wavelengths) of Mn, Fe, and Pb are observed: Fe I - 404.76 nm, 406.63nm, 407.46 nm, Mn I - 403.07 nm, 403.4483 nm, Pb I - 405.78 nm.

The results indicate the danger to use plants grown in contaminated soils as food, for peoples but also for animals, but also opens the possibility to use specific cultures in contaminated soils as a method for decontamination and soil bioremediation.

Figure 1: The laser induced emission spectrum for a contaminated soil from Zlatna region in the spectral range 397-409 nm

**Acknowledgements:** The authors from INFPR acknowledge the financial support of the Romanian National Authority for Scientific Research and Innovation, through NUCLEU project PN1647/2016.

# MAPLE prepared heterostructures with oligoazomethine: fullerene derivative mixed layer for photovoltaic applications

A. Stanculescu<sup>1</sup>, M. Socol<sup>1</sup>, O. Rasoga<sup>1</sup>, L. Vacareanu<sup>2</sup>, M. Grigoras<sup>2</sup>, G. Socol<sup>3</sup>, F. Stanculescu<sup>4</sup>,  
C. Breazu<sup>1,4</sup>, M. Girtan<sup>5</sup>

<sup>1</sup>National Institute of Materials Physics, 405 A Atomistilor Street, P.O. Box MG-7, Bucharest-Magurele, 077125 Romania,

<sup>2</sup>P. Poni Institute of Macromolecular Chemistry, 41 A Gr. Ghica Voda Alley, 700487-Iasi, Romania

<sup>3</sup>National Institute for Laser, Plasma and Radiation Physics, Str. Atomistilor, Nr. 409, PO Box MG-36, Magurele, 077125, Romania

<sup>4</sup>University of Bucharest, Faculty of Physics, 405 Atomistilor Street, P.O. Box MG-11, Bucharest-Magurele, 077125 Romania

<sup>5</sup>University of Angers, Photonics Laboratory, University 2, Bd. Lavoisier 49045, Angers, France  
sanca@infim.ro

Organic solar cells show advantages over the inorganic solar cells because can be manufactured with low cost materials at low temperature processes on different substrates, including flexible substrates.

The performances of this type of solar cells can be enhanced identifying new donor materials showing optimized absorption spectra, energy levels and transport properties and optimizing the preparation method of the active layer.

An improved charge carrier transport between the donor and acceptor component can be obtained by the use of an active layer with a morphology characterized by interpenetrating networks assuring an increased contact area surpassing the conversion efficiency characterizing the bi-layer organic solar cells. This condition is satisfied by the active layer consisting in a mixture “blend” of donor and acceptor organic components determining a bulk or dispersed heterojunction. Therefore the organic heterostructure with mixed active layer represents an alternative to bi-layer heterostructure showing improved exciton dissociation and charge carriers transport.

The performances of the solar cell are determined by: 1) increased dissociation of the excitons generated by light absorption at the interface between donor and acceptor controlled by the morphology of the mixed layer; 2) efficient charge carrier extraction and collection by the electrodes controlled by the roughness of the organic film which is in contact with the electrode; 3) energetic driving force involved in exciton dissociation and rapid charge transfer processes at the donor/acceptor interfaces determined by the difference between the energy of the lowest unoccupied molecular orbital of donor and acceptor must compensate the binding energy of the exciton.

This paper presents some studies on the organic layers prepared from a mixture of an oligoazomethine (p type conduction) and a fullerene derivative, [6,6]-phenyl C61 butyric acid butyl ester/[C60]PCB-C4 (n type conduction), blended in 1:1 and 1:2 ratios. The new donors are characterized by a central unit of 2,5-diamino3,4-dicyanothiophene and electron donating carbazole (LV4) or triphenylamine (LV5) groups at both ends and the selected acceptor [C60]PCB-C4 shows an increased solubility resulting in improved film morphology with effect on the properties. The mixed layers have been deposited on Si, glass/ITO substrates by matrix-assisted pulsed laser evaporation (MAPLE) using chloroform and dimethyl sulfoxide (DMSO) as solvents, and the radiation  $\lambda=248$  nm of KrF\* excimer laser. The fluence was the same for all deposition while the number of pulses was at least one order of magnitude higher (60000-75000) for target realized in DMSO compared to those realized in chloroform (2500-7000) confirming that the laser evaporation process is strongly affected by matrix solvent.

Details about the structure and morphology have been obtained by XRD, AFM and SEM emphasizing the effect of the composition and solvent. Spectroscopic methods (UV-Vis, PL, FTIR) and I-V measurements in dark and under illumination have confirmed that these mixed layers prepared by MAPLE are adequate for solar cells applications. We have evaluated the parameters for solar cell structure realized with each type of mixed layer, identifying the structure showing the best parameters. The higher photovoltaic effect was shown by the solar cell structure realized with mixed layer of LV4 and [C60]PCB-C4 in the ratio 1:1 deposited by MAPLE from a chloroform matrix.

# Functionalization of medical grade PDMS processed by ns-laser pulses

N.E. Stankova<sup>1</sup>, P.A. Atanasov<sup>1</sup>, Ru.G. Nikov<sup>1</sup>, R.G. Nikov<sup>1</sup>, N.N. Nedyalkov<sup>1</sup>, K.N. Kolev<sup>2</sup>, Dr.M. Tatchev<sup>2</sup>, E.I. Valova<sup>2</sup>, J.S. Georgieva<sup>2</sup>, St.A. Arnyanov<sup>2</sup>, N. Fukata<sup>3</sup>, K. Grochowska<sup>4</sup>, G. Śliwiński<sup>4</sup>

<sup>1</sup>Institute of Electronics, Bulgarian Academy of Sciences, Tzarigradsko chaussee 72, Sofia 1784, Bulgaria,

<sup>2</sup>Rostislav Kaischew Institute of Physical Chemistry, Bulgarian Academy of Sciences, Acad. G. Bonchev Str., block 11, Sofia 1113, Bulgaria,

<sup>3</sup>International Center for Materials for NanoArchitecture (MANA), National Institute for Materials Science (NIMS), Japan,

<sup>4</sup>Photophysics Department, The Szevalski Institute, Polish Academy of Sciences, 14 Fiszerza St, 80-231 Gdańsk, Poland  
nesttankova@yahoo.com

Medical grade polydimethylsiloxane (PDMS) elastomer is a widely used in medicine as implants, e.g. shunts and pacemakers, long term neural implants, micro-channeled tracks as electrodes for neural interfaces for monitoring and/or stimulation of neural activity<sup>1-5</sup>, because of its remarkable properties: neutrality and chemical stability, very low electrical conductivity and transparency to visible and near infra-red light.

The as prepared medical grade PDMS sheets with thickness of 190  $\mu\text{m}$  are processed by a ns-Nd:YAG laser system comprises basic ( $\lambda = 1.064 \mu\text{m}$ ), 2nd ( $\lambda = 532 \text{ nm}$ ), 3rd ( $\lambda = 355 \text{ nm}$ ) and 4th ( $\lambda = 266 \text{ nm}$ ) harmonic generations. It delivers pulses of 15 ns at repetition rate of 10 Hz. A special attention is paid on the comparison between the qualities of the trenches produced by focused none manipulated and homogenized laser beam at 355 nm. The processed trenches are viewed and analyzed by laser microscopy,  $\mu$ -Raman and optical spectrometry, and scanning electron microscope. Selective Pt or Ni metallization of the laser processed traces is produced successfully via electroless plating.

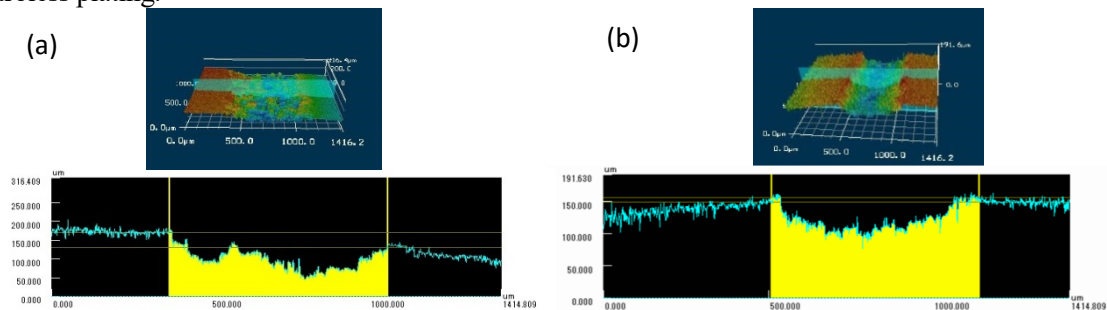


Figure 1: 3D Laser microscope images of the tracks produced by (a) non manipulated and (b) homogenized laser beam irradiated at 355 nm and their profiles, respectively.

1. C. Hassler, T. Boretius, T. Stieglitz, "Polymers for neural implants", *J. of Polymer Science Part B: Polymer Physics* **49** (1), 18-33 (2011);
2. Liang Guo, G.S. Guvanasen, Xi Liu, C. Tuthill, T.R. Nichols, S.P. DeWeerth, "A PDMS-based integrated stretchable microelectrode array (is MEA) for neural and muscular surface interfacing", *IEEE Transactions on Biomedical Circuits and Systems*, **7** (1), 1-10 (2013);
3. Mohamad Hajj Hassan, Vamsy Chodavarapu, Sam Musallam, "Review: NeuroMEMS: Neural Probe Microtechnologies", *Sensors*, **8** (10), 6704-6726 (2008);
4. S. Lacour, S. Benmerah, E. Tarte, J. Fitz Gerald, J. Serra, S. McMahon, J. Fawcett, O. Graudejus, Z. Yu, B. Morrison, "Flexible and stretchable micro-electrodes for in vitro and in vivo neural interfaces", *Medical and Biological Engineering and Computing*, **48** (10), 945954 (2010);
5. M. Schuettler, S. Stiess, B.V. King, G. J. Suaning, "Fabrication of implantable microelectrode arrays by laser cutting of silicone rubber and platinum foil", *J. Neural Eng.*, **2** (1) S121 (2005).

## Role of Substrate Morphology on the Characteristics of Noble Nanoparticles Produced by Laser-induced Deposition

N. Stefan<sup>1</sup>, N. E. Stankova<sup>2</sup>, F.M. Miroiu<sup>1</sup>, C. Hapenciu<sup>1</sup>, C. Ristoscu<sup>1</sup>, I.N. Mihailescu<sup>1</sup>, At. N. Tzonev<sup>3</sup>,

<sup>1</sup>National Institute for Lasers, Plasma, and Radiation Physics (INFLPR), Magurele, Bucuresti, Romania,

<sup>2</sup>Institute of Electronics, Bulgarian Academy of Sciences, 72 Tzarigradsko shose Blvd., Sofia 1784, Bulgaria,

<sup>3</sup>Department of Solid State Physics and Microelectronics, Faculty of Physics, University of Sofia, 5 J. Bouchier Blvd., Sofia, Bulgaria,  
stefan.nicolaie@inflpr.ro

Metallic nanoparticles have generated a great interest in different fields due to their unique properties, which made them suitable for applications such as chemical imaging<sup>1</sup>, solar cells<sup>2</sup>, biomaterials<sup>3</sup>, adsorption of organic molecules<sup>4</sup>, surface-enhanced Raman scattering<sup>5</sup>, and sensors and biosensors<sup>6</sup>.

We investigate the size, shapes and distribution of gold nanoparticles in dependence on the surface morphology of substrates. The nanoparticles are grown on substrates (Si, SiO<sub>2</sub>, glass and thin films of ITO, WO<sub>3</sub>, TiO<sub>2</sub>) with different crystal phases and roughness by using pulsed laser deposition technique. The morphology of the metal nanoparticles has been investigated by scanning electron microscopy and atomic force microscopy. The influence



of the gold nanoparticles morphology on their optical properties has been determined by studying of the surface plasmon resonance with UV-VIS spectroscopy.

1. R. B. P. Elmes, K. N. Orange, S. M. Cloonan, D. C. Williams, and T. Gunnlaugsson, "Luminescent ruthenium(II) polypyridyl functionalized gold nanoparticles; their DNA binding abilities and application as cellular imaging agents," *Journal of the American Chemical Society*, **133**(40), 15862–15865 (2011);
2. I.-K. Ding, J. Zhu, W. Cai et al., "Plasmonic back reflectors: plasmonic dye-sensitized solar cells," *Advanced Energy Materials*, **1**(1), 52–57 (2011);
3. H. Hermawan, D. Dubé, and D. Mantovani, "Degradable metallic biomaterials for cardiovascular applications," in *Metals for Biomedical Devices*, M. Niinomi, Ed., chapter 16, pp. 379–404, Woodhead Publishing, Cambridge, UK, (2010);
4. S. L. Tait, Z. Dohnálek, C. T. Campbell, and B. D. Kay, "Methane adsorption and dissociation and oxygen adsorption and reaction with CO on Pd nanoparticles on MgO(1 0 0) and on Pd(1 1 1)," *Surface Science*, **591**, no. 1–3, pp. 90–107 (2005);
5. K. Grochowska, G. Śliwiński, A. Iwulska, M. Sawczak, N. Nedyalkov, P. Atanasov, G. Obara, M. Obara, "Engineering Au Nanoparticle Arrays on SiO<sub>2</sub> Glass by Pulsed UV Laser Irradiation", *Plasmonics*, **8**, Issue 1, pp 105-113, (2013);
6. K. Saha, S. S. Agasti, C. Kim, X. Li, and V. M. Rotello, "Gold nanoparticles in chemical and biological sensing," *Chemical Reviews*, **112**, no. 5, pp. 2739–2779 (2012).

## Inter-diffusion studies in stacks of nano-layers of alternating W and B

C. Surdu-Bob<sup>1</sup>, A.M. Vlaicu<sup>2,1</sup>, A. Anghel<sup>1</sup>, M. Badulescu<sup>1</sup>, R. Gavrilă<sup>3</sup>, B. Bită<sup>3</sup>

<sup>1</sup>Low Temperature Plasma Lab., National Institute for Lasers, Plasma and Radiation Physics, Magurele – Romania

<sup>2</sup>National Institute for Materials Physics, Magurele – Romania

<sup>3</sup>Microtechnology Institute – Baneasa, Romania  
cristina.surdubob@plasmacoatings.ro

Multilayers are used in every field, from consumer electronics to medical, aerospace, military and cosmology. The synthesis of quality nano-multilayers is a challenge of technology, as there are important requirements that need to be fulfilled by these structures, such as smoothness and abrupt interfaces, with minimal intermixing – at the nanoscale.

Film growth and surface phenomena strongly depends on the energy and flux of film precursors. In this work, we present and discuss XRR data on inter-diffusion in W and B stacks of nano-layers synthesized using an anodic arc plasma (the Thermionic Vacuum Arc – TVA). Characterization of bi-layer quality in terms of extent of inter-layer diffusion and also film density is presented. Spectrum fitting in XRR spectra of multiple nano-layers gives calculated information on the roughness of each layer. The obtained roughness is the expression of interlayer diffusion and real film roughness.

It is known that low energy ions deposit on the surface with no displacement and produce porous and rough surfaces but with minimal layer inter-diffusion while higher energy ions give opposite results. Inter-layer improvement by modulation of ion energy is discussed. In our anodic plasma, the distribution of ion energies is practically monoenergetic and ion energy values are modulated via plasma voltage. A direct control of ion energy is thus obtained, allowing optimization of nano-multilayers.

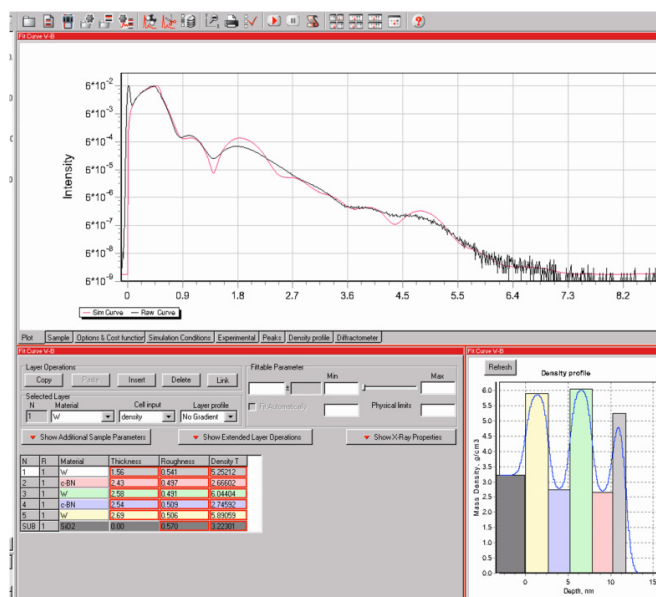


Figure 1: XRR spectrum of a W-B nano-multilayer

1. E.O. Filatova, I.V. Kozhevnikov et al, X-ray and photoelectron spectroscopic nondestructive methods for thin films and interfaces study. Application to SrTiO<sub>3</sub> based heterostructures, *Microelectronic Engineering Name*, **109**, 13-16 (2013);

2. N. Ghafoor, Growth and Nano-structural Studies of Metallic Multilayers for X-ray Mirrors (Linköping University, Linköping, Sweden), PhD Thesis (2005).

# Fabrication of Periodic ZnO Microdot Arrays by Laser Interference Patterning

S. Takao, M. Yamasaki, R. Tasaki, K. Oda, M. Higashihata, D. Nakamura, T. Okada

Graduate school of information science and electrical engineering, Kyushu University, Japan  
takao@laserlab.ees.kyushu-u.ac.jp

Zinc oxide (ZnO) has attracted widely attention for its direct wide band gap of 3.37 eV and large exciton binding energy of 60 meV at room temperature, which is much larger than the thermal energy at room temperature (26 meV). In addition, important features of ZnO are low toxicity and biocompatibility. Thus, it is known that ZnO is one of the most prospective material candidates for ultraviolet (UV) emitting devices and biosensors. To develop such devices, periodic micro/nano structuring of ZnO is very important for the optical characterization and surface wettability control. We have succeeded in fabricating periodic ZnO microdot arrays by four-beam interference patterning in air at room temperature. In this contribution, we report the selective micropatterning of a ZnO film by interference laser processing and UV lasing from ZnO submicron droplet under pulsed laser excitation.

ZnO microdot arrays were fabricated by four-beam interference pattern, which is produced by a transmittance grating and lens arrays. The third harmonics of a Q-switched Nd:YAG laser ( $\lambda = 355$  nm, 10 ns, 180 mJ/cm<sup>2</sup>) was used as the patterning laser. Various interference pattern can be achieved by changing the phase and intensity of the beams before irradiation to the ZnO film in air at room temperature. In the experiment, the phase of a laser beam was changed by passing through a sapphire substrate. The ZnO film with a thickness of approximately 1  $\mu$ m was prepared by pulsed laser deposition on a sapphire substrate. The surface morphology and optical characteristics were investigated by scanning electron microscope (SEM) and microscopic spectroscopy, respectively.

Fig. 1(a) shows the low-magnification SEM image of patterned ZnO film, where 20 pulses of interference pattern were irradiated at the same spot. Fig. 1(b) shows 60 degree-tilted view of the high-magnification SEM image of the ZnO microdot arrays. Well-aligned ZnO microdot arrays were formed by the simple interference patterning. The diameter and height of the microdots were 2.4  $\mu$ m and 2.6  $\mu$ m, respectively. The aspect ratio of height to diameter of microdot gradually increased with increasing number of laser pulses. However, more than 20 pulses reduced the aspect ratio. ZnO spherical droplet with a diameter of 400-500 nm was formed on the top of some microdots, as shown at the center of Fig. 1(b). The droplets may generated during laser irradiation, and deposited on the patterned surface. Fig. 1(c) shows the photoluminescence (PL) spectrum of the ZnO droplet excited by the third harmonics of a Q-switched Nd:YAG laser. It shows the whispering gallery mode lasing from the spherical droplet, and the quality factor was estimated to be about 500.

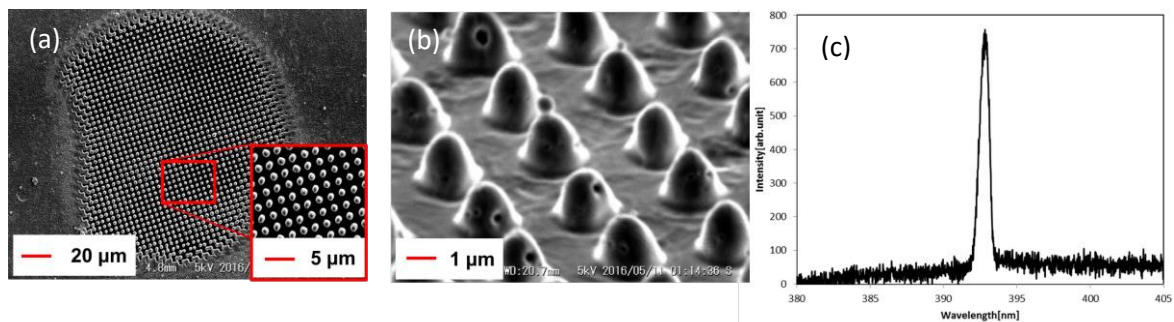


Figure 1: SEM images of the ZnO microdot arrays with (a) low-magnification and (b) 60 degree-tilted view of high-magnification, and (c) photoluminescence spectrum from the ZnO droplet on the microdot under excitation of the pulsed 355 nm Nd:YAG laser.

1. Y. Nakata, et al. J. Appl. Phys. 42, 1452 (2003);
2. K. Okazaki, et al. Appl. Phys. Lett. 101, 211105 (2012).

# Femtosecond laser-induced reductive sintering to fabricate Ni-based alloy micropatterns

K. Tamura, M. Mizoshiri, J. Sakurai, S. Hata

Department of Micro-Nano Systems Engineering, Graduate School of Engineering, Nagoya University  
Furo-cho, Chikusa-ku, Nagoya, Aichi, 464-8603 Japan  
tamura.kenki@h.mbox.nagoya-u.ac.jp

Direct writing process is a key technology in 3D additive manufacturing. However, it is difficult to apply this process to fabricating metal microstructure because raw metal powder is easily oxidized by reducing the powder size. On the other hand, laser-induced reductive sintering of metal oxide nanoparticles (NPs) was proposed to fabricate metal micropatterns.<sup>1,2</sup> To reduce the thermal diffusion and reoxidation, we have studied femtosecond laser-induced reductive sintering using NiO NPs.<sup>3</sup> In this presentation, we applied femtosecond laser-induced reductive sintering using NiO NPs to forming Ni-based alloy micropatterns. The crystal structures of the fabricated micropatterns were examined.

The wavelength, pulse duration, and repetition rate of the femtosecond laser were 780 nm, 120 fs, and 80 MHz, respectively. The numerical aperture of an objective lens to focus femtosecond laser pulses was 0.80. Raw materials of NiO NPs (<50 nm size) and Cr NPs (<35-45 nm size) were mixed with ethylene glycol (EG) and polyvinylpyrrolidone (PVP) using ultrasonic waves. The concentration of NiO NPs, Cr NPs, EG, and PVP were 23.5 wt%, 23.5 wt%, 43 wt%, and 10 wt%, respectively. The prepared NiO/Cr NP solution was spin-coated on a glass substrate (thickness 1.3 mm) with the spinning rate of 5000 rpm. After irradiating femtosecond laser pulses, non-reduced and non-sintered NiO NPs and Cr NPs were removed by rinsing the substrate into EG and ethanol. The crystal structures were analyzed by X-ray diffraction (XRD) analysis. The surface structure was observed with field emission-scanning electron microscope (FE-SEM).

Figures 1 shows FE-SEM images of the surface of the micropatterns which were fabricated with the pulse energy of 0.62 nJ and the laser scan speed was varied in 1-15 mm/s. The micropatterns were written by raster scanning pitch of 15  $\mu\text{m}$ . The surface structures were dramatically different in the laser scan speed. The dark lines in Figs. 1(a) and 1(b) were formed by laser ablation at the center of the focal spot.

XRD spectrum of the micropattern which were fabricated at the laser scanning speed 1-20 mm/s were shown in Fig.2. The high diffraction peak at  $\sim 44^\circ$  which possibly corresponds to Ni(1 1 1), Cr(1 1 0),  $\text{Cr}_{0.25}\text{Ni}_{0.75}$ (1 1 1) was observed. However, Cr peak at  $81.7^\circ$  was decreased by decreasing the laser scanning speed, and was nearly disappeared at the laser scanning speed of 1 mm/s and 5 mm/s. These results indicate that almost all Cr NPs were consumed by generating compounds such as  $\text{Cr}_{0.25}\text{Ni}_{0.75}$  or  $\text{Cr}_2\text{O}_3$  under these conditions. The diffraction peak at  $44.011^\circ$  in Fig. 2(b), which corresponds to  $\text{Cr}_{0.25}\text{Ni}_{0.75}$ (1 1 1), also indicates the generation of the Ni alloy.

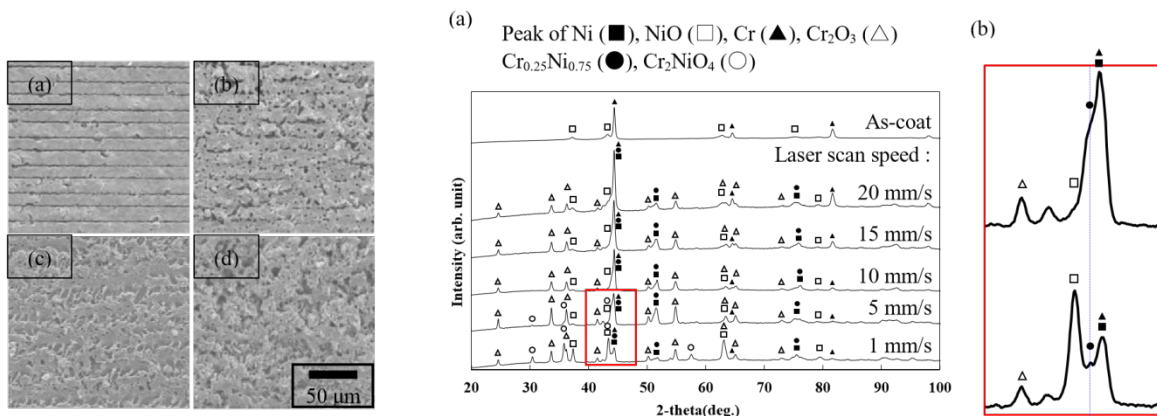


Figure 1: Surface microstructure at scanning speed of (a) 1 mm/s, (b) 5 mm/s, (c) 10 mm/s, (d) 15 mm/s

Figure 2: (a) XRD spectrum of Ni-based alloy micropattern and (b) enlarged one

1. B. Kang, S. Han, J. Kim, S. Ko, M. Yang, One-Step Fabrication of Copper Electrode by Laser-Induced Direct Local Reduction and Agglomeration of Copper Oxide Nanoparticle, *Journal of Physical Chemistry*, **C115**, 23664 (2011);
2. D. Lee, D. Paeng, H. K. Park, and C. P. Grigoropoulos, Vacuum-Free, Maskless Patterning of Ni Electrodes by Laser Reductive Sintering of NiO Nanoparticle Ink and Its Application to Transparent Conductors, *ACS NANO*, **8**, 9807 (2014);
3. K. Tamura, M. Mizoshiri, J. Sakurai, S. Hata, Patterning properties of nickel microstructures using femtosecond laser induced reduction, *Proceedings of 7th International Congress on Laser Advanced Material Processing*, art.no. 15-036 (2015).

# In vitro evaluation of antitumoral and antibacterial activities of Curcumin loaded biodegradable copolymer

I. Tirca<sup>1,2</sup>, V. Marascu<sup>1,3</sup>, S. Brajnicov<sup>1,2</sup>, V. Dinca<sup>1</sup>, D. Pelinescu<sup>4</sup>, I. Sarbu<sup>4</sup>,  
V. Mitran<sup>5</sup>, A. Campean<sup>5</sup>, M. Dinescu<sup>1</sup>,

<sup>1</sup>National Institute for Laser, Plasma and Radiation Physics, RO-077125 Magurele, Bucharest, Romania

<sup>2</sup>University of Craiova, Faculty of Sciences, RO-200585, Craiova, Romania

<sup>3</sup>University of Bucharest, Faculty of Physics, RO-077125, Magurele, Bucharest, Romania

<sup>4</sup>University of Bucharest, Faculty of Biology, Department of Genetics, RO-060101, Bucharest, Romania

<sup>5</sup>University of Bucharest, Faculty of Biology, Department of Biochemistry and Molecular Biology, Bucharest, Romania  
maria.dinescu@infpr.ro

The current study presents the development of novel biodegradable copolymer-Curcumin coatings which were evaluated *in vitro* for antitumoral and antibacterial complex coatings applications. The chemical- physical structural stability of delivery system and effective release of Curcumin are crucial for controlling and tuning the drug delivery. To meet this challenge, the bioactive element (Curcumin) was embedded in the biodegradable Polyvinyl Alcohol-Polyethylene Glycol graft coatings using Matrix Assisted Pulsed Laser Evaporation (MAPLE) method. The strategy used in this study for manufacturing hybrid coatings with various roughness and porosity was to tailor target characteristics (solvent, composition, concentration of Curcumin) and deposition parameters (laser fluence, number of pulses). Coatings characterization involved morphological methods (Atomic Force Microscopy, Scanning Electron Microscopy) while the compositional aspects of the thin films was evidenced by Fourier Transform Infrared Spectroscopy (FTIR) and UV-Vis spectroscopy. Degradation studies were performed by spectroellipsometry (SE) and surface changing by AFM studies. *In vitro* studies were performed for evaluating the capacity of the hybrid coatings to influence or inhibit the development of pathogenic microorganisms and osteosarcoma cells. Antimicrobial activity of copolymer- Curcumin coatings was assessed against three pathogenic strains belonging to *Staphylococcus aureus*, *Escherichia coli* and *Candida albicans*. The most sensitive strains to copolymer- Curcumin coating samples was *Staphylococcus aureus* ATCC 5063. Furthermore, the study demonstrates that Curcumin exhibits efficacy against the osteosarcoma cell lines MG-63, being able to inhibit proliferation and to promote cell death. Our results provide evidence for the potency of the Curcumin copolymer based coatings as a future treatment of osteosarcomas as well as obtaining tailored antibacterial surfaces.

## Susceptibility of bacteria to photo-chemically generated agents starting from phenothiazine derivatives

T. Tozar<sup>1</sup>, A. Stoicu<sup>1</sup>, V. Nastasa<sup>1</sup>, M. Popa<sup>2</sup>, C. Chifriuc<sup>2</sup>, I. R. Andrei<sup>1</sup>, M.L. Pascu<sup>1</sup>

<sup>1</sup>National Institute for Laser, Plasma and Radiation Physics, Laser Department, 409 Atomistilor, 077125, Magurele, Romania

<sup>2</sup>Research Institute of the University of Bucharest, 93-95 Splaiul Independentei, Sector 5 77206, Bucharest, Romania  
tatiana.alexandru@infpr.ro

An important issue of global health nowadays is the evolution of multidrug resistance (MDR) in both Gram-positive and Gram-negative bacteria, which has a great impact on global economy. The biggest concern is focused on the Gram-negative bacteria, because they are more resistant to current antibiotics, due to their outer membrane that acts as an extra layer of protection and that is responsible for the defense against toxic compounds. In this case, an urgent need for developing new drugs, in fighting MDR bacteria, exists. The antimicrobial activity of unirradiated and irradiated Phenothiazines is known, but it is necessary to evaluate the safety of the photo-products for human use prior to exposure. In addition, an important application of Phenothiazines is the direct use on tissues or impregnation with them of materials applied in treatments of biological targets accessed *via* their surfaces.

Thioridazine (TZ) and chlorpromazine (CPZ), dissolved in ultrapure water, at 2 mg/mL were irradiated with a 6.5 mJ, 266 nm pulsed laser beam generated by a Nd:YAG laser (Continuum, Excel Technology laser, model Surelite II, 6-ns full time width at half maximum, 10-Hz pulse repetition rate) as fourth harmonic of the fundamental beam, for time intervals between 1 and 240 minutes. The optical pathlength was 1 cm, the area of the beam spot on the cuvette was 0.38 cm<sup>2</sup>, and the beam fluence was 17.1 J/cm<sup>2</sup>. The techniques used to identify/measure the obtained photoproducts were absorption spectroscopy, Thin Layer Chromatography (TLC), Laser Induced Fluorescence (LIF), FTIR, surface tensions measurements, and Liquid Chromatography - tandem Time of flight Mass Spectroscopy (LC/MS TOF).

The antimicrobial activity was tested *in vivo* by performing susceptibility tests of micro-organisms to the mixture of photo-products using two methods: minimum inhibitory concentration (MIC) and minimum biofilm

eradication concentration (MBEC). The micro-organisms tested were bacteria, both gram-positive and gram-negative, and fungi.

The results suggest that the effect of TZ and CPZ irradiated with 266 nm (UV) laser beam is the generation of new species with antimicrobial activity. The MIC results showed an enhanced antimicrobial activity of the photoproducts mixture against bacterial strains and the MBEC assay showed the susceptibility to the photoproducts of bacterial cells growing in biofilms.

This method could constitute a fast and inexpensive approach in developing new antimicrobial agents. The photoproducts are obtained in a short time, without any use of additional chemical agents and time-consuming synthetic chemistry and are able to fight MDR acquired by bacteria. The results obtained on different bacterial strains by exposing them to TZ solutions irradiated with a UV laser beam are promising in fighting MDR bacteria.

The most remarkable differences have been observed as a function of the irradiation process on the photoproducts derived from CPZ and TZ. These photoproducts have higher in vitro cytotoxicity against the studied cell cultures, suggesting that this approach may be useful for the development of compounds more bioactive than parental species.

*Acknowledgements:* This work has been financed by the National Authority for Research and Innovation in the frame of Nucleus programme- contract 4N/2016 and by CNCS – UEFISCDI by project number PN-II-PT-PCCA-2011-3.1.-1350.

## Refractive Index Imaging with Nanoscale Resolution Enabled by Laser Near-Field Dipole Excitation

D. E. Tranca, S. G. Stanciu, R. Hristu, C. Stoichita and G. A. Stanciu

Center for Microscopy - Microanalysis and Information Processing, University Politehnica of Bucharest  
denis.tranca@cmmip-upb.org

The laser imaging domain comprises a large amount of different optical imaging techniques, many of them – like Confocal Laser Scanning Microscopy<sup>1</sup> and Non-linear Laser Microscopy Techniques<sup>2,3</sup> – being developed up to a mature level. These techniques based on far-field investigations have a theoretical resolution given by Abbe's theory<sup>4</sup> which is restrictive for many applications. However, other new laser imaging techniques based on far-field or near-field are in developing process and their results are very promising for nanoscale investigations. In this category is situated the Scattering Scanning Near-field Optical Microscopy (s-SNOM)<sup>5</sup> which has rapidly grown in the last decade. The reported s-SNOM results are related to achievements such as nano-resolution capabilities<sup>6</sup> and complex dielectric function measurements<sup>7</sup>. The technique consists in illuminating the tip of a nano-probe – which can be the probe of an Atomic Force

Microscope (AFM) – with a laser beam coming from lateral side of the probe. According to the Optical PointDipole Model (OPDM)<sup>8</sup>, the laser excites an oscillating point-dipole in the tip which radiates light (with the same frequency as the incident beam) that can be collected on the same path as the incident beam. When the tip is in close proximity to the surface of a sample (at distances known as “near-field”, which roughly means much smaller than the half of the wavelength) the optical properties of the sample's surface influence the dipole radiation in terms of amplitude and phase. Therefore, detection of the light radiated from the dipole enables optical nanoscale resolution.

Recent developments allowed researchers to achieve quantitative information from s-SNOM imaging. Our team developed a method which permits the measurement of the dielectric function of the materials from a sample when one of the materials (i.e. the substrate) is known<sup>9</sup>. This is possible by correlating the experimental results with the theoretical results predicted by the OPDM. However, the dielectric function can be related to the refractive index and in this present work we report nanoscale refractive index measurements of different samples (including biological cells).

Our new technique permits measurement of the local surface refractive index in every pixel of the s-SNOM image; therefore, a map of the refractive index can be created. The information about the complex refractive index can be related to many other specific sample parameters.

*Acknowledgements:* This work has received support from the European Community's Seventh Framework Programme (FP7/20122015) under grant agreement no. 280804 (LANIR, [www.lanir.eu](http://www.lanir.eu)) and no. 212533 (BioElectricSurface, [www.bioelectricsurface.eu](http://www.bioelectricsurface.eu)). This communication reflects the views only of the authors, and the Commission cannot be held responsible for any use which may be made of the information contained therein. The presented work has been supported as well by the Romanian Executive Agency for Higher Education, Research, Development and Innovation Funding through the research grants PN-II-PT-PCCA-2011-3.2-1162 (NANOLASCAN) and PN-II-RU-TE-2014-4-1803 (MICRONANO).

1. C.J.R. Sheppard, T. Wilson, The theory of the direct-view confocal microscope, *Journal of Microscopy*, **124**, 107-117 (1981);

2. W. Denk, J.H. Strickler, W.W. Webb, Two-photon laser scanning fluorescence microscopy, *Science*, **248**, 73-76 (1990);

- P.J. Campagnola, L.M. Loew, Campagnola, P. J., & Loew, L. M. (2003). Second-harmonic imaging microscopy for visualizing biomolecular arrays in cells, tissues and organisms. *Nature Biotechnology*, **21**, 1356-1360 (2003);
- E. Abbe, Beiträge zur Theorie des Mikroskops und der mikroskopischen Wahrnehmung, *Archiv für mikroskopische Anatomie*, **9**, 413-418, 1873;
- S. Patane, P.G. Gucciardi, M. Labardi, M. Allegrini, Apertureless near-field optical microscopy, *La Rivista del Nuovo Cimento*, **27**, 1-46 (2004);
- A.J. Huber, J. Wittborn, R. Hillenbrand, Infrared spectroscopic near-field mapping of single nanotransistors, *Nanotechnology*, **21**, 235702:1-6 (2010);
- AA. Govyadinov, I. Amenabar, F. Huth, P.S. Carney, R. Hillenbrand, Quantitative Measurement of Local Infrared Absorption and Dielectric Function with Tip-Enhanced Near-Field Microscopy, *Journal of Physical Chemistry Letters*, **4**, 1526-1531 (2013);
- B. Knoll, F. Keilmann, Enhanced dielectric contrast in scattering-type scanning near-field optical microscopy, *Optical Communications*, **182**, 321-328 (2000);
- D.E. Tranca, S.G. Stanciu, Hristu, C. Stoichita, S.A.M. Tofail, G.A. Stanciu, High-resolution quantitative determination of dielectric function by using scattering scanning near-field optical microscopy, *Scientific Reports*, **5**, 11876:1-9 (2015).

## Laser Induced Selective Phase Transition of Molybdenum Disulphide Nanoplatelet Arrays

R. Trusovas<sup>1</sup>, G. Račiukaitis<sup>1</sup>, G. Niaura<sup>2</sup>, A. Jagminas<sup>3</sup>

<sup>1</sup> Department of Laser Technologies, Center for Physical Sciences and Technology, Savanoriu Ave. 231, Vilnius LT-02300, Lithuania

<sup>2</sup> Department of Organic Chemistry, Center for Physical Sciences and Technology, Sauletekio Ave. 3, Vilnius LT-10222, Lithuania

<sup>3</sup> Department of Electrochemical Materials Science, Center for Physical Sciences and Technology, Sauletekio Ave. 3, Vilnius LT-10222, Lithuania  
romualdas.trusovas@fmc.lt

In recent years, single and few-layered molybdenum disulphide (MoS<sub>2</sub>) has attracted much interest from researchers due to its outstanding electrical, optical and catalytical properties<sup>1</sup>. Unlike graphene, this 2D material possesses band gap<sup>2</sup>. Therefore, it becomes attractive for nano-electronic applications while MoS<sub>2</sub> nanoplatelet arrays are prospective for utilization as catalyst for electrochemical and photocatalytical hydrogen generation from water solutions.

In this research, we report on the new approach for MoS<sub>2</sub>-based 2D materials synthesis improvement by laser-induced excitation. This effect was obtained for densely packed few-layered nanoplatelet arrays fabricated onto the Ti substrate by one-pot hydrothermal synthesis from three times lower concentrated ammonium heptamolybdate and thiourea solution at significantly higher temperatures than reported in<sup>3</sup>.

By this way, densely packed and well adherent to the substrate nanoplatelet array composed of a mixture of amorphous and crystalline molybdenum sulphides was formed. Scanning electron microscopy (SEM), X-ray diffraction (XRD), X-ray energy dispersive (EDX) spectroscopy and Raman investigations were used for MoS<sub>2</sub> nanoplatelets investigation (Figure 1).

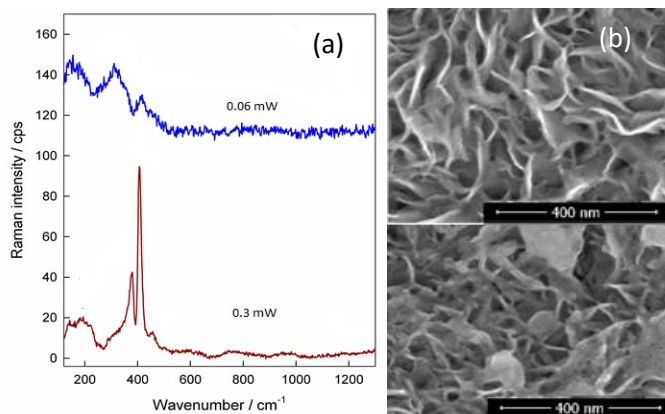


Figure 1: (a) Raman spectra of MoS<sub>2</sub> sample observed with 0.06 mW and 0.3 mW 532 nm CW laser power in the wavenumber region from 120 to 1300 cm<sup>-1</sup>. (b) SEM images of nonstoichiometric MoS<sub>2</sub> nanoplatelets, formed at the Ti substrate before (top) and after (bottom) 532 nm CW laser excitation at 3 mW average power.

Our studies showed that continuous wave (CW) laser and nanosecond laser irradiation induces phase transformation in MoS<sub>2</sub> nanoplatelets. Furthermore, laser irradiation causes reduction of MoO<sub>x</sub> species simultaneously increasing the percentage of MoS<sub>2</sub> content in investigated material.

- B. Radislavljevic, A. Radenovic, J. Brivio, A. Kis, Single-Layer MoS<sub>2</sub> Transistors. *Nature Nanotechnology* **6**, 147-150 (2011);
- K.K. Kam, B.A. Parkinson, Detailed photocurrent spectroscopy of the semiconducting group VIB transition metal dichalcogenides, *Journal of Physical Chemistry*, **86**, 463-467 (1982);
- Z. Lu, W. Zei, X. Yu, H. Zhang, Y. Li, X. Sun, Y. Li, X. Sun, X. Wang, H. Wang, J. Wang, J. Luo, X. Lei, L. Jiang. Ultrahigh Hydrogen Evolution Performance of Under-Water "Superaerophobic" MoS<sub>2</sub> Nanostructured Electrodes, *Advanced Materials*, **26**, 2683-2687 (2014).

# Experimental Setup for Detection of Accelerated Particles Generated by High Power (PW) Laser-Solid Target Interaction

L. Tudor<sup>1,2</sup>, M. Gugu<sup>1</sup>, M. Cernaianu<sup>1</sup>, F. Rotaru<sup>1</sup>, C. Manailescu<sup>1</sup>, S. Kisiov<sup>1</sup>, A. Cucoanes<sup>1</sup>, D. C. Popescu<sup>1,2</sup>, E. Stancu<sup>3</sup>, D. Stutman<sup>1</sup>, F. Negoita<sup>1</sup>, D. Ursescu<sup>1,3</sup>

<sup>1</sup>ELI-NP, Horia Hulubei National Institute for Physics and Nuclear Engineering Magurele, Ilfov, Romania

<sup>2</sup>University Politehnica of Bucharest, Bucharest, Romania

<sup>3</sup>National Institute for Lasers, Plasma and Radiation Physics, Măgurele, Romania  
lucian.tudor@eli-np.ro

This poster contains an overview for the experimental setup used for detection and characterization of charged particles resulted from high power (PW) laser-solid target interactions. This setup has been successfully used at ELI-NP – CETAL February-March 2016 experiments, for detection of accelerated particles produced by high power lasers. It contains Radiochromic films (RCF), CR 39 plastic detector, used along with electrostatic deflector. These detectors are suitable to be used in strong electromagnetic pulses (EMP) environment, for high fluxes of accelerated particles. The detectors can be exchanged automatically in the Interaction Chamber without breaking the vacuum.

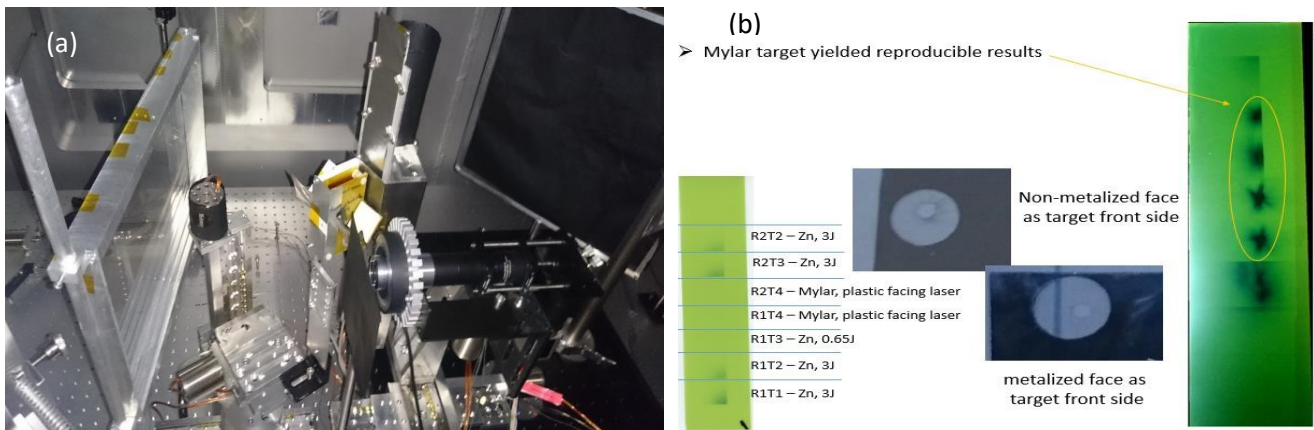


Figure 1: (a) Experimental Setup configuration. (b) RCF's impressed by 4 sets of target types used (Fe 2um, Mylar 12um, Al 0.8um, Zn10um)

1. N. Sinenian, M. J. Rosenberg, M. J.-E. Manuel, The response of CR-39 nuclear track detector to 1-9 MeV protons, PSFC/JA-11-46, 1-14 (2012);
2. A. E. Breschi, M. Galimberti, D. Giuliotti, L. A. Gizzi, "Spectral and angular characterization of laser-produced proton beams from dosimetric measurements", Central Laser Facility Annual Report, 21-22, (2004/2005).

## Femtosecond laser irradiation to fluorescent molecules-loaded poly(lactic-co-glycolic acid)

T. Umemoto<sup>1</sup>, A. Shibata<sup>1</sup>, S. Yada<sup>1</sup>, M. Terakawa<sup>1,2</sup>

<sup>1</sup>School of Integrated Design Engineering, Keio University, 3-14-1 Hiyoshi, Kohoku-ku, Yokohama, 223-8522, Japan

<sup>2</sup>Department of Electronics and Electrical Engineering, Keio University, 3-14-1, Hiyoshi, Kohoku-ku, Yokohama, 223-8522, Japan  
terakawa@elec.keio.ac.jp

Tissue scaffolds which consist of a biodegradable polymer can provide a space for cell growth as well as releasing growth factors with its degradation, which enables us to promote tissue regeneration. The precise processing of biodegradable polymers has been realized by using ultrashort pulsed lasers and recently been demonstrated to obtain different degradation period after laser processing depending on the laser wavelength.<sup>1,2</sup> In this study, we have investigated the release of fluorescent molecules loaded in a poly(lactic-co-glycolic acid) (PLGA) substrate after irradiating femtosecond laser pulses, which is aimed at controlled release of the molecules from tissue scaffolds triggered by laser irradiation. PLGA is one of typical biodegradable polymers which have been receiving increasing attention as a material for a tissue scaffold. Femtosecond laser pulses at 800 nm and 400 nm in central wavelengths were focused and scanned on a surface of a PLGA substrate containing Rhodamine B. The laser fluences were 0.70 J/cm<sup>2</sup> and 0.15 J/cm<sup>2</sup> for 800 nm and 400 nm, respectively. The substrates were fully immersed in a phosphate-buffered saline (PBS) in vials. Vials were placed in a water bath maintained at 37 °C. Weight change was measured at different time to evaluate the water absorption. The amount of released fluorescent molecules in exchanged medium was measured every 2 days using a spectrofluorometer.

Figure 1 shows the water absorption of PLGA substrates containing the fluorescent molecules. The water absorption of the 400 nm laser-irradiated PLGA substrates was greater than that of the non-laser-irradiated substrates and 800 nm laser-irradiated PLGA substrates. The amount of Rhodamine B molecules released from 400 nm laser-irradiated PLGA substrates was greater than those of the other conditions, especially 2 to 12 days after the laser irradiation. These results show the potential of femtosecond laser processing to control the release of loaded molecules from biodegradable scaffolds.

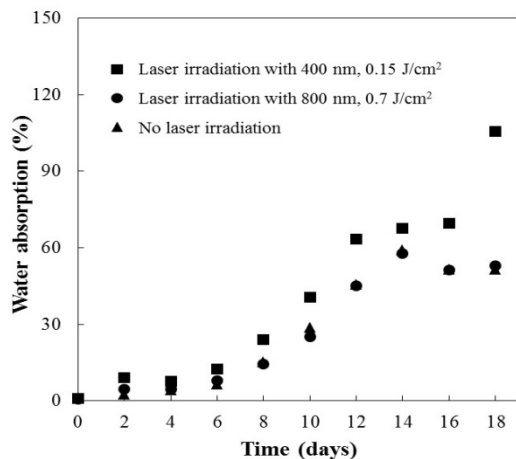


Figure 1: Water absorption to Rhodamin B-loaded PLGA

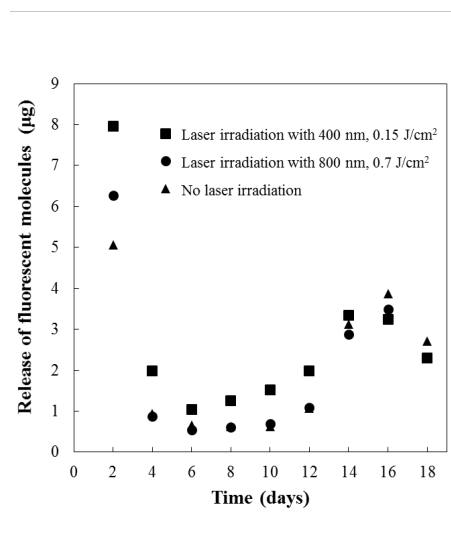


Figure 2: Release of Rhodamin B from the substrates after laser irradiation

1. S. Yada, M. Terakawa, Femtosecond laser induced periodic surface structure on poly-L-lactic acid, *Optics Express*, **23**, pp. 531-539, (2015);
2. A. Shibata, S. Yada, M. Terakawa, Biodegradability of poly(lactic-co-glycolic acid) after irradiation of femtosecond laser pulses, The 13th Conference on Laser Ablation (COLA-2015), September 2015.

## Polyaniline grafted lignin coatings fabricated by MAPLE for medical applications

A. Visan<sup>1</sup>, O. Fufa<sup>1</sup>, C. Matei<sup>1</sup>, M. Socol<sup>2</sup>, C. Luculescu<sup>1</sup>, R. C. Popescu<sup>3</sup>, D. Savu<sup>3</sup>, R. Cristescu<sup>1</sup>, I. N. Mihailescu<sup>1</sup>, D. Craciun<sup>1</sup>, G. Socol<sup>1</sup>

<sup>1</sup>National Institute for Lasers, Plasma and Radiation Physics, Magurele, Ilfov, Romania

<sup>2</sup>National Institute of Materials Physics, Magurele, Ilfov, Romania

<sup>3</sup>Life and Environmental Physics Department, Horia Hulubei National Institute of Physics and Nuclear Engineering, Magurele, Ilfov, Romania.  
gabriel.socol@infpr.ro

Thin films of polyaniline (PANI) grafted Lignin were deposited by matrix assisted pulsed laser evaporation (MAPLE) technique using dimethylsulfoxide (DMSO) as a matrix solvent. The Lignin addition facilitated the directional alignment of the monomer and improve the solubility of the polyaniline conducting polymer. In order to find the optimal deposition parameters, we conducted a study of laser fluence (0.3 - 0.5 mJ/cm<sup>2</sup>).

The structures were studied by SEM, XRD, AFM, FTIR, UV-VIS and were submitted to biological assays. It follows that the deposited thin films exhibit a convenient nanostructured surface for bone implants. We demonstrated that polyaniline grafted Lignin can be transferred in form of thin films without altering their initial composition.

The obtained structures are corrosion resistant, as resulted from electrochemical measurements. Biocompatibility assay (MTT, imunostaining and cellular morphology) showed that PANI grafted Lignin films are not cytotoxic for bone cells, which encourages further assessment of this type of biomaterials for their application in controlled drug release at implantation sites by electrical impuls stimulation.



## Muramidase embedded into degradable polymers blends for antimicrobial applications

A. Visan<sup>1</sup>, N. Stefan<sup>1</sup>, M. Miroiu<sup>1</sup>, C. Nita<sup>1</sup>, G. Dorcioman<sup>1</sup>, O. Rasoga<sup>2</sup>, I. Zgura<sup>2</sup>, C. Breazu<sup>2</sup>, I. Iordache<sup>1</sup>, A. Stanculescu<sup>2</sup>, R. Cristescu<sup>1</sup>, M.C. Chifiriuc<sup>3</sup>, L. Sima<sup>4</sup>, I.N. Mihailescu<sup>1</sup>, G. Socol<sup>1</sup>

<sup>1</sup>National Institute for Lasers, Plasma and Radiation Physics, Magurele, Ilfov, Romania

<sup>2</sup>National Institute of Materials Physics, Magurele, Ilfov, Romania

<sup>3</sup>Faculty of Biology, University of Bucharest, Microbiology Immunology Department, Aleea Portocalelor 1-3, Sector 5, 77206 Bucharest, Romania

<sup>4</sup>Institute of Biochemistry, Splaiul Independentei 296, Bucharest, Romania  
gabriel.socol@inflpr.ro

Muramidase embedded into blends of polyethylene glycol (PEG) and polycaprolactone (PCL) were developed via Matrix Assisted Pulsed Laser Evaporation (MAPLE) and Dip Coating techniques for long-term delivery applications. Different polymer compositions were synthesized and evaluated to optimize drug release profile from fabricated coatings. The main surface features which affect and guide cellular and bacterial adhesion like roughness (AFM), and wettability measurements were investigated. The effect of muramidase incorporation on crystallinity of polymers, chemical composition (FTIR) and antimicrobial properties of coatings against *Escherichia coli* and *Staphylococcus aureus* were also evaluated. In vitro cell culture tests on PCL-PEG-muramidase coatings showed appropriate viability, good spreading and normal cell morphology. The release tests of muramidase, along with all investigations essentially signify that these biodegradable composite coatings are potential promising candidates for local protein delivery applications.

## Antimicrobial calopocarpin-polyvinylpyrrolidone composite coatings fabricated by MAPLE

A.Visan<sup>1</sup>, M. Miroiu<sup>1</sup>, M.C. Chifiriuc<sup>2</sup>, I.N. Mihailescu<sup>1</sup>, G. Socol<sup>1</sup>, R. Cristescu<sup>1</sup>

<sup>1</sup>National Institute for Lasers, Plasma and Radiation Physics, Magurele, Ilfov, Romania

<sup>2</sup>Faculty of Biology, University of Bucharest, Microbiology Immunology Department, Bucharest, Romania  
rodica.cristescu@inflpr.ro

Flavonoids have a wide range of biological and pharmacological applications being isolated and characterized from medicinal plants. Among them, calopocarpin (3,9-dihydroxy-2-(3,3dimethylallyl)pterocarpan) is a highly antifungal isoflavonoid, which may be extracted and isolated from *Colopogonium mucunoides* or a series of tropical plants around the world belonging to the *Erythina* genus of the *Leguminosae* Family.

In this study we used matrix assisted pulsed laser evaporation (MAPLE) in order to obtain composite biopolymeric coatings based on polyvinylpyrrolidone and natural flavonoid (calopocarpin) as bioactive substance. To identify optimal deposition parameters, we conducted a laser fluency (0.2-0.5 J/cm<sup>2</sup>) study. The coatings were physico-chemical characterized using Fourier transform infrared spectroscopy, infrared microscopy, scanning electron microscopy, Grazing incidence X-ray diffraction and atomic force microscopy. The antimicrobial assay of the microbial biofilms formed on these coatings was determined by the viable cell counts method.

The results confirmed that the flavonoid-containing coatings exhibited an increased resistance to microbial colonization, highlighting the potential and perspective of MAPLE technique to be used for the fabrication of anti-biofilm surfaces.

# Comparison of different routes for the manufacture of intercalated dodecyl sulfate Mg,Al-layered double hydroxides composite thin films using laser techniques

A. Vlad<sup>1</sup>, I. Tirca<sup>1</sup>, R. Birjega<sup>1</sup>, A. Matei<sup>1</sup>, M. Dumitru<sup>1</sup>, M. Dinescu<sup>1</sup>, V. Marascu<sup>1</sup>, R. Zavoianu<sup>2</sup>, M. C. Corobea<sup>3</sup>

<sup>1</sup>National Institute for Lasers, Plasma and Radiation Physics, Bucharest-Magurele, Romania

<sup>2</sup>University of Bucharest, Faculty of Chemistry, Department of Chemical Technology and Catalysis, Bucharest, Romania

<sup>3</sup>National R.&S. Institute for Chemistry and Petrochemistry, ICECHIM, Bucharest, Romania  
angela.vlad@gmail.com

Layered double hydroxides (LDHs), also known as hydrotalcite-like compounds, have a potential as nanocontainers of corrosion inhibitors in self-healing corrosion protection coatings. The anionic exchange capability of LDHs can be utilized to incorporate surfactant organic anions into the interlayer space for preparing organo-LDHs. To convert the LDH hydrophilic surface to hydrophobic one and hence, increase the accessibility of the interlayer region is beneficial for a wider range of applications. The dodecyl sulfate (DS) anions intercalation into the interlayer of LDH by weakening the electrostatic force between the layers increase the hydrophobic character of the LDH's surface. We investigate the manufacture of DS- modified Mg,Al based LDH thin film using different approaches :i) direct pulsed laser deposition (PLD) from DS-modified Mg,AlLDHs; ii) intercalation during LDH reconstruction by immersion as deposited pristine LDH and calcinated LDH films in a DS solution. The DS-Mg,Al-LDH targets were prepared by co-precipitation and by reconstruction via the "memory effect", respectively. For the PLD experiments an Nd:YAG laser working laser working at different wavelengths (266 nm, 532 nm and 1064 nm), and having a 10 Hz pulse repetition rate was used. The morphology of the thin films was investigated by atomic force microscopy (AFM) and the crystallographic structure of the powders and films was checked by X-ray diffraction. FTIR spectroscopy was used to evidence DS interlayer intercalation, both for powders and the deposited films. Contact angle measurements were performed in order to establish the wettability properties of the as-prepared thin films.

Correlations of the methods used for the preparation of DS-Mg,Al-LDH thin films with their structural, morphological and hydrophobic properties were evidenced.

## Ultrashort laser beam focusing into bulk glass: Modeling based on Maxwell's and non-linear Schrödinger equations and effects of boundary condition

V.P. Zhukov<sup>1,2</sup>, N.M. Bulgakova<sup>3,4</sup>, M.P. Fedoruk<sup>1,5</sup>

<sup>1</sup>Institute of Computational Technologies SB RAS, 6 Lavrentyev Ave., 630090 Novosibirsk, Russia

<sup>2</sup>Novosibirsk State Technical University, 20 Karl Marx ave., 630073, Novosibirsk, Russia

<sup>3</sup>HiLASE Centre, Institute of Physics ASCR, Za Radnici 828, 25241 Dolní Břežany, Czech Republic

<sup>4</sup>Institute of Thermophysics SB RAS, 1 Lavrentyev Ave., 630090 Novosibirsk, Russia

<sup>5</sup>Novosibirsk State University, 1 Koptug Ave., 630090 Novosibirsk, Russia  
zukov@ict.nsc.ru

Two approaches for modeling of femtosecond laser pulse propagation inside transparent dielectrics are most frequently used, based on Maxwell's equations and the nonlinear Schrödinger equation (NSE). The latter is easier for numerical solving as it requires considerably smaller computer resources. However, its applicability becomes doubtful for situations when a dense, highly localized free-electron plasma is excited which scatters light to large angles. This contradicts to main assumptions of the Schrödinger model, unidirectionality of light propagation. Additionally, for very short laser pulses, below  $\sim 100$  fs, the assumption of a slowly varying envelop which is a basis of the NSE can become invalid.

In this work, the above-mentioned modeling approaches are compared for irradiation parameters typically used for modification of optical glasses. Simulations are performed for fused silica irradiated at 800 nm. The results show significant difference between Maxwell and Schrödinger solutions even at relatively moderate NA ( $\sim 0.25$ ) which dramatically increases with further NA increase.

It is known that the spatial Fourier transform of a Gaussian beam entering the sample contains the terms with  $k_{\perp} > 2\pi/\lambda$ . For Maxwell's equations, this yields in an imaginary  $z$ -component of the wave number, resulting in small-scale perturbations of laser intensity near the focal region. To avoid these effects connected with large values of  $k_{\perp}$ , the boundary conditions with cut-off  $k_{\perp}$  and a smoothing procedure are proposed which suppress perturbations. The results of the Maxwell-based  $k_{\perp}$  model with such conditions are close to the Schrödinger-based solution even at NA  $\sim 0.4$ .

The questions on what are realistic boundary conditions, which would accurately describe beam focusing, and whether the Schrödinger-based model is valid for simulations of laser beams tightly focused into the bulk of transparent media call for further studies. Simulations demonstrate that even small variations of spatial pulse shape can cause considerable changes in locally absorbed laser energy and, hence, in material modification.

*Acknowledgements:* This research is supported by the Russian Foundation for Basic Research (RFBR project No. 15-01-02432). The work of M.P. Fedoruk is supported by Russian Science Foundation (Project No. 1204 14-21-00110).

## Toward modeling of interaction of dichromatic laser pulses with transparent dielectrics

V.P. Zhukov<sup>1,2</sup>, N.M. Bulgakova<sup>3,4</sup>

<sup>1</sup>*Institute of Computational Technologies SB RAS, 6 Lavrentyev Ave., 630090 Novosibirsk, Russia*

<sup>2</sup>*Novosibirsk State Technical University, 20 Karl Marx ave., 630073, Novosibirsk, Russia*

<sup>3</sup>*HiLASE Centre, Institute of Physics ASCR, Za Radnicí 828, 25241 Dolní Břežany, Czech Republic*

<sup>4</sup>*Institute of Thermophysics SB RAS, 1 Lavrentyev Ave., 630090 Novosibirsk, Russia*  
zukov@ict.nsc.ru

Laser microprocessing of materials can be more effective when using spatially and/or temporally shaped laser pulses. Last years, an attention is increasing to dichromatic laser pulses applied simultaneously or with a delay. When the pulses with different wavelength are applied sequentially, widely adopted monochromatic models can be used for simulations of material processing conditions. However, for adequate modelling of the action of overlapping laser pulses of different wavelengths on dielectric materials, description of photo- and impact ionizations as well as the Kerr effect require considerable revisions.

In this work, the Keldysh theory of photoionization is generalized for the case of the bi-wavelength irradiation with the electric field of  $E = E_1 \cdot \cos(\omega_1 t) + E_2 \cdot \cos(\omega_2 t + \varphi)$ ,  $\varphi$  is the phase shift. Two cases are considered, with integer and non-integer ratios between laser frequencies  $\omega_1$  and  $\omega_2$ . It has been shown that, for dichromatic pulses, the photoionization rate is usually larger than that for each monochromatic pulse of the same intensity. The ionization rate also depends on mutual orientation of polarization directions of the electric fields  $E_1$  and  $E_2$ . It is smaller for the case of perpendicular polarizations compared to parallel ones. The circular polarization, which can be considered as a particular case of a dichromatic pulse with perpendicular polarizations and equal frequencies, yields in a smaller photoionization rate compared to the linear one that is in line with experimental observations.

The impact ionization in dichromatic cases can be described as a sum of the Joule heating terms from the waves of both frequencies. The description of the Kerr effect is shown to require introduction of terms proportional to  $|E_1|^2|E_2$  and  $|E_2|^2|E_1$ .

*Acknowledgements:* This research is supported by the Russian Foundation for Basic Research (RFBR project No. 15-01-02432).

